Terms and Conditions of Use of Digitised Theses from Trinity College Library Dublin

Copyright statement

All material supplied by Trinity College Library is protected by copyright (under the Copyright and Related Rights Act, 2000 as amended) and other relevant Intellectual Property Rights. By accessing and using a Digitised Thesis from Trinity College Library you acknowledge that all Intellectual Property Rights in any Works supplied are the sole and exclusive property of the copyright and/or other IPR holder. Specific copyright holders may not be explicitly identified. Use of materials from other sources within a thesis should not be construed as a claim over them.

A non-exclusive, non-transferable licence is hereby granted to those using or reproducing, in whole or in part, the material for valid purposes, providing the copyright owners are acknowledged using the normal conventions. Where specific permission to use material is required, this is identified and such permission must be sought from the copyright holder or agency cited.

Liability statement

By using a Digitised Thesis, I accept that Trinity College Dublin bears no legal responsibility for the accuracy, legality or comprehensiveness of materials contained within the thesis, and that Trinity College Dublin accepts no liability for indirect, consequential, or incidental, damages or losses arising from use of the thesis for whatever reason. Information located in a thesis may be subject to specific use constraints, details of which may not be explicitly described. It is the responsibility of potential and actual users to be aware of such constraints and to abide by them. By making use of material from a digitised thesis, you accept these copyright and disclaimer provisions. Where it is brought to the attention of Trinity College Library that there may be a breach of copyright or other restraint, it is the policy to withdraw or take down access to a thesis while the issue is being resolved.

Access Agreement

By using a Digitised Thesis from Trinity College Library you are bound by the following Terms & Conditions. Please read them carefully.

I have read and I understand the following statement: All material supplied via a Digitised Thesis from Trinity College Library is protected by copyright and other intellectual property rights, and duplication or sale of all or part of any of a thesis is not permitted, except that material may be duplicated by you for your research use or for educational purposes in electronic or print form providing the copyright owners are acknowledged using the normal conventions. You must obtain permission for any other use. Electronic or print copies may not be offered, whether for sale or otherwise to anyone. This copy has been supplied on the understanding that it is copyright material and that no quotation from the thesis may be published without proper acknowledgement.

Development of the recombinant Semliki Forest virus vector as a gene therapy agent for the central nervous system

A thesis submitted to the University of Dublin, Trinity College

For the Degree of Doctor of Philosophy

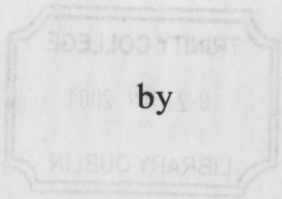

by

Alan Jerusalmi

Department of Microbiology,

Moyne Institute of Preventive Medicine,

Trinity College, Dublin

December 2003

For my parents

Declaration

This thesis is submitted by the undersigned to the University of Dublin, Trinity College for the examination of Doctorate of Philosophy. The work herein is entirely my own work and has not been submitted as an exercise for a degree to any other university. The librarian of Trinity College Dublin has my permission to lend or copy this thesis upon request.

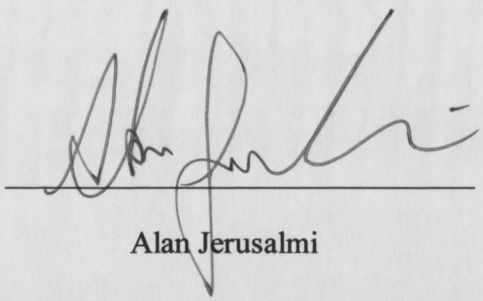

Alan Jerusalmi

Acknowledgements

First of all I would like to thank my supervisor Professor Greg Atkins for his help, guidance and support throughout the entire length of my project. I am very grateful for all the encouragement you have given me. Thank you for all your help.

I would also like to sincerely thank and acknowledge Professor Brian Sheahan, who has been like a second supervisor providing a great deal of help in all areas of the research. Special thanks for all the hours spent in analyzing enormous amounts of brains and spinal cord sections.

A special thanks to all in the virology lab past and present. Mags, who has been like a co-supervisor, providing a great deal of help with all aspects of animal work; Dot, our senior medical technologist for offering much needed help in everything including maintaining a well stocked chocolate drawer, providing much needed sugar for all the late night spent working. Jamie and Christopher, who welcomed me into Ireland with open arms, and have been not only great friends, but also excellent drinking partners. Kathrina, it's been a great adventure. Marina, Gowda, Sareen, Francis and Jerry, many thanks for all the help. Barbara, John, and Sarah who recently joined the lab, it's been entertaining.

For all in the Moyne who provided a great working environment, and for the many friends I made there, most of which I will carry for the rest of my life.

Many thanks to everyone in the prep-room, especially Paddy and Joe for all the last minute autoclavings.

Thanks to the multiple sclerosis society of Ireland and the Wellcome trust for funding me for the past 3 years.

Finally I would like to thank my parents Raphael and Miriam, and my brother Daniel for all the encouragement throughout my stay here in Dublin. Thank you for all the confidence you have expressed in me and for being very supportive of all my work.

Summary

Multiple sclerosis (MS) is a neurological disease of the central nervous system (CNS), and a major case of disability in young adults. It is characterized by the presence of inflammatory infiltrates containing autoreactive T cells, resulting in demyelination and axonal loss within the CNS. One of the greatest challenges in the treatment of MS is to get the therapeutic agent to successfully cross the blood-brain barrier, and exert an activity inside the CNS.

Semliki Forest virus (SFV) is an enveloped positive-stranded RNA virus that has been developed into an RNA expression vector. SFV is a neurotropic virus that has been extensively exploited as a model for the study of viral neuropathogenesis. The SFV4 strain of SFV, derived from an infectious clone, induces lethal encephalitis when given intranasally (i.n.) to adult mice. Avirulent strains such as A7 do not kill infected mice older than 14 days, but induce CNS demyelination. Experiments with both virulent and avirulent strains of SFV have shown that SFV can utilize olfactory pathways as a route of entry into the brain and have indicated that axonal transport and macrophages play a role in the transport of virus from nerve endings in the olfactory mucosa.

The SFV vector system utilized in this experiment consists of a self-replicating RNA vector (rSFV). In it, a heterologous gene replaces the SFV structural proteins, while the structural proteins are supplied *in trans* by helper RNAs to form encapsidated particles. A split-helper RNAs system in which two separate RNAs supply the capsid and spike protein prevents the production of replication-proficient viruses and greatly increases the biosafety of the vector. Particles produced are capable of expressing the cloned genes transiently during a single round of virus multiplication. Since the rSFV vector system induces little damage when administered as vaccine vectors, and has been shown to express cloned reporter genes in cultured brain slices, studies to access the feasibility of using i.n. infection by rSFV as a means of protein delivery to the CNS were conducted.

The current study successfully demonstrates that recombinant particles are able to induce high levels of expression of a reporter gene in the CNS following i.n. administration and infection of the nasal mucosa. Upon infection, viral RNA replication is confined to the nasal mucosa, and only the expressed protein enters the CNS, thus minimizing vector-induced

damage to the CNS. The safety of this vector was further verified by routine histological analyzes, where brain samples were consistently negative for pathology lesions. The therapeutic potential of this finding was tested by the effect of cytokine expression on the course of a model autoimmune disease of the CNS.

Experimental autoimmune encephalomyelitis (EAE) is a demyelinating CNS disease induced in susceptible strains of mice following inoculation of spinal cord homogenate, myelin proteins or peptides derived from myelin proteins. It is a T-cell mediated autoimmune disease that in some respects is similar to human MS. Because of its autoimmune nature, various attempts have been made to treat EAE with cytokines or with cytokine-expressing vectors with limited success. It has been shown that intramuscular injection of plasmid-based DNA vectors expressing the cytokines TGF-β or IL-4 inhibits the development of EAE. Previous work on a non-replicative herpes virus vector expressing IL-4 has shown that intracerebral administration of this vector inhibits EAE. An adenovirus vector expressing IL-10 has been shown to inhibit EAE when given intracerebrally and i.n. administration of IL-10 given as protein to rats also inhibits EAE.

The cytokines IL-10 and IL-4, which have been extensively researched in the treatment of EAE, were cloned into the rSFV vector system. Administration of the cytokine by the i.n. route, successfully changed the cytokine profile in animals by up-regulating the production of other T_H2 cytokines. One problem with the use of SFV vectors in the treatment of EAE is that it has been shown that the wild-type avirulent virus, when given peripherally, can potentiate or exacerbate EAE. It is possible; therefore, that administration of the SFV vector, in the absence of cytokine gene expression, could exacerbate EAE. In this study, we show that this is indeed the case, but that expression of IL-10 by the vector ameliorates the disease, as has been shown for other vector systems and routes of delivery. We conclude that SFV vectors may be useful for the delivery and expression of therapeutic genes in the CNS.

An alternative to the use of viral vectors encoding cytokines has been the use of polyunsaturated fatty acid in the treatment of MS. It has been previously demonstrated that a derivative of the omega-6 polyunsaturated fatty acid, linoleic acid has beneficial anti-inflammatory properties. Previous studies on EAE have shown the compound to be effective in protecting animals from the clinical effects commonly observed in EAE. This study utilizes a number of synthetic polyunsaturated fatty acid compounds, in the treatment of EAE.

Publications

Jerusalmi A., M. M. Morris-Downes, B. J. Sheahan, and G. J. Atkins (2003). Reporter and cytokine gene expression in the mouse central nervous system after intranasal administration of Semliki Forest virus recombinant particles. *Molecular Therapy* 8:886-894

Jerusalmi A., M. M. Morris-Downes, B. J. Sheahan, and G. J. Atkins (2003). An expression Vector for the Central Nervous System. International Patent Application Number PCT/IE03/00089.

Jerusalmi A. (2000) Identification and characterization of a newly discovered reovirus strain. *Thesis (M.S.) - Florida Atlantic University, Florida, USA.*

Jerusalmi A., M. M. Morris-Downes, B. J. Sheahan, and G. J. Atkins (2003) Treatment of experimental autoimmune encephalomyelitis by intranasal administration of IL-10 with a Semliki Forest virus vector system. Abstract in *Multiple Sclerosis* 7-Supplement 1:S48

Jerusalmi A., M. M. Morris-Downes, B. J. Sheahan, and G. J. Atkins (2003) Treatment of experimental autoimmune encephalomyelitis by intranasal administration of cytokines with a Semliki Forest virus vector system. Abstract in *Preceedings and Programme ESVP 200*: 57

Jerusalmi A., M. M. Morris-Downes, B. J. Sheahan, and G. J. Atkins (2002) Transient reporter gene expression in the mouse olfactory bulb following intranasal administration of Semliki Forest virus recombinant particles. Abstract in *XIIth International Congress of Virology*:189

Jerusalmi A., M. M. Morris-Downes, B. J. Sheahan, and G. J. Atkins (2001) The use of a Semliki Forest virus expression vector for the central nervous system. Abstract in *Multiple Sclerosis* 7-Supplement 1:S10

Presentations

1. The use of a Semliki Forest virus expression vector for the central nervous system. **Jerusalmi A.**, M. M. Morris-Downes, B. J. Sheahan, and G. J. Atkins. Oral and Poster presentation at the 17th Congress of the European Committee for Treatment and Research in Multiple Sclerosis. Dublin, Ireland. September 12th 2001.

2. Transient reporter gene expression in the mouse olfactory bulb following intranasal administration of Semliki Forest virus recombinant particles. **Jerusalmi A.**, M. M. Morris-Downes, B. J. Sheahan, and G. J. Atkins. Oral presentation at the 12th International Congress of Virology. Paris, France. August 1st 2002.

3. The use of a SFV expression vector for the central nervous system. **Jerusalmi A.**, M. M. Morris-Downes, B. J. Sheahan, and G. J. Atkins. Oral Presentation at the 1st Symposium on Semliki Forest Virus. Edinburgh, Scotland. February 14th 2003.

4. Treatment of experimental autoimmune encephalomyelitis by intranasal administration of cytokines with a Semliki Forest virus vector system. **Jerusalmi A.**, M. M. Morris-Downes, B. J. Sheahan, and G. J. Atkins. Oral Presentation at the 21st Annual Meeting of the European Society of Veterinary Pathology. Dublin, Ireland. September 11th 2003

5. Treatment of experimental autoimmune encephalomyelitis by intranasal administration of IL-10 with a Semliki Forest virus vector system. **Jerusalmi A.**, M. M. Morris-Downes, B. J. Sheahan, and G. J. Atkins. Poster presentation at the 19th Congress of the European Committee for Treatment and Research in Multiple Sclerosis. Milan, Italy. September 18th 2003.

Table of Contents

Dedication ii
Declaration iii
Acknowledgements iv
Summary v
Publications vii
Presentations viii
Table of contents ix
Index of tables xiii
Index of figures xiv
Abbreviations xviii

Chapter one - General introduction

1.1 Semliki Forest Virus 2
1.1.1 Classification of the Semliki Forest virus 2
1.1.2 Virion Structure 2
1.1.3 Genomic structure and organization 4
1.1.4 Life cycle of Semliki Forest virus 4
1.1.4.1 Viral entry 4
1.1.4.2 Viral RNA replication 5
1.1.4.3 Synthesis of the structural proteins and viral assembly 6
1.1.5 Effects of replication on infected cells 7
1.1.6 Strains of SFV 9
1.1.7 SFV pathogenesis in the CNS 9
1.2 Semliki Forest virus expression systems 11
1.2.1 rSFV vector system 11
1.2.2 SFV vectors and tumor therapy 12

1.2.3 SFV vectors as vaccines 12
1.2.4 SFV vectors and its potential for CNS disease treatments 13

1.3 Multiple Sclerosis 14
1.3.1 Classification of disease 14
1.3.2 Etiology of disease 15
1.3.3 Epidemiology 18
1.3.4 Symptoms 19
1.3.5 Diagnosis 19
1.3.6 Current treatments 20

1.4 Experimental Autoimmune Encephalomyelitis 21
1.4.1 Classification of disease 21
1.4.2 Current treatments 22
1.4.2.1 EAE treatment with IL-10 22
1.4.2.2 EAE treatment with IL-4 24
1.4.2.3 TGF-β treatment of EAE 24

1.5 The central nervous system 25
1.5.1 Cells of the central nervous system 25
1.5.2 Myelin biogenesis 28
1.5.2.1 Myelin formation 28
1.5.2.2 Myelin protein autoantigens 28
1.5.3 Mouse olfactory bulb 30
1.5.3.1 Layers of the main olfactory bulb 30
1.5.3.2 Cells of the main olfactory bulb 31

1.6 Cytokines in CNS disease treatments 32

1.7 Fatty acids in the treatment of EAE 34

1.8 Objectives of study 35

Chapter two - Expression of recombinant SFV particles in the mouse central nervous system

2.1 Introduction 37
2.2 Experimental procedures 38
2.3 Results 53
2.4 Discussion 54

Chapter three - Cloning and *in-vitro* expression of IL-4 and IL-10 in the SFV expression vector system

3.1 Introduction 59
3.2 Experimental procedures 60
3.3 Results 74
3.4 Discussion 75

Chapter four - *In-vivo* expression and analyses of SFV particles expressing different cytokines

4.1 Introduction 78
4.2 Experimental procedures 79
4.3 Results 82
4.4 Discussion 85

Chapter five - Treatment of experimental autoimmune encephalomyelitis with rSFV vectors

5.1 Introduction 89
5.2 Experimental procedures 91
5.3 Results 96
5.4 Discussion 100

Chapter six - Treatment of experimental autoimmune Encephalomyelitis with linoleic acid

6.1 Introduction 104

6.2 Experimental procedures 105

6.3 Results 107

6.4 Discussion 108

Chapter seven – General discussion

7.1 Discussion 111

Chapter eight – References

8.1 References 120

Index of tables

Chapter two

Table 2.1 Protein expression following rSFV-EGFP infection

Table 2.2 Table 2.2 RNA expression following rSFV-EGFP infection

Table 2.3 pathological analyses following i.n. administration of virus and vector

Chapter four

Table 4.1 Statistical analyses of IL-4 levels in tissue homogenates

Table 4.2 Statistical analyses of IL-10 levels in tissue homogenates

Table 4.3 Statistical analyses of IFN-γ levels in tissue homogenates

Chapter five

Table 5.1 Analysis of EAE mice treated with rSFV particles

Table 5.2 Analysis of EAE mice treated with rSFV particles

Table 5.3 Analysis of EAE mice treated with rSFV particles

Table 5.4 Pathology analysis of EAE mice treated with rSFV particles

Table 5.5 Analysis of EAE mice treated with rSFV particles

Table 5.6 Pathology analysis of EAE mice treated with rSFV particles

Chapter six

Table 6.1 Table 6.1 Analysis of EAE mice study 1 treated with fatty acid compounds

Table 6.2 Table 6.2 Analysis of EAE mice study 2 treated with fatty acid compounds

Index of figures

Chapter one

Figure 1.1 Schematic structure of SFV virion

Figure 1.2 SFV genomic structure and organization

Figure 1.3 Processing of structural proteins and viral release

Figure 1.4 Schematic diagram of rSFV particle production

Figure 1.5 The SFV vector system

Figure 1.6 World distribution of Multiple Sclerosis

Figure 1.7 Classification of disease progression in MS

Figure 1.8 Myelin formation by oligodendrocytes

Figure 1.9 Demyelination

Figure 1.10 Location of olfactory bulb in mouse skull

Figure 1.11 Layers of the main olfactory bulb

Chapter two

Figure 2.1 Maps of the Semliki Forest virus expression vectors

Figure 2.2 Confirmation of recombinant and helper SFV plasmids

Figure 2.3 Purified recombinant and helper plasmids

Figure 2.4 Linearized recombinant and helper plasmids

Figure 2.5 In vitro SP6 RNA transcription

Figure 2.6 rSFV-EGFP particle titration

Figure 2.7 Cryosection of perfused TA muscle

Figure 2.8 Cryosections of brain samples viewed under GFP filter

Figure 2.9 Layered images of brain cryosections

Figure 2.10 Immunohistochemical analyses of brain cryosections

Figure 2.11 RNA expression following i.n. infection with rSFV-EGFP particles

Figure 2.12 Histological staining of rSFV-EGFP infected mice

Figure 2.13 Histological staining of SFV4 infected mice

Chapter three

Figure 3.1 Strategy for cloning

Figure 3.2 RT-PCR on spleen samples for IL-10

Figure 3.3 IL-10 gene sequence

Figure 3.4 Purified IL-10 DNA

Figure 3.5 Digested IL-10 DNA

Figure 3.6 pSFV1

Figure 3.7 IL-10 insert in pSFV1

Figure 3.8 IL-10 insert orientation in pSFV1

Figure 3.9 IL-4 gene sequence

Figure 3.10 Purified IL-4 DNA

Figure 3.11 Digested IL-4 DNA

Figure 3.12 IL-4 insert in pSFV1

Figure 3.13 IL-4 insert orientation in pSFV1

Figure 3.14 In vitro SP6 RNA transcription

Figure 3.15 rSFV-IL10 particle titration

Figure 3.16 IL-10 sequence analyses

Figure 3.17 IL-4 sequence analyses

Figure 3.18 Expression of IL-10 in BHK-21 cells

Figure 3.19 Expression of IL-4 in BHK-21 cells

Figure 3.20 Secreted levels of IL-10 in different cell lines

Figure 3.21 Secreted levels of IL-4 in different cell lines

Figure 3.22 TGF-β latent complex and sequence

Chapter four

Figure 4.1 IL-4 levels in mice following particle administration

Figure 4.2 IL-4 levels in mice following particle administration

Figure 4.3 IL-10 levels in mice following particle administration

Figure 4.4 IL-10 levels in mice following particle administration

Figure 4.5 IFN-γ levels in mice following particle administration

Figure 4.6 IFN-γ levels in mice following particle administration

Chapter five

Figure 5.1 EAE model disease

Figure 5.2 Effect of 3 inoculations of rSFV on EAE

Figure 5.3 Effect of 3 inoculations of rSFV on EAE

Figure 5.4 Effect of 4 i.m. inoculations of rSFV on EAE

Figure 5.5 Effect of 4 i.m. inoculations of rSFV on EAE

Figure 5.6 Effect of 4 i.n. inoculations of rSFV on EAE

Figure 5.7 Effect of 4 i.n. inoculations of rSFV on EAE

Figure 5.8 Comparison of i.n and i.m. treatment of rSFV on EAE

Figure 5.9 Effect of 5 i.p. inoculations of rSFV on EAE

Figure 5.10 Effect of 5 i.p. inoculations of rSFV on EAE

Figure 5.11 Effect of 5 i.n. inoculations of rSFV on EAE

Figure 5.12 Effect of 5 i.n. inoculations of rSFV on EAE

Figure 5.13 Analyses of 5 rSFV treatments on EAE

Figure 5.14 Pathology lesions of EAE mice

Figure 5.15 Pathology lesions of EAE mice

Figure 5.16 Effect of 5 early i.n. inoculations of rSFV on EAE

Figure 5.17 Effect of rSFV on EAE induced on SJL mice

Figure 5.18 Effect of rSFV on EAE induced on SJL mice – 2

Figure 5.19 Comparison of all rSFV treatments on C57BL/6 mice

Chapter six

Figure 6.1 Effect of omega-6 fatty acid study 1 on EAE
Figure 6.2 Effect of omega-6 fatty acid study 1 on EAE
Figure 6.3 Effect of omega-6 fatty acid study 2 on EAE
Figure 6.4 Effect of omega-6 fatty acid study 2 on EAE
Figure 6.5 Effect of omega-6 fatty acid study 2 on EAE

Abbreviations

a.a. – amino acid

ATCC – American type culture collection

BHK – baby hamster kidney

bp – base pair

C – capsid

cDNA – complimentary DNA

CNS - central nervous system

CSF – cerebrospinal fluid

DAB – diaminobenzidine

DAPI – 4, -6, diamidino-2-phenylindole

ddNTP – dideoxynucleosidetriphosphates

DGLA - dihomogamma-linolenic acid

DNA – deoxyribonucleicacid

dNTP – deoxynucleosidetriphosphates

dpi - days post infection

dsDNA - double stranded deoxyribonucleicacid

dsRNA – double stranded ribonucleic acid

DTT – Dithiotreitol

EAE – experimental autoimmune encephalomyelitis

ECACC – European collection of animal cultures

EDTA - ethylenediaminetetra-acetic acid

EGFP – enhanced green fluorescent protein

ELISA – enzyme linked immunosorbent assay

ER – endoplasmic reticulum

FCS – foetal calf serum

g - gravitational force

GLA - gamma-linolenic acid

hepes – N-2-hydroxyethyl-piperazine-N'-2-ethanesulphonic acid

HSV-1 - herpes simplex virus

HLA – human lymphotrophic antigen

H_2O_2 - hydrogen peroxide

h.p.i. – hours post infection

HRP – horseradish peroxidase

i.c. – intra-cerebral

IFN – interferon

Ig – immunoglobin

IL – interleukin

i.m. – intra-muscular

i.n. – intra-nasal

i.p. – intra peritoneal

LIV – Louping Ill virus

MBP – myelin basic protein

MCS – multiple cloning site

MHC – major histocompatibility complex

MAG – myelin-associated glycoprotein

MOG – myelin oligodendrocyte glycoprotein

m.o.i. - multiplicity of infection

MS – multiple sclerosis

MRI – magnetic resonance imaging

mRNA – messenger RNA

NK – Natural Killer cells

NsP – non-structural protein

ORF – open reading frame

PBS – phosphate buffered saline

PCR – polymerase chain reaction

p.f.u. – plaque forming units

PLP – proteolipid protein

PNS – peripheral nervous system

PPMS – primary-progressive MS

PRMS – progressive-relapsing MS

r.p.m. – revolutions per minute

RNA – ribonucleic acid

RNase – ribonuclease

RRMS – relapsing-remitting MS

RT – room temperature

s.c. – subcutaneous

SCH – spinal cord homogenate

SFV – Semliki Forest virus

SIN – Sindbis virus

SPMS – secondary-progressive MS

TA - tibia anterior

TGF – transformation growth factor

TNF – tumor necrosis factor

TRITC – rhodamine isothiocyanate

Tris - Tris-(hydroxymethyl)-aminomethane

Chapter 1

General Introduction

1 INTRODUCTION

1.1 Semliki Forest Virus

1.1.1 Classification of the Semliki Forest virus

The Semliki Forest virus (SFV) was first isolated from mosquitoes in the Semliki rain forest, western Uganda in 1944 (Smithburn and Haddow 1944). The virus belongs to the genus *Alphavirus*, of the family *Togaviridae*. It is naturally transmitted to vertebrates (avian and mammalian hosts) by mosquitoes, creating a life cycle between the two. Most human infections of SFV are subclinical; however, there have been two cases of disease associated with the virus. The first case was reported in 1979, when a laboratory worker in Germany developed fever and headache followed by seizures, coma, and died of encephalitis. The individual had been working on the Osterrieth strain of SFV, and had a 1-year history of "purulent bronchitis". SFV was isolated from the brain and spinal fluid, with no viral antibody detected until the time of death, 1 week later. His history of chronic pulmonary infection and failure to produce antiviral antibody suggests that he had an immunodeficiency disorder involving antibody production (Willems *et al,* 1979). A second set of cases were reported in 1987 when SFV was isolated from serum samples of individuals in the Central African Republic with fever, persistent headache, myalgias, and arthralgias (Mathiot *et al,* 1990).

1.1.2 Virion Structure

SFV is a small virus, measuring about 65 nm in diameter. The viral particle contains 4 viral proteins. The virion consists of a nucleocapsid made up of 240 copies of the capsid (C) protein and a single molecule of RNA of approximately 11.4 kb. A lipid-containing envelope derived from the host cell plasma membrane surrounds the nucleocapsid. A total of 80 viral spikes are inserted into this envelope, consisting of three envelope glycoproteins E1, E2, and E3. The nucleocapsid and viral envelope are organized into T=4 icosahedral lattices (figure 1.1) (Choi *et al,* 1991, von Bonsdorff and Harrison 1975).

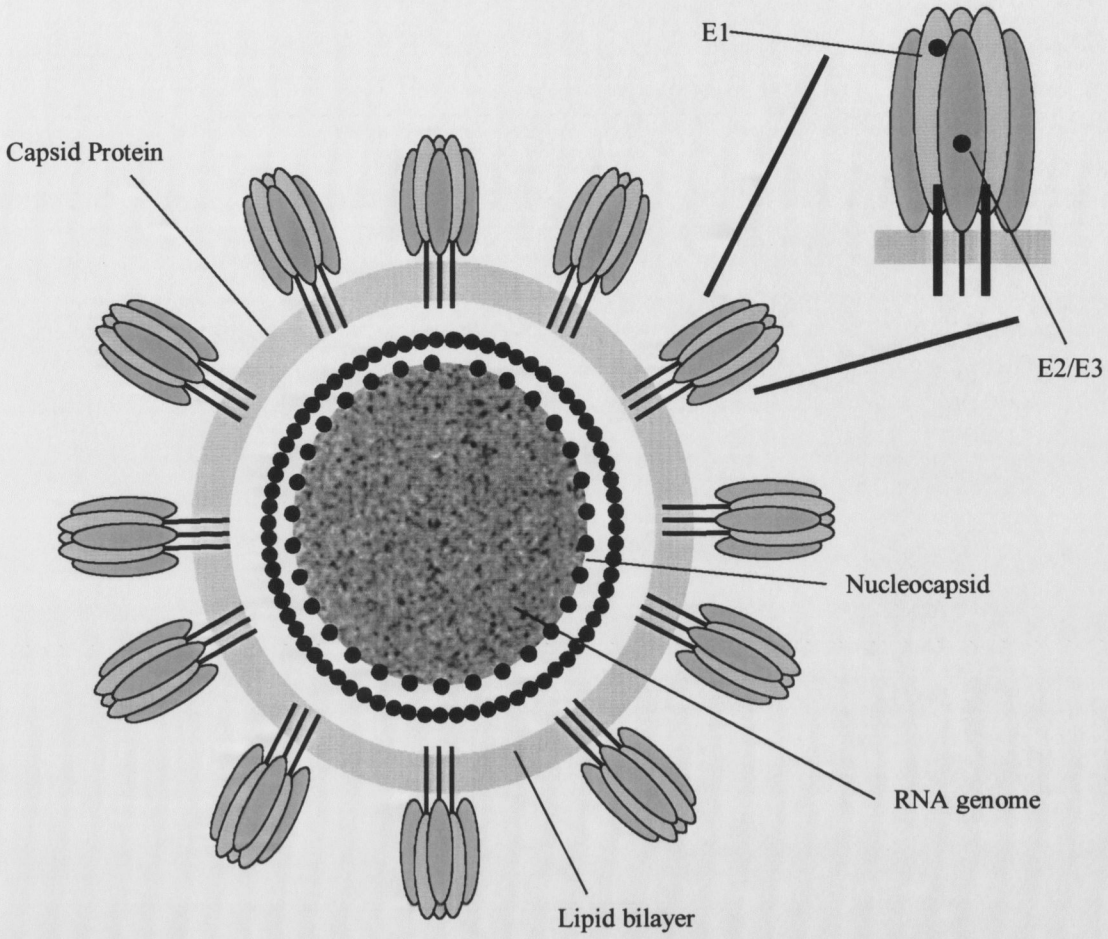

Figure 1.1 Schematic structure of SFV virion

The SFV virion consists of a nucleocapsid containing 240 C-protein copies and a single-stranded RNA genome of positive polarity. The host-derived lipid membrane contains 80 spikes, each composed of three copies of the E1, E2 and E3 glycoproteins.

The C protein has 267 amino acids (a.a.) and an apparent molecular weight of 30 kDa. It contains an RNA-binding domain residing in the N-terminus and a conserved C-terminal domain similar to chymotrypsin-like serine proteases (Choi *et al,* 1991, Melancon and Garoff 1987, Weiss *et al,* 1989). Once synthesized the C protein folds to act as a protease cleaving itself off the nascent chain (Hahn and Strauss 1990, Melancon and Garoff 1987). This reveals an N-terminal signal sequence that is recognized by the signal recognition particle targeting the nascent chain-ribosome complex to the endoplasmic reticulum (ER) membrane (Bonatti *et al,* 1984, Garoff *et al,* 1978) where it is later cleaved to the three structural membrane proteins p62, 6K and E1 (Garoff *et al,* 1990, Liljestrom and Garoff 1991b, Melancon and Garoff 1986).

Each viral spike consists of three copies each of the glycoproteins E1/E2/E3. The three interact to give 240 heterotrimers on the surface, assembled into 80 spikes (Garoff *et al,* 1974). The E1 protein has a size of about 49 kDa containing 438 a.a. It has a hydrophobic transmembrane region separating the N-terminal glycosylated ectodomain from two C-terminal arginine residues, situated on the inside of the viral membrane (Bron *et al,* 1993, Wahlberg *et al,* 1992, Wahlberg and Garoff 1992). The E1-E1 interactions are responsible for maintaining spike stability, as suggested by cross-linking studies (Wahlberg *et al,* 1992). The E2 glycoprotein whose major function lies in its receptor-binding subunit, has a similar size to E1, with 422 a.a. and about 42 kDa molecular weight. It contains an N-terminal ectodomain (Simmons and Garoff 1980), a hydrophobic transmembrane region and a large 31 a.a. C-terminal sequence within the viral membrane interacting with the virion nucleocapsid (Metsikko and Garoff 1990, Skoging *et al,* 1996). E2 is formed from a precursor, p62, which also contains a smaller 66 a.a. glycoprotein E3. The p62 protein forms a heterodimer with E1 via its E3 domain in the ER (Lobigs *et al,* 1990, Wahlberg *et al,* 1989). This is then transported out of the plasma membrane, where virus budding occurs through spike nucleocapsid interactions (Barth *et al,* 1992, Suomalainen *et al,* 1992, Zhao and Garoff 1992). The full function of the E3 protein has not yet been fully understood. It does remain associated with the SFV virion, and the N-terminus functions as a signal peptide for p62 during viral replication (Sariola *et al,* 1995); however it is discarded in several other alphaviruses (de Curtis and Simons 1988). Apart from the four structural proteins, small amounts of the viral 6K protein is found in SFV virions. The function of this 60 a.a., 6 kDa membrane protein is unclear. It is not involved

in virus infectivity, but it may play a role in viral budding (Liljestrom *et al,* 1991, Lusa *et al,* 1991).

1.1.3 Genomic structure and organization

The overall structure and organization of the SFV genome is illustrated in figure 1.2. It has a size of approximately 11.4 kb, and it consists of a single-stranded positive RNA genome (Garoff *et al,* 1980, Takkinen 1986). The genome is arranged in two modules, capped with a 5' 7-methylguanosine residue, and a 3' polyadenylated tail (Sawicki and Gomatos 1976). Two thirds of the genome at the 5' end, encodes for the non-structural proteins (nsPs) required for transcription and replication of the RNA. They are the nsP1, nsP2, nsP3 and nsP4, formed from a polyprotein precursor by a process of post-translational cleavage from the parental 42S RNA. (Glanville *et al,* 1976, Lachmi and Kaariainen 1976). The remaining one-third at the 3' end codes for the structural proteins. They are translated from a smaller subgenomic 26S RNA species and are also produced as a polyprotein (Wengler and Wengler 1976). The structural proteins are translated in the following order: C, p62, 6K and E1 (Keranen and Kaariainen 1975). The E2 and E3 glycoproteins are derived from the post-translation cleavage of the p62 polyprotein.

1.1.4 Life cycle of Semliki Forest virus

1.1.4.1 Viral entry

Alphaviruses have a broad host range and replicate in a variety of different cell types, as well as in many different species. The viral protein E2 is responsible for the interactions with cell receptors (Dubuisson and Rice 1993). Different proteins have been suggested as functional receptors for SFV. Early studies first suggested the HLA and the H2 histocompatibility antigens as cell surface receptors (Helenius *et al,* 1978); however, it was later proved that the presence of these antigens is not essential for infectivity (Oldstone *et al,* 1980). Due to its broad host range, it is possible that the virus uses a

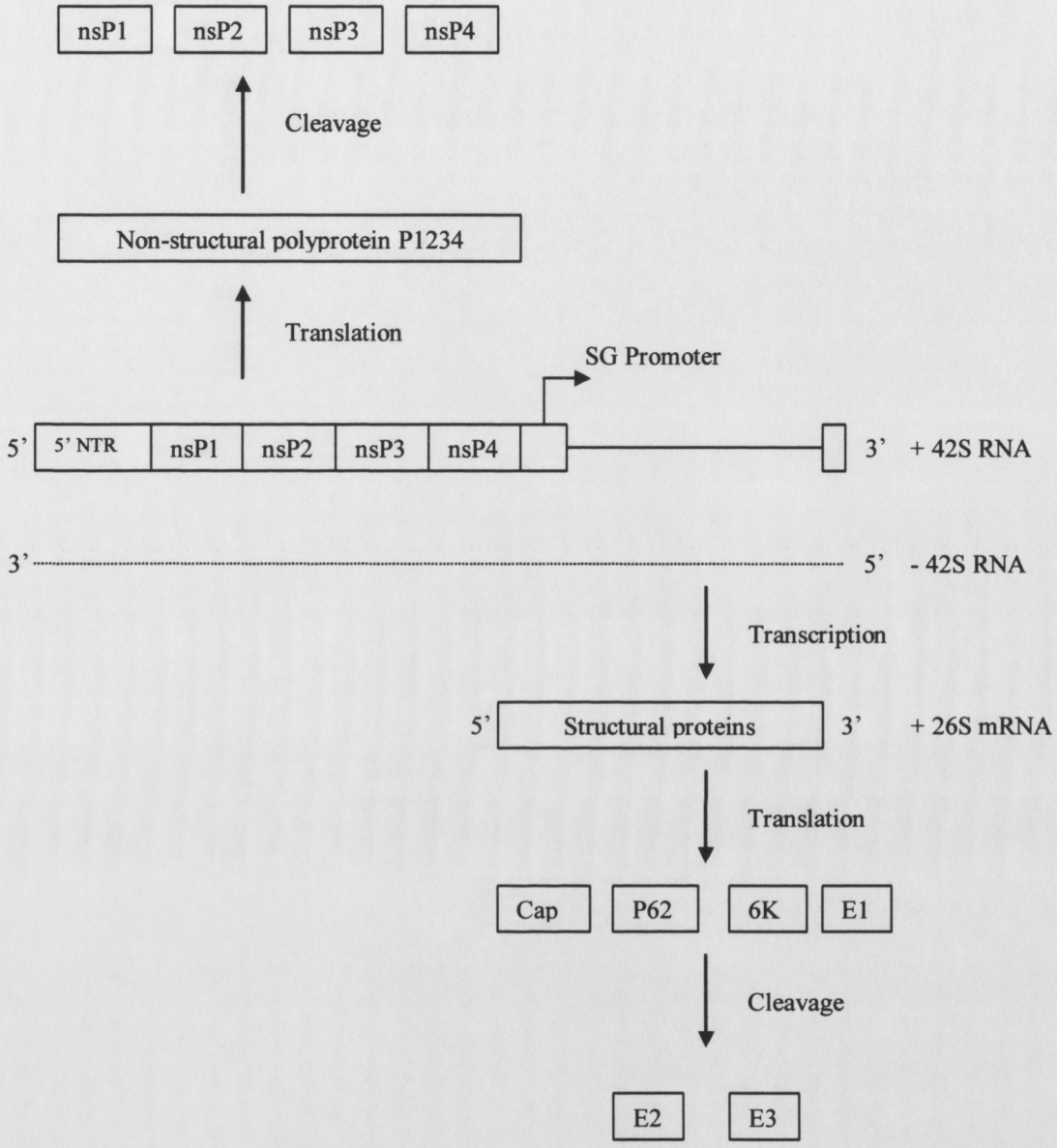

Figure 1.2 SFV genomic structure and organization

The 4 non-structural proteins (nsPs) are encoded in the 5' two-thirds of the genome, translated as the polyprotein P1234. The polyprotein is then processed to nonstructural proteins nsP1-nsP4, through the action of the nsP2 and nsP4 autoproteases. The structural proteins are transcribed following formation of a complementary strand, and translated as a polyprotein; they are then cleaved to form the spike proteins.

variety of different molecules for attachment or else uses a ubiquitous surface molecule as a receptor (Strauss *et al,* 1994).

The virus gains entry to the cell by receptor mediated endocytosis, a pathway which normally functions for uptake of receptor-ligand complex (DeTulleo and Kirchhausen 1998). Once internalized, the low-pH environment of the endosome induces a conformational change in the viral spike proteins, which results in dissociation of the E1/E2 heterodimer and conformational changes within the E1 and E2 subunits (Wahlberg and Garoff 1992). The newly formed E1 trimer mediates fusion of the viral membrane with the endosomal membrane (Wahlberg *et al,* 1992). This fusion requires the presence of cholesterol and sphingolipid in the target membrane (Nieva *et al,* 1994, Phalen and Kielian 1991, Smit *et al,* 1999).

Following fusion, there is release of the nucleocapsid into the cytoplasm. This is followed by uncoating of the virus by cell ribosomes, which releases viral RNA and subsequently leads to initiation of translation (Singh and Helenius 1992).

1.1.4.2 Viral RNA replication

RNA replication takes place in the cytoplasm of infected cells, more specifically in 0.6-2.0 2 μm wide cytoplasmic vacuoles (CPV-1) derived from endosomes and lysosomes (Froshauer *et al,* 1988, Peranen and Kaariainen 1991). The RNA genome is 11,442 nt long, it is 5' capped and 3' polyadenylated of positive polarity, and thus can function directly as an mRNA.

Viral replication begins with translation of the 5' ORF that constitutes two-thirds of the genome coding for the non-structural precursor polyprotein (Takkinen 1986). Following translation, this precursor is cleaved into the four non-structural proteins nsP1, nsP2, nsP3, and nsP4, which comprise the viral replicase. Protein nsP1 encodes a methyl transferase responsible for virus-specific capping activity and initiation of minus strand synthesis (Mi *et al,* 1989, Mi and Stollar 1991). The nsP4 protein is responsible for cleaving the polyprotein into its four subcomponents (Ding and Schlesinger 1989, Hardy and Strauss 1989). No known function is yet associated with the phosphoprotein nsP3 (Li *et al,* 1990); however, it may be required in some capacity for RNA synthesis (LaStarza *et al,* 1994). The SFV RNA polymerase activity is located in the protein nsP4 (Hahn *et al,*

1989, Sawicki *et al,* 1990). Once the nsP proteins have been synthesized they are responsible for the formation and replication of the plus strand 42S genome into full-length minus strands, which serve as templates for production of new 42S genomic RNAs. They also serve as template for the synthesis of the subgenomic 26S RNA. These contain the final third of the genome and synthesis is initiated by the 26S promoter located on the 42S minus stand (Grakoui *et al,* 1989, Levis *et al,* 1990).

1.1.4.3 Synthesis of the structural proteins and viral assembly

All structural proteins are translated from the 26S subgenomic RNA very early (2 to 3 hours post infection) in the replication cycle. The proteins are synthesized as a polyprotein precursor in the order C-E3-E2-6K-E1 (Garoff *et al,* 1982). Once synthesized, the C protein is autoproteolytically cleaved off the nascent polypeptide chain; it multimerizes and associates with genomic RNA to form nucleocapsids (Aliperti and Schlesinger 1978, Hahn and Strauss 1990, Melancon and Garoff 1987). Cleavage reveals an N-terminal signal sequence in the nascent chain that directs co-translational translocation of the p62 ectodomain into the ER lumen. The uncleaved N-terminal signal sequence is also transferred to the ER lumen where it becomes glycosylated. The p62, E1 and 6K proteins appear to move as a group following synthesis, through the ER, to their ultimate location on the host-cell plasma membrane. Other signal peptidase sequences are located at the COOH-terminus of the p62 and 6K proteins, to promote 6K and E1 translocation, respectively (Liljestrom and Garoff 1991b, Melancon and Garoff 1986). Subsequent cleavage by host cell peptidases generates p62, 6K and E1 proteins (Barth *et al,* 1995).

The p62 and E1 associate to form a heterodimer complex in the ER. This complex, resistant to low pH, interacts with 6K and is transported out to the plasma membrane, via the Golgi apparatus, where 6K dissociates and virus budding takes place through spike nucleocapsid interactions (Lusa *et al,* 1991, Wahlberg *et al,* 1989). 6K may function to select specific lipids for insertion into the membrane bilayer facilitating efficient viral budding due to a cholesterol requirement in viral assembly (Marquardt *et al,* 1993). During this migration the p62 precursor is cleaved into mature E2 and E3 glycoproteins (de Curtis and Simons 1988, Sariola *et al,* 1995), making the viral spike sensitive to low pH.

This facilitates formation of the E1-E2 heterodimer, which leads to fully infectious virus (Lobigs and Garoff 1990, Salminen *et al,* 1992), with E3 remaining transiently associated with the viral spike.

Genomic RNA and C proteins are rapidly associated into nucleocapsids (Soderlund 1973). The interaction between the C proteins in the nucleocapsid with the cytoplasmic tail of E2 leads to the budding of viral particles at the plasma membrane (Garoff and Simons 1974, Skoging *et al,* 1996, Suomalainen *et al,* 1992). A schematic representation of the processing of structural proteins and viral release is demonstrated in figure 1.3.

1.1.5 Effects of replication on infected cells

Infection of vertebrate cell with alphaviruses, leads to inhibition of host-cell protein synthesis and cell death. In contrast, infection of invertebrate cells leads to a persistent infection, with no significant cell damage. The mechanism behind the persistent infection in mosquito cell lines is not known (Brown and Condreay 1986, Karpf and Brown 1998). Most vertebrate cells once infected undergo apoptosis and die within a few days; however, cells naturally resistant to apoptosis, such as fully differentiated macrophages, muscle cells and neurons are killed by necrosis (Atkins *et al,* 1990, Balluz *et al,* 1993, Frolov and Schlesinger 1994, Glasgow *et al,* 1997). Structural proteins are produced in very high amounts during the first 24 hours of infection, and about 10^4 p.f.u are released per infected BHK-21 cell. After 6 hours of infection, only viral proteins are produced, with host cell synthesis being completely shut down (Liljestrom and Garoff 1991a). An extensive cytopathic effect is observed in infected cells, characterized by cell rounding, shrinkage, and cytoplasmic blebbing (Levine *et al,* 1993). Since synthesis of viral structural proteins is not required for cytopathic effect, it is mediated by viral RNA replication (Frolov and Schlesinger 1994).

Two different types of persistent infections have been described in vertebrate cells. In BHK cells using defective interfering particles, virtually all cells were infected; however, synthesis of virus-specific RNA and protein were greatly reduced (Weiss *et al,* 1980). The virus in this model underwent genetic mutation, which interferes with the replication of the genomic RNA, leading to inhibition of viral RNA replication and virus production. This mutation resulted in a less cytopathic mutant capable of persistent

Figure 1.3 Processing of structural proteins and viral release

All structural proteins are translated from the 26S subgenomic RNA. The C protein is autoproteolytically cleaved off and associates with genomic RNA to form nucleocapsids. The p62, E1 and 6K proteins are translocated to the ER, directed by an NH_2-terminal sequence in p62, where co- translational cleavage of the remaining polypeptide occurs. The p62 and E1 proteins associate to form a heterodimer complex, interact with 6K and are transported out to the plasma membrane, via the Golgi apparatus, where 6K dissociates and virus budding takes place through spike nucleocapsid interactions. (Adapted from Schlesinger & Schlesinger, 1996).

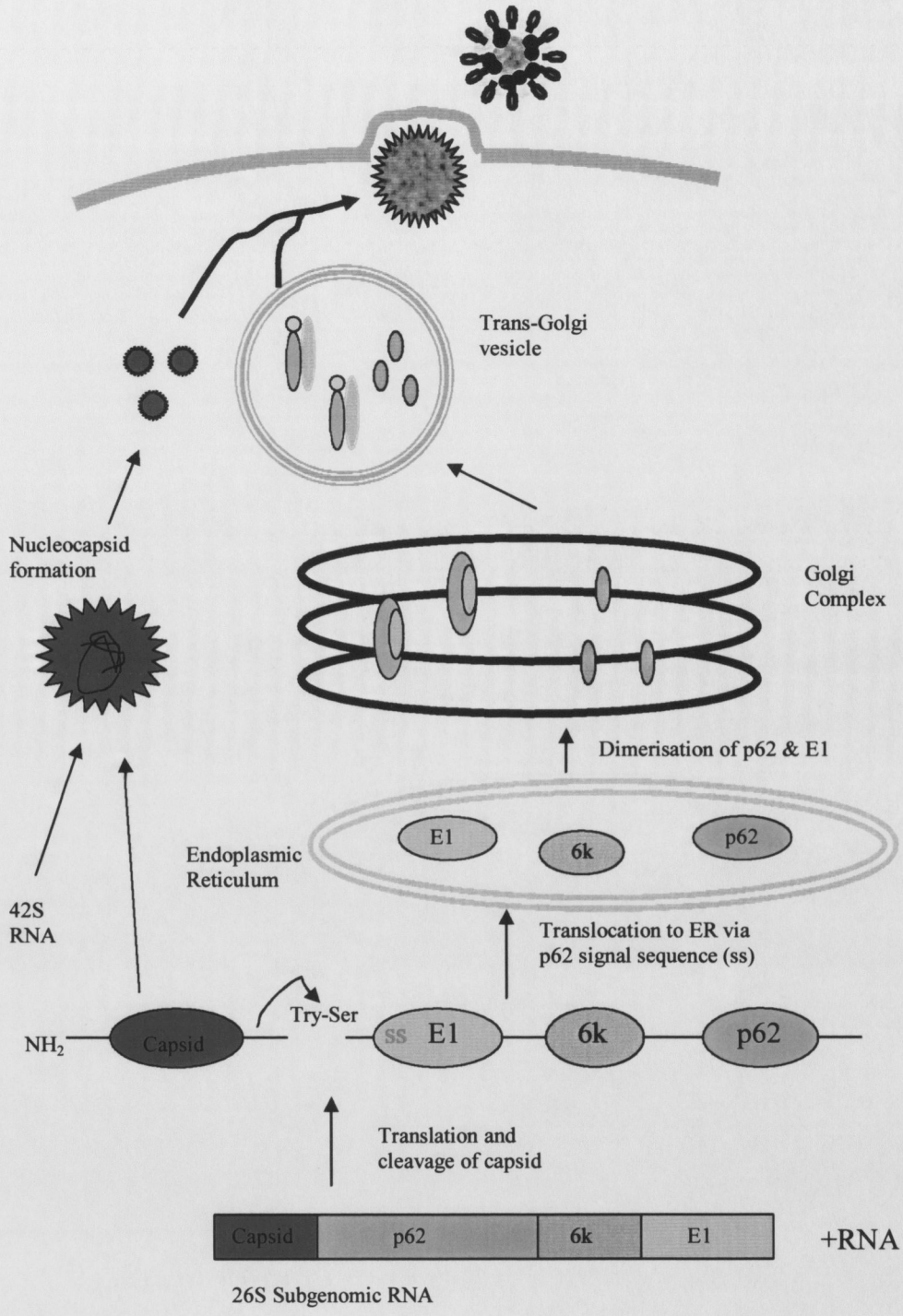

Figure 1.3 Processing of structural proteins and viral release

infections in BHK cells. A mutation in the nsP2 region that converted Pro^{726} to Ser is the most likely reason for this change in infection type (Dryga *et al,* 1997). A second model utilized Sindbis virus (SIN) replicons that expressed a gene coding for an enzyme that destroys puromycin (*pac* gene) in BHK cells. In the presence of puromycin, only cells capable of clearing this compound can survive. Therefore, several surviving nonocytopathic replicons were isolated (Frolov *et al,* 1999). The most analyzed mutant contained a mutation of a single a.a. in the nsP2 protein from Pro^{726} to Leu (same a.a. as previous mutant). Both studies suggest the nsP2 protein may have some undefined function affecting host-cell survival (Rikkonen 1996).

Other cellular genes have more recently been shown to cause a significant decrease in virus replication, leading to a persistent infection. The protein *bcl-2*, an antiapoptotic agent, has been shown to play a role in establishing persistent infection. This was accomplished by SIN and SFV infection of the rat prostate carcinoma cell line (AT-3 cells), which expresses the human *bcl-2* gene, where viral replication was restricted by 10 to 100 fold compared to control cell lines (Levine *et al,* 1993, Scallan *et al,* 1997, Ubol *et al,* 1994). The low titers obtained from infection indicated only a small number of cells (AT-3) were productively infected, as was the case with previous examples. This type of persistent infection by SIN was later linked to a single a.a. in the E2 glycoprotein (Ubol *et al,* 1994). It was later shown that for SFV, this might not necessarily occur. Recent studies have shown that SFV encodes a function which leads to inactivation of *bcl-2* by proteolytic cleavage, which makes it able to multiply in *bcl-2* expressing cells (Grandgirard *et al,* 1998).

While cellular factors dictating alphaviral-induced apoptosis are well examined, a number of viral factors dictating cell death are still unknown. Synthesis of structural proteins has been linked to the mechanisms of SIN induced apoptosis. This is easily observed by the delayed cell death following infection of BHK cells transfected with virus lacking these proteins (Despres *et al,* 1995). That is not the case however for SFV, where deletion of structural proteins does not prevent the viral cytopathic effects of the virus on infected cells (Glasgow *et al,* 1998). This leaves the non-structural proteins and/or viral replication responsible for the apoptotic trigger seen in infected cells. It was demonstrated that p53-independent apoptosis was induced in cells by the non-structural region of SFV, and that induction was also dependent on viral RNA synthesis (Glasgow *et al,* 1998). The induction of dsRNA-dependent protein kinase and viral replication as a result of SFV

infection could also trigger cell death pathways (Favre *et al,* 1996, Grandgirard *et al,* 1998).

1.1.6 Strains of SFV

The original SFV strain is designated L10 (Smithburn and Haddow 1944). This strain is neurovirulent for mice and causes lethal encephalitis by infecting the central nervous system (CNS). An avirulent strain designated A7 was later isolated from mosquitoes in Mozambique (McIntosh *et al,* 1961). Strains currently used in laboratories were derived from these two isolates. The A7[74] strain was derived by further selection for avirulence from the A7 strain (Bradish *et al,* 1971). Two other mutants from the original L10 strain are designated M9 and M136, which induce immune-mediated demyelination (Atkins *et al,* 1985). The original infectious clone of SFV was apparently derived from the L10 strain, though it appears to have lost some of its virulence due to multiple passages in cell culture (Glasgow *et al,* 1991). The infectious clone derived from this prototype strain is designated pSP6-SFV4, and transcription of this strain leads to a virulent form of the virus labeled SFV4.

1.1.7 SFV pathogenesis in the CNS

All SFV strains can be classified as virulent or avirulent, depending on the type of infection they generate. The original strain L-10 and its derivative SFV4 are the virulent strains, while A7 and its derivatives are avirulent. Both strains infect the same type of cells in culture, and *in vivo*. The rate at which multiplication takes place in some cells is the main distinguishing factor between the two. In the CNS, virulent strains tend to grow to a much higher titer, leading to fatal death of the neurons. Avirulent strains on the other hand, multiply much slower, causing less neuronal damage, and as a result, are cleared from the CNS by the immune system (Atkins and Sheahan 1982, Atkins *et al,* 1990, Balluz *et al,* 1993, Fazakerley *et al,* 1993, Gates *et al,* 1985). A similar death mechanism is seen in cultured neurons, where the efficiency of multiplication is different depending on the strain used. Experiments utilizing SFV4 and A7 showed that infection of cultured neurons was 10-fold higher for virulent strains then avirulent strains (Glasgow *et al,* 1997). Little

difference is found for infection of glial cells. Glial cells consist of a mixture of proliferating oligodendrocytes and astrocytes, where oligodendrocytes are successfully infected by SFV, and astrocytes undergo a slow infection. Avirulent strains tend to grow slower then virulent strains in these cells, but reach higher titers (Atkins *et al,* 1990, Glasgow *et al,* 1997).

Depending on route of infection, a notable difference can be detected in mice following infection with either virulent or avirulent strains. Intraperitoneal (i.p.) and subcutaneous (s.c.) infection of mice with SFV4 leads to a lethal encephalitis by neuronal damage in a proportion of mice. Avirulent strains however do not kill the mice, and lead to protection against challenge with virulent strains. It does lead to immune mediated demyelination in some mice. Intranasal (i.n.) infection with SFV4 kills every mouse by lethal encephalitis; there is widespread neuronal destruction with viral RNA and antigens detected in neurons and oligodendrocytes. With the avirulent strain, neuronal damage is seen in the olfactory bulbs, followed by demyelination of the CNS (Atkins *et al,* 1990, Balluz *et al,* 1993, Sheahan *et al,* 1996). All strains of SFV are lethal to neonatal mice (reviewed in Atkins *et al,* 1996)

The demyelination seen in mice infected with avirulent strains is likely to be a result of oligodendrocyte infection. It has been demonstrated that the immune mediated demyelination is triggered by the generation of myelin debris produced by damage to oligodendrocytes. This results in the presentation of normally sequestered myelin antigens to T-helper cells, in addition, the release of cytokines during virus infection could amplify this process (Balluz *et al,* 1993). Furthermore, Balb/c nu/nu mice show a less severe demyelination compared to immune-competent mice, and demyelination can be prevented by *in vivo* depletion of CD8+T-lymphocytes (Fazakerley and Webb 1987, Subak-Sharpe *et al,* 1993). A difference in demyelination is detected between BALB/c and SJL mice. In BALB/c demyelination is maximal at 14 days after i.p. infection, at a time where infectious virus has been cleared from the CNS. The lesions are then repaired. In SJL mice, demyelinating lesions persist up to a year following infection with the M9 mutant (Donnelly *et al,* 1997b, Smyth *et al,* 1990)

1.2 Semliki Forest virus expression systems

1.2.1 rSFV vector system

Many characteristics of SFV make it a good candidate for an expression system. The genome is of positive polarity, therefore functions as a mRNA, and infectious RNA molecules can be obtained by transcription from a full-length cDNA copy of the genome. SFV has a very efficient replication, since the infecting RNA molecule codes for its own replicase. Furthermore, replication takes place in the cytoplasm of infected cells. This eliminates problems encountered in conventional nuclear cDNA expression systems such as mRNA splicing, limitations in transcription factors, problems with capping efficiency, and mRNA transport. A very late onset of cytopathogenic effects allows for an extensive time frame (4 h to 24 h after infection) where a very high expression level of the structural proteins is combined with negligible morphological changes. SFV has a broad host range, and most people outside of Africa have no pre-existing immunity against the virus. In culture, SFV has been shown to infect a range of different cells, including mammalian, avian, reptilian, amphibian and insect (Clark *et al,* 1973, Griffin 1986, Leake *et al,* 1977, L'Heritier 1970, Stollar 1980). Finally, SFV is of low pathogenicity for humans, making it safe to handle.

The SFV vector system utilized in this study consists of an RNA replicon derived from the virus genome, where recombinant particles are produced based on the co-transfection of BHK-21 cells with three separate RNAs (figure 1.4) (Liljestrom and Garoff 1991a, Smerdou and Liljeström 1999).

The vector RNA lacks the structural protein genes, which are supplied (in trans) by a split helper system. The replicon vector contains the replicase gene, the sub-genomic promoter followed by a multiple cloning site where a heterologous gene could be inserted, and the 5' and 3' ends of the genome required for replication. The helper vectors contain the complete sequence present in the viral sub-genomic RNA, as well as the 3' and 5' replication signals from the genomic RNA, but do not encode the viral replicase. They supply the packaging system needed for vector production. Two independent RNAs provide in *trans* the capsid and spike proteins (figure 1.5). This leads to increased bio-safety, where a high level of protection is obtained due to requirement of at least two mutation events in order to generate full-length genomes. A further mutation to the capsid

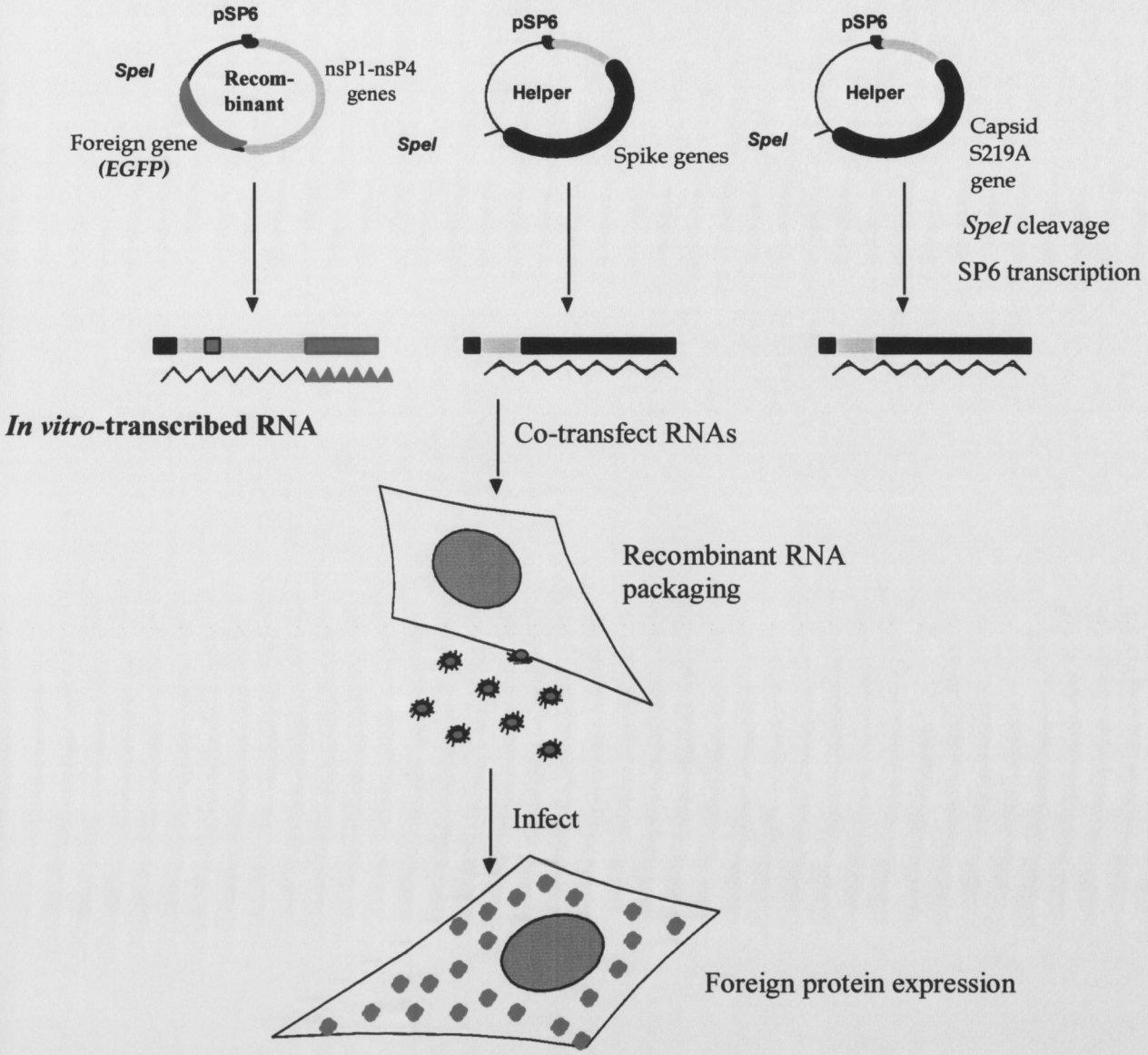

Figure 1.4 Schematic diagram of rSFV particle production

SFV structural proteins are replaced with a foreign gene in the recombinant plasmid, and supplied in two separate helper plasmids. Helper molecules lack the majority of viral non-structural sequences, except those essential for translation of viral structural proteins. *In vitro-* transcribed RNA from all 3 SFV constructs are used to co-transfect, where the rRNA-encoded replicase amplifies both RNA species in BHK-21 cells. The helper molecules supply viral structural proteins *in trans*. The capsid protein only packages the rRNA molecule, as both helper molecules lack the SFV packaging signal. Recombinant particles are produced and released. These particles are used to infect new cells, or animals, and induce a high-level of foreign protein expression. As the infecting RNA lacks the structural genes of the virus, new infectious virions are not formed, and they are thus suicide rSFV particles. (Adapted from Berglund *et al*, 1996).

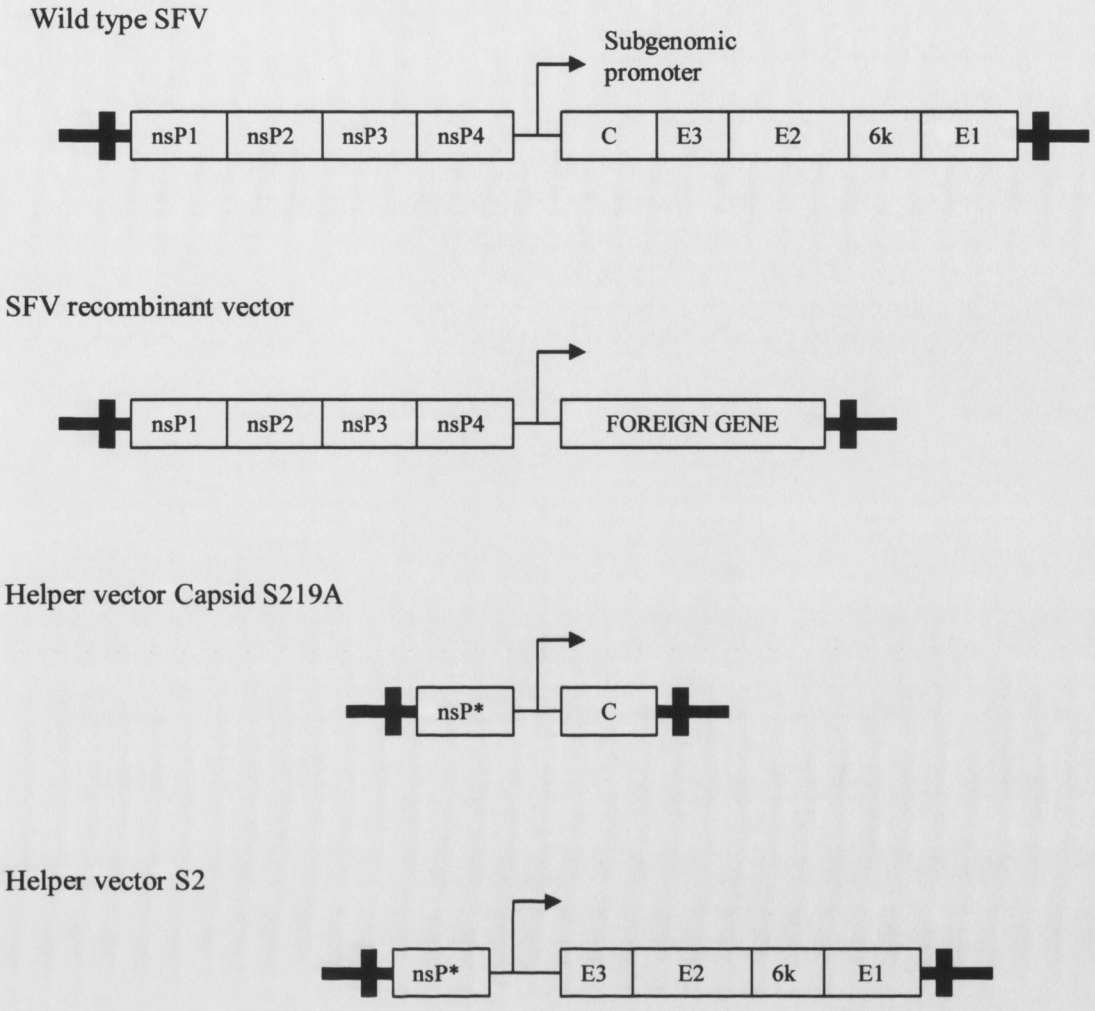

Figure 1.5 The SFV vector system

The representation of the RNA transcribed from the parental pSP6-SFV4 plasmid of the wild-type SFV is shown at the top. The recombinant vector was derived by manipulation of the SFV4 genome, where structural genes under the control of the subgenomic promoter were replaced with foreign genes. The helper RNAs encode all of the structural proteins of SFV; however they are supplied as two separate plasmids. Each helper RNA has nearly the complete replicase region deleted, including the packaging signal.

gene abolishes the self-cleaving activity of the protein. (Liljestrom and Garoff 1991a, Smerdou and Liljeström 1999). The recombinant particles produced by this vector system contain RNA encoding the cloned gene, and express them transiently during a single round of virus multiplication only. The system is capable of producing particles of very high titer, and infects a number of cells.

1.2.2 SFV vectors and tumor therapy

The rSFV vector system has been previously studied for its use as an anti-cancer agent. It has been recently shown that direct infection of murine tumors with rSFV particles can inhibit tumor growth and induce regression in the *p53*-deleted human non-small cell lung carcinoma cell line H358a. Pathological analyses of rSFV treated tumors indicated that tumor inhibition was not due to induction of an immune response, rather consistent with an initial induction of apoptosis followed by a large depletion of tumor cells by oncotic necrosis (Murphy *et al,* 2000). The apoptotic characteristic of the vector lies within the non-structural region of the SFV (Glasgow *et al,* 1998), which is maintained in the vector. This allows for insertion of genes in place of the structural region, which could modify or enhance its pro-apoptotic or anti-tumor properties. One experimental study involved the insertion of the *Bax* gene to enhance cytopathic and anti-tumor potential of the vector, as well as to counteract the anti-apoptotic *Bcl*-2 gene. This insert augmented the p53-independent apoptosis characteristic of the SFV vector (Murphy *et al,* 2001). Both anti-tumor studies performed with the SFV vector show that there is a considerable potential for this system to be used for genotoxic cancer therapy.

1.2.3 SFV vectors as vaccines

The development of SFV as a vector system has opened a wide spectrum of opportunities for vaccine development. The vector has many advantages over other expression systems. SFV has the potential to infect a broad host of cells, and most people and animals have no pre-existing immunity against the vector. As an RNA vector, replication is cytoplasmic so there is no risk of integration into the chromosome; and the

virus genome does not persist in the tissue (Atkins *et al,* 1996, Atkins *et al,* 1999, Tubulekas *et al,* 1997, Zhou *et al,* 1994). The safety of this system for vaccine use has been previously exploited. SFV vectors have shown the ability to induce humoral and cell-mediated immunity against several diseases (Berglund *et al,* 1997, Berglund *et al,* 1999, Fleeton *et al,* 1999, Fleeton *et al,* 2000). Following intra-muscular (i.m.) inoculation with rSFV particles, the cloned protein was detected at the injection site only, with very mild lesions (animals fully recovered), whereas administration of DNA leads to widespread dispersal, and prolonged persistence. Furthermore, rSFV particles did not persist beyond 7 days, as opposed to DNA which can persist for months (Morris-Downes *et al,* 2001a, Wolff *et al,* 1992). Compared to DNA immunization encoding the same antigens, rSFV particles induce stronger immune responses (Berglund *et al,* 1999, Brand *et al,* 1998, Fleeton *et al,* 1999, Zhou *et al,* 1995). In Cheviot cross lambs, particles encoding Louping Ill virus (LIV) antigens induced a robust immune response, giving complete protection following peripheral LIV challenge (Morris-Downes *et al,* 2001b).

1.2.4 SFV vectors and its potential for CNS disease treatments

The SFV vector system has never before been used as a means for delivery into the CNS. There is however a great potential for this system to be used in the treatment of CNS diseases. Extensive research on the neuropathogenesis of SFV has demonstrated that following i.n. infection, the virus follows axonal transport along olfactory tracts from nerve endings in the olfactory mucosa, reaching the CNS via the olfactory bulb (Sammin *et al,* 1999, Sheahan *et al,* 1981, Sheahan *et al,* 1996). With the high levels of heterologous protein expression observed from the rSFV vector system, it is theoretically possible to insert the cloned genes directly into the CNS of animals by the non-invasive i.n. method of delivery. Current research has indicated that high levels of protein expression were indeed detected in the olfactory bulb area of the CNS following i.n. inoculation of rSFV particles expressing a reporter gene. It was further demonstrated that no damage as a result of infection was detected in brains of infected mice, and no vector RNA was measured in areas of the CNS (Jerusalmi *et al,* 2003).

1.3 Multiple Sclerosis

1.3.1 Classification of disease

Multiple sclerosis (MS) is an inflammatory demyelinating disease of the central nervous system of unknown etiology. The most common form of the disease affects young adults between the ages of 20-40 years, leading to significant neurological disability after a period of about 10-15 years. It is believed a number of factors may be involved in the etiology of MS, including immunological, environmental, genetic, and infectious. Worldwide, MS occurs at a greater frequency in higher latitudes, away from the equator (figure 1.6), and it is more common in woman than in man. Ireland is one of the countries with the highest incidence of MS in the world, with an incidence of about 1 in 1000 people.

The exact course of MS in individual patients is uncertain. Even though the disease affects people in a variety of ways, in general, it follows several known patterns. Doctors group four of the patterns together under the heading "chronic progressive MS": Relapsing-remitting MS (RRMS), secondary-progressive MS (SPMS), primary-progressive MS (PPMS) and Progressive-relapsing MS (PRMS). A fifth type is classified as Benign MS.

Benign MS is characterized by mild to moderate symptoms, which do not worsen or lead to permanent disability. It is present in 10 to 15 percent of people with MS. In relapsing-remitting MS, one or two flare-ups of MS occur every 1 to 3 years, followed by periods of remission. The flare-ups typically appear suddenly, last a few weeks or months, and then gradually disappear. Symptoms may accumulate with each recurrence. About 75 percent of people with MS begin with this form, and more than half will have this form of the disease at any one time. In primary progressive MS, deterioration occurs without periods of remission when symptoms first appear. About 15 percent of people with MS begin with this pattern of the disease. After years of relapsing-remitting MS, at least half the people enter a stage of continuous deterioration known as secondary-progressive MS. In it, sudden relapses may occur, superimposed upon the continuous deterioration that has developed. Primary-progressive MS with the addition of sudden episodes of new symptoms or worsened existing ones is characterized as progressive-relapsing MS. This

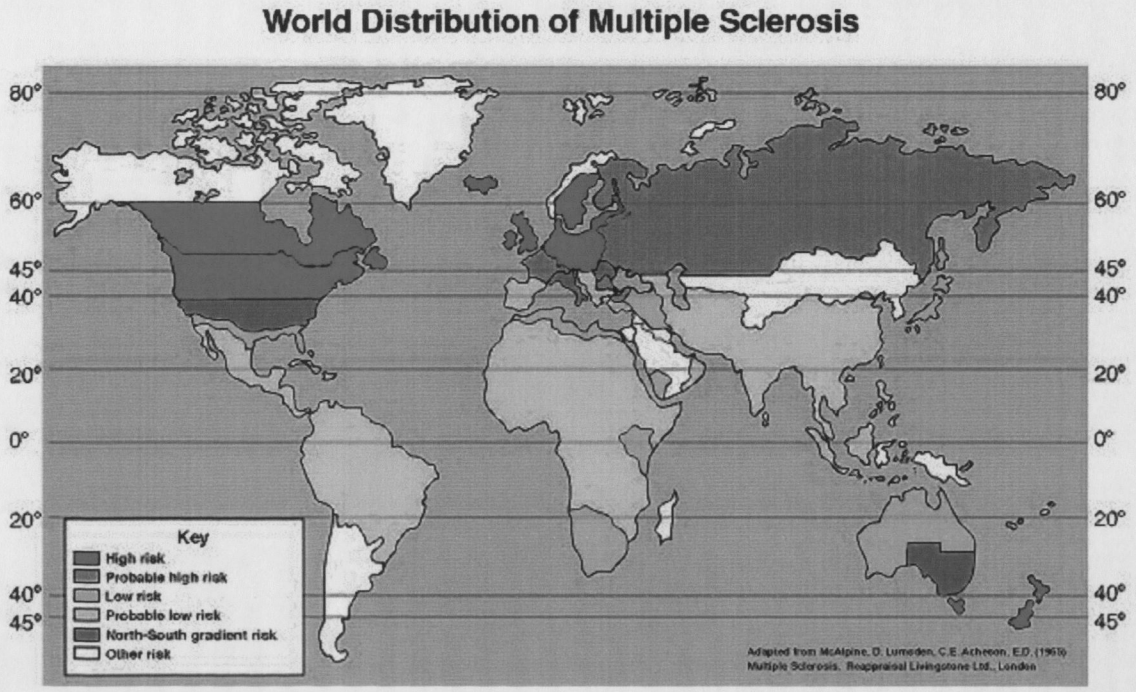

Figure 1.6 World distribution of Multiple Sclerosis

The geographic distribution of MS around the world is very specific. Worldwide, MS occurs with much greater frequency in higher latitudes (above40° latitude) away from the equator, than in lower latitudes, closer to the equator. As seen by the figure, North America, and northern Europe have the highest incidence of MS in the world. Adapted from http://melib.med.utah.edu/kw/ms

form is rare, occurring in approximately 10 percent of people with MS, and behaves in a manner similar to primary progressive MS (figure 1.7).

The necessity for early treatment in MS is becoming increasingly clear. Current MS treatment can be classified into two categories: treatments that address symptom management, and treatments that change the course of the disease by modifying the number and severity of attacks and the progression of disability. There has been a significant progress in both types of treatments in the last decade.

1.3.2 Etiology of disease

The cause of MS is still not known; extensive scientific research indicates that a combination of several factors may be involved. These involve genetic, immunologic, environmental and an infectious agent.

To date, there has been no conclusive evidence that MS is a genetic disease. There are many difficulties in defining the role of genes in MS. There is however evidence that points to a genetic component to the cause of the disease. People with a first-degree relative such as a parent or sibling with MS have an increased risk of developing the disease, compared to the general population. Concordant siblings tend to share age of the onset of symptoms rather then year of onset, suggesting that inherited rather then environmental factors are responsible for familial aggregation (Ebers *et al,* 1995). Common genetic factors have been identified in some families where there is more than one person with MS. Some researchers theorize that MS develops because a person is born with a genetic pre-disposition to react to some environmental agent that, upon exposure, triggers an autoimmune response. Risk for MS is also affected in part by a person's ethnic background and other factors that have not yet been clearly identified. The frequent occurrence of MS in certain ethnic backgrounds (i.e. northern Europeans) compared to others (African and Asian) irrespective of geographic location furthers proves that there is a complex genetic etiology in MS (Oksenberg and Barcellos 2000). The observation that resistant groups reside in high-risk areas, also suggests a genetic resistance (Milanov *et al,* 1999). The identical twin of a person with MS has a 1 in 3 chance of developing the disease (Mumford *et al,* 1994, Sawcer and Goodfellow 1998). The fact that identical twins of people with MS do not contract MS, and that more than 80% of people with MS do not

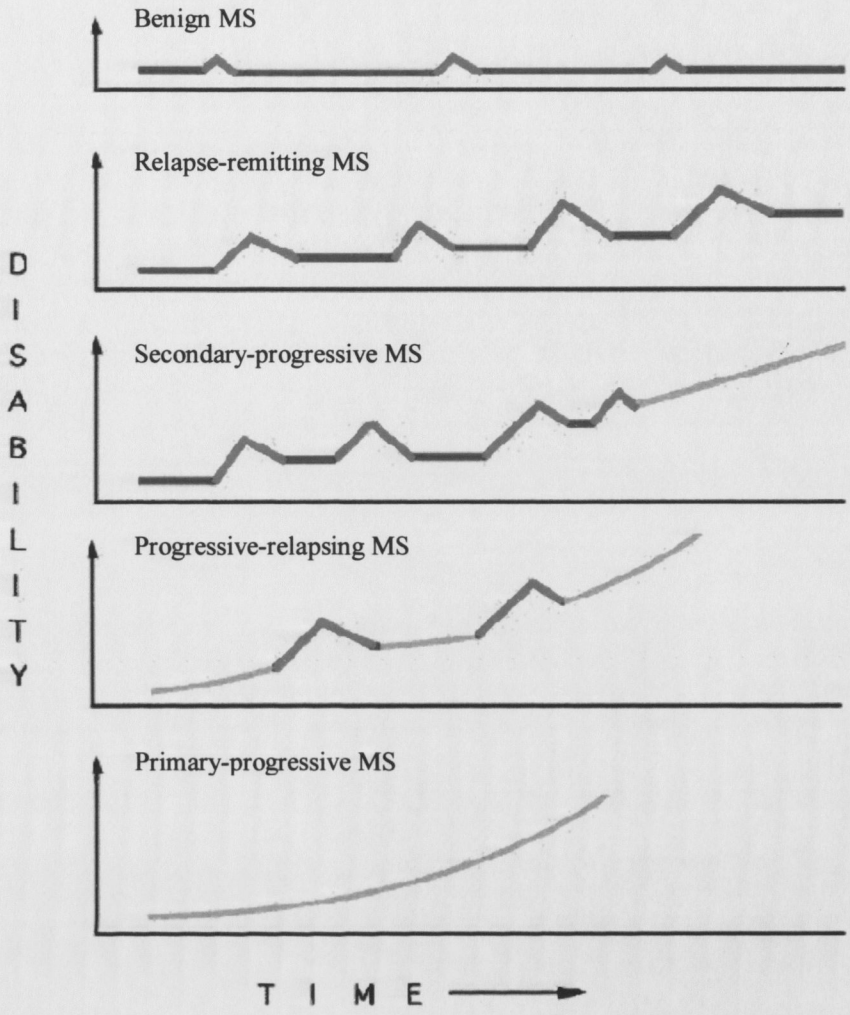

Figure 1.7 Classification of disease progression in MS

The different types of disease progression are described. The blue line represents stable disease; the red line represents a relapse, while the yellow line represents disease progression. In benign MS there are mild infrequent sensory exacerbations with full recovery. In RRMS there are episodes of exacerbations and remissions where not all symptoms resolve completely. Relapses become more severe with time. When the condition worsens with the accumulation of neurological signs and symptoms, it is classified as SPMS. In this form, relapses become more severe while remissions are less complete, shorter in duration, and eventually non-existent. The course of MS becomes steadily progressive. A rare form of MS, PRMS will develop to PPMS with addition of sudden episodes of new symptoms or worsened existing ones. This form is very rare. Finally, in PPMS there is no history of relapse in these patients. Disease begins with a slow progression of neurological deficits, and gradually worsens over time. Adapted from http://melib.med.utah.edu/kw/ms

have a first-degree relative with MS, demonstrates conclusively that MS is not directly inherited and that factors other than genetics must also be involved. It is likely that nutritional, infectious, geographical, and other environmental influences acting on genetically susceptible individuals affect susceptibility.

It is generally accepted that MS involves an autoimmune process directed against the CNS. The exact antigen, or target that the immune cells are sensitized to attack, remains unknown. Traditionally, T_H1 cells recognize components of the myelin sheath and initiate a self-propagating auto-destructive process within the CNS (Wekerle *et al,* 1986). Since T-cells alone are not capable of producing the typically large and confluent demyelinating plaques seen in MS, additional amplification factors are required. Recent research indicated these may vary between patients (Lucchinetti *et al,* 2000). In addition to infiltrating T-cells, elevated levels of CNS immunoglobulin (Ig) are also characteristics of MS (Tourtellotte *et al,* 1980). The oligoclonal nature of this antibody, suggests that it is comprised of a small number of different antibody molecules. The exact mechanism of tissue damage in MS is not known. It has been proposed however, that cytokine products of activated T-cells, macrophages, or astrocytes may contribute to lesion development. TNF-α is present in brain lesions of MS (Hofman *et al,* 1989, Selmaj *et al,* 1991), levels in the cerebrospinal fluid (CSF) parallel MS disease activity (Beck *et al,* 1988, Hauser *et al,* 1990), and inhibitors to TNF-α block acute experimental autoimmune encephalomyelitis (EAE) (Genain *et al,* 1995, Monastra *et al,* 1993, Ruddle *et al,* 1990). The myelin forming protein myelin basic protein (MBP) has also been implicated in MS, where MBP-reactive T-cells exist in the circulation of patients (Jingwu *et al,* 1992, Joshi *et al,* 1993, Martin *et al,* 1992, Zamvil and Steinman 1990). Furthermore, indirect evidence for antibody participation includes the findings of elevated levels of CSF Ig, CSF anti-MBP, and anti-myelin oligodendrocytes glycoprotein (MOG) antibodies (Panitch *et al,* 1980, Warren *et al,* 1994, Xiao *et al,* 1991).

The possible role for environmental factors in the etiology of MS has been demonstrated by the different geographic gradients of disease frequency and changes in prevalence in migrants. A very clear geographic distribution of this disease around the world is demonstrated in figure 1.6. A significantly higher incidence of the disease is found in the northernmost latitudes of the northern and the southern hemispheres compared to southernmost latitudes. This directly correlates with climate, where sun exposure, and temperatures play a key role. Low temperature and a high level of humidity may have

effects on the immune system, or be conducive to frequent respiratory tract infections. The lack of direct sunlight in the winter influences vitamin D levels, which has been suggested by researchers to be protective in MS (Cantorna *et al,* 1996, Embry *et al,* 2000, Issa *et al,* 1998, Nieves *et al,* 1994). Epidemiological and migration studies have shown that if the exposure to a higher risk environment occurs at a young age (before 15 years old), the migrant assumes the higher risk of the environment. Furthermore, natives of areas of high risk who immigrate to areas of lower risk before the age of 15, assume the risk of the new environment (Kurtzke *et al,* 1998, Kurtzke 2000). These data suggest that exposure to some environmental agent that occurs before puberty may predispose a person to develop MS later on in life.

Much controversy has been created over the etiology of MS. Since initial exposure to numerous viruses, bacteria and other microbes occurs during childhood, and since viruses are well recognized as causes of demyelination and inflammation, it is possible that a virus or other infectious agent is the triggering factor in MS (Allen and Brankin 1993, Atkins *et al,* 2000). Numerous viruses and bacteria, including measles virus, canine distemper virus, human herpes virus-6 and *Chlamydia pneumonia* have been or are being investigated to determine if they are involved in the development of MS, with many of these detected in CNS autopsy tissue from MS patients (Christensen *et al,* 1998, Haahr *et al,* 1994, Moore 1997, Waksman and Reingold 1986). No single virus however has been consistently isolated from MS patients. Several studies have proved that viral infections could trigger the clinical attacks in RRMS (Cassetta and Granieri 2000), and the high susceptibility to viral infections in childhood, could contribute to neuroallergic reactions, such as MS at later stages (Wender and Zwyrzykowska-Kierys 1984). One of the most compelling arguments supporting the notion that MS is caused by exogenous antigens is the analysis of an MS epidemic in the Faroe Islands (North Atlantic). MS was completely absent there until World War II when the first cases were described and linked to the arrival of British troops (Kurtzke and Hyllested 1975, Kurtzke *et al,* 1993). There is still insufficient evidence supporting the hypothesis that an infectious agent could cause MS, nonetheless the evidence suggesting that the etiology could be viral is increasing.

No single factor can safely be ascribed as the main cause of MS. However, taken together they suggest that each factor plays an important role in determining the etiology of the disease. A plausible explanation would be that when young people with a genetic

predisposition to MS are exposed to an environmental factor, most likely linked to an infectious agent, there is a high risk of developing MS later on in life.

1.3.3 Epidemiology

There are multiple factors that combine to increase the risk of developing MS. The geographic distribution of MS around the world is very specific. In general MS is a disease of temperate climates. A significantly higher incidence of the disease is found in higher latitudes (above 40° latitude) away from the equator, than in lower latitudes, closer to the equator (Baum and Rothschild 1981). It is also clear from migration studies that individuals, who migrate before the age of 15, acquire the risk of the region to which they migrated, whereas individuals that migrate later in life carry the risk of their geographic origin (Kurtzke 1993, Kurtzke 2000). It has been difficult to assess whether this is due to differences in genetic background or to a variety of exogenous factors. Thus, in all probability these studies suggest that MS is ordinarily acquired in early adolescence with a lengthy latency before the onset of symptoms.

Population studies show the difference in susceptibility to MS between populations of different ethnicity. MS is more common among Caucasians (particularly those of northern European ancestry). Native Americans and Hutterites very infrequently suffer from MS, as opposed to other residents of North America. MS is uncommon in Japan, China and South America. It is rare among the indigenous people of equatorial Africa and among native Inuit in Alaska (Compston 2000, Oksenberg and Barcellos 2000). When the racial differences are correlated, White populations are at greater risk than Asian or African populations. MS is approximately twice as common in females than in males. Onset is typically during early to middle adulthood. Ten percent of cases begin before the age of 18. The mean age on onset for men is slightly later than in woman. There have been certain outbreaks or "clusters" of MS identified, but the cause and significance of these outbreaks is not known. Though no single gene has been identified as a marker for MS, in certain populations, a genetic marker, or trait, has been found to occur more frequently in people with MS than in those who do not have the disease (Baranzini *et al,* 2002, Compston 2000). Research is ongoing to identify the multiple genes that are associated with susceptibility in people to MS.

1.3.4 Symptoms

MS symptoms generally appear in people aged 20 to 40 years, and women are more likely than men to have the disease. Since demyelination can occur in any part of the brain or spinal cord, symptoms depend on the area affected. When it occurs in the nerve pathways that bring signals to muscles, it causes problems with movement (motor symptoms), while demyelination in the nerve pathways that carry sensations to the brain causes disturbances in sensation (sensory symptoms). Common early symptoms are tingling, numbness, or other peculiar feelings in the arms, legs, trunk, or face. A person may lose strength or dexterity in a leg or a hand. Some people develop symptoms in the eyes only and may experience double vision, partial blindness and pain in one eye, dim or blurred vision, or loss of central vision (optic neuritis). Early symptoms may include mild emotional or intellectual changes. These vague indications of demyelination in the brain sometimes begin long before the disease is recognized. Multiple sclerosis follows a varied and unpredictable course. In many people, the disease starts with an isolated symptom, followed by months or years without further symptoms. In others, symptoms become worse and more generalized within weeks or months. A relapse of the disease can occur spontaneously or can be triggered by an infection such as influenza. As relapses become more frequent, disability worsens and may become permanent.

1.3.5 Diagnosis

The possibility of the disease should be considered in younger people who suddenly develop blurred vision, double vision, or motor and sensory abnormalities in different parts of the body. A pattern of relapses and recoveries can strengthen the diagnosis. If MS is suspected, a thorough evaluation of the nervous system is carried out. There is no single diagnostic test. The diagnosis of MS is a clinical diagnosis based on dissemination of lesions in time (based on clinical history and clinical examination) and dissemination of lesions in space (as adjudged by Magnetic Resonance Imaging). Para-clinical tests such as examination of CSF and visual and auditory evoked responses can be of assistance in making the diagnosis.

1.3.6 Current treatments

MS treatment is as complex as the disease. To date, no single cure exists, rather numerous drugs and therapies are used to treat many symptoms of the disease. Recent studies suggest that earlier treatments lead to a lesser damage to the CNS, as well as a slower disease progression. The following drug therapies and treatment options are currently in use:

Five disease-modifying drugs are currently in use. Four are used for treating RRMS. These include interferon beta 1-a (Avonex (Biogen Inc), and Rebif (Serono biotech & beyond)), interferon beta 1-b (Betaseron (Berlex Inc)) and glatiramer acetate (Copaxone (Teva Pharmaceutical Industries Ltd.)), which reduce the number and severity of attacks, and in some cases slow the onset of disability. Betaseron, Rebif and Copaxone are injected into the skin, and Avonex into the muscle. Interferon beta is a cytokine that mediates antiviral, antiproliferative and immunomodulatory activities in response to viral infection and other biological inducers. In some clinical trials on MS patients, IL-10 levels in CSF were higher in patients treated with interferon beta. Glatiramer acetate is a synthetic compound made from substances found in myelin. It is not clearly understood how it helps in MS, but it seems to act by modifying immune processes that are currently believed to be responsible for the pathogenesis of MS. All of these are known to have side effects. Novantrone (Serono biotech & beyond) (mitoxantrone) is used for the treatment of SPMS, PRMS, and RRMS. This drug, administered intravenously, was originally developed as an anti-cancer agent. Since it also seems to decrease the relapses, and slow the progression of disability, it is used in MS. *In vitro* it was shown to inhibit B-cell, T-cell, and macrophage proliferation and impair antigen presentation, as well as the secretion of interferon gamma, TNF-α, and IL-2 (Burns *et al,* 1988, Fidler *et al,* 1986a, Fidler *et al,* 1986b, Wang *et al,* 1986). This drug has many potential serious side effects, since it promotes the suppression of the immune system.

Steroids are still used to reduce inflammation caused by MS, and manage acute attacks of the disease. High doses of the steroid can be administered intravenously, however they have serious side effects. More commonly prescribed steroids include dexamethasone (Decadron) (De Keyser *et al,* 1999), methylprednisolone (Solu-Medrol) (La Mantia *et al,* 1994, Martinez-Caceres *et al,* 2002, Newman *et al,* 1982, van de Wyngaert *et al,* 2001), and prednisone (Deltasone) (Losy *et al,* 1994, Wender *et al,* 1999).

A treatment known as plasmapheresis (plasma exchange) is used for patients that do not respond well to steroids treatment. This involves replacing the plasma from blood of MS patients with another fluid. This leads to removal of antibodies that may attack myelin. Plasma free blood is then transfused into patients. Mixed success has been achieved with this form of treatment (Dau 1991, McLeod 2003, McQuillen 1991).

1.4 Experimental Autoimmune Encephalomyelitis

1.4.1 Classification of disease

Experimental Autoimmune Encephalomyelitis, also called Experimental Allergic Encephalomyelitis, is an animal model of the human disease MS. First observed in 1933 when it was confirmed that immunization of experimental animals with myelinated tissue regularly led to what is now called EAE (Hurst 1932, Rivers *et al,* 1933). The original method was very long and tedious, and in 1947 it was shown that the use of Freud's adjuvant resulted in rapid development of the disease in a high proportion of injected animals (Kabat *et al,* 1947, Morgan 1947). In 1954 and 1956 it was shown that the myelin proteins MBP and proteolipid protein (PLP) could also induce EAE (Kies *et al,* 1956, Waksman *et al,* 1954). To date, EAE has been the subject of numerous scientific papers in the 70 years since its discovery. Like MS, EAE is not a single disease in a single species, but its different forms resemble the various forms and stages of MS. EAE is a T-cell mediated acute or chronic-relapsing, acquired, inflammatory and demyelinating autoimmune disease of the CNS (Gold *et al,* 2000, Zamvil and Steinman 1990). It is mediated by myelin-reactive CD4+ T-cells, expressing a T_H1 phenotype that produces pro-inflammatory cytokines such as TNF-β and IFN-γ (Hohlfeld 1997). The disease is characterized by a pleomorphic cellular infiltrate within the CNS with varying degrees of demyelination, generating characteristic paralyses displaying graduation from reduced tail tone to pelvic limb paralysis (Heber-Katz 1995). Cytokines produced by T_H2 cells such as IL-10 and TGF-β have been associated with the spontaneous recovery from EAE (Issazadeh *et al,* 1995, Kennedy *et al,* 1992). To induce the disease, animals are immunized with the whole or parts of various proteins that make up myelin. These proteins induce an autoimmune response in the animals, where the immune system mounts

an attack on its own myelin as a result of exposure to the protein. The animals develop a disease process that resembles MS in humans. Several proteins or parts of proteins can be used to induce EAE, including: MBP, PLP, MOG, and spinal cord homogenate (SCH). To date, EAE has been induced in a number of different animal species including mice, rats, guinea pigs, rabbits, macaques, rhesus monkeys and marmosets. For various reasons, including the number of immunological tools, the availability and lifespan of the animals and the resemblance of the induced disease to MS, mice and rats are the most commonly used species. Not all mice or rats have a natural propensity to acquire EAE. Moreover, different breeds will develop different forms of the disease.

The main disadvantage in working with EAE is that the disease is not an exact copy of MS; therefore, a number of significant assumptions have to be made when proposing EAE as an animal model for MS. Another factor to take into consideration is the ethics involved. When animals are given EAE, it is undeniable that the animals involved undergo a considerable amount of suffering.

1.4.2 Current treatments

A number of different treatments for EAE are currently underway. These vary greatly in nature. Some involve use of cytokines, cytokine receptors, peptides, fatty acids, and synthetic compounds among others. The mode of delivery also varies between each treatment, involving peripheral administrations, oral, nasal, as well as more traumatic inoculations such as intra-cerebral (i.c.). It keeping with the context of the study, only treatments with the same cytokines as used in this project will be discussed (IL-4, IL-10, and TGF-β). A more in-depth description of each cytokine is presented in section 1.6

1.4.2.1 EAE treatment with IL-10

IL-10 has been widely used in attempts to treat EAE. Studies have shown that animals which spontaneously recover from EAE correlate with an expansion of T_H2 cells producing IL-10 (as well as IL-4) (Kennedy *et al,* 1992, Khoury *et al,* 1992). Furthermore, low IL-10 levels have been detected in animals with chronic relapsing EAE (Issazadeh *et*

al, 1996). Both findings strongly suggest IL-10 plays a key role in prevention and recovery of EAE. Studies on IL-10-deficient as well as transgenic mice greatly supported the findings. It was demonstrated that IL-10 deficient mice develop a more severe EAE compared to wild type mice (genetically matched), and that mice transgenic for IL-10 are completely resistant to EAE (Bettelli *et al,* 1998, Cua *et al,* 1999, Samoilova *et al,* 1998).

The use of recombinant IL-10 to treat EAE has yielded contradictory results. The most effective results came from systemic delivery of IL-10 to the CNS. It was demonstrated that i.c delivery of IL-10 by a replication-deficient adenovirus was effective in suppressing EAE when delivered 2-3 days before the onset of disease (Cua *et al,* 2001). The amount of IL-10, as well as the mode in which it is delivered also plays a role in the outcome of EAE. Croxford et al demonstrated this by comparing the outcomes of IL-10 delivered i.c. by three different modes. IL-10 was delivered by a single injection of retrovirus-immortalized fibroblasts producing IL-10 (IL-10.tsf), adenovirus coding for IL-10, and the protein alone at day 12 post induction of EAE. From all treatments, only animals given IL-10.tsf showed a statistical amelioration of EAE. This is possibly due to the ability of the immortalized cells to produce IL-10 for a much longer time period compared to viral or direct protein delivery (Croxford *et al,* 2001). A much lower dose of IL-10 delivered by the adenovirus in the above study could explain the difference in outcomes between the two. Studies on i.n delivery of IL-10 protein showed that when delivered in multiple doses following disease induction, it was effective in disease suppression (Xiao *et al,* 1998). Furthermore, IL-10 given both orally and i.n. in conjunction with MOG and/or MBP antigens, produced an enhanced tolerance to EAE (Slavin *et al,* 2001). When EAE was treated i.n. with a rSFV vector expressing IL-10 similar results were obtained. When multiple administrations of the vector were delivered, there was an inhibition of EAE; however when lower amounts were given, the treatment yielded no significant results (Jerusalmi *et al,* 2003). There has been a number of other studies where IL-10 has shown to ameliorate or completely suppress the course of EAE (Nagelkerken *et al,* 1997, Rott *et al,* 1994, Xu *et al,* 2000b, Young *et al,* 2000), while other studies showed the opposite effect (Cannella *et al,* 1996, Croxford *et al,* 1998). Given the results, it seems that the amount of IL-10 delivered, the location, as well as time of delivery have a profound effect in disease outcome.

1.4.2.2 EAE treatment with IL-4

Similarly to IL-10, IL-4 has been used in a wide range of EAE studies, and just like IL-10, results have been ambiguous. A more severe clinical outcome of EAE is observed in IL-4 knockout mice compared to wild-type mice (genetically matched). Furthermore, increased perivascular inflammation and demyelination of the CNS was detected in addition to higher levels of T_H1 cytokines (IFN-γ, IL-1, TNF) in the spinal cord tissue (Bettelli *et al,* 1998, Falcone *et al,* 1998). In contrast to data from IL-10 transgene mice, IL-4 transgenic mice develop a similar disease compared to their non-transgenic littermates (Bettelli *et al,* 1998).

Studies on EAE treatment with IL-4 have yielded a variety of results. The delivery of IL-4 by a non-replicative herpes simplex virus by an i.c. route, was effective in suppressing EAE. This was demonstrated in two studies, where the administration date varied. One study involved treating mice induced for EAE before the appearance of the disease (days 0 and 7 post-immunization), while the other involved treating mice at the time of appearance of first EAE symptoms. In both cases, severity of EAE was lower, and so was the number of inflammatory infiltrates (Martino *et al,* 1998, Martino *et al,* 2000a). Other studies utilizing the same vector have had similar results (Furlan *et al,* 1998). The combined nasal or oral administrations of IL-4 and MBP have also been effective in ameliorating the course and severity of EAE (Inobe *et al,* 1998, Xu *et al,* 2000a). This effect however was not observed when the protein only was administered, without addition of MBP. IL-4 has also been shown to stimulate increased levels of TGF-β, thus, having a positive effect on the outcome of EAE (Inobe *et al,* 1998, Inobe *et al,* 1996). In contrast, IL-4 has been shown to inhibit the effects of IL-10 and increase the severity of EAE (Nagelkerken *et al,* 1997). IL-4 clearly plays a role in EAE recovery. Similar to IL-10, the timing and mode of delivery is a key factor in determining the outcome of treatment.

1.4.2.3 TGF-β treatment of EAE

TGF-β has been shown in a wide number of studies to successfully treat EAE. It was demonstrated that peripheral treatment of EAE with TGF-β has a significant effect on inhibiting the proliferative response of reactive T-cells, preventing the development of

EAE, or reducing the severity of the disease. This is further supported by the presence of this molecule in the inflammatory areas of the brain and spinal cord during the course of EAE (Cautain *et al,* 2001, Johns *et al,* 1991, Kuruvilla *et al,* 1991, Racke *et al,* 1991, Racke *et al,* 1992). The protective effect of TGF-β in EAE was based on in vitro study where TGF-β inhibited the adoptive transfer of EAE by preventing activation and proliferation of encephalitogenic precursors (Racke *et al,* 1991). Further evidence for the involvement of TGF-β in EAE recovery has been demonstrated in experiments where administration of anti-TGF-β increased severity of EAE (Johns and Sriram 1993, Racke *et al,* 1992, Santambrogio *et al,* 1993). A proposed mechanism for the protective effects of TGF-β on EAE was suggested, where TGF-β protects against EAE by antagonizing the production and effects of TNF. This leads to an interference in the entry of lymphoid cells into the CNS, as well as interference in subsequent inflammatory processes inside the CNS (Cautain *et al,* 2001, Santambrogio *et al,* 1993). It has been further demonstrated that TGF-β can prevent the incidence of relapses in EAE mice (Kuruvilla *et al,* 1991).

1.5 The central nervous system

1.5.1 Cells of the central nervous system

Two major classes of cells compose the central nervous system; neurons, specialized for communication, and supporting cells known as neuroglia. Neurons are among the most ancient of all specialized animal cell types. Due to their ability to send and receive signals, they are responsible for most of the functional characteristics of the nervous tissue. Neurons are mainly composed of a cell body, where the nucleus is located, dendrites and a single axon. Dendrites are short branching processes that receive signals from other neurons. Each neuron contains several dendrites branching in many directions. A single axon of varying length conducts impulses away from the cell body. The diameter of an axon is uniform throughout its length, and it is usually surrounded by a myelin sheath, laid by oligodendrocytes. It consists of many layers of plasma membrane (lipoprotein composition), and begins near the origin of the axon, and ends short of its terminal branching. Interruptions along the length of the myelin are known as nodes of Ranvier, and indicate points where regions formed by different oligodendrocytes adjoin.

The function of the myelin sheath is to insulate the axon between the nodes of Ranvier allowing for conduction of nerve impulses. The area between the end of an axon and beginning of a dendrite is known as a synapse. It is there that impulses are transmitted from one neuron to another. Axonal transport involves the transport of proteins distally within axons; however the mechanisms of which are not fully understood. There are a few neurons in the body with no axons where dendrites act in both directions, both sending and receiving impulses. The shape and size of neurons are dependent on their structural function.

Neuroglial cells have important ancillary functions, and are further divided into astrocytes, oligodendrocytes, ependymal cells and microglia. Astrocytes are the most common cellular elements in the brain, outnumbering neurons about 10 to 1. Astrocytes are active and dynamic cells, involved in many aspects of the central nervous system functions. They are variable cells with deep indentations having moderately dispersed chromatin, and numerous processes. They do not represent a uniform population of cells, in that cell properties from one brain region differ from those of other regions. Astrocytes are interconnected to each other via gap junctions allowing for ionic and metabolic coupling (Dermietzel *et al,* 1991, Fisher and Kettenmann 1985, Massa and Mugnaini 1982, Nedergaard *et al,* 1995), which is responsible for long distance communication and functional responses in areas of the brain distant from primary site (Cornell-Bell *et al,* 1990, Dani *et al,* 1992). They contain receptors to most neurotransmitters and neuropeptides (Kimelberg 1988, Murphy and Pearce 1987), in addition to secondary messenger signals that provide key intracellular communication with neurons. There is much evidence indicating astrocytes represent dynamic cells possessing a high rate of metabolic activity and pleiotropic functions responsible for the regulation of the CNS microenvironment. Furthermore, they fill spaces among neurons and their processes, and due to the rigidity of filaments found in astrocytes, there is a possibility they provide physical support for other cellular elements in the nervous system. They might also be involved in phagocytosis of myelin debris in MS, as demonstrated in EAE where reactive astrocytes are a prominent histopathological feature (Cammer *et al,* 1990, Goldmuntz *et al,* 1986), besides having a high degree of proliferation (Smith *et al,* 1987). Astrocytes are involved in immune/inflammatory phenomena, and have a significant cooperation with cells of the immune system. They are immunocompetent cells, which have an important role in augmenting the immune system, and are among the first cells to respond to CNS

injury. Gliosis, characterized by the presence of reactive astrocytes is the best-recognized cellular response to CNS injury. Cytokines such as IL-1, IFN-γ and TNF are among the factors involved in the production of reactive astrocytes (Barna *et al,* 1990, Giulian and Lachman 1985, Yong *et al,* 1991). Other growth factors (EGF, PDGF, and FGF) have also been implicated in production of reactive astrocytes in response to injury (Besnard *et al,* 1987, Leutz and Schachner 1981, Perraud *et al,* 1988). Astrocyte swelling following CNS injury occurs very rapidly, as described in EAE (Eng *et al,* 1989, Goldmuntz *et al,* 1986). This swelling may eventually lead to production of increased intracranial pressure and brain stem dysfunction. Glutamate is also released by swollen astrocytes, which may lead to excitotoxic injury (Kimelberg *et al,* 1990).

Oligodendrocytes occur in rows among myelinated axons in the CNS. Their cytoplasmic processes form and remain continuous with the myelin sheaths. Each oligodendrocyte cell is connected to several myelinated nerve fibers. It is responsible for production and maintenance of myelin sheaths of axons in the CNS, where one cytoplasmic process provides myelin for one internode of an axon. They wrap layer upon layer of their own plasma membrane in a tight spiral around the axon, thereby insulating the axonal membrane so no current leaks across it. Schwann cells are the counterparts of oligodendrocytes in the peripheral nervous system (PNS). They are able to invade the CNS in order to regenerate new myelin sheaths around demyelinated axons (Ross and Romrell 1989); but, only in the absence of astrocytes (Graca *et al,* 2001).

Microglia are characterized by highly specialized morphology, and compose 5% of the neuroglial population. Resting microglial cells are found in both white and gray matter, and are evenly spread in the tissue, with very little overlapping of their processes. Resting microglial cells are equivalent to resident macrophages of other tissues, and they can acquire phagocytic properties in response to a variety of stimuli (Duchen 1984, Rao and Lund 1989, Streit *et al,* 1988). As a result, they may be involved in protection from viruses, microorganisms, or even the formation of tumors.

1.5.2 Myelin biogenesis

1.5.2.1 Myelin formation

Myelin is formed by oligodendrocytes in the CNS, and by Schwann cells in the PNS. Because oligodendrocytes are multi-processed cells, a single one is capable of myelinating segments of many axons, while an individual Schwann cell forms a myelin sheath around only one PNS axon. Oligodendrocyte cells wrap layer upon layer of their own plasma membrane concentrically around an axon to form a segment of myelin sheath about 1 mm long. Lipoprotein added to the central part of oligodendrocytes diffuses laterally within the plasmalemma and is quickly incorporated into the whole surface of the cell (including myelin sheath of all internodes associated with oligodendrocytes), causing the myelin to enlarge. Consequently, myelin is composed mainly of lipoprotein. The myelin begins near the origin of an axon and terminates just short of its terminal branching. The myelin sheath is interrupted at regularly spaced regions called nodes of Ranvier (Rumbsy 1978, Williams and Deber 1993). In the nodes, voltage-gated sodium channels are present, and ionic movements of impulse conduction occur. The myelin sheath insulates axons between the nodes and allows for an almost instantaneous conduction of an action potential from one node to the next. The thickness of the myelin sheath and distance between nodes is directly dependent on the axon's diameter and length. Thicker nerve fibers allows for a faster conduction of nerve impulse (figure 1.8).

1.5.2.2 Myelin protein autoantigens

Several proteins have emerged as prominent autoantigens in autoimmune diseases of the CNS, including many myelin proteins (figure 1.9). Myelin-associated glycoprotein (MAG) is produced by myelin-forming oligodendrocytes and Schwann cells, and located in the CNS and in higher abundance in the PNS. More specifically, it is located in the periaxonal membrane of developing myelin, absent from the compact myelin (Quarles 1989). A member of the immunoglobulin gene super family, it contains a cytoplasmic domain, a transmembrane domain, and 5 heavily glycosylated extracellular immunoglobulin-like domains (Salzer *et al,* 1987). Furthermore, it shares immunological

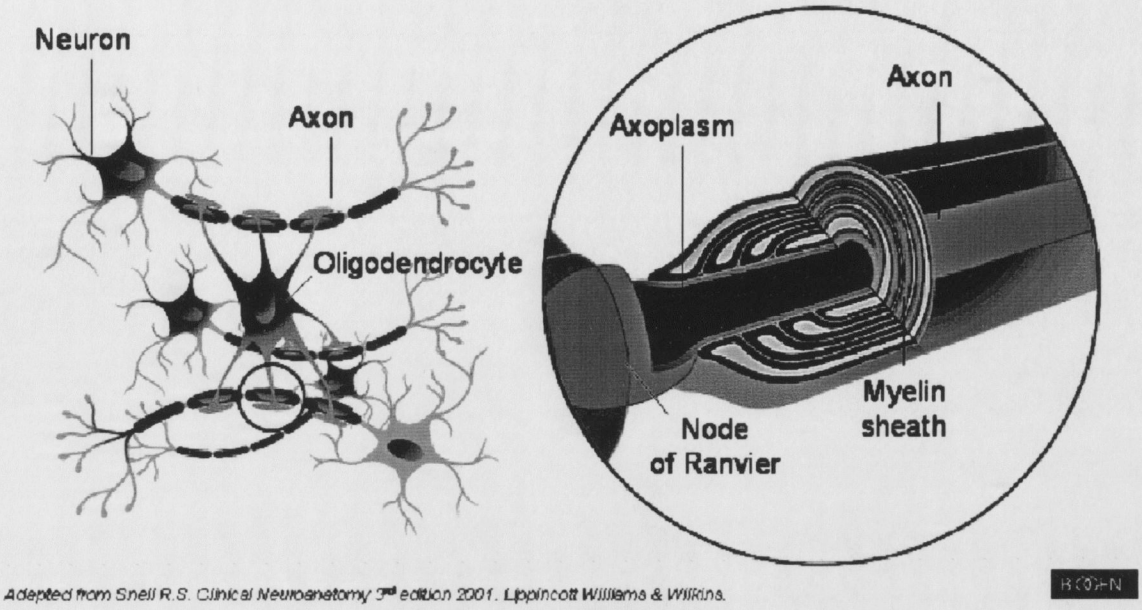

Figure 1.8 Myelin formation by oligodendrocytes

Oligodendrocytes occur in rows among myelinated axons in the CNS. Their cytoplasmic processes form and remain continuous with the myelin sheaths. Each oligodendrocyte cell is connected to several myelinated nerve fibers. They wrap layer upon layer of their own plasma membrane concentrically around an axon to form a segment of myelin sheath about 1 mm long. The myelin begins near the origin of an axon and terminates just short of its terminal branching, with regularly interrupted spaces known as nodes of Ranvier. The myelin sheath insulates the axonal membrane so no current leaks across it, allowing for an almost instantaneous conduction of an action potential from one node to the next. The thickness of the myelin sheath and distance between nodes is directly dependent on the axon's diameter and length. Adapted from Snell R.S. Clinical Neuroanatomy 3rd edition 2001. Lippincott Williams & Wilkins

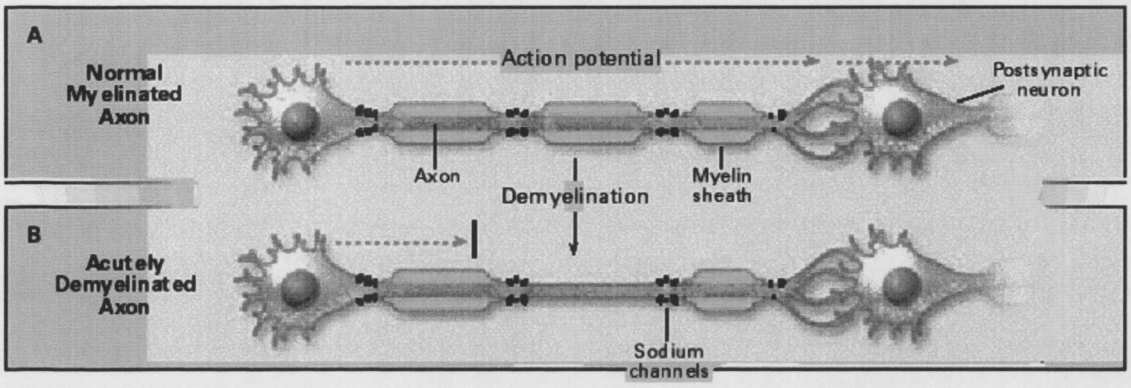

Figure 1.9 Demyelination

In a normal myelinated axon, nerve impulses or action potential travels from one node of Ranvier to the next, where voltage-gated sodium channels are present. The myelin sheath insulates axons between the nodes and allows for an almost instantaneous conduction of an action potential from one node to the next. In a demyelinated axon, there is a partial or full destruction of this myelin sheath. A partial destruction leads to a slower transfer of nerve impulses between axons, while in acute demyelinated axons, there is no myelin left, leading to an interruption of this action potential, stopping communication between axons. Adapted from http://www.albany.net/~tjc/myelin-axon

epitopes with natural killer cells (NK) (Kruse *et al,* 1984). MAG has been implicated in the pathogenesis of MS; however, with an unclear role. It was found to be one of the earliest myelin proteins lost at the lesion margin, on studies conducted on acute MS plaques (Itoyama *et al,* 1980). Further studies have found small but significant MAG antibody response in the CSF of MS patients versus controls (Moller *et al,* 1989), as well as B-cells producing antibodies against MAG (Baig *et al,* 1991). In addition, T-cells producing IFN-γ have also been identified in response to MAG (Link *et al,* 1992).

Myelin basic protein is an abundant protein found in the myelin sheath of the CNS and PNS myelin. It is associated with the cytoplasmic side of the oligodendrocyte membrane (Omlin *et al,* 1982). The compaction of the CNS myelin by adjoining opposing membrane structures may be a result of the interaction of the negative phospholipids in the myelin with the highly cationic protein MBP (Lees and Brostoff 1984). Similar isoforms compose human MBP, while rodent MBP is composed of several isoforms (Barbarese *et al,* 1978, Kamholz *et al,* 1988). Since expression of isoforms is tightly regulated, it is postulated that they each have different functions (Barbarese *et al,* 1978). Its role in EAE has been well documented, and the encephalogenic epitope has been defined in many different laboratory animals.

Proteolipid protein is an extrinsic membrane protein of high abundance comprising 50% of the total protein in the CNS myelin. It does not appear until later in the developing human brain (Kronquist *et al,* 1987). It is conserved between species, and exists in multiple forms containing very strong hydrophobic domains (Kronquist *et al,* 1987, Macklin *et al,* 1987, Nave *et al,* 1987). It is effective in inducing EAE, and has been implicated in the pathogenesis of MS. The specific role in MS has not been identified, though PLP specific T-cell lines have been isolated from MS patients (Trotter *et al,* 1991). Furthermore, in MS T-cells produce IFN-γ and B-cells produce antibodies in response to PLP (Sun *et al,* 1991b, Trotter *et al,* 1991).

Myelin oligodendrocyte glycoprotein is found on the extracellular surface of myelin and oligodendrocytes in the CNS (Brunner *et al,* 1989, Linington *et al,* 1988). Quantitatively, compared to other myelin proteins, MOG is classified as a minor myelin protein (Lebar *et al,* 1986, Linington *et al,* 1984). It is suggested that MOG plays a role in myelin completion and maintenance, since its expression lags behind MBP during myelination (Matthieu and Amiguet 1990, Scolding *et al,* 1989). MOG may play an important role in autoimmunity as a target of antibody mediated demyelination. *In vitro*, it

was shown that antibodies directed against MOG either directly induce demyelination of brain cell culture (Honegger *et al,* 1989), or that it induces macrophages to phagocytize oligodendrocytes (Scolding and Compston 1991). Experimental models showed that treatment with monoclonal antibodies to MOG augmented EAE (Linington *et al,* 1988, Schluesener *et al,* 1987). It may play a role as an autoantigen in MS, since B-cells producing antibodies to MOG, and MOG-reactive T-cells were found in patients, but rarely in controls (Sun *et al,* 1991a). Furthermore, it appears that these cells had been sequestered to the CNS, since they were found in more abundance in the CSF compared to the blood. Unlike MBP-reactive cells, which were found in both MS and normal patients, MOG-reactive cells are rarely found in controls (Pette *et al,* 1990).

1.5.3 Mouse olfactory bulb

The olfactory bulb lies immediately behind the perforated cribiform bony plate that separates the nasal cavity and cranial cavities (figure 1.10). The nasal cavity is covered by the olfactory epithelium, and olfactory receptors are neuroepithelial cells combining the functional characteristics of a peripheral receptor and sensory neurons. These receptors are bipolar neurons possessing a unique dendrite extending among supporting cells to the nasal surface ending as a small olfactory vesicle. To reach the main olfactory bulb, each olfactory receptor cell emits a single unmyelinated axon, which joins others forming fascicles that pass the foramina and engulf the entire non-peduncular surface of the main olfactory bulb, forming the fibrous outer layer. They terminate in the glomeruli layer of the olfactory bulb, and establish synaptic contacts with mitral and tufted cells, which are the only output cells of the main olfactory bulb.

1.5.3.1 Layers of the main olfactory bulb

The first processing station of the olfactory pathway, the main olfactory bulb, has a typical cortical appearance with its cellular elements arranged in a tangential and radial fashion. From its surface to the ependymal zone, six well-defined layers can be distinguished. The outermost nerve layer is formed by fascicles of olfactory nerve. This

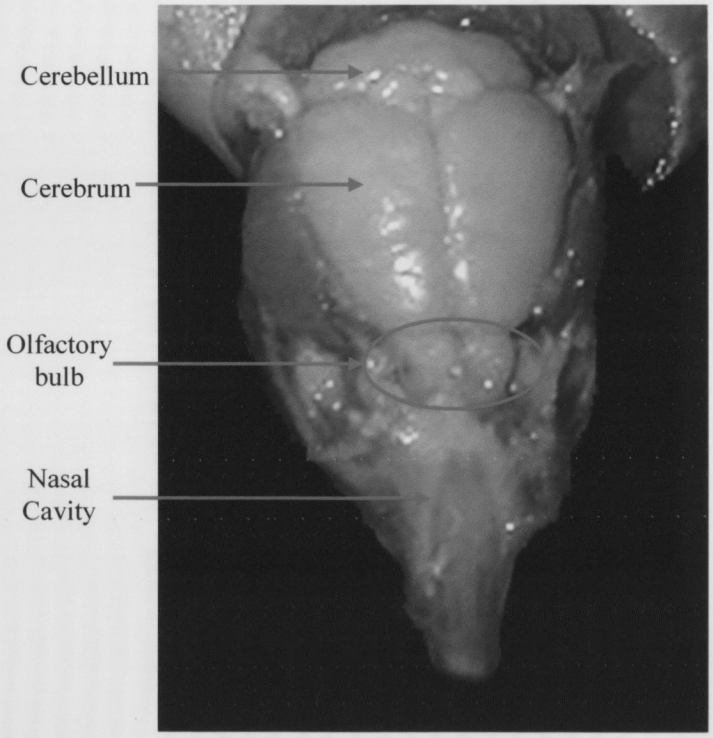

Figure 1.10 Location of olfactory bulb in mouse skull

The olfactory bulb lies immediately behind the perforated cribiform bony plate that separates the nasal cavity and cranial cavities. The nasal cavity is covered by the olfactory epithelium, and olfactory receptors are neuroepithelial cells.

layer forms a dense plexus around the bulb. The glomeruli layer, where incoming olfactory nerve fibers form synaptic contact with dendrites of mitral and tufted cells is composed of one or two rows of spheric acellular islands surrounded by numerous interneurons. The next layer, the external plexiform, consists of tufted cells and a dense dendritic plexus. Next, the mitral cells layer consists of mitral cells embedded in a dense matrix of granule cells. A dense plexus of myelinated fibers is found in the thin internal plexiform layer, and finally the internal granule cell layer contains numerous clusters of small granule cells. These layers can be easily distinguished in Nissl stained sections as described in figure 1.11.

1.5.3.2 Cells of the main olfactory bulb

Four types of cells compose the olfactory bulb. They can be further classified as main projection, or intrinsic neurons. The main projection neurons are the mitral and tufted cells, while periglomerular and internal granular cells compose the intrinsic neurons. Mitral cells compose the main source of olfactory bulb projection fibers. Primary apical dendrites proceed straight through the external plexiform layer to reach single glomeruli where it branches extensively, while several secondary dendrites stand horizontally in the external plexiform layer (Orona *et al,* 1984). Their axons proceed to deeper layers to form merging bundles on the lateral olfactory tract projecting to various olfactory areas of the forebrain (Kishi *et al,* 1984, Shepherd 1972). Similar to mitral cells, tufted cells send their axons into the olfactory tracts. These cells form a heterogeneous group of neurons that also project their axons to olfactory areas of the forebrain (Haberly and Price 1977, Macrides and Schneider 1982, Scott 1981). The intrinsic neurons forming a dense population of cells around the glomeruli layer are known as periglomerular cells. The internal granular layer is composed of intrinsic cells known as internal granular cells. Their dendrites extend radially towards the surface of the main olfactory bulb as well as inwards. They receive intrinsic input from mitral and tufted cells in synapses in the external plexiform layer, and their extrinsic axons contact both peripheral and central dendrite processes of the internal granular cells (Price and Powell 1970a, Price and Powell 1970b).

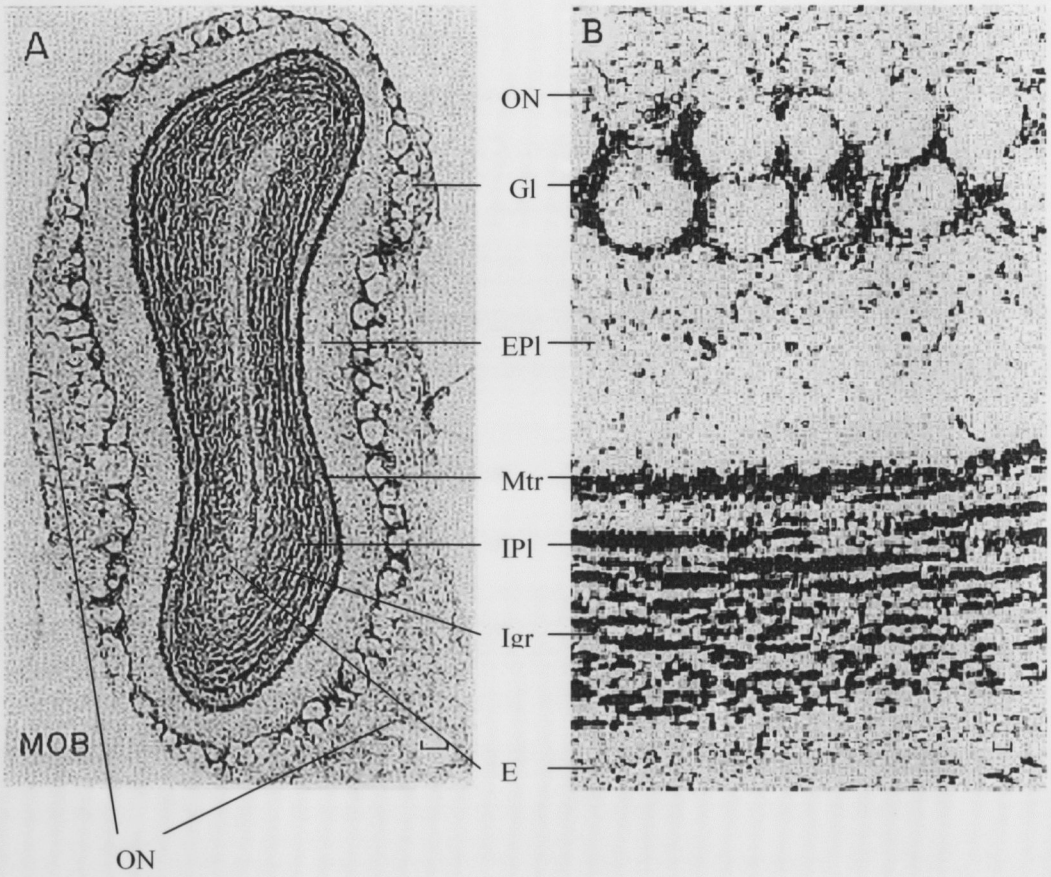

Figure 1.11 Layers of the main olfactory bulb

The main olfactory bulb has its cellular elements organized in a tangential and radial fashion. Seven layers can be distinguished in a Nissl stained section. **(A)** Low magnification of a coronal section through the main olfactory bulb. The outermost olfactory nerve layer (ON) engulfs the entire bulb, and contains the incoming axons from receptor cells in olfactory epithelium, which in turn terminate in the round acellular glomeruli. **(B)** An enlarged portion of the olfactory bulb showing all layers in detail. Gl, glomeruli layer; EPl, external plexiform layer; Mtr, mitral cell layer; IPl, internal plexiform layer; Igr, internal granule cell layer; E, ependymal layer (adapted from Switzer *et al,* 1985)

1.6 Cytokines in CNS disease treatments

A number of cytokines and cytokine receptors are currently being studied for their effect as CNS disease treatments. Cytokines are soluble regulatory proteins or glycoproteins of low molecular weight secreted by cells in response to a number of inducing stimuli. They normally function as intercellular messenger molecules that evoke particular biological activities after binding to receptors on target cells. Macrophages and T_H cells are the two main cell types to secrete cytokines. Once released, cytokines can activate an entire network of interacting cells. Each individual cytokine is a very potent molecule that can cause changes in cell proliferation, differentiation, and movement at nano to picomolar concentrations. The fact that cytokines are secreted proteins also means that the site of their expression does not necessarily predict the sites at which they exert their biological function. Many cytokines show stimulating or inhibitory activities and may synergize or antagonize the actions of other factors. A single cytokine may elicit reactions under certain circumstances, which are the reverse of those shown under other circumstances. The type, duration, and extent of cellular activities induced by a particular cytokine can be influenced considerably by the micro-environment of a cell, the type of neighboring cells, cytokine concentrations, the combination of other cytokines present at the same time, and even on the temporal sequence of several cytokines acting on the same cell. Under such circumstances combinatorial effects allow a single cytokine to transmit diverse signals to different subsets of cells. Almost all cytokines are pleiotropic effectors showing multiple biological activities. In addition, multiple cytokines often have overlapping activities and a single cell frequently interacts with multiple cytokines with seemingly identical responses. One of the consequences of this functional overlap is the observation that one factor may frequently functionally replace another factor altogether or at least partially compensate for the lack of another factor. Since most cytokines have ubiquitous biological activities, their significance as normal regulators of physiology is often difficult to assess.

The term type-1 cytokines refers to cytokines produced by T_H1 T-helper cells while type-2 cytokines are those produced by T_H2 T-helper cells. Due to the inflammatory nature of MS, anti-inflammatory cytokines produced mainly by T_H2 cells are the most commonly used in such treatments. The three such cytokines employed in the current research are IL-10, IL-4 and TGF-β.

IL-10 is secreted by T_H2 subsets of CD4+ T-cells. It blocks cytokine production of both T-cells and NK cells by inhibiting accessory cells (macrophage and monocyte) function. It further inhibits a broad spectrum of activated macrophage and monocyte functions, including monokine synthesis, and expression of MHC class II and co-stimulatory molecules (de Waal Malefyt *et al,* 1991, Ding and Shevach 1992, Fiorentino *et al,* 1991). Of crucial importance to the anti-inflammatory activity of IL-10, are its inhibitory effects on IL-1 and TNF production, since these have a synergistic activity on inflammatory pathways and tend to amplify their response (Gruber *et al,* 1994). A critical function in limiting inflammatory responses was suggested for IL-10, following *in vivo* studies with IL-10 deficient (IL-10 -/-) mice exhibiting inflammatory bowel disease, more severe EAE, and other exaggerated inflammatory responses (Berg *et al,* 1995a, Berg *et al,* 1995b, Bettelli *et al,* 1998, Kuhn *et al,* 1993, Samoilova *et al,* 1998). Spontaneous recovery from EAE has been associated with elevated levels of T_H2 cells producing IL-10 (Kennedy *et al,* 1992), while low IL-10 production was associated with chronic relapsing EAE (Issazadeh *et al,* 1996).

Also secreted by T_H2 cells, IL-4 has multiple biological effects on B-cells, T-cells, and other non-lymphoid cells. It enhances expression of class II MHC antigens on B-cells, can promote their capacity to respond to other B-cell stimuli and to present antigens for T-cells (Yoshimoto and Paul 1994). Furthermore, it inhibits activation of NK-cells induced by IL-2. It also determines that B-cells switch to the expression of IgE and IgG (Gascan *et al,* 1991). IL-4 appears to play an important role in the establishment of a functional T_H2 immune response. *In vitro*, it stimulates growth of T and B-cells, deactivates inflammatory macrophages and regulates the induction of type-2 cells, in addition to inhibiting the development of type-1 cells (Harber *et al,* 2000, McKenzie *et al,* 1993, McKenzie 2000, Mossman and Coffman 1989).

TGF-β is a pleiotropic cytokine with immense anti-inflammatory and immune-suppressive properties, synthesized by almost all cell types. It is involved in tissue remodeling, wound repair, development, and haematopoiesis. It enhances growth of T-cells, induces T-cell expression of specific cytokines and enhances their capacity to respond to stimulation (Cerwenka *et al,* 1994). Conflicting data has been reported regarding the influence of TGF-β on T_H differentiation, and it has been shown that it can inhibit the production and response to cytokines associated with each subset (Bridoux *et al,* 1997, Chen *et al,* 1994). There is a notable antagonistic relationship between TGF-β and

IL-12 and IFN-γ, which have more clearly related it with a T_H2 differentiation (Marth *et al,* 1997, Strober *et al,* 1997). TGF-β plays a role in the generation and regulation of dendritic cells (Riedl *et al,* 1997, Strobl *et al,* 1996). Furthermore, TGF-β inhibits B-cell proliferation (Holder *et al,* 1992, Lomo *et al,* 1995),which may serve as an important regulatory feedback loop to limit expansion of an activated population.

1.7 Fatty acids in the treatment of EAE

A different approach to the treatment of MS and EAE has been in the use of polyunsaturated fatty acids. The omega-6 fatty acid linoleic acid has been shown to have beneficial effects in MS and EAE (Dworkin *et al,* 1984, Hughes *et al,* 1980, Meade *et al,* 1978). An essential fatty acid to human health, omega-6 fatty acid cannot be made in the body. There are several different types of omega-6 fatty acids, and most are consumed in the diet from vegetable oils as linoleic acid. In the body, linoleic acid is converted to gamma-linolenic acid (GLA), and then further broken down to arachidonic acid. Both of these can be consumed directly from food: arachidonic acid in meats and GLA from several plant-based oils. In excess, linoleic acid and arachidonic acid are unhealthy and promote inflammation. In contrast, GLA on its own may actually reduce inflammation. When GLA is taken as a supplement, it does not get converted to arachidonic acid, rather to a substance called dihomogamma-linolenic acid (DGLA). DGLA competes with arachidonic acid and prevents the negative inflammatory effects that arachidonic acid would otherwise cause in the body (Fan *et al,* 1995, Harbige *et al,* 1995, Phylactos *et al,* 1994). In addition, DGLA becomes part of a specific series of substances, called prostaglandins, which have been shown to have physiological immunoregulatory functions (Fan *et al,* 1995, Goetzl *et al,* 1995, Phipps *et al,* 1991). Prostaglandins can be potent anti-inflammatory mediators inhibiting interferon gamma production in antigens stimulated T-cell clones (Harbige *et al,* 1997, Watanabe *et al,* 1994). Since these polyunsaturated fatty acids are an element of myelin, studies have been conducted to see if taking an oral supplement might alter the course of multiple sclerosis. Research has shown that levels of TGF-β1 in peripheral blood mononuclear cells were elevated in humans taking omega-6 fatty acid supplements (Fisher and Harbige 1997). Animal studies conducted on Lewis rat

found that a high linoleic acid-rich oil partially suppressed EAE (Mertin and Stackpoole 1978, Mertin and Stackpoole 1979).

1.8 Objectives of study

- Use the non-invasive i.n. method of inoculation to deliver proteins into the mouse central nervous system utilizing the rSFV expression system with a reporter gene.
- Clone and incorporate different anti-inflammatory cytokine genes (IL-4 and IL-10) into the rSFV vector system.
- Establish levels of secreted cytokines both *in-vitro* and *in-vivo* following administration of the rSFV expression system.
- Set up a working model of experimental autoimmune encephalomyelitis, an animal model for the human disease multiple sclerosis.
- Determine the therapeutic effects of the rSFV vector system expressing cytokines in the treatment of EAE following i.n. treatment.
- Test the effectiveness of different synthetic made GLA compounds in the treatment of EAE

Chapter 2

Expression of recombinant SFV particles in the mouse central nervous system

2.1 INTRODUCTION

Extensive research has been performed on the pathogenicity of the Semliki Forest virus in the CNS. It is known that the virus is capable of replicating in the CNS of mice, and depending on the strain produce either a lethal encephalitis or an immune mediated demyelination (Atkins *et al,* 1985, Balluz *et al,* 1993, Sheahan *et al,* 1996). When virulent strains are administered intranasally a lethal threshold of damage to neurons in the CNS takes place, which results in the death of the mice (Smyth *et al,* 1990). Since infection with avirulent strains progresses at a slower pace then virulent strains, it leads to an autoimmune demyelination which does not kill infected mice (Balluz *et al,* 1993). Further research has demonstrated that following i.n. infection of mice (and rats), the virus follows axonal transport along olfactory tracts from nerve endings in the olfactory mucosa, reaching the CNS via the olfactory bulb (Sammin *et al,* 1999, Sheahan *et al,* 1996).

Based on these findings, preliminary studies were conducted to determine the feasibility of employing the rSFV expression system for the delivery of heterologous proteins to the CNS. The safety of this system for vaccine use has been previously demonstrated. SFV vectors have shown the ability to induce humoral and cell-mediated immunity against several diseases (Berglund *et al,* 1997, Berglund *et al,* 1999, Fleeton *et al,* 1999, Fleeton *et al,* 2000, Zhou *et al,* 1994). Furthermore, following i.m. inoculation with rSFV particles the cloned gene was detected at the injection site only, with very mild lesions and animals recovering fully (Morris-Downes *et al,* 2001a). Compared to DNA or RNA immunization encoding the same antigens, rSFV particles induced stronger immune responses (Fleeton *et al,* 2000, Fleeton *et al,* 2001). This same system has also been previously studied for its use as an anti-cancer agent. It has been recently shown that direct injection of murine tumors with rSFV particles can inhibit tumor growth and induce regression in the *p53*-deleted human non-small cell lung carcinoma cell line H358a. Pathological analyses of rSFV treated tumors indicated that tumor inhibition was not due to induction of an immune response, rather consistent with an initial induction of apoptosis followed by a large depletion of tumor cells by oncotic necrosis (Murphy *et al,* 2000).

A number of viral vectors are currently being used as delivery agents for the CNS, including herpes simplex virus, adeno-associated virus, and lentivirus among others. All of these are capable of expressing the cloned protein in the CNS of animals, some with a long duration of expression. The main problem with these vectors is they all rely on an i.c.

delivery route. This inoculation method is very traumatic to animals, making multiple injections over a short period of time very unwelcome. Furthermore, these are all DNA vectors, requiring the viral vector to enter the nucleus of infected cells, resulting in a much longer persistence of infection compared to RNA vectors like rSFV.

To determine the feasibility of utilizing the Semliki Forest virus vector system as a CNS vector, experiments were conducted testing the effects of infecting Balb/c mice i.n. with rSFV particles expressing the Enhanced Green Fluorescent Protein (EGFP) reporter gene. EGFP is commonly used as a reporter gene for a variety of reasons. It is a relatively small protein, 240 amino acids, which readily diffuses throughout the cytoplasm and cell processes. Its expression does not noticeably alter the tissue environment, since it is immunologicaly inactive. Finally, it can be visualized under fluorescent optics without the addition of substrates, both in live cells and fixed tissue. The current study assesses the location and duration of protein expression, RNA expression, as well as pathology associated with infection following i.n. inoculation of mice with rSFV-EGFP.

2.2 EXPERIMENTAL PROCEDURES

2.2.1 MATERIALS

2.2.1.1 Cell Lines

The Baby Hamster Kidney 21 (BHK-21) cell line was obtained from the American Type Culture Collection (ATCC) (Maryland, USA). The BHK cell line, sBHK, was a gift from Prof. P. Liljeström, (Microbiology and Tumorbiology center, Karolinska Institute, Stockholm, Sweden). BHK medium, newborn calf serum (NCS), fetal calf serum (FCS), tryptose phosphate broth, HEPES, and trypsin EDTA were from Gibco (UK), Penicillin-streptomycin-L-glutamine solution was from Sigma (UK).

2.2.1.2 Expression Vectors

The SFV expression vector, pSFV-EGFP, and helper vectors, pSFV-Helper S2 and pSFV-Helper CS219A (figure 2.1) were a gift from Prof. P. Liljeström.

2.2.1.3 Molecular Biology Reagents

Tri Reagent used for RNA extraction was purchased from Sigma. Primers used for PCR amplification were as follows:

Mouse GAPDH F	5'-ACCACCATGGAGAAGGCTG-3'
Mouse GAPDH R	5'-CTCAGTGTAGCCCAGGATGC-3'
EGFP F	5'-CTGGACGGCGACGTAAACGGCCAC-3'
EGFP R	5'-AGCTGCACGCTGCCGTCCTCGATG-3'
SFV nsP3 F	5'-GCGGAATTCCTCATCTTTTCCCCTCCCGA-3'
SFV nsP3 R	5'-CGCGAATTCATCGACCTCGTGCTCGTCAA-3'

All primers were obtained from MWG (UK), with the exception of the SFV nsP3, which was obtained from the Genetics department at TCD. The restriction enzymes *EcoRI* and *SpeI* were from New England Biolabs (NEB) (MA, USA), Taq DNA polymerase, recombinant RNAsin ribonuclease inhibitor, AMV reverse transcriptase, Oligo(dT) primer, dNTP mixture, $MgCl_2$, reverse transcriptase buffer, nuclease-free water and PCR molecular weight markers were from Promega (Promega, Wisconsin, USA). The plasmid purification kits for mini- and midi-preps were from QIAGEN Ltd. (West Sussex, UK). SP6 RNA polymerase and $m^7G(5')ppp(5')G$ were from Amersham Pharmacia Biotech (Uppsala, Sweden).

2.2.1.4 Particle production

A Sorvall RC 5C plus centrifuge with a SS-34 rotor, and a Beckman L8-M ultracentrifuge were used for all spins during particle production. Ultracentrifuge tubes and the SW40Ti rotor and swing buckets were from Beckman-Coulter Instruments Inc. (CA, USA). Sucrose was from BDH Ltd (Poole, UK)

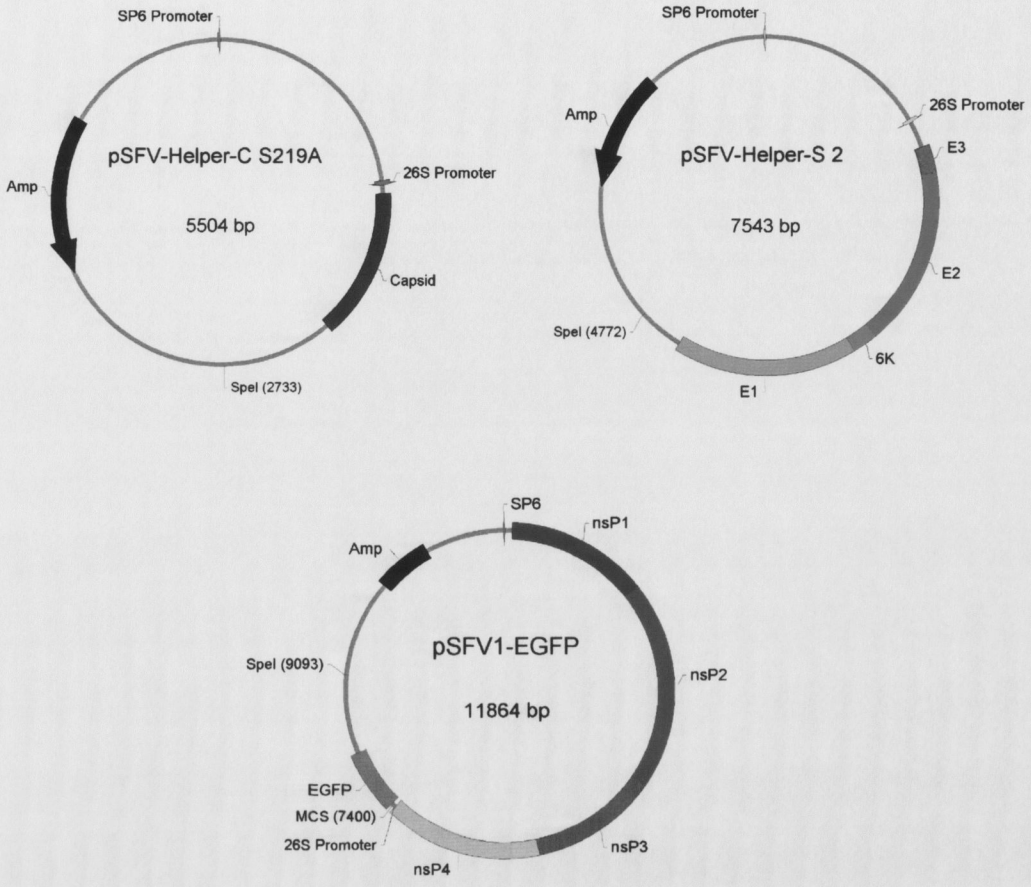

Figure 2.1 Maps of Semliki Forest virus expression vectors

The recombinant vector pSFV-EGFP as well as helper vectors, pSFV-Helper S2 and pSFV-Helper CS219A is shown. The recombinant vector incorporates the four genes encoding the SFV replicase complex (nsP1-4), but lack the structural genes (C, p62, 6K, E1), which are located on the helper vectors. All plasmids contain the unique *SpeI* site used for linearization, and SP6 promoter, which drives *in-vitro* transcription.

2.2.1.5 Microscopy

A Nikon Eclipse E400 Epiflourescence microscope was used for both bright field and fluorescence microscopy. The following Nikon filters were used for fluorescence detection: GFP filter at 460-500 nm, DAPI filter at 340-380 nm, and G2A filter at 510-560 nm.

2.2.1.6 Mice

Male and female Balb/c mice aged 40-60 days were obtained from the Bio Resources unit (TCD). Mice were maintained in accordance with the principles outlined in S1 17/94 European Communities regulations 1994, for care and use of laboratory animals. Syringes (1.0 ml and 0.5 ml microfine insulin) and needles, (21G and 29G), were from Becton Dickenson, (Le pont de Claix, France).

2.2.1.7 Histological and pathological studies

A CM 1900 cryostat was from Leica Microsystems (Nussloch, Germany). OCT compound, DABCO, and Diamino-2-phenylindole (DAPI) were from Sigma. Isopentane, paraformaldehide (PFA), Haematoxylin Harris, Eosin aqueous solution, and DPX solutions were from BDH Ltd. Cork discs were purchased from Raymond Lamb (East Sussex, UK). Mowiol was from Calbiochem Novabiochem (Nottingham, UK). Neutral buffered formaldahyde (NBF) was obtained by diluting formaldehyde solution (BDH) 1 :10 in water and adding 9 g of sodium chloride (Sigma).

2.2.1.8 Antibodies

Mouse monoclonal anti-CNPase antibody (C5922), and a mouse monoclonal anti-MAP1 antibody (M4278) were obtained from Sigma. Rabbit anti-mouse IgG TRITC-

conjugated antibody was from DAKO (Glostrup, Denmark). Normal rabbit serum was from Vector Laboratories Inc.(CA, USA). Tween 80 was from MERK (Germany).

2.2.1.9 Miscellaneous

Lambda molecular weight marker, 10X loading dye, Phenol : Chloroform : isoamyl alcohol and agarose were from Promega. One kb DNA ladder was from NEB. Electroporation cuvettes were from BTX (San Diego, USA). Solvents were mainly from BDH Ltd. All other chemicals were of AnalaR or molecular biology grade as required and were purchased from Sigma or BDH Ltd. T.N.E. buffer: 50 mM Tris, 0.1 M NaCl and 1 mM EDTA were dissolved in 800 ml distilled water, pH adjusted to 7.4 and volume to 1 liter. Phosphate buffered-saline (PBS) was from Oxoid (Hampshire, UK), ampicillin was from Sigma, noble agar was from Difco (Detroit, USA), and crystal violet from ClinTech. (Exess, UK), lysing matrix D tube was from Q-Biogen (UK).

2.2.2 METHODS

2.2.2.1 Cell Culture

The BHK-21 cell line was used for SFV4 virus growth and recombinant SFV particle production. Cells were cultured in 75cm^2 tissue culture flasks containing BHK-21 medium, supplemented with 5% (vol/vol) NCS, 5% (vol/vol) tryptose phosphate broth, 100 U/ml penicillin, 100 μg/ml streptomycin in 200 mM L-glutamine, and maintained at 37°C in a humidified atmosphere of 5% CO_2. For particle production, BHK medium contained 5% (vol/vol) FCS and 2% (vol/vol) 1M Hepes in addition to tryptose phosphate broth, L-glutamine and antibiotics. Cells were seeded at 1 x 10^5 ml^{-1} for growing (ATCC recommendation) in a total volume of 15 ml medium, and passaged when confluent as follows: Cell monolayers were washed twice with phosphate buffered saline (PBS, pH6.7) and incubated with 0.25% (wt/vol) trypsin/EDTA at 37°C until detachment was evident (1-3 min), the flask tapped to complete detachment and medium added to terminate trypsinization. Cells were then split and returned to the incubator. A second BHK cell line

(sBHK) was utilized for recombinant SFV particle titration. It was cultured in the same medium as that used for particle growth, and propagated in the same manner. For titration experiments, cells were seeded at 1 x 10^5 ml^{-1} in a total volume of 2 ml per well in 6-well dishes.

2.2.2.2 Virus

A working stock of the virulent SFV4 strain of SFV was obtained by allowing seed-stock SFV4 to infect BHK-21 cells in a 75 cm^2 flask for 1 h, with rocking movements every 15 min to achieve a homogenous infection. The virus inoculum was removed from the monolayer and cells were given fresh BHK medium and incubated at 37^{0}C in a humidified atmosphere of 5% CO_2 until full cytopathic effect was observed (approximately 24 h). To harvest the virus, supernatants were removed, centrifuged at 700 x *g* for 10 min to remove cellular debris, filtered through 0.2 μm filters, and stored in 0.5 ml aliquots at – 70^{0}C. Virus titer was established by plaque assay.

2.2.2.3 Plaque assay

BHK-21 cells seeded at 1 x 10^5 ml^{-1} in a total volume of 2 ml per plate (60 mm) were infected with varying dilutions of SFV4 for 1 h at 37^{0}C in a humidified atmosphere of 5% CO_2, with rocking movements every 15 min. The virus inoculum was removed from the monolayer and cells were given 3 ml of medium containing a 50:50 solution of overlay medium and 1.8% (wt/vol) noble agar, and incubated at 37^{0}C in a humidified atmosphere of 5% CO_2 for approximately 48 h. Cells were then fixed in formal saline, and stained with crystal violet. Viral titer was measured by counting plaques, and expressed as plaque forming units (pfu).

2.2.2.4 Preparation of recombinant and helper SFV plasmids

2.2.2.4.1 Preparation of competent *E. coli* DH5α cells

Escherchia coli strain DH5α cells were used for transformation of recombinant SFV and 'helper' SFV plasmids. 500 ml of *E. coli* cells were grown in L broth shaking at 37°C until the optical density at 600 nm reached 0.45-0.55. The culture was then chilled on ice for 2 h after which the culture was centrifuged at 800g for 20 min at 4°C. The bacterial pellet was resuspended in 500 ml of titration buffer (100 mM $CaCl_2$, 70 mM $MgCl_2$, 40 mM NaOAc) and incubated on ice for 45 min. The bacteria were then pelleted by centrifugation at 700g for 10 min and the pellet resuspended in 50 ml titration buffer. 15% (vol/vol) 80% glycerol was added to the competent bacterial cell suspension, which were then aliquoted and stored at -70°C.

2.2.2.4.2 Transformation of Bacterial Cells

Competent DH5α cells were transformed with recombinant (rSFV-EGFP) and Helper SFV plasmids (pSFV-Helper S2 and pSFV-Helper CS219A) by incubating 200 µl of competent cells with each plasmid DNA for 1 h on ice, followed by heat shocking of cells for 2 min at 42°C. Cells were then cooled on ice for 10 min before being transferred to 1 ml of L broth without any drug selection. Cells were allowed to recover for 1 h shaking at 37°C before the addition of 100 µg ampicillin. Cells were allowed to grow for a further 1 h. Transformed colonies were then plated onto L-agar containing 100 µg/ml ampicillin and incubated overnight at 37°C.

2.2.2.4.3 Verification of plasmid DNA from E. coli DH5α

Pure isolated colonies of recombinant plasmids were inoculated in 30 ml of L-broth containing 100 µg/ml ampicillin. Cells were grown for 18 h shaking at 37°C. From each culture, a 20 ml aliquot was removed and mixed with 15% (wt/vol) 80% glycerol. These

were then stored at -70°C in 1 ml aliquots. The remaining culture was used to purify the plasmid, using the QIAGEN Miniprep Plasmid Purification Kit. This prep is based on a modified alkaline lysis protocol. Cells were harvested by centrifugation (1000g, 10 min, 4°C). Each pellet was resuspended in 250 µl of buffer P1 (10 mM EDTA, 100 µg/ml RNAse A, 50 mM Tris-HCL, pH 8.0), and transferred to a microfuge tube. Cells were lysed by the addition of 250 µl of buffer P2 (200 mM NaOH, 1% (wt/vol) SDS). 350 µl of buffer N3 was added, and mixed gently prior to centrifugation (10,000g, 10 min). The supernatant was applied to a QIAprep column and further centrifuged (10,000g, 1 min). The column was then washed with 500 µl of buffer PB, to remove all trace of nuclease activity. The column was again washed with 750 µl of buffer PE, and centrifuged twice (10,000g, 1 min). Clean DNA was eluted in 30 µl of water by centrifugation (10,000g 1 min). Each DNA was digested for 1 h at 37°C with *EcoRI* enzyme to confirm correct plasmids. Products were confirmed by mixing a 1 µl aliquot with 1µl loading buffer (33% (vol/vol) glycerol, 0.05% (wt/vol) bromophenol blue, 0.05% (wt/vol) xylene cyanole FF) and running this on a 0.8% (wt/vol) agarose gel (0.8% agarose, 3.0µl 10 mg/ml ethidium bromide in 40 ml TBE) in TBE at 75 mA (figure 2.2)

2.2.2.4.4 Isolation of plasmid DNA from E. coli DH5α

A glycerol stock from each plasmid was incubated in 50 ml of L broth containing 100 µg/ml ampicillin by shaking for 18 h at 37°C. Plasmids were purified using the QIAGEN Plasmid Midi Purification Kit. Cells were harvested by centrifugation (6,000g, 15 min, 4°C). Each pellet was gently resuspended in 4 ml of buffer P1, and then lysed with 4 ml of buffer P2 for 5 min. Four ml ice-cold P3 (3 M potassium acetate, pH 5.5) was then added to precipitate the genomic DNA, cell debris, proteins and SDS. After 15 min incubation on ice, samples were centrifuged (20,000g, 35 min, 4°C) and then supernatant transferred to a new tube, and centrifuged as before for 20 min. The new supernatant containing plasmid DNA was applied to a QIAGEN-tip 100, which had been equilibrated with 4 ml of buffer QBT (750 mM NaCl, 15% (vol/vol) isopropanol, 0.15% (vol/vol) Triton X-100, 50 mM MOPS, pH 7.0). Once loaded, the QIAGEN-tip was washed with twice with 10 ml of buffer QC (1.0 M NaCl, 15% (vol/vol) isopropanol, 50 mM MOPS, pH 7.0). Plasmid DNA was then eluted in 5 ml of buffer QF (1.25 M NaCl, 15% (vol/vol)

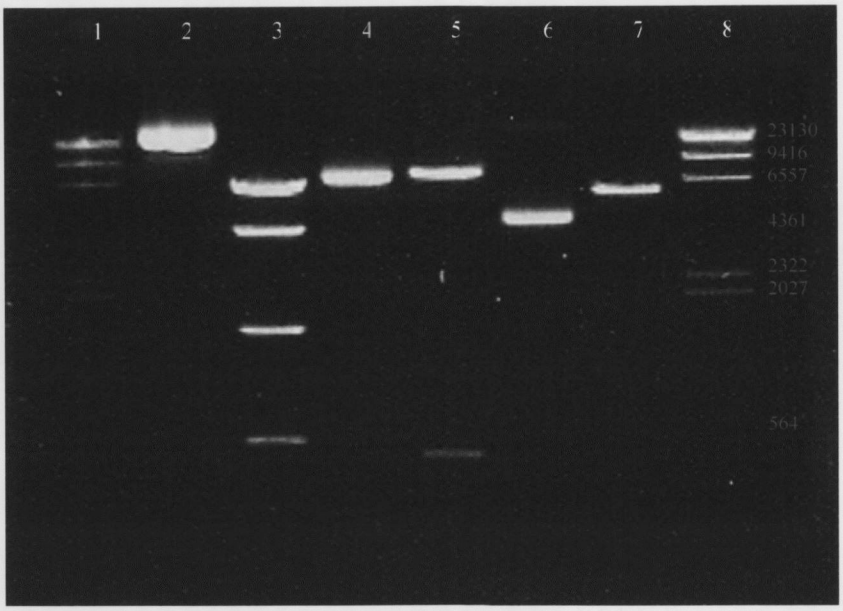

Figure 2.2 Confirmation of recombinant and helper SFV plasmids

Helper and recombinant (rSFV-EGFP) plasmids were digested with the restriction enzyme EcoRI as outlined in section 2.2.2.4.3. Uncut plasmids, as well as digested plasmids with showing appropriate sizes are demonstrated. *Lane 1 and 8*; 0.125 μg and 0.25 μg Lambda (Hind111) DNA molecular weight marker. *Lane 2*; 1.0 μl of undigested rSFV-EGFP DNA. *Lane 3*; 1.0 μl of digested rSFV-EGFP DNA. *Lane 4*; 1.0 μl of undigested rSFV-Helper S2 DNA. *Lane* 5; 1.0 μl of digested rSFV- Helper S2 DNA. *Lane 6*; 1.0 μl of undigested rSFV- Helper CS219A DNA. *Lane 7*; 1.0 μl of digested rSFV- Helper CS219A DNA. 0.8% (wt/vol) agarose gel, stained with ethidium bromide.

isopropanol, 50 mM Tris-HCL, pH 8.5). Three and half ml of room temperature (RT) isopropanol was added to precipitate the DNA. The solution was then aliquoted into 5 microfuge tubes. The tubes were then centrifuged (13,000g, 30 min, 4°C), the supernatant removed, and DNA pellets washed with 70% (vol/vol) ethanol. The tubes were centrifuged (13,000g, 10 min, 4°C), and pellets were dried for 30 min to 1 h on air, then in a SpeediVac (2,000g, 5 min) and redissolved in sterile dH_2O (20 µl/tube) before storing at -20°C. Clean plasmid concentration was assessed by mixing a 1 µl aliquot with 1µl loading buffer and running this on a 0.8% (wt/vol) agarose gel. The concentration of plasmid was estimated from this gel by comparing band intensity with that of 5 and 10 µl Lambda molecular weight marker [5 µl Lambda (*HindIII* & *EcoRI*), 20 µl loading buffer, 75µl TBE] (figure 2.3). Midi-prep plasmid concentrations were further estimated on a GeneQuant DNA/RNA spectrophotometer.

2.2.2.5 Preparation of recombinant and helper SFV RNA

2.2.2.5.1 *SpeI* linearization of plasmid DNA

For the production of both helper and recombinant SFV viral RNA, each plasmid was linearized with the *SpeI* restriction enzyme. This is a unique restriction site in the infectious clone preceding the non-structural protein genes. A total of 10 µg SFV plasmid DNA was linearized in final reaction volumes of 50 µl, containing 5 µl of *SpeI* buffer (50 mM NaCl, 10 mM Tris-HCL, 10 mM $MgCl_2$, 1 mM DTT, pH 7.9), and 35 U of *SpeI*. After digestion at 37°C for 16-18 h, each linearized plasmid DNA was pooled and brought to a final volume of 100 µl. Each DNA was brought to 200 µl with the addition of 100 µl of sterile dH_2O. Twenty µl of 3M Sodium Acetate (pH 5.2) was added, and mixed with 200 µl of Phenol: Chloroform: Isoamylalcohol (25:24:1) by vortexing for 10 sec. The mixture was then centrifuged (13,000g, 2.5 min) and the aqueous (top) layer decanted into a fresh tube. The previous step repeated to this aqueous layer, then 800 µl of the ether part of a ether: water (2:1) mixture added. After vortexing for 10 sec, the mixture was again centrifuged (13,000g, 1 min). The top layer was carefully removed by suction using a 200 µl pipette tip attached to a vacuum pump. Five hundred µl of 100% ethanol (-20°C) was

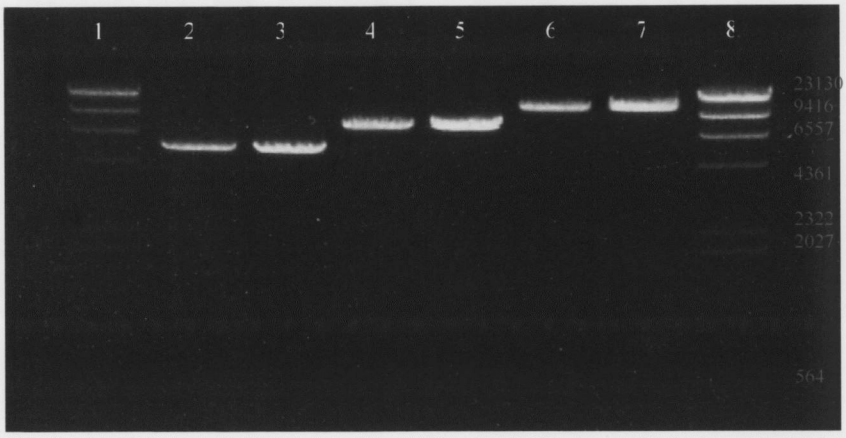

Figure 2.3 Purified recombinant and helper SFV plasmids

Helper and recombinant (rSFV-EGFP) plasmids were purified using the QIAGEN Midi prep purification kit as described in section 2.2.2.4.4. Purified product was then linearised for *in-vitro* transcription. The amount needed for linearization was calculated based on band intensity obtained from above gel. *Lane 1 and 8*; 0.125 μg and 0.25 μg Lambda (Hind111) DNA molecular weight marker. *Lane 2 and 3*; 0.5 μl and 1.0 μl each of SFV-Helper CS219A DNA. Lane *4 and 5*; 0.5 μl and 1.0 μl each of SFV-Helper S2 DNA. *Lane 6 and 7*; 0.5 μl and 1.0 μl each of rSFV-EGFP DNA. 0.8% (wt/vol) agarose gel, stained with ethidium bromide.

added to each tube, inverted a few times to mix, and incubated overnight at -20°C. The tubes centrifuged (13,000g, 30 min, 4°C), and supernatant decanted. One ml of 70% ethanol (-20°C) was added and again centrifuged (13,000g, 15 min, 4°C). All ethanol was removed, and pellet dried in a SpeediVac (2,000g, 10 min). The pellet was then resuspended (using RNAse free tips) in 100 µl of nuclease-free water before storage at -20°C. Plasmid DNA concentration was assessed by mixing a 1 µl aliquot with 1 µl loading buffer and running this on a 0.8% (wt/vol) agarose gel. The concentration of plasmid was estimated from this gel by comparing band intensity with that of 5 and 10 µl Lambda (*HindIII* and *EcoRI*) DNA molecular weight marker (figure 2.4).

2.2.2.5.2 *In vitro* SP6 RNA transcription

For the production of helper and recombinant SFV viral RNA, SP6 RNA polymerase, was used to initiate *in vitro* RNA transcription from the clean *SpeI*-linearised plasmids. Standard reaction mixtures contained 0.5 µg DNA template, 1 x SP6 buffer [40 mM N-2-hydroxyrthyl-piperazine-N'-2-ethansulphonic acid-KOH (Hepes-KOH), pH7.4, 6 mM MgOAc, 2 mM spermidine-HCL], 1 mM $m^7G(5')ppp(5')G$, 5 mM dithiotreitol, 1 mM each rATP, rCTP, rUTP, 500 µM rGTP, 60 U recombinant RNAsin, and 50 U of SP6 RNA polymerase in 50 µl volume. The reactions were incubated at 37°C for 1 h 50 min and transcripts were analyzed by electrophoresis on a 0.6% (wt/vol) agarose gel (figure 2.5).

2.2.2.5.3 High titer rSFV-EGFP virus particle production

2.2.2.5.3.1 Electroporation

BHK-21 cells were propagated as described in section 2.2.2.1. For electroporation, five 75 cm^2 tissue culture flasks, containing ~80% confluent BHK-21 cells were used. Cell monolayers were washed, and trypsinized as previously described. Each flask was resuspended in 10 ml of fresh BHK medium, and pooled in two tubes prior to centrifugation (400g, 10 min). Pellets were resuspended in 20 ml PBS, and centrifuged as before. The *in vitro*-transcribed RNA reactions were divided into five 150 µl aliquots,

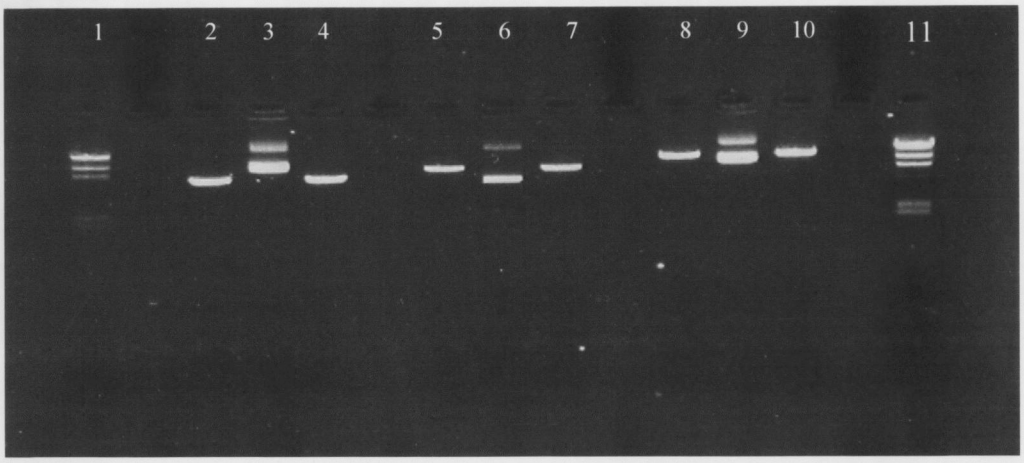

Figure 2.4 Linearized recombinant and helper SFV plasmids

Helper and recombinant (rSFV-EGFP) plasmids were linearized prior to transcription using the unique restriction site Spe1 found on all SFV plasmids as described in section 2.2.2.5.1. Linearized plasmid concentrations obtained from this figure were used to calculate amount of DNA needed for transcription. *Lane 1 and 11*; 0.125 μg and 0.25 μg Lambda (Hind111) DNA molecular weight marker. *Lane 2, 4 and 3*; 0.5 μl, 1.0 μl of digested rSFV- Helper CS219A DNA and undigested control, respectively. *Lane 5, 7 and 6*; 0.5 μl, 1.0 μl of digested rSFV- Helper S2 DNA and undigested control, respectively. *Lane 8, 10 and 9*; 0.5 μl, 1.0 μl of digested rSFV-EGFP DNA and undigested control, respectively. 0.8% (wt/vol) agarose gel, stained with ethidium bromide.

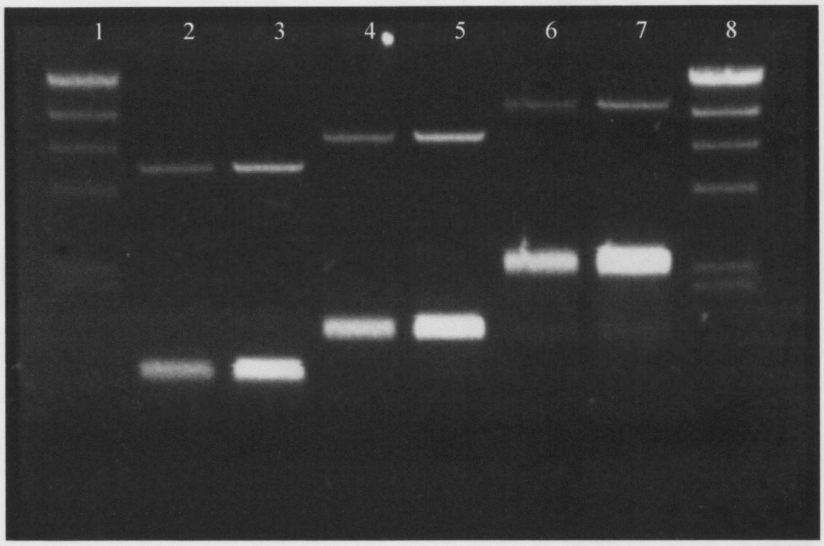

Figure 2.5 In vitro SP6 RNA transcription

Helper and recombinant (rSFV-EGFP) plasmids were transcribed as outlined in section 2.2.2.5.2. *Lane 1 and 8*; 0.125 μg and 0.25 μg Lambda (Hind111) DNA molecular weight marker. *Lane 2 and 3*; 0.5 μl and 1.0 μl each of SFV-Helper CS219A RNA. Lane *4 and 5*; 0.5 μl and 1.0 μl each of SFV-Helper S2 RNA. *Lane 6 and 7*; 0.5 μl and 1.0 μl each of rSFV-EGFP RNA. 0.6% (wt/vol) agarose gel, stained with ethidium bromide.

with each tube containing 50 µl each SFV-EGFP, SFV-Helper S2 and SFV-Helper CS219A RNA. Cells were resuspended in 2 ml of PBS per tube, and pooled. Eight hundred µl of cell suspension was added to the 150 µl RNA mixture, and placed in a 0.4 µm electroporation cuvette. The cuvette was then electroporated at 0.85 kV and 25 µF capacitance, using a BioRad Gene Pulser 11. Following 2 pulses, cells were mixed with 20 ml of fresh BHK particle medium, transferred to a 75 cm^2 tissue culture flask and incubated for 36 h at 33°C in a humidified atmosphere of 5% CO_2. This was repeated for all RNA aliquots.

2.2.2.5.3.2 Harvesting high titer rSFV particles

Thirty-six hours following electroporation, tissue culture supernatants, containing rSFV-EGFP particles were removed from the 5 culture flasks and pooled (100 ml). The pooled supernatant was centrifuged (6,000g, 30 min, 4°C) to remove cellular debris, and further clarified by centrifugation (6,000g, 15 min, 4°C), before being pooled into a glass conical flask kept on ice. Nine ml aliquots of particle supernatant were placed in 6 Beckman SW40Ti ultracentrifuge tubes. A 20% (wt/vol) sucrose cushion was carefully placed beneath this solution, and the tubes topped up and balanced with a further 2 ml rSFV supernatant. The tubes were placed into 6 SW40Ti swing buckets, balanced and the rSFV-EGFP particle centrifuged (30,000g, 2.0 h, 4°C). Following ultracentrifugation, the supernatant was immediately removed, the sides of the tubes dried with sterile cotton tips, and each pellet was resuspended in 150 µl of TNE buffer (50 mM Tris-HCL, pH 7.4, 100 mM NaCl, 0.1 mM EDTA). The above ultracentrifugation step was repeated with remaining supernatant. The rSFV-EGFP pellets were incubated on ice at 4°C. Following overnight resuspension, particles were further resuspended by gentle pipetting, removed from tubes and pooled. Each tube was further washed with 100 µl of TNE buffer. After 15 min incubation on ice, tubes were vortexed and resuspensions pooled with previous into a final volume of 2 ml, which were then aliquoted into 50-200 µl volumes, on ice, and rapidly frozen using dry-ice-cooled ethanol or liquid nitrogen, before storing at -70°C.

2.2.2.5.3.3 High titer rSFV particle titration

For particle titration, the sBHK cell line was seeded at 1 x 10^5 cm^{-1} onto glass coverslips, contained within each well of a 6-well plate, and incubated until confluent. Serial dilutions (10 µl, 1 µl, 0.1 µl, 0.01 µl) of rSFV-EGFP particles, in duplicate, were used to infect successive wells of confluent sBHK cell monolayers, in a total volume of 500 µl infection medium for 1 h, with rocking movements every 15 min to achieve a homogenous infection. The cells were then replaced with fresh BHK medium and incubated at 37°C in a humidified atmosphere of 5% CO_2. Following 18 h incubation with rSFV-EGFP particles, medium was removed, the coverslips washed twice in PBS and the cells were fixed in 4% (wt/vol) paraformaldehyde for 20 min. Coverslips were again washed twice with PBS, and mounted onto glass slides in Mowiol-DABCO solution. Particle titers were obtained by examining cells microscopically for the presence of EGFP fluorescence using a specific EGFP filter at a wavelength of 488nm (figure 2.6). Particle titers were calculated at a magnification of x 400 and expressed as IU/ml.

2.2.2.6 Protein expression following rSFV-EGFP infection

2.2.2.6.1 *In vivo* experimentation

A total of 46 Balb/c mice were used for this study. All mice infected i.n. with rSFV-EGFP received approximately 10^7 IU in a volume of 20 µl per nostril, and sampled at 16 hours post infection (hpi), 1, 2, 3, 4, 5, 6, 8, 10, 14, and 21 dpi. Positive control mice were infected i.m. with 10^6 IU in 50 µl volume injected into each tibia anterior (TA) muscle, and sampled at 3 days post-infection (dpi). Negative control mice were given 20 µl of PBS i.n., and sampled at 3 dpi.

2.2.2.6.2 Preparation of cryosections

At designated time points mice were anaesthetized with halothane and perfused via the left ventricle with PBS followed by 4% PFA for 5 min. Mice were left in fixative for

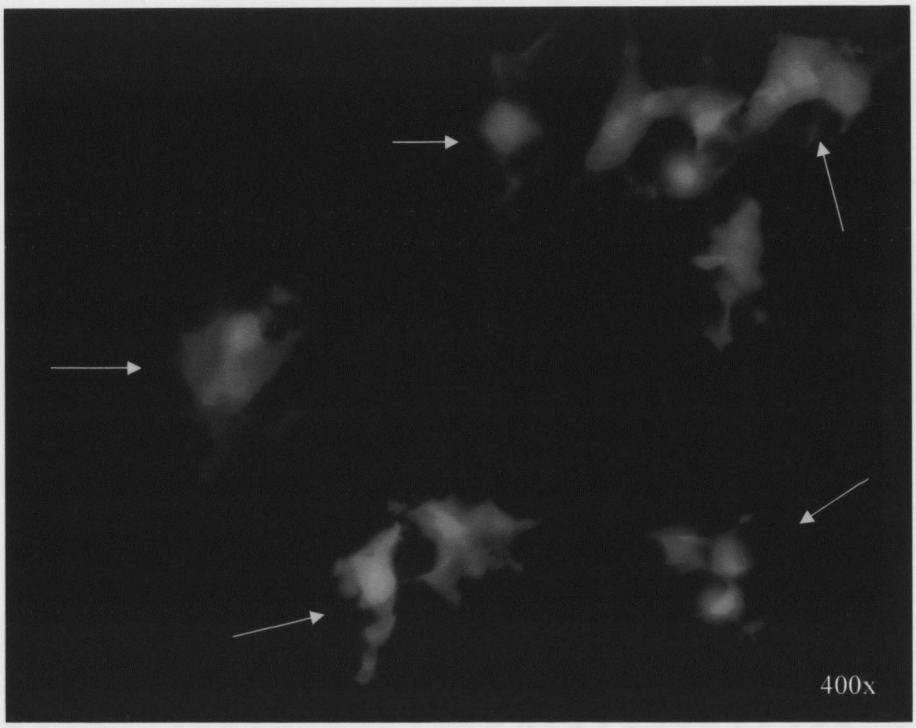

Figure 2.6 rSFV-EGFP particle titration

Titration of rSFV-EGFP particles was carried out as described in section 2.2.2.5.3.3. Titer was calculated by counting all sBHK cells fluorescing (arrows) under the GFP filter at a (488nm wavelength), and multiplying by appropriate factors. Titer was expressed as IU/ml. Titers ranging from 1.0×10^9 to 1.0×10^{10} IU/ml were routinely obtained.

1-2 h prior to removal of tissue. For histological analysis on frozen brain sections, excised olfactory bulbs and remaining brain were immediately embedded in OCT compound on cork discs, and rapidly frozen in liquid-nitrogen-cooled isopentane, before storing at -70°C. Cryosections of seven μm thick were placed on glass slides that were pre-coated with 0.5% (wt/vol) gelatin, and fixed with 4% (wt/vol) PFA solution. For protein expression visualization, sections were counterstained using a nuclear stain, DAPI, and mounted onto coverslips using mowiol. Control muscle sections were also prepared in same manner. Sections were visualized by fluorescent microscopy using filters at 488 and 400 nm for EGFP and DAPI detection, respectively. For routine histology, fixed cryosections were stained with haematoxylin for 8 min, washed in water, and cleared in 1% acid alcohol (1 ml HCl in 99 ml 70% ethanol) for 10 sec. Sections were then washed in water until a blue color was visible, and counterstained for 5 min with eosin. After a brief water wash, sections were dehydrated in a series of alcohol washes (70%, 95%, and 100%), cleared in xylene and mounted onto coverslips using DPX solution.

2.2.2.7 RNA analyses following rSFV-EGFP infection

2.2.2.7.1 *In vivo* experimentation

A total of 49 Balb/c mice were used for this study. All mice infected i.n. with rSFV-EGFP received approximately 10^7 IU in a volume of 20 μl per nostril, and were sampled at 16 hpi, 1, 3, 5, 7, and 10 dpi. Control animals received 10^7 pfu of SFV4 while negative controls were mock-infected PBS, and sampled at 1 and 3 dpi.

2.2.2.7.2 RNA extraction

At designated time points both the olfactory bulb and remaining brain, or the nasal passage were removed from infected mice. Total RNA was extracted from the tissue and mixed with Tri Reagent on a lysing matrix D tube. For every 50-100 mg of tissue, 1 ml of Tri Reagent was added; while 1.5 ml were added for 75-150 mg (1 ml added to olfactory bulbs, and 1.5 ml to each half of remaining brain, and to nasal passage). Tissue was

homogenized in a FastPrep Instrument (FP 120, Anachem) at 5.5 pulse for 45 sec (for brain and nasal passage, tissue was homogenized twice), and then incubated on ice for 10 min. The mixture was then centrifuged (12,000g, 10 min, 4°C) and supernatant transferred to a microfuge tube. After 5 min incubation at RT, 200 µl of chloroform (per ml of Tri Reagent used) was added to tube, and mixture centrifuged (12,000g, 15 min, 4°C). Colorless aqueous phase was transferred to a new tube, mixed with 500 µl of isopropanol (per ml of Tri Reagent), and incubated at RT for 10 min. The mixture was centrifuged (12,000g, 10 min, 4°C), the supernatant was removed and the pellet washed with 1 ml of 75% ethanol (-20°C) by vortex. The mixture was again centrifuged (12,000g, 10 min, 4°C), ethanol was removed and RNA resuspended in 20 µl of nuclease-free water before storage at -70°C. RNA concentration was measured on a GeneQuant DNA/RNA spectrophotometer.

2.2.2.7.3 RT-PCR

First strand cDNA was synthesized from 1 µg mouse RNA tissue sample in a 20 µl reaction using Promega's reverse transcription system. Each reaction contained 5mM $MgCl_2$, 1X reverse transcription buffer (10mM Tris-HCl [pH 9.0], 50 mM KCl, 0.1% Triton X-100), 1mM each dNTP, 1 U recombinant RNAsin ribonuclease inhibitor, 15 U high concentration AMV reverse transcriptase (RT), and 0.5 µg oligo $(dT)_{15}$ primers. The mixture was incubated for 60 min at 42°C, 5 min at 99°C and 5 min at 4°C. The cDNA (20 µl) was set up in a 100 µl PCR reaction with the following final concentrations: 200 µM cDNA reaction dNTPs, 2 mM $MgCl_2$, 1X reverse transcription buffer, 0.1 µM forward and reverse SFV or EGFP primers, and 2.5 U of TaqDNA Polymerase. The following temperature profile was used in the PCR reaction: 1 min at 94°C followed by 30 cycles of incubations at 94°C for 30 s, 55°C for 30 s 72°C for 30 s with a final extension of 5 min at 72°C. Negative control samples contained cDNA from RNA extracted from PBS mock-infected mouse tissues, whereas positive control cDNA for nsP3 and EGFP amplification was prepared from tissue of mice injected i.n. with SFV4, and i.m. with rSFV-EGFP. Internal controls for the RT-PCR procedure included samples with either no RNA or no RT added. Oligonucleotide primers were designed from a non-structural region of SFV

(nsP3) and the coding region of the EGFP reporter molecule. Oligonucleotide primers that produce a 508 bp product of the GAPDH protein were used to demonstrate the integrity of the DNA. The amplified products were analyzed on 1% agarose gels stained with ethidium bromide.

2.2.2.8 Immunohistochemistry following rSFV-EGFP infection

2.2.2.8.1 *In vivo* experimentation

Five Balb/c mice were used for this experiment. All mice were infected i.n. with 10^7 IU of rSFV-EGFP in a volume of 20 µl per nostril, and sampled at 3 dpi.

2.2.2.8.2 Immunohistochemistry

All mice were perfused with 4% PFA, and cryosections prepared as described in section 2.2.2.6.2. For immunohistochemical analysis, olfactory bulb cryosections were labeled with antibodies that detect oligodendrocytes (anti-CNPase)(Sprinkle 1989), and antibodies that selectively label neurons with a stronger staining of axons than dendrites (anti-MAP1)(Huber and Matus 1984). The optimal dilution for each antibody was determined using an antibody dilution series. Fixed sections were washed in sterile distilled water followed by 2 x PBS for 5 min and blocked with rabbit antiserum (50 µl/ml) in PBS for 1.5 h at 37°C in a dark humidified chamber. Sections were then incubated overnight at 4°C in primary antibody diluted in PBS (anti-CNPase 1:10, and anti-MAP1 1:25) in a dark humidified chamber. Sections were then washed twice in PBS tween (0.05% vol/vol) for 10 min, twice in PBS alone for 5 min, and then incubated in a TRITC-conjugated rabbit anti-mouse Immunoglobulin (1:20 dilution) for 1 h at 37°C in a dark humidified chamber. Slides were again washed twice in PBS tween and PBS alone, counterstained with DAPI (2.5 µg/µl) for 20 minutes, washed in PBS and dH_2O and mounted using Mowiol-DABCO solution. Negative controls included sections with and without primary or secondary antibodies. Sections were visualized using a fluorescent microscope with a G2A filter at 510-560 nm, a DAPI filter, and a GFP filter.

2.2.2.9 Pathology following rSFV-EGFP infection

2.2.2.9.1 Animal infection

Thirty-two Balb/c mice were used for this experiment. A total of 20 mice were infected i.n. with 10^7 IU of rSFV-EGFP as previously described, 6 mice used as positive controls were infected i.n. with 10^7 pfu of SFV4, while negative controls were mock infected i.n. with PBS. Virus infected mice were sampled at days 3 and 5, while particle infected mice were sampled at 5, 7, 8, and 14 dpi. Mock-infected mice were sampled at 5 dpi.

2.2.2.9.2 Paraffin embedding and sectioning for pathology

All mice were perfused as described in section 2.2.2.6.2 with NBF being used as opposed to 4% PFA. Paraffin embedding and sectioning of brains and nasal passage were performed by Ms. Marie Moore (Veterinary Pathology Laboratory, University College, Dublin). Excised brains, and nasal passages were immediately fixed in 10% NBF prior to paraffin embedding. Samples were dehydrated in a graded alcohol series of washes; 50% (vol/vol) alcohol for 60 min, 70% (vol/vol) alcohol for 60 min and 90% (vol/vol) alcohol for 60 min, before being placed into two absolute alcohol washes, for 40 min each. Samples were then immersed in a 1:1 solution of absolute alcohol: xylene solution, for 60 min, before being washed 3 times in absolute xylene, for 40 min each. This was followed by four individual immersions in paraffin wax, for 40 min each. Tissue was then mounted onto blocks prior to sectioning. Six to eight μm thick paraffin sections were prepared using a microtone, placed onto standard slides and acetone fixed for routine histological analysis.

2.3 RESULTS

2.3.1 Persistence and location of protein expression in mice

Following i.n. inoculation of mice with rSFV-EGFP particles, the duration and location of EGFP expression was determined by fluorescent microscopy. In order to determine whether the fixative used would have an adverse effect on protein expression, control mice infected i.m. with particles were perfused and cryosections prepared (figure 2.7). Since protein expression was detected, cryosections of brain tissue were prepared. Cryosections of brain samples exhibited bright green staining indicative of protein expression (figure 2.8). Protein expression was first detected at 24 hours post-infection, and remained visible through day 14. No protein could be seen at day 21. Detectable EGFP expression was limited to the olfactory bulb region of the brain throughout the time course of the experiment (Table 2.1). The main layers of the olfactory bulb are described in figure 1.11. By overlaying the figure of protein expression under the GFP filter with that of the DAPI filter, we were able to determine where in the olfactory bulbs expression was located, as well as the type of cells were expressing EGFP (figure 2.9). Protein expression was confined to cells surrounding the glomeruli areas of the olfactory bulb. This result was further confirmed by immunohistochemical analyses of olfactory bulb cryosections. In this region, the axons from receptor cells in the olfactory epithelium terminate, and establish synaptic contacts with cells found in the olfactory bulb. No protein was detected in control mice mock-infected with PBS.

2.3.2 Immunohistochemical analyses

To confirm findings that protein expression was in fact restricted to the incoming axons into the olfactory bulbs, olfactory bulb sections taken from mice infected with rSFV-EGFP were labeled for axons, as well as oligodendrocytes. Within the olfactory bulb area, no oligodendrocytes were found to be expressing EGFP. Cells surrounding the glomeruli areas of the olfactory bulb that were expressing EGFP were also positively labeled with the MAP1 antibody (figure 2.10). This area contains the incoming axons from the receptor cells in the olfactory epithelium.

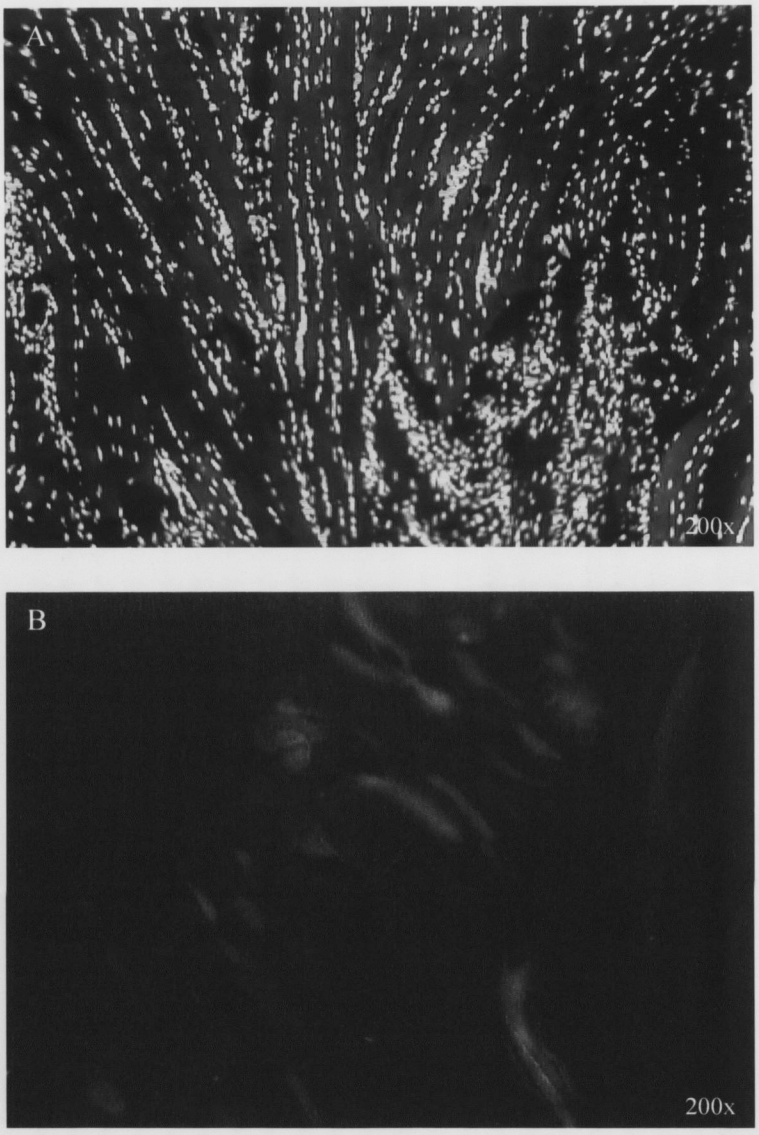

Figure 2.7 Cryosection of perfused TA muscle

In order to determine if perfusing animals with 4% (wt/vol) PFA has an adverse effect on fluorescent protein expression, cryosections of the TA muscle of mice infected i.n. with rSFV-EGFP were prepared as described in section 2.2.2.6.2. Sections were then visualized in a fluorescence microscope. **(A)** Cryosection of TA muscle visualized under a DAPI filter at a wavelength of 400nm. **(B)** Same section now visualized under a GFP filters at 480nm.

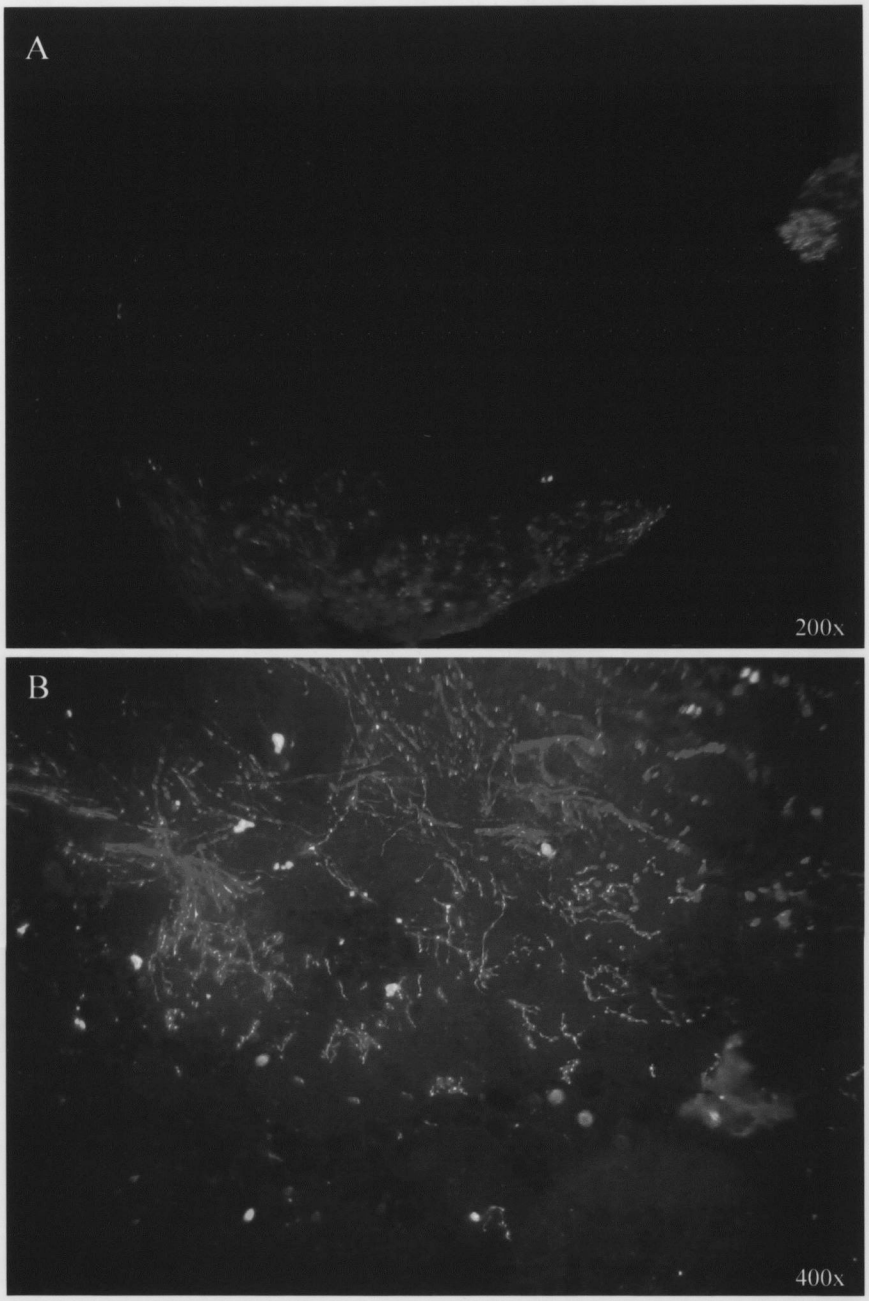

Figure 2.8 Cryosections of brain samples views under GFP filter

Cryosections of brain samples exhibiting bright green staining indicative of protein expression. Brain tissue taken from mice infected i.n. with rSFV-EGFP and post fixed in 4% PFA **(A)** Cryosection prepared from brain tissue taken at 5 dpi, visualized at 200x magnification. **(B)** Cryosection prepared from brain tissue taken at 2 dpi, visualized at 400x magnification.

Table 2.1 Protein expression following rSFV-EGFP infection

Balb/c mice infected i.n. with rSFV-EGFP were sampled at different time points for protein expression. EGFP was visualized by fluorescence microscopy on fixed cryosections prepared from frozen olfactory bulb and remaining brain tissues of infected mice.

Time	Olfactory Bulbs	Brain
16 hpi	0/4[a]	0/4
1 dpi	4/4	0/4
2 dpi	3/5	0/5
3 dpi	4/4	0/4
4 dpi	4/5	0/5
5 dpi	4/5	0/5
6 dpi	5/5	0/5
8 dpi	2/5	0/5
10 dpi	2/3	0/3
14 dpi	1/3	0/3
21 dpi	0/3	0/3

[a] Number of mice positive / number tested

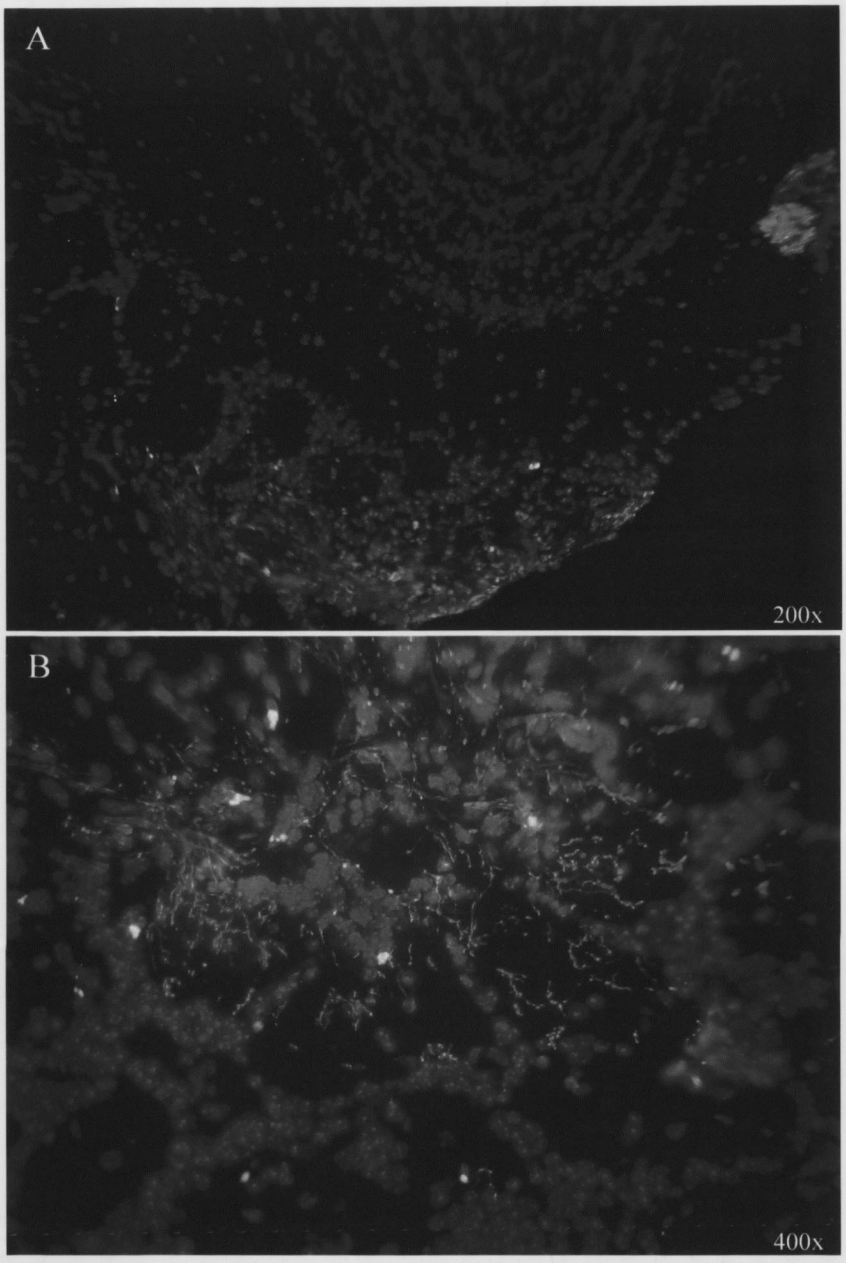

Figure 2.9 Layered images of brain cryosections

Cryosections of brain samples exhibiting bright green staining indicative of protein expression can be seen in figure 2.8. To determine where in the olfactory bulb expression is taking place, an overlay of a section viewed under both the GFP and DAPI filter was composed. **(A)** Cryosection prepared from brain tissue taken at 5 dpi, visualized at 200x magnification. **(B)** Cryosection prepared from brain tissue taken at 2 dpi, visualized at 400x magnification.

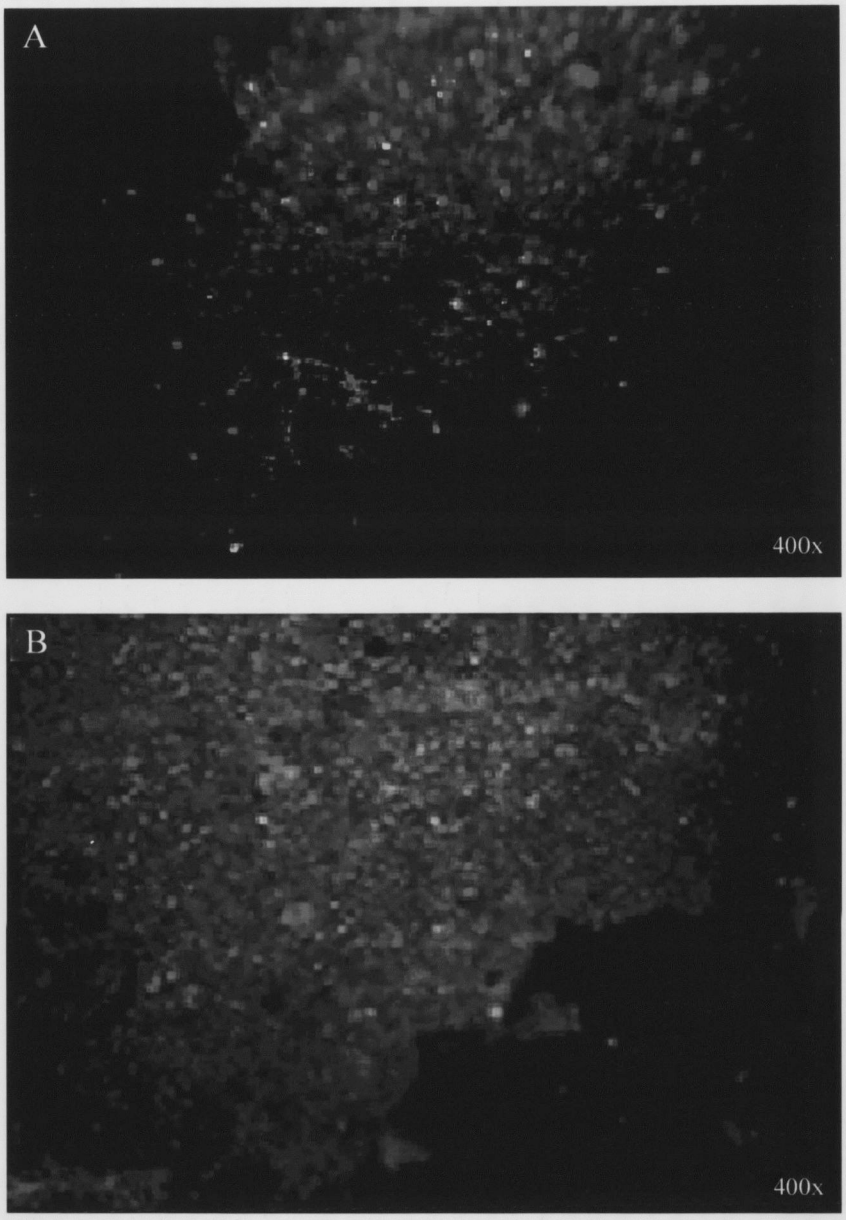

Figure 2.10 Immunohistochemical analyses of brain cryosections

Cryosections of olfactory bulb tissue of mice infected i.n. with rSFV-EGFP. Sections were prepared for immunohistochemistry as described in section 2.2.2.8.2. **(A)** Section labeled with anti-CNPase antibody, oligodendrocytes labeled in red. No oligodendrocytes are expressing EGFP. **(B)** Section labeled with anti-MAP1 antibody, axons labeled in red. Note overlapping of axons and green staining indicative of EGFP expression.

2.3.3 Persistence and location of rSFV-EGFP in mice

RNA from the nasal passages, olfactory bulb, and brains from mice infected i.n. with rSFV-EGFP was isolated at different time points and examined for the presence of vector RNA using both viral nsP3 and EGFP primers. RNA was also isolated from mice infected with SFV4 or PBS mock-infected and used as positive and negative controls, respectively. No bands were visible at any time points for RNA extracted from the olfactory bulbs or remaining areas of the brains of rSFV-EGFP infected mice, with either set of primers. Both RNA's were detected in the nasal passages of infected mice as early as 16 hpi (table 2.2). Maximum RNA expression was detected at 24 hpi. A small amount of RNA was still present at 7 dpi, while no expression was detected at 10 dpi (figure 2.11). RT-PCR performed on tissue taken from PBS mock-infected mice was consistently negative for both set of primers, while samples from SFV4 infected mice were positive for nasal passage, olfactory bulb, and remaining brains only when the SFV-nsP3 primer was used (data not shown).

2.3.4 Pathology in mice following administration of particles and SFV4

In order to establish pathological changes associated with particle administration, mice were infected with either rSFV-EGFP, SFV4 or PBS mock-infected. No pathological changes were observed in brain tissue prepared from rSFV-EGFP or PBS mock-infected mice (figure 2.12). Brain sections of mice infected with SFV4 revealed perivascular cuffing and mild neuronal degeneration at 3 dpi, with massive neuronal necrosis observed at 5 dpi (figure 2.13). These were consistent with previous findings (Balluz *et al,* 1993, Donnelly *et al,* 1997b, Smyth *et al,* 1990). Table 2.3 summarizes pathology data for all animals in the study.

2.4 DISCUSSION

The main aim of the current experiment was to test the feasibility of utilizing the SFV expression vector system for delivery of heterologous genes to the CNS. There has

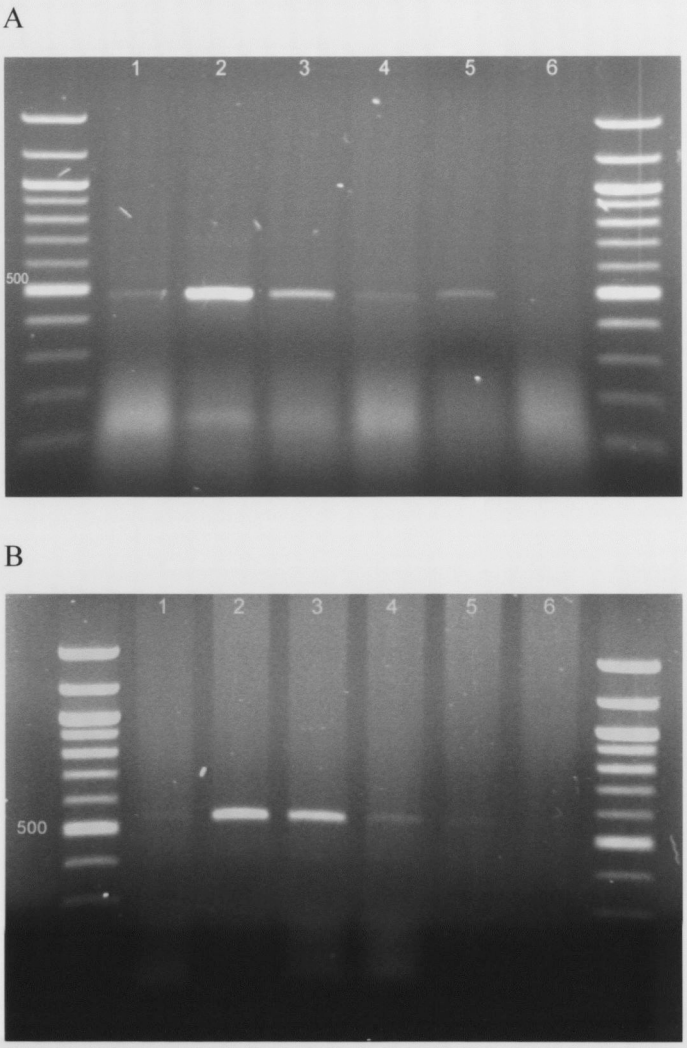

Figure 2.11 RNA expression following i.n. infection with rSFV-EGFP particles

Detection by agarose gel (1.0 % (wt/vol)) electrophoresis (stained with ethidium bromide) was performed for RT-PCR products from total RNA extracted from the nasal passages of infected Balb/c mice. Ten µl of each product was loaded as follows: *Lane 1*. 16 hpi. *Lane 2*. 1 dpi. *Lane 3*. 3 dpi. *Lane 4*. 5 dpi. *Lane 5*. 7 dpi. *Lane 6*. 10 dpi. **(A)** Representative gel of the 482 bp product from the EGFP gene. **(B)** Representative gel of the 520 bp product from the SFV-nsP3 region. In each case the outermost lanes show molecular weight markers (1 kb ladder).

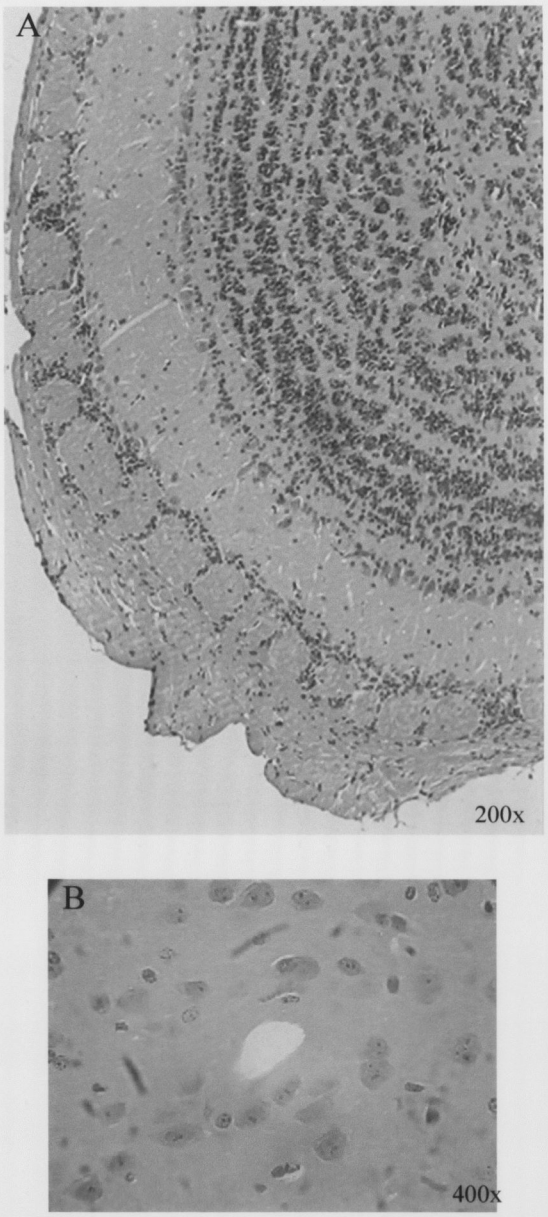

Figure 2.12 Histological staining of rSFV-EGFP infected mice

Histological staining of olfactory bulb from mouse infected i.n. with rSFV-EGFP. The brain was removed at 7 dpi, and post fixed in 10% (vol/vol) formal buffered saline, prior to staining with haematoxylin and eosin as described in section 2.2.2.9.2. **(A)** Olfactory bulb. No abnormalities were found. **(B)** Normal blood vessels, with no cuffing.

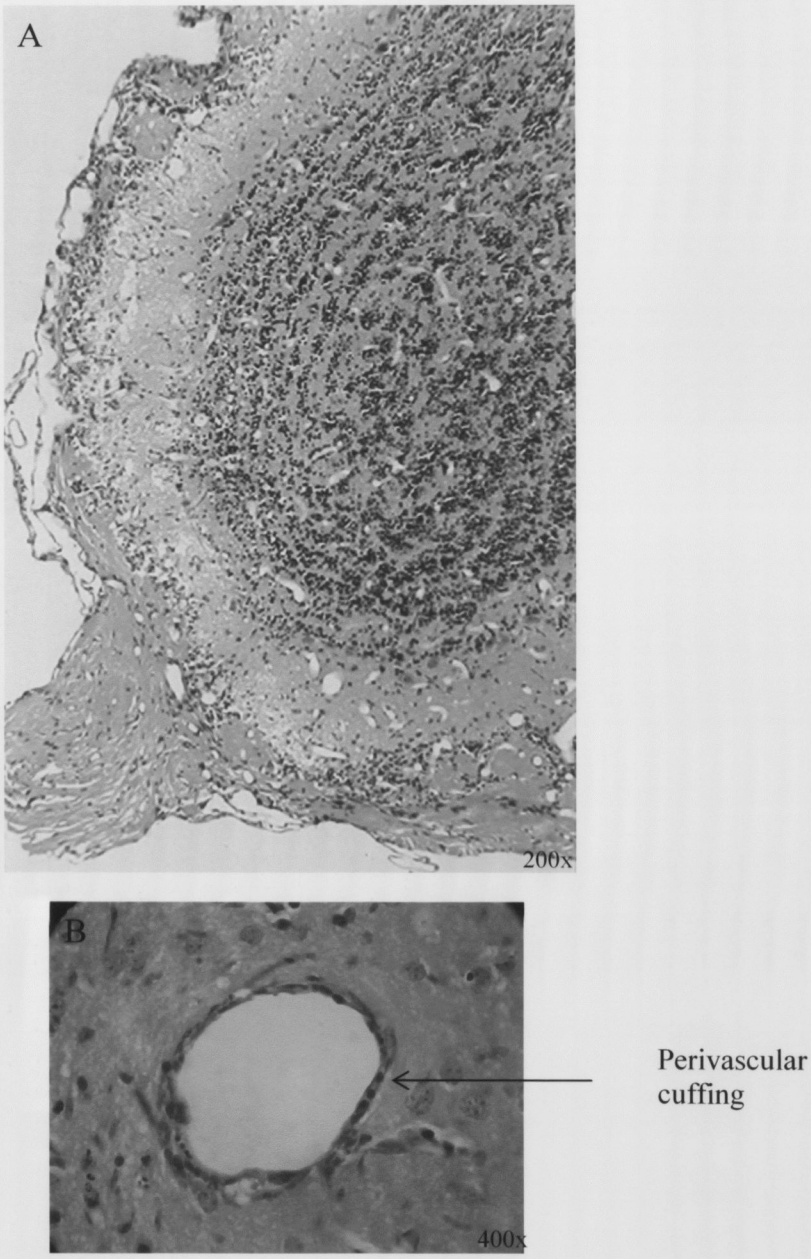

Figure 2.13 Histological staining of SFV4 infected mice

Histological staining of olfactory bulb from a mouse infected i.n. with SFV4. The brain was removed at 5 dpi, and post fixed in 10% (vol/vol) formal buffered saline, prior to staining with haematoxylin and eosin as described in section 2.2.2.9.2. **(A)** Olfactory bulb. Note necrosis of neurons and edema around glomeruli area. **(B)** Perivascular cuffing with lymphocytes.

Table 2.3 Pathological analyses following i.n. administration of virus and vector

Balb/c mice were infected i.n. with either rSFV-EGFP, SFV4, or PBS mock-infected. Paraffin sections of brain and nasal passage tissue were analyzed by routine histology by Professor Brian J. Sheahan (Department of Veterinary Pathology, Faculty of Veterinary Medicine, University College Dublin, Ireland), at different time points.

Sample	Infection	dpi	Mice	Histology results
Nasal P.	rSFV-EGFP	5	1	Occasional intra-epithelial aggregates of neutrophils
Nasal P.	rSFV-EGFP	5	1	NAD[a]
Nasal P.	rSFV-EGFP	5	1	Perivascular lymphocytes in respiratory submucosa
Brain	rSFV-EGFP	5	3	NAD
Nasal P.	rSFV-EGFP	6	1	NAD
Nasal P.	rSFV-EGFP	7	2	Small number of lymphocytes in olfactory submucosa
Nasal P.	rSFV-EGFP	7	1	NAD
Brain	rSFV-EGFP	7	3	NAD
Nasal P.	rSFV-EGFP	8	2	NAD
Nasal P.	rSFV-EGFP	14	2	NAD
Nasal P.	rSFV-EGFP	14	1	Nuclear debris / neutrophils in mucosal glands
Brain	rSFV-EGFP	14	3	NAD
Brain	SFV4	3	3	Perivascular cuffing and neuronal degeneration
Brain	SFV4	5	3	Massive neuronal necrosis
Nasal P.	PBS	5	1	Intraephitelial deposits of necrotic debris
Nasal P.	PBS	5	2	NAD
Brain	PBS	5	3	NAD

[a] No Abnormalities Detected

been extensive research on the neuropathogenisity of the Semliki Forest virus when given i.n. to mice. Damage to the CNS is mainly dependent on viral strain, where virulent strains such as L-10 and SFV4 cause lethal encephalitis, and avirulent strains like the A7 do not kill adult mice; however, they do cause an immune-mediated demyelination of the CNS (Atkins *et al,* 1985, Sammin *et al,* 1999, Sheahan *et al,* 1996). The ability of the virus to replicate in neurons, and oligodendrocytes within the CNS is of key importance to the pathology observed (Balluz *et al,* 1993). Another factor contributing to pathology observed with infection is the pace with which viral multiplication takes place. Virulent strains kill cells at a much faster pace then avirulent strains, therefore the difference in outcome between encephalitis, and demyelination (Atkins *et al,* 1990, Donnelly *et al,* 1997b, Smyth *et al,* 1990).

The SFV vector system has a number of advantages over other vector systems. It is a non-replicating system, where the cloned proteins are expressed transiently during a single round of viral replication. RNA replication occurs in the cytoplasm, so there is no risk of genetic integration in the chromosomes (Liljestrom and Garoff 1991a, Smerdou and Liljeström 1999). Very few viral proteins are expressed by the system, with only a low level expression of non-structural proteins in infected cells. Additionally, the virus has a very broad host-range, and most people have no pre-existing immunity against this vector (Atkins *et al,* 1996, Atkins *et al,* 1999).

By using a vector which expresses only the reporter gene EGFP, it was possible to show that protein encoded by recombinant particles was capable of penetrating the CNS via the olfactory bulb area of the brain, by a non-invasive method, which causes no damage to recipient cells. Protein expressed by the foreign gene inserted into the vector was expressed in the incoming axons from the receptor cells in the olfactory epithelium that terminate in the glomeruli area of the olfactory bulbs. This area is of significance; within it synaptic contacts between the incoming axons, and dendrites from cells within the olfactory bulb are established. Axons from those cells extend to the anterior olfactory nucleus area of the brain. Expression levels of the protein on the CNS were high, especially during the first 48 hours following inoculation. Protein expression was detected in the same locations within the olfactory bulb throughout the time course of the experiment. This finding together with the fact that all RNA transcription took place in the nasal passage of all infected animals, suggests that duration of expression is dependent on the half-life of the protein used, and the viral vector is not traveling any further into the

brain. It is not surprising that EGFP was not seen in any other areas of the brain. Expression of EGFP is localized and typically only found in infected cells, and by its very nature, the protein does not get secreted. The findings also suggest that RNA replication of the viral vector is taking place in the cells of the olfactory mucosa, which have the capability to regenerate themselves if any damage is caused, as is the case in any viral infection of the upper respiratory tract. Viral RNA persisted only for 7 days in infected mice following inoculation, which was consistent with previous findings (Morris-Downes *et al,* 2001a), as opposed to dispersing in the host and persisting for many weeks, which is the case for DNA vectors (Donnelly *et al,* 1997a). Histological analyses of brain tissue of mice infected i.n. with rSFV-EGFP showed no pathology associated with particle administration. Infected tissue remained healthy for the entire duration of the experiment. This is not the case for vector administration by the i.c. route, where cells are routinely damaged by physical trauma due to the injection procedure.

Many studies have been conducted utilizing different viral vectors for delivery into the CNS with mixed results. A modified herpes simplex virus (HSV-1) showed the vector able to infect neurons within the cortex, thalamus, and striatum of rats following stereotactic injection. Protein expression was reported for up to 5 weeks, and though the vector alone caused no damage, tissue damage was seen as a result of infection method (Sandler *et al,* 2002). Other studies utilizing HSV-1 vectors delivered to the CNS by stereotactic means have found similar results in that a long lasting and even high levels of expression was detected, with some damage to recipient cells (Fukuda *et al,* 2003, Lilley *et al,* 2001). Adeno-associated virus vectors have also been used for gene delivery into the CNS. Researchers also reported long-term expression of protein following delivery into different regions of the brain by stereotactic means (Klein *et al,* 1999, Peel *et al,* 1997, Peel and Klein 2000). Gene transfer into the CNS has also been conducted using recombinant lentivirus vectors. In one particular study, utilizing EGFP, researchers demonstrated transgene expression for over 3 months, following injections into the striatum and hippocampus of the mouse brain (Blomer *et al,* 1997, Lai and Brady 2002). Though most researchers were able to deliver genes to different areas to the CNS, tissue damage was noted, not as a result of the vector, but as a result of mechanical damage from injection process.

In conclusion, it is clear that new methods for gene delivery to the CNS are needed. The present study shows that SFV recombinant particles are capable of penetrating the

CNS after intranasal infection via the olfactory bulb by a novel non-invasive method. This, combined with previous studies that have demonstrated the safety and efficacy of rSFV vectors (Morris-Downes *et al,* 2001a) demonstrates they are potential candidates to be developed as therapeutic agents for the CNS.

Chapter 3

Cloning and in-vitro expression of IL-4 and IL-10 in the SFV expression vector system

3.1 INTRODUCTION

Once established that the SFV vector system is capable of expressing its cloned protein in the olfactory bulb area of the CNS, it was necessary to determine how other genes would behave under the same system. Though a good marker for protein expression, EGFP is not suitable to determine effectiveness when used as a therapeutic gene for autoimmune diseases. EGFP is immunologically inactive, expressed locally on infected cells, and it does not get secreted. Cytokines are secreted low molecular weight soluble proteins, which act as chemical communicators between cells. It has been demonstrated that *in vitro* cytokines are capable of causing changes in cell proliferation, differentiation, and movement even at picomolar concentrations (Callard and Gearing 1994). In order to establish how cytokine delivery by the vector system could affect the course of neurological disorders, such as EAE, two T_H2 producing cytokines were cloned into the vector system. A third cytokine was cloned into the SFV vector system by M.M. Morris-Downs, and utilized in this study. Since the main aim of the project was to use the SFV vector system to treat EAE, two cytokines frequently used in the treatment of EAE were selected.

IL-10 is a multifunctional cytokine with diverse effects on most hemapoietic cell types. It can be expressed by a variety of cells in response to an activation stimulus. It is most commonly described as a regulatory cytokine since it plays a major role in limiting and terminating inflammatory responses (Moore *et al,* 2001). This mechanism is down regulating the production of pro-inflammatory cytokines, such as IL-1 and TNF, and preventing uncontrolled T-cell-mediated tissue destruction. In doing so, it exerts synergistic activities on inflammatory pathways and processes (Harber *et al,* 2000, Moore *et al,* 2001). IL-4 is one of the key cytokines in determining whether a T_H1 or T_H2 response develops. *In vitro*, IL-4 stimulates growth of T and B-cells, deactivates inflammatory macrophages and regulates the induction of type 2 cells, in addition to inhibiting the development of type-1 cells (Harber *et al,* 2000, McKenzie *et al,* 1993, McKenzie 2000, Mossman and Coffman 1989). TGF-β1, also cloned into the SFV vector system, is a potent immunoregulatory cytokine. It has the ability to both modulate the production and antagonize the response of cells to inflammatory cytokines. It has also been implicated in suppression of primary autoimmune disease and in mediating the effects of tolerance (D'Orazio and Niederkorn 1998, Letterio and Roberts 1998). All three

mentioned cytokines: IL-10, IL-4 and TGF-β1, can be easily detected in mice following infection with SFV. IL-10 and IL-4 RNA detected in spleens of infected mice were used for cloning and incorporation into the rSFV vector system. This chapter describes how each was cloned and incorporated into the SFV vector system, and experiments to detect secretion following infection of different cell lines.

3.2 EXPERIMENTAL PROCEDURES

3.2.1 NEW MATERIALS

3.2.1.1 Cell Lines

In addition to BHK-21, the cell lines L-929 and Cos-7 were obtained from the European Collection of Animal Cell Culture (ECACC) (Salisbury, Wiltshire, UK), and the cell line Balb-3T3 was obtained from ATCC. DMEM medium and sodium pyruvate were from Gibco.

3.2.1.2 Expression Vectors

The SFV expression vector, pSFV-1 which contains the 4 non-structural SFV proteins as well as a 3' MCS to facilitate insertion of the heterologous gene was a gift from Prof. P. Liljeström. A SFV vector expressing TGF-β was obtained from M.M. Morris-Downes, rSFV-TGFb.

3.2.1.3 Molecular Biology Reagents

The following primers from MWG were used:

Murine IL-10 F	5'-GTAGGATCCACGAGCACCATGCCTGGCTCAGCA-3'
Murine IL-10 R	5'-GCCGGATCCCGCTTAGCTTTTCATTTTGATCAT-3'
Murine IL-4 F	5'-TATGGATCCAGCACCATGGGTCTCAACCCCCAG-3'

Murine IL-4 R	5'-CGCGGATCCGACCTACGAGTAATCCATTTGC -3'
Insert F	5'-GGCACACAGAATTCTGATTGG-3'
Insert R	5'-CGCTGCGTAGGGATGTAATTCAATTAATTACCCG-3'
Mouse β-actin F	5'-GTGGGCCGCTCTAGGCACCAA-3'
Mouse β-actin R	5'-CTCTTTGATGTCACGCACGCTTTC-3'

The restriction enzymes *BamHI*, *EcoRV*, *BSU36I*, and *XmnI* were from NEB, Shrimp Alkaline Phosphatase (SAP) was from Roche (Penzberg, Germany), T4 DNA ligase from Promega, and quick ligation kit from NEB. The PCR purification kit, nucleotide extraction, and the gel extraction kit were from QIAGEN Ltd. DNA molecular weight markers XIV and XVII were from Roche. A 100 bp DNA ladder was from NEB.

3.2.1.4 Mice

Male Balb/c mice aged 40-60 days were obtained from the Bio Resources unit. Mice were maintained in accordance with the principles outlined in S1 17/94 European Communities regulations 1994, for care and use of laboratory animals. Syringes (1.0 ml) and needles, (25G), were from Becton Dickenson.

3.2.1.5 Antibodies

Purified rat anti-mouse IL-4 monoclonal antibody, purified rat anti-mouse IL-10 monoclonal antibody, and purified rat anti-mouse, human, pig TGFβ monoclonal antibody were obtained from BD PharMingen (BD Biosciences). The VectaStain Elite ABC kit containing blocking serum, biotinylated antibody, and VECTASTAIN reagent was from Vector Laboratories Inc. Hydrogen Peroxide (H_2O_2) was from BDH.

3.2.1.6 Enzyme Linked Immunoabsorbant Assay

The OptEIA mouse IL-10 set, mouse IL-4 set and human TGF-β set were from BD PharMingen. The substrate 3,3',5'5-Tetramethylbenzidine (TMB) was from Sigma. All

ELISA plates were rinsed on a MultiWash II washer from Tri Continent, and absorbance read using a Multiskan RC reader from ThermoLabsystems. IL-10 coating buffer: 0.2 M sodium phosphate (11.8 g Na_2HPO_4, 16.1 g NaH_2PO_4 in 1 L H_2O; pH 6.5); IL-4 and TGF-β coating buffer: 0.1 M Carbonate (8.40 g $NaHCO_3$, 3.56 g Na_2CO_3 in 1 L H_2O; pH 9.5). Assay diluent: PBS with 10% (vol/vol) heat inactivated fetal bovine serum. Wash buffer: PBS with 0.05% (vol/vol) Tween 20.

3.2.1.7 Western blot

PVDF membrane and BM chemiluminescence blotting substrate (POD) were from Roche. Acrylamide/Bis [30% (w/v) Acrylamide : 0.8% (w/v) Bis-Acrylamide stock solution] and all other chemicals used were from Sigma. X-ray film and automated developer (X-OMAT 1000 Processor) were from Kodak.

3.2.1.8 Miscellaneous

Trypan Blue, Tween 20, 3,3'-Diaminobenzidine Tetrahydrochloride (DAB), and methyl green were from Sigma.

3.2.2 METHODS

3.2.2.1 rSFV-IL10 cloning

For cloning the IL-10 gene into the SFV expression vector, pSFV-1, a strategy was designed using the unique *BamHI* restriction site in the pSFV-1 MCS. This strategy is illustrated in figure 3.1.

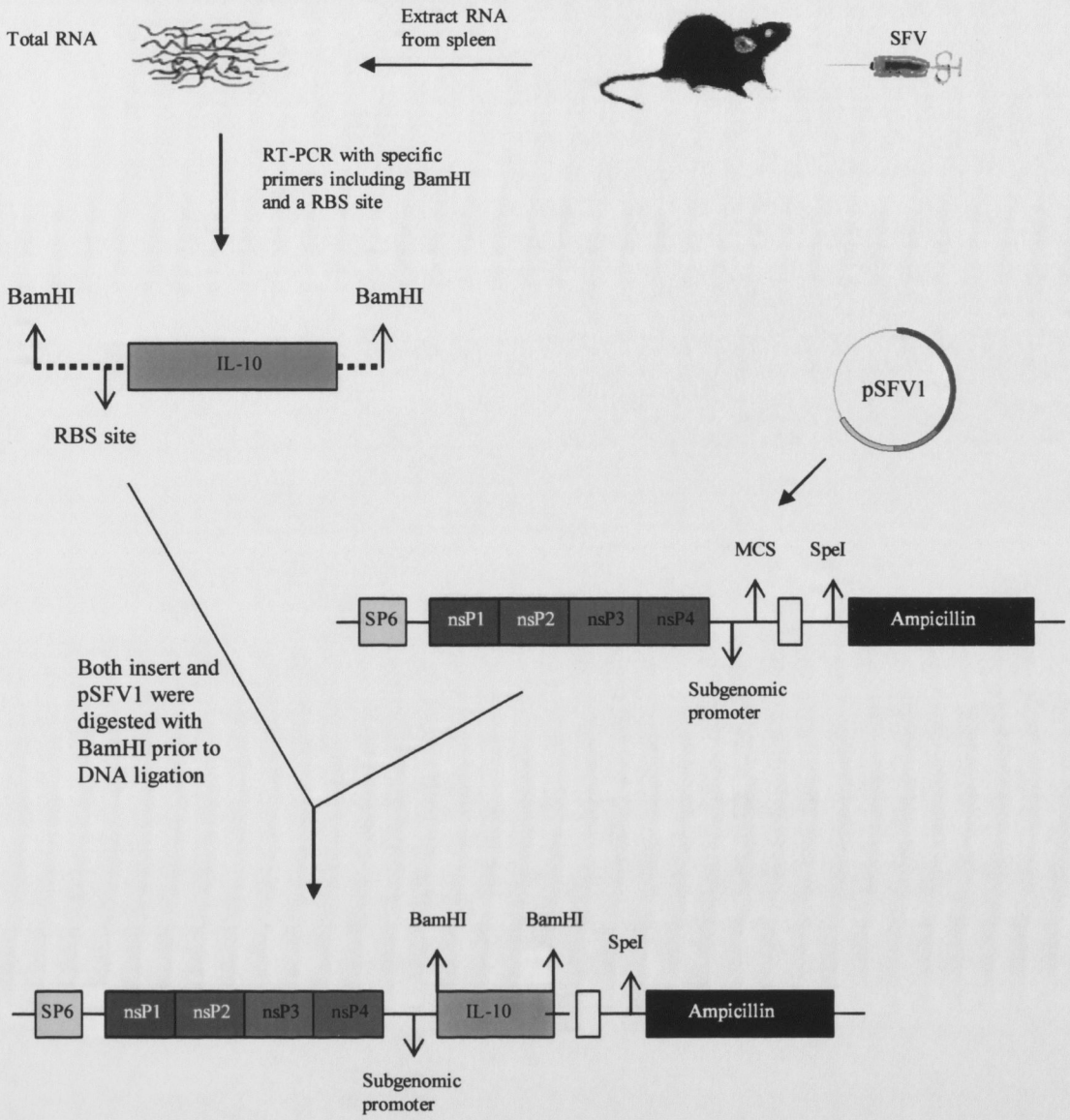

Figure 3.1 Strategy for cloning

Mice were infected i.p. with SFV, and RNA from infected spleens removed. RT-PCR with primers specific for the coding region of IL-10 including the restriction site *BamHI* and a RBS site was used to produce the insert DNA used for ligation. The plasmid pSFV-1 was digested with *BamHI* (found in the MCS) dephosphorylated using SAP, and ligated to insert DNA IL-10. The resultant clone was screened for presence of insert by restriction enzyme, and correct clones sent for sequencing.

3.2.2.1.1 DNA Amplification

Total RNA was isolated from the spleens and brains of Balb/c mice infected i.p. at 3, 5, 7, and 10 dpi (4 mice per time point), as described in section 2.2.2.7.2. The integrity of this RNA was checked using primers specific for mouse β-actin and mouse GAPDH as described in section 2.2.2.7.3 (figure 3.2). RNA concentration was measured on a GeneQuant DNA/RNA spectrophotometer. To facilitate cloning of IL-10 into the pSFV-1 vector, the forward primer was designed to include the first 15 nucleotides of the coding region of the IL-10 gene (figure 3.3). In addition, this primer also incorporated the native SFV ribosome-binding site (RBS) sequence, and a *BamHI* restriction site, to facilitate ligation with pSFV-1. The sequence of the reverse primer includes the final 21 nucleotides of the coding region of the IL-10 gene, and a *BamHI* restriction site. The sequence of primers used in IL-10 amplification is indicated with the *BamHI* sites in *italics*, the RBS sequence underlined, and the IL-10 start codon in bold:

IL-10 F 5'-GTA*GGATCC*ACGAGCACC**ATG**CCTGGCTCAGCA-3'

IL-10 R 3'-GCC*GGATCC*CGCTTAGCTTTTCATTTTGATCAT-5'

Standard PCR reactions were carried out as described in section 2.2.2.7.3. Since more cDNA was synthesized from spleens taken from day 5, these were used to clone IL-10 (figure 3.3). RNA was amplified using different temperature profiles, in order to achieve a maximum amplification of product. The following temperature profile yielded the highest amplification: 2 min at 95°C, 3 min at 80°C, followed by 30 cycles of incubations at 95°C for 30 s, 49°C for 30 s 72°C for 4 min with a final extension of 15 min at 72°C. PCR products were analyzed by electrophoresis of a 10 μl aliquot on a 1.0% (wt/vol) agarose gel.

3.2.2.1.2 Preparation of the IL-10 insert

In order to achieve a very concentrated product, following PCR amplification, the 537 bp IL-10 fragment was purified using a combination of the QIAGEN PCR purification and gel extraction kits. Both kits rely on the selective binding properties of a silica-gel membrane in a spin-column to bind the DNA. Special buffers are then utilized to remove impurities, and recover DNA. The products of 12 separate RT-PCR reactions were

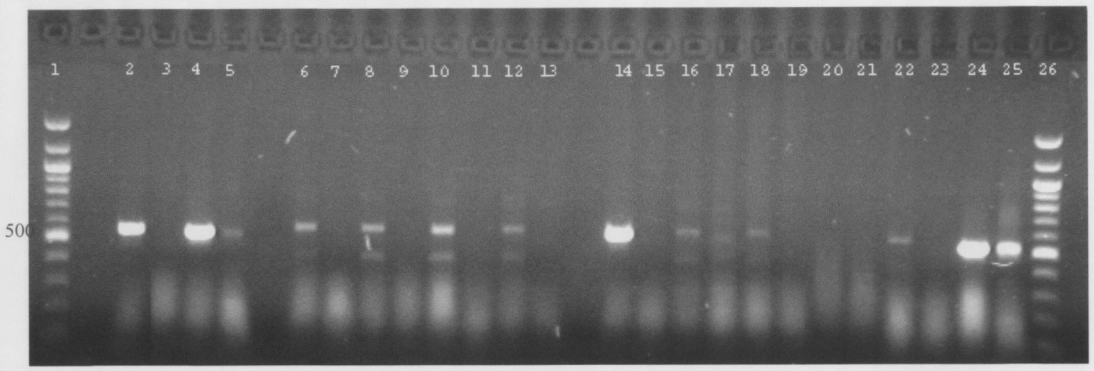

Figure 3.2 RT-PCR on spleen samples for IL-10

Total RNA was isolated from spleens (4 each) of Balb/c mice infected i.p. at 5 and 7 dpi. The integrity of this RNA was checked by RT-PCR using primers specific for mouse β-actin and mouse GAPDH. The presence of the IL-10 gene transcript was determined using specific primers, as outlined in section 3.2.2.1.1. PCR products were analyzed by electrophoresis of a 10 μl aliquot on a 1.0% (wt/vol) agarose gel. In each instance, first sample (lane) represents RT-PCR carried out with all reagents, while second sample (lane) represents internal RT-PCR controls where no reverse transcriptase was added. *Lane 1;* 1 kp DNA ladder. *Lanes 2 and 3;* mouse β-actin at 5 dpi. *Lanes 4 and 5;* mouse GAPDH at 5 dpi. *Lanes 6 and 7;* IL-10, spleen 1 at 5 dpi. *Lanes 8 and 9;* IL-10, spleen 2 at 5 dpi. *Lanes 10 and 11;* IL-10, spleen 3 at 5 dpi. *Lanes 12 and 13;* IL-10, spleen 4 at 5 dpi. *Lanes 14 and 15;* mouse β-actin at 7 dpi. *Lanes 16 and 17;* IL-10, spleen 1 at 7 dpi. *Lanes 18 and 19;* IL-10, spleen 2 at 7 dpi. *Lanes 20 and 21;* IL-10, spleen 3 at 7 dpi. *Lanes 22 and 23;* IL-10, spleen 4 at 7 dpi. *Lanes 24 and 25;* mouse GAPDH at 7 dpi. *Lane 26;* 1 kp DNA ladder. Higher amounts of IL-10 were detected in samples taken from spleens at 5 dpi.

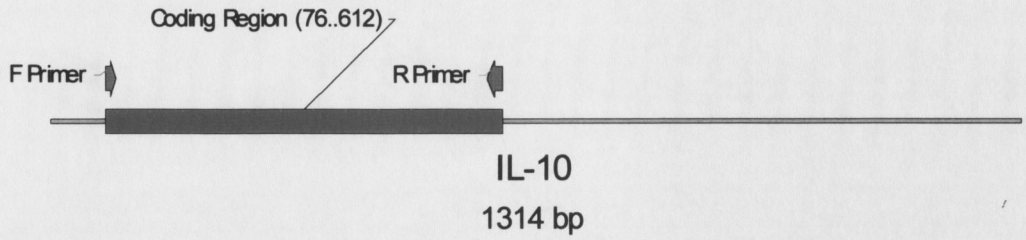

atgcctggctcagcactgctatgctgcctgctcttactgactggcatgaggatcagcaggggccagtacagccgggaagacaata
actgcacccacttcccagtcggccagagccacatgctcctagagctgcggactgccttcagccaggtgaagactttctttcaaaca
aaggaccagctggacaacatactgctaaccgactccttaatgcaggactttaagggttacttgggttgccaagccttatcggaaatg
atccagttttacctggtagaagtgatgccccaggcagagaagcatggcccagaaatcaaggagcatttgaattccctgggtgagaa
gctgaagaccctcaggatgcggctgaggcgctgtcatcgatttctcccctgtgaaaataagagcaaggcagtggagcaggtgaa
gagtgattttaataagctccaagaccaaggtgtctacaaggccatgaatgaatttgacatcttcatcaactgcatagaagcatacatg
atgatcaaaatgaaaagctaa

Figure 3.3 IL-10 gene sequence

The coding region of the mouse IL-10 gene is a 537 bp sequence, which contains the precursor and mature form of the gene required for production and secretion of protein by cells. The forward primer was designed to include the first 15 nucleotides of this region, as well as a *BamHI* restriction site and the native SFV ribosome-binding site. The reverse primer was designed to include the final 21 nucleotides of the coding region of the IL-10 gene, and a *BamHI* restriction site.

purified using the QIAGEN PCR purification kit. To each PCR reaction mix, 5 volumes of buffer PB were added and mixed (500 µl of buffer to 100 µl PCR reaction). This buffer allows for binding of the PCR product and removal of primers of up to 40 nucleotides. Samples were added to QIAquick column (4 PCR reactions per column) and centrifuged (10,000g, 1 min) to allow for binding of DNA. The column was then washed with 750 µl of buffer PE to remove unwanted primers and impurities, and centrifuged (10,000g, 1 min) twice. Final DNA was eluted in 50 µl of nuclease-free water per column by centrifugation (10,000g, 1 min). To further concentrate the DNA product all 4 IL-10 tubes were pooled (200 µl), mixed with 35 µl of loading dye, and run on a 1.0% (wt/vol) agarose gel for purification using the QIAGEN gel extraction kit (figure 3.4A). DNA fragments were excised from the agarose gel with a clean scalpel, weighed and mixed with buffer QG at a rate of 3 volumes of buffer to 1 volume of gel (300 µl of buffer to 100 µg of gel). The mixture was incubated for 10 min at 50°C (tubes mixed every 2-3 min). This buffer solubilizes the agarose gel slice, and provides appropriate conditions for binding of DNA to the silica membrane. Once the gel was completely dissolved, isopropanol was added and mixed (1 volume per volume of gel). The mixture was added to 2 QIAquick columns and centrifuged (10,000g, 1 min). The columns were washed with 500 µl of buffer QG to remove all traces of agarose, and centrifuged (10,000g, 1 min). They were then further washed with 750 µl of buffer PE and centrifuged (10,000g, 1 min) twice. Purified DNA was eluted in 30 µl of nuclease-free water per column, and pooled (figure 3.4B). IL-10 DNA was digested with *BamHI* to create the necessary 'sticky' ends. A total of 4 reactions with the following mixture were digested at 37°C for 2 h: 15 µl IL-10 DNA, 2 µl water, 2 µl 10X NEBuffer *BamHI* (150 mM NaCl, 10 mM Tris-Hcl, 10 mM $MgCl_2$, 1 mM dithiothreitol pH 7.9), and 20 U *BamHI*. Digested reactions were purified using the QIAGEN nucleotide removal kit. Pooled digested DNA (80 µl) was mixed with 800 µl buffer PN, which promotes the absorption of both oligonucleotides more then 17 bases and DNA fragments up to 10 kb to the silica membrane. The mixture was added to a MinElute column, and centrifuged (6,000g, 1 min) to allow binding of DNA. The column was then washed with buffer PE and centrifuged (6,000g, 1 min), then further centrifuged (10,000g, 1 min). Purified IL-10 DNA was eluted in 10.5 µl of nuclease-free water. Final product was analyzed and quantified by electrophoresis of a 0.5 µl aliquot on a 1.2% (wt/vol)

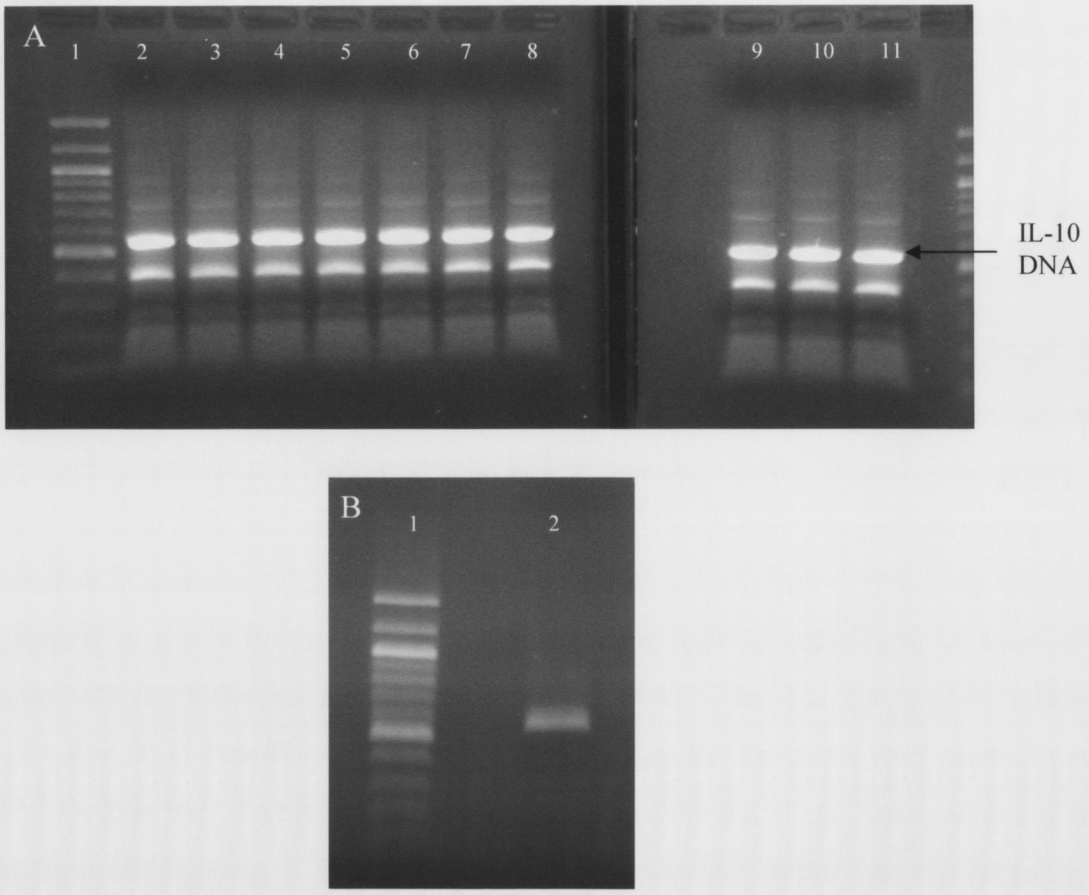

Figure 3.4 Purified IL-10 DNA

Following PCR amplification of IL-10 DNA was purified using a PCR purification kit (outlined in section 3.2.2.1.2). **(A)** Purified IL-10 insert was further concentrated using a gel extraction kit (as outlined in same section), by excising pooled product from a 1.0% (wt/vol) agarose gel. *Lane 1;* 100 bp DNA ladder. *Lanes 2-11;* PCR purified IL-10 DNA **(B)** Excised fragments were again purified and concentrated prior to digestion with BamHI. Final product seen on a 1.0% (wt/vol) agarose gel, stained with ethidium bromide. *Lane 1;* 100 bp DNA ladder. *Lane 2;* 1.0 µl purified IL-10 DNA.

agarose gel (figure 3.5). A concentration of approximately 120 ng/μl of DNA was measured by comparison to a 500 bp DNA ladder.

3.2.2.1.3 Preparation of recombinant SFV expression vector

The 11.3 kbp plasmid pSFV-1 vector containing a MCS (*BamHI-XmaI-SmaI*) for use in the construction of recombinant plasmids, and an ampicillin resistance site for bacterial screening was used to prepare the SFV expression vector. Plasmid was grown in DH5α competent cells and purified using the QIAGEN midi-prep plasmid purification kit as described in sections 2.2.2.4.2 and 2.2.2.4.4, respectively. pSFV-1 DNA was digested with *BamHI* to create the necessary 'sticky' ends for ligation with IL-10. A total of 6 reactions with the following mixture were digested at 37°C for 2 h: 1.4 μl pSFV1 DNA, 15.6 μl water, 20 U *BamHI*, and 2 μl 10X NEBuffer *BamHI*. Reactions were stored frozen at -20°C for later use. To remove the phosphate group from the 5' end, thus preventing the vector from self-ligating, 1 U of SAP and 0.9 μl 10X SAP buffer was mixed to each previously digested pSFV1 DNA and incubated at 37°C for 30 min. SAP was then inactivated by heating at 65°C for 15 min. DNA was then purified using a QIAGEN nucleotide removal kit as described in section 2.2.2.5.2 (1 QIAquick column was used), and eluted in 40 μl of nuclease-free water. The resulting digested plasmid was analyzed by electrophoresis of a 1 μl aliquot on a 0.8% (wt/vol) agarose gel (figure 3.6). Final DNA concentration was approximately 150 ng/μl as measured by comparison to a 1 kb DNA ladder.

3.2.2.1.4 DNA ligation

Linearized pSFV-1 was ligated to the purified IL-10 DNA at a ratio of 1:5 vector to insert. A ligation mixture containing 1 μl of pSFV1, 12 μl of IL-10, 10 μl 2X quick ligase buffer (132 mM Tris-HCl, 20 mM $MgCl_2$, 2 mM dithiothreitol, 2mM ATP and 15% polyethylene glycol (PEG 6000) pH 7.6), and 1 μl quick T4 DNA ligase were combined in a 21 μl reaction mix and incubated for 5 min at room temperature. The mixture was

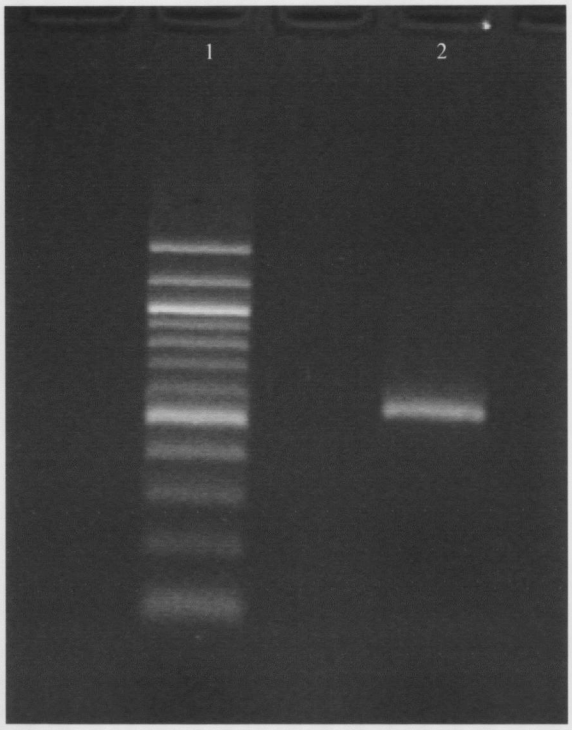

Figure 3.5 Digested IL-10 DNA

Purified IL-10 DNA insert was digested with BamHI for ligation to pSFV1 as outlined in section 3.2.2.1.2. *Lane 1;* 0.5 μg of 100 bp DNA ladder. *Lane 2;* 0.5 μl Digested IL-10. Visualized on a 1.0% (wt/vol) agarose gel, stained with ethidium bromide. IL-10 DNA was estimated to contain a concentration of 120 μg/μl by comparing it to the DNA ladder.

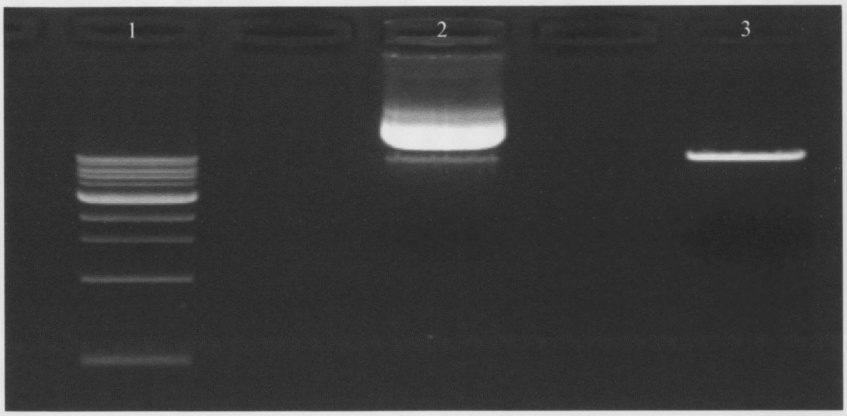

Figure 3.6 pSFV1

The pSFV-1 plasmid was grown on competent cells, and purified as outlined in section 3.2.2.1.3. Clean DNA was then digested with BamHI and prepared for ligation to both IL-10 and IL-4. *Lane 1;* 0.5 μg of 1 kb DNA ladder. *Lane 2;* 1.0 μl midi-prep pSFV-1. *Lane 3;* 1.0 μl BamHI digested pSFV-1. Visualized on a 1.0% (wt/vol) agarose gel, stained with ethidium bromide. pSFV-1 DNA was estimated to contain a concentration of 150 μg/μl by comparison to the DNA ladder.

briefly chilled on ice, and stored frozen at -20°C. A control ligation was carried out using only pSFV1 DNA.

3.2.2.1.5 Transformation of bacterial cells

Transformation of competent cells was performed as outlined in section 2.2.2.4.2, with the following modification: all 21 µl ligation mixture as well as control ligation mixture was added to competent cells.

3.2.2.1.6 Screening for recombinant plasmids by restriction digestion

To confirm the presence and orientation of insert, 8 putative positive clones grown on ampicillin agar plates were inoculated into 10 ml L-broth containing 100 µg/ml ampicillin and incubated shaking overnight at 37°C. Plasmids were purified using the QIAGEN miniprep plasmid purification kit, as described in section 2.2.2.4.3. After purification, plasmids were digested with *BamHI* as previously described, and run on 0.8% (wt/vol) agarose gels. Five colonies were found to contain an insert (figure 3.7). These were further digested with *BSU36I* and *EcoRV* to check insert orientation. The reaction mixture contained 1 µl plasmid DNA, 4 µl buffer Neb 3 (100 mM NaCl, 50 mM Tris-Hcl, 10 mM $MgCl_2$, 1 mM dithiothreitol pH 7.9), 10 U *Bsu36I* and 20 U *EcoRV* in a total volume of 20 µl. Digested products were analyzed by electrophoresis of a 1 µl aliquot on a 0.8% (wt/vol) agarose gel. The following 3 fragment sizes should be detected for correct orientation: 4097, 4639, and 2852 nucleotides. Four out of the five plasmids contained the insert in the correct orientation (figure 3.8).

3.2.2.1.7 Sequencing of pSFV1-IL10

All 4 clones with the correct insert were sent for sequencing to LARK technologies Inc. (UK) using insert primers. The sequenced obtained was blasted against the NCBI database, and then paired to the original sequence for the coding region of IL-10 obtained

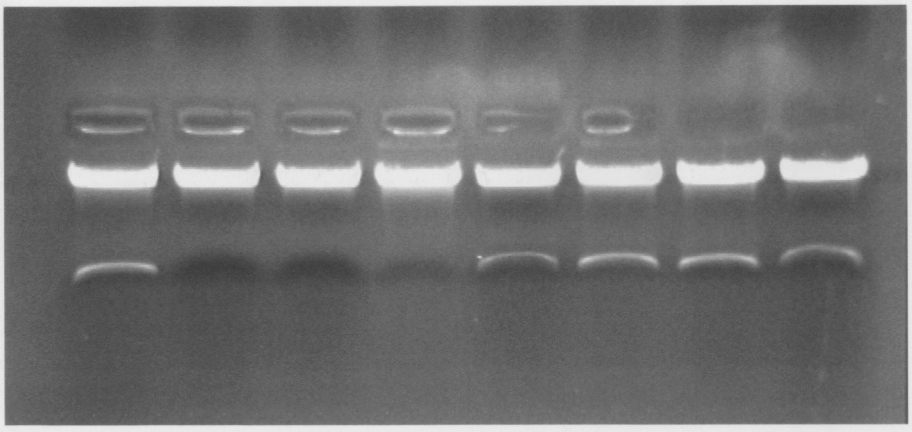

Figure 3.7 IL-10 insert in pSFV1

To confirm presence of IL-10 insert into pSFV1, putative clones grown on ampicillin agar plates, were digested with BamHI as outlined in section 3.2.2.1.6, and run on 0.8% (wt/vol) agarose gel. Out of a possible 8, 5 colonies were found to contain an insert. These were labeled as IL-10 clones 1-5.

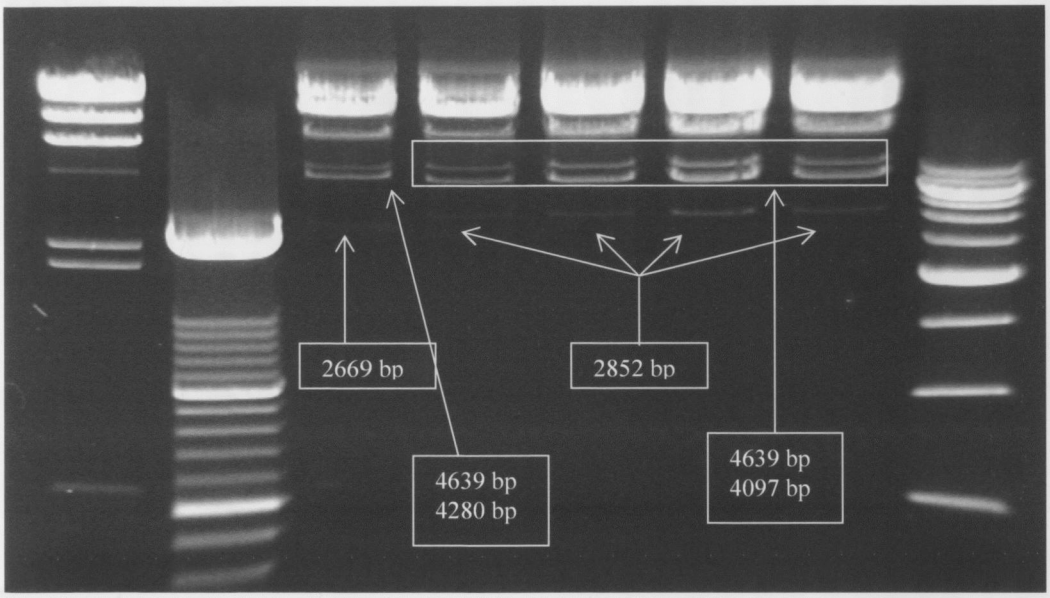

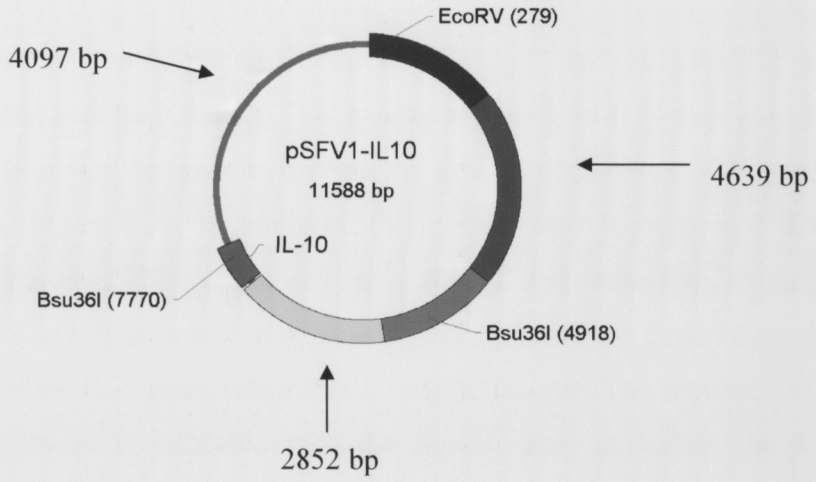

Figure 3.8 IL-10 insert orientation in pSFV1

To confirm the orientation of the IL-10 insert in pSFV1, IL-10 clones 1-5 were double digested with BSU36I and EcoRV as outlined in section 3.2.2.1.6. *Lane 1*; Lambda (HindIII) DNA molecular weight marker. *Lane 2;* DNA molecular weight marker XIV. *Lanes 3-7;* IL-10 clones 1-5 *Lane 8*; DNA molecular weight marker XVII. 0.8% (wt/vol) agarose gel, stained with ethidium bromide. Correct fragment sizes for clones were 4639, 4097, and 2852 bp, which were found in clones 2-5.

from the GenBank database. A glycerol stock was prepared from the correct clone as described in section 2.2.2.4.3.

3.2.2.2 rSFV-IL4 cloning

For cloning the IL-4 gene into the SFV expression vector, pSFV-1, a similar strategy to that used for cloning IL-10 was designed also using the unique *BamHI* restriction site in the pSFV-1 MCS.

3.2.2.2.1 DNA Amplification

The same RNA used previously for amplifying IL-10 was tested for presence of IL-4, as described in section 3.2.2.1.1. To facilitate cloning of IL-4 into the pSFV-1 vector, the forward primer was designed to include the first 18 nucleotides of the coding region of the IL-4 gene (figure 3.9). In addition, this primer also incorporated the native SFV ribosome-binding site (RBS) sequence, and a *BamHI* restriction site, to facilitate ligation with pSFV-1. The sequence of the reverse primer included the final 22 nucleotides of the coding region of the IL-4 gene, and a *BamHI* restriction site. The sequence of primers used in IL-4 amplification is indicated with the *BamHI* sites in *italics*, the RBS sequence underlined, and the IL-4 start codon in bold:

IL-4 F 5'- TAT*GGATCC*AGCACC**ATG**GGTCTCAACCCCCAG-3'

IL-4 R 3'- CGC*GGATCC*GACCTACGAGTAATCCATTTGC-5'

Standard PCR reactions were carried out as described in section 2.2.2.7.3. Spleens from day 7 were used to synthesize cDNA. RNA was amplified using same temperature profile used for amplifying IL-10 (2 min at 95°C, 3 min at 80°C, followed by 30 cycles of incubations at 95°C for 30 s, 49°C for 30 s, 72°C for 4 min with a final extension of 15 min at 72°C). PCR products were analyzed by electrophoresis of a 10 µl aliquot on a 1.0% (wt/vol) agarose gel.

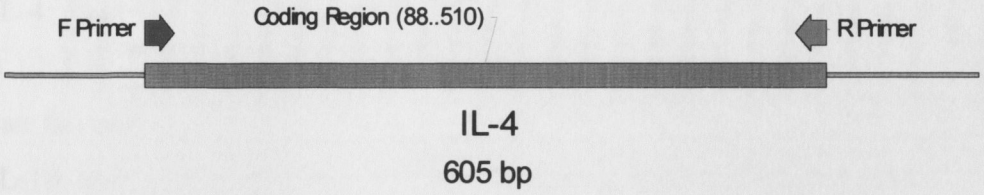

atgggtctcaacccccagctagttgtcatcctgctcttctttctcgaatgtaccaggagccatatccacggatgcgacaaaaatcactt
gagagagatcatcggcattttgaacgaggtcacaggagaagggacgccatgcacggagatggatgtgccaaacgtcctcacag
caacgaagaacaccacagagagtgagctcgtctgtagggcttccaaggtgcttcgcatattttatttaaaacatgggaaaactccat
gcttgaagaagaactctagtgttctcatggagctgcagagactctttcgggcttttcgatgcctggattcatcgataagctgcaccatg
aatgagtccaagtccacatcactgaaagacttcctggaaagcctaaagagcatcatgcaaatggattactcgtag

Figure 3.9 IL-4 gene sequence

The coding region of the mouse IL-4 gene is a 423 bp sequence, which contains the precursor and mature form of the gene required for production and secretion of protein by cells. The forward primer was designed to include the first 18 nucleotides of this region, as well as a *BamHI* restriction site and the native SFV ribosome-binding site. The reverse primer was designed to include the final 22 nucleotides of the coding region of the IL-10 gene, and a *BamHI* restriction site.

3.2.2.2.2 Preparation of the IL-4 insert

To achieve a highly concentrated product following PCR amplification, the 423 bp IL-4 fragment was purified in the same manner used for IL-10, as outlined in section 3.2.2.1.2. Purified PCR product prior to gel extraction, and prior to digestion with *BamHI* can be seen on figure 3.10. Clean DNA fragment was digested as outlined previously for IL-10, and a final concentration of approximately 280 ng/µl was achieved (figure 3.11)

3.2.2.2.3 Preparation of recombinant SFV expression vector

The same pSFV1 expression vector used for cloning rSFV-IL10 was used for IL-4. The procedure is outlined in section 3.2.2.1.3

3.2.2.2.4 DNA ligation

Linearized pSFV-1 was ligated to the purified IL-4 DNA at a ratio of 1:10 vector to insert. A ligation mixture containing 1 µl of pSFV1, 5 µl of IL-10, 2 µl 10X ligase buffer (300 mM Tris-HCl (pH 7.8), 100 mM $MgCl_2$, 100 mM DTT and 10 mM ATP), and 3 U T4 DNA ligase were combined in a 20 µl reaction mix and incubated overnight at 16°C. A control ligation was carried out using only pSFV1 DNA.

3.2.2.2.5 Transformation of bacterial cells

Transformation of competent cells was performed as outlined in section 2.2.2.4.2, with the following modification: all 20 µl ligation mixture and control mixture was added to competent cells.

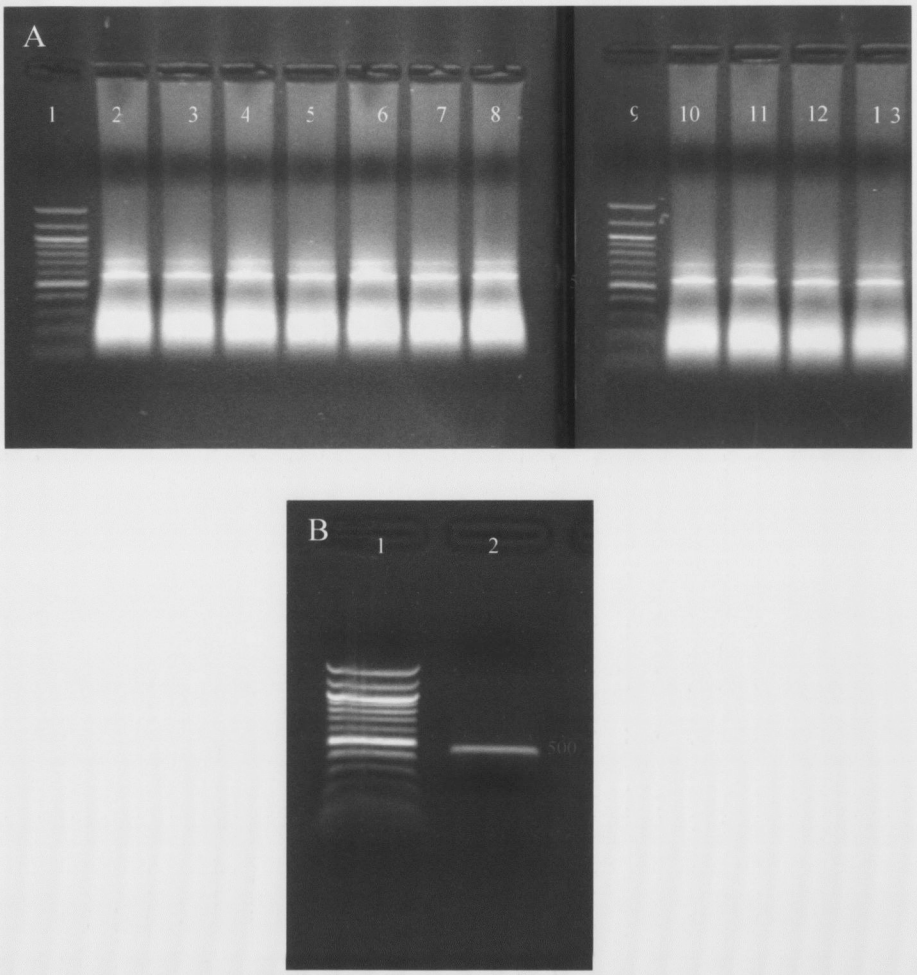

Figure 3.10 Purified IL-4 DNA

Following PCR amplification IL-4 DNA was purified using a PCR purification kit (outlined in section 3.2.2.2.2). **(A)** Purified IL-4 insert was further concentrated using a gel extraction kit (as outlined in same section), by excising pooled product from a 1.0% (wt/vol) agarose gel. *Lanes 1 and 9;* 100 bp DNA ladder. *Lanes 2-8 and 10-13;* PCR purified IL-4 DNA **(B)** Excised fragments were again purified and concentrated prior to digestion with BamHI. Final product seen on a 1.0% (wt/vol) agarose gel, stained with ethidium bromide. *Lane 1;* 100 bp DNA ladder. *Lane 2;* 1.0 µl purified IL-4 DNA.

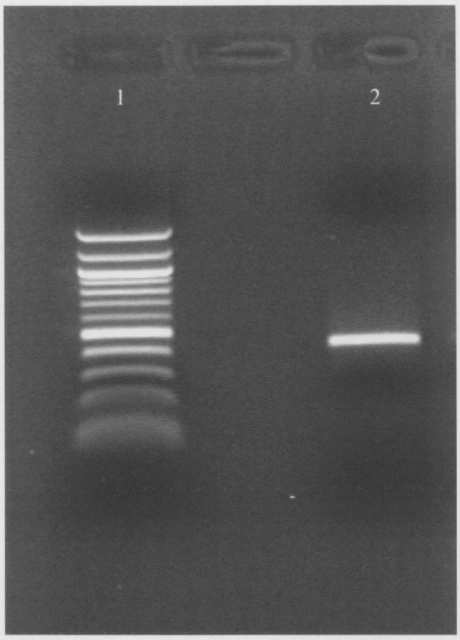

Figure 3.11 Digested IL-4 DNA

Purified IL-4 DNA insert was digested with BamHI for ligation to pSFV1 as outlined in section 3.2.2.2.2. *Lane 1;* 0.5 μg of 100 bp DNA ladder. *Lane 2;* 0.5 μl Digested IL-4. DNA was visualized on a 1.0% (wt/vol) agarose gel, stained with ethidium bromide. IL-4 DNA was estimated to contain a concentration of 280 μg/μl by comparison to the DNA ladder.

3.2.2.2.6 Screening for recombinant plasmids by restriction digestion

To confirm presence and orientation of insert, 26 putative positive clones grown on ampicillin agar plates were inoculated into 10 ml L broth containing 100 μg/ml ampicillin and incubated shaking overnight at 37°C. Plasmids were purified using the QIAGEN miniprep plasmid purification kit, as described in section 2.2.2.4.3. After purification, plasmids were digested with *BamHI* as previously described, and run on 0.8% (wt/vol) agarose gels. Thirteen colonies were found to contain an insert (figure 3.12). These were further digested with *XmnI* to check insert orientation. Reaction mixture contained 1 μl plasmid DNA, 2 μl buffer Neb 2 (50 mM NaCl, 10 mM Tris-HCl, 10 mM $MgCl_2$ and 1 mM dithiothreitol pH 7.9), 10 U *XmnI* in a total volume of 20 μl. Digested products were analyzed by electrophoresis of a 1 μl aliquot on a 0.8% (wt/vol) agarose gel. The following 2 fragment sizes should be detected for correct orientation: 2585, and 8886 nucleotides. Nine out of the possible plasmids contained the insert in the correct orientation (figure 3.13).

3.2.2.2.7 Sequencing of pSFV1-IL4

Five of the possible correct clones were sent for sequencing to LARK technologies Inc. using insert primers. Sequence obtained was blasted against the NCBI database, and then paired to the original sequence for the coding region of IL-4 obtained from the GenBank database. A glycerol stock was prepared from the correct clone as described in section 2.2.2.4.3

3.2.2.3 Detection of protein expression

3.2.2.3.1 DNA amplification and *in vitro SP6* RNA transcription

pSFV1-IL10 and pSFV1-IL4 were amplified and purified as outlined for pSFV-EGFP in section 2.2.2.4.4. *SpeI* linearization, cleanup and *in vitro* transcription of pSFV1-IL10 and pSFV1-IL4 recombinant RNA was performed as outlined for the transcription of

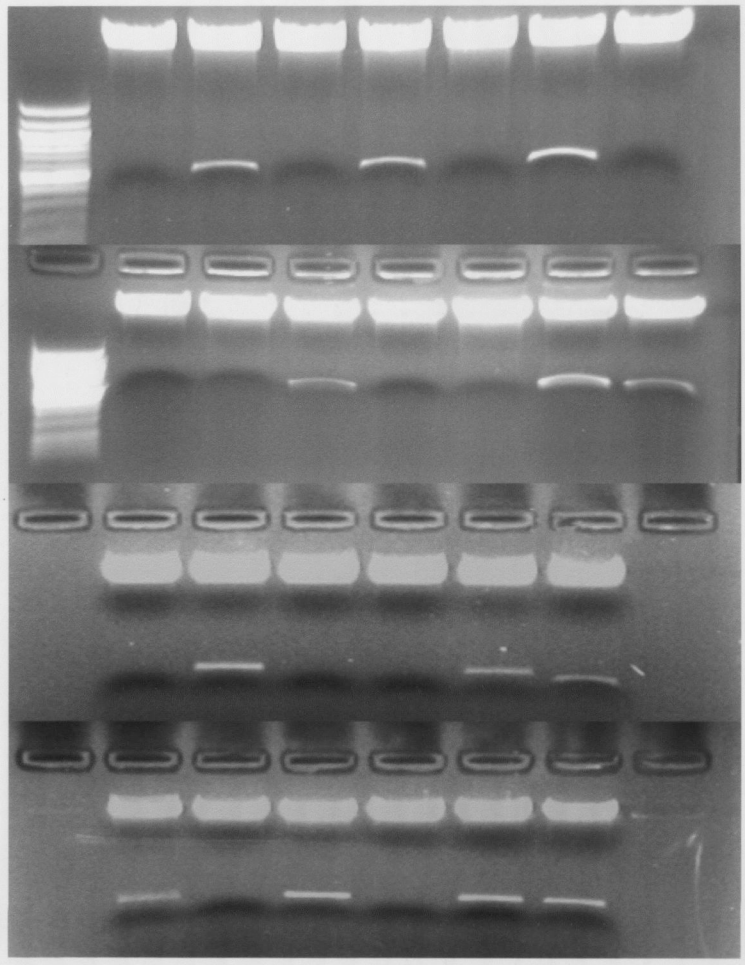

Figure 3.12 IL-4 insert in pSFV1

To confirm presence of IL-4 insert into pSFV1, putative clones grown on ampicillin agar plates, were digested with BamHI as outlined in section 3.2.2.2.6, and run on 0.8% (wt/vol) agarose gels. Out of a possible 26, 13 colonies were found to contain an insert. These were labeled as IL-4 clones 1-13.

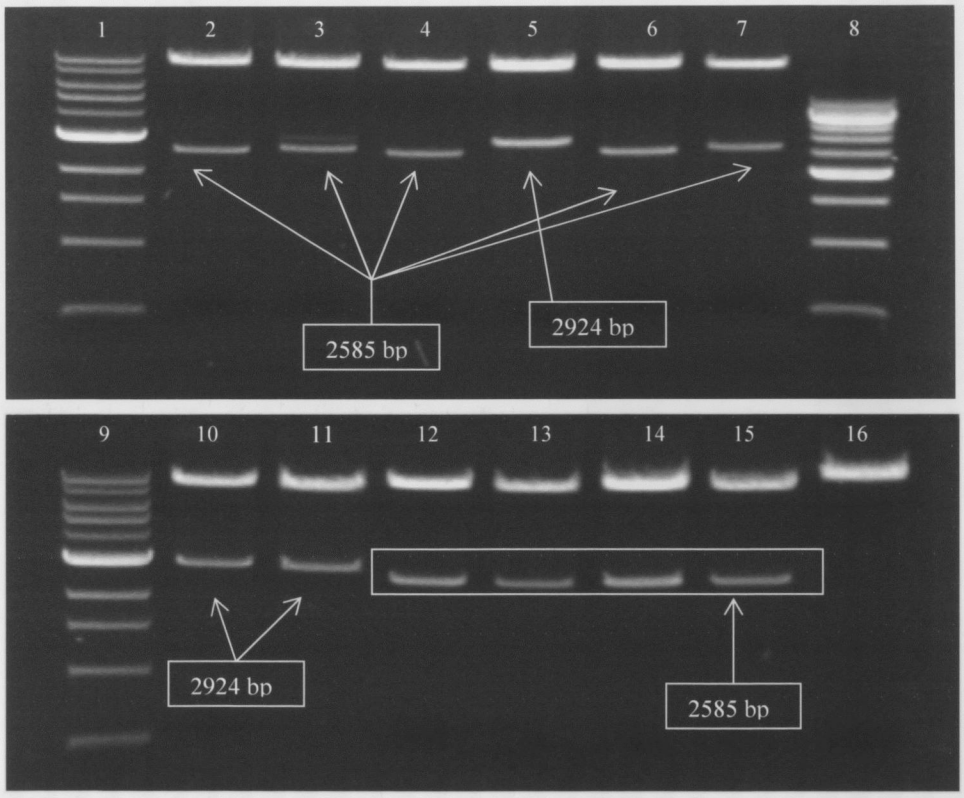

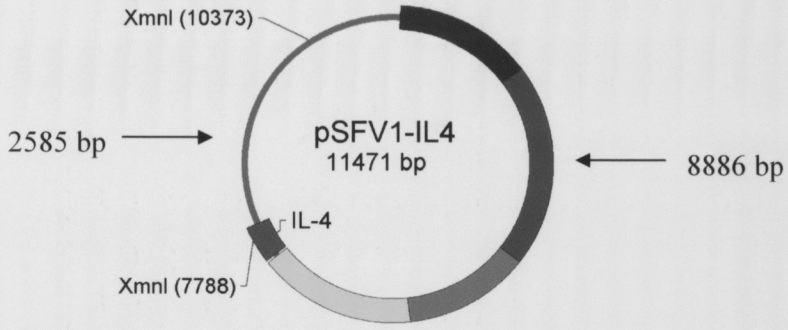

Figure 3.13 IL-4 insert orientation in pSFV1

To confirm the orientation of the IL-4 insert in pSFV1, IL-4 clones 1-13 were digested with XmnI as outlined in section 3.2.2.2.6. *Lanes 1 and 9*; 1 kb DNA ladder. *Lanes 2-7 and 10-16;*.IL-4 clones 1-13 *Lane 8*; DNA molecular weight marker XIV. 0.8% (wt/vol) agarose gel, stained with ethidium bromide. Correct fragment sizes for clones were 2585, and 8886 bp, which were found in clones 1-3, 5, 6, and 9-12.

pSFV-EGFP RNA, in sections 2.2.2.5.1 and 2.2.2.5.2, respectively. Recombinant RNA transcripts were analyzed by agarose gel electrophoresis, on a 0.6% (wt/vol) agarose gel (figure 3.14).

3.2.2.3.2 Electroporation

In vitro-transcribed pSFV1-IL4 and pSFV1-IL10 RNA was transfected by electroporation into ~80% confluent BHK-21 cells, as outlined in section 2.2.2.5.3.1, with the following modifications. Only recombinant RNAs (pSFV1-IL4 and pSFV1-IL10 RNA) were electroporated into BHK-21 cells, and following electroporation, cells were grown on sterile glass coverslips contained within each well of a 6-well plate. Cells were then incubated for 18-20 h at 37°C in a humidified atmosphere of 5% CO_2. Negative controls were performed with pSFV-EGFP and PBS only electroporated into separate BHK-21 cells.

3.2.2.3.3 Immunocytochemistry

Following incubation, medium was removed from wells, and cells washed with PBS. Cells were then fixed with formalin (5% (vol/vol) in PBS) for 15 min at room temperature (RT). Cells were washed twice in PBS for 5 min each, and post-fixed in acetic acid: ethanol (1:2) for 5 min at -20°C. Cells were washed twice in PBS for 5 min, and quenched for 10 min in 3% (vol/vol) H_2O_2 in PBS to remove endogenous peroxidase activity. Cells were then washed twice in PBS for 5 min prior to blocking in rabbit serum (15 µl in 1 ml PBS) for 20 min in a humidified chamber (HC) at 37°C. Serum was removed and cells stained with primary antibody (IL-10, or IL-4 diluted 1:100 in PBS) for 1 h in a HC at 37°C. Following incubation cells were washed twice with PBS-tween (0.05% (vol/vol) tween-80 in PBS) for 10 min, and then twice with PBS for 5 min. Biotinylated antibody (5 µl antibody and 15 µl serum in 1 ml PBS) was added for 30 min at RT in HC. Cells were again washed in PBS tween followed by PBS as described above, then incubated in VECTASTAIN Elite ABC reagent (20 µl reagent A and 20 µl reagent B in 1 ml PBS) for 30 min at RT in HC. Cells were washed in PBS for 5 min, incubated in

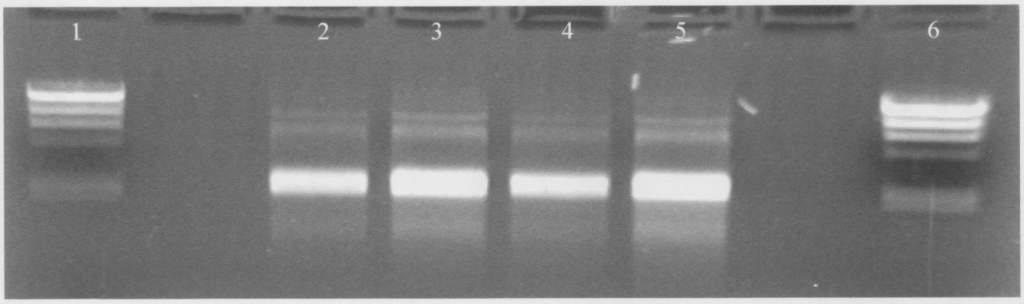

Figure 3.14 In vitro SP6 RNA transcription

Recombinant (pSFV1-IL4 and pSFV1-IL10) plasmids were transcribed as outlined in section 3.2.2.3.1. *Lane 1 and 6*; 0.125 μg and 0.25 μg Lambda (Hind111) DNA molecular weight marker. *Lane 2 and 3*; 0.5 μl and 1.0 μl each of pSFV1-IL4 RNA. Lane *4 and 5*; 0.5 μl and 1.0 μl each of pSFV1-IL10 RNA. 0.6% (wt/vol) agarose gel, stained with ethidium bromide.

DAB for 2 min, and washed in running tap water for 5 min. Cells were then counterstained in methyl green (2% (wt/vol) in 0.1M Sodium Acetate) for 10 min, washed in water, dehydrated in 3 butanol washes, cleared in 3 xylene washes and mounted on slides in DPX. Alternatively, as opposed to using methyl green and butanol, cells were counterstained with Haematoxylin Harris for 20 sec, cleared in water and differentiated for 10 sec in 1% (vol/vol) HCl (in 70% ethanol). Cells were then dipped 3 times in ammonia water (2 ml NH_3 in 500 ml H_2O), dehydrated in a series of ethanol washes (75%, 90%, and 100%), cleared in 3 xylene washes and mounted on slides in DPX.

3.2.2.4 Detection of protein secretion

3.2.2.4.1 Particle production

The production of rSFV-IL4, rSFV-IL10, and rSFV-TGFb was performed as outlined in section 2.2.2.5 for rSFV-EGFP, utilizing the plasmids pSFV1-IL4, pSFV1-IL10, and pSFV1-TGFb.

3.2.2.4.2 Particle titration

Titration of rSFV-IL4, rSFV-IL10, and rSFV-EGFP was carried out in a manner similar to that of rSFV-EGFP outlined in section 2.2.2.5.3.3. Following incubation, cells were fixed with 5% (vol/vol) formalin, and coverslips stained with specific antibodies (IL-4, IL-10, and TGF-β) as described in section 3.2.2.2.2. Particle titers were obtained by examining cells microscopically for the presence of substrate (figure 3.15). Particle titers were calculated from counts at a magnification of x 400 and expressed as IU/ml.

3.2.2.4.3 *In vitro* cytokine secretion

To confirm the vectors were secreting the cloned cytokines, a number of cell lines were infected and their medium harvested for the presence of the specific cytokine. The

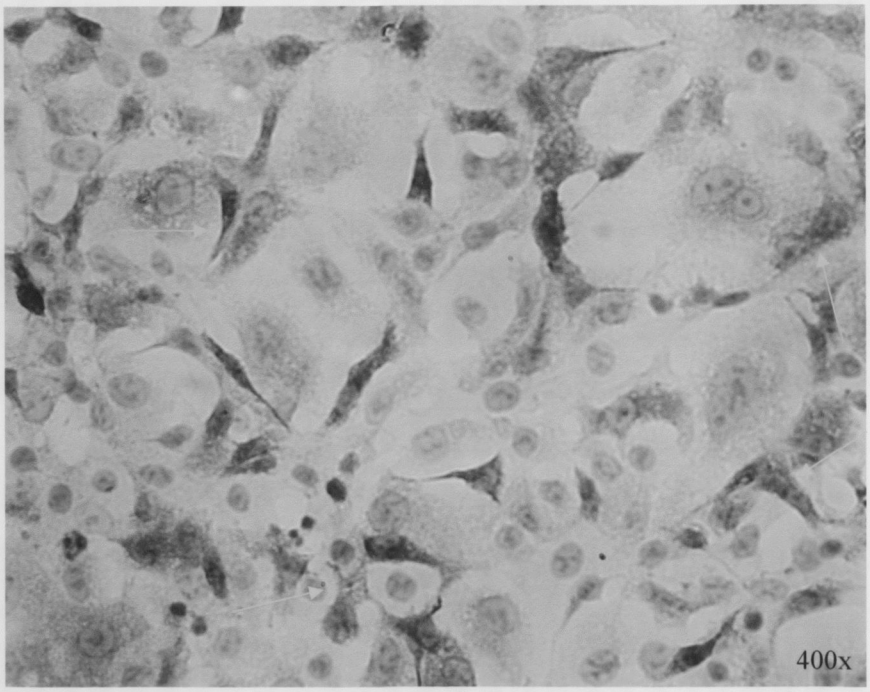

Figure 3.15 rSFV-IL10 particle titration

Titration of rSFV-IL10 particles was carried out as described in section 3.2.2.4.2. Titer was calculated by microscopically counting all sBHK cells labeled with substrate (arrows) and multiplying by appropriate factors. rSFV-IL4 and rSFV-TGFb were titrated in same manner (not shown). Titer was expressed as IU/ml. Titers ranging from 1.0×10^9 to 6.0×10^9 IU/ml were routinely obtained.

cell lines BHK-21, Balb-3T3, L-929, and Cos-7 were seeded at $1x10^4$ ml^{-1} in 96 well plates. BHK-21 cells were cultured in BHK-21 medium, supplemented with 5% (vol/vol) NCS, 5% (vol/vol) tryptose phosphate broth, 100 U/ml penicillin, 100 μg/ml streptomycin in 200 mM L-glutamine. Remaining cell lines were cultured in Dulbecco's modified Eagle medium supplemented with 5% (vol/vol) fetal calf serum, 1% (vol/vol) sodium pyruvate, 100 IU/ml penicillin and 100 μg/ml streptomycin. Cell medium was removed and cells infected with rSFV-IL4, rSFV-IL10, rSFV-TGFb, and rSFV-EGFP at a multiplicity of infection (m.o.i.) of 10, 50 and 100. Cells were also mock-infected with TNE buffer. Following incubation at 37^0C in a humidified atmosphere of 5% CO_2 for 1 h, the virus inoculum was removed from the monolayer and cells were given 300 μl of fresh medium. After 24 h incubation at 37^0C in a humidified atmosphere of 5% CO_2, supernatant was removed and cell debris removed by centrifugation (10,000g, 10 min). Supernatant containing secreted cytokines was stored at -70°C.

3.2.2.4.3.1 ELISA

Supernatant samples were tested for the presence of cytokines by use of a capture ELISA specific for IL-4, IL-10 or TGF-β. Wells of a 96 well plate were coated with 100 μl/well of capture antibody diluted in coating buffer (1:250 dilution), and incubated overnight at 4°C. Wells were washed 3 times with 300 μl/well of wash buffer, and plates blocked for 1 h at RT with 200 μl/well of assay diluent. Wells were again washed 3 times with wash buffer, and incubated sealed for 2 h at RT with 100 μl/well of either standard (serial dilutions in assay diluent) or samples. Plates were washed as before with 5 total washes, and then incubated sealed for 1 h at RT with 100 μl/well of working detector (detection antibody and avidin-HRP reagent diluted in assay diluent; 1:500 for IL-4, and 1:250 for IL-10 and TGF-β). Plates were again washed as before, but with 7 total washes. 100 μl/well of TMB substrate was added, and plates incubated at RT in the dark for 30 min, before addition of stop solution (2N H_2SO_4). Absorbances were read at 450 nm within 30 minutes of adding stop solution.

3.2.2.4.3.2 Western blot

Supernatant samples were further tested for the presence of rSFV-TGFb by western blot analyses. A 10% separating gel was prepared by mixing 2.5 ml of 1.5M Tris HCl pH 8.8, 3.33 ml of acrylamide/bis , 4.0 ml of dH_2O, 100 µl of 10% SDS, 30 µl 20% APS, and 5 µl of Temed. Mixture was placed in a gel plate, overlayed with iso-butanol and allowed to polymerize for 1 h. After polymerization, butanol was removed, and a stacking gel (625 µl of 0.5M Tris HCl pH 6.8, 333 µl of acrylamide/bis 1.5 ml of dH_2O, 25 µl of 10% SDS, 12.5 µl 20% APS, and 2.5 µl of Temed) was added on top of the separating gel. A comb was placed in the stacking gel to create wells, and allowed to polymerize for 30 min. The comb was removed, and wells rinsed with a syringe containing running buffer. Samples were mixed with 2X loading dye (3.2 ml dH_2O, 2.5 ml 0.5M Tris HCl pH 6.8, 2.3 ml 10% SDS, 1 ml glycerol, 1 ml 2-βmercaptoethanol, 200 µl bromophenol blue) and heated in a boiling water bath for 8 min. The gel was placed in a tank filled with running buffer (3.03g Tris, 14.41g glycine, 1.0g SDS dissolved in dH_2O to 1L), and samples added to wells. The gel was run at 100 V for stacking gel and 150 V for separating gel for about 1.5 h. The samples were transferred to a piece of PVDF western blotting membrane in transfer buffer (28.8g glycine, 6g Tris base dissolved in dH_2O to 1.6 L, pH 8.3) for 1 h at 100 V. The membrane was blocked overnight in 3% skim milk (3g skim milk powder, 88 ml dH_2O, and 10 ml 10X Towbin's saline [140 ml 0.5M Tris HCl pH 6.8, 20 ml 1.5M Tris HCl pH 8.8, and 90g NaCl in 1L dH_2O]). The membrane was incubated in primary antibody (mouse anti-human TGF-β) diluted in blocking solution for 1.5 h. The membrane was washed 3 times in wash buffer (0.5g Tween 20,100 ml 10X Towbin's and 900 ml H_2O) for 10 min. The membrane was incubated in biotynilated secondary antibody (diluted in blocking solution) for 1.5 h. The membrane was again washed 3 times as before, drained and sealed in plastic. The corner of the plastic was opened, POD blotting mixture added, and the bag sealed again. After 1 min the bag was opened, the liquid expelled and the bag resealed. The membrane was exposed in X-ray film for 30 sec, and developed in an automated developer.

3.3 RESULTS

3.3.1 Sequencing of pSFV1-IL10

Out of the possible 5 clones obtained, 4 were observed to be in the correct orientation by restriction digestion (figure 3.8). Clones were sent for sequencing in order to determine which one would contain the complete undamaged IL-10 gene. Only clones 1 and 2 contained a 100% homology to the original sequence, with remaining clones containing a homology of 98% and 90% for clones 3 and 4 respectively. Correct orientation of all clones was further confirmed by sequencing. Nucleotide sequence obtained from clone 1 was blasted against the NCBI database, and an E-value of 0.0 was obtained for a match to the mouse IL-10 gene. Figure 3.16 describes the findings from blasting the cloned sequence to original sequence obtained from the GenBank database, which were 100% base match.

3.3.2 Sequencing of pSFV1-IL4

Five out of the 9 possible clones found in correct orientation were sent to be sequenced (remaining clones were stored for later, if needed). Only one of the clones returned a 100% homology to original IL-4 sequence (figure 3.17). Correct orientation was also confirmed from the sequence obtained. This sequence was blasted against the NCBI database, and an E-value of 0.0 was obtained for a match to the mouse IL-4 gene.

2.3.3 *In vitro* cytokine expression

Expression of both IL-10 and IL-4 were visualized in BHK-21 cells transfected by electroporation with rSFV-IL10 RNA and rSFV-IL4 RNA respectively using immunocytochemistry. As a control, cells transfected with rSFV-IL4 RNA, rSFV-EGFP RNA, and PBS buffer were found to be expressing no IL-10 (figure 3.18). Similarly, control cells treated with rSFV-IL10, rSFV-EGFP, and PBS buffer were found not to be expressing IL-4 (figure 3.19).

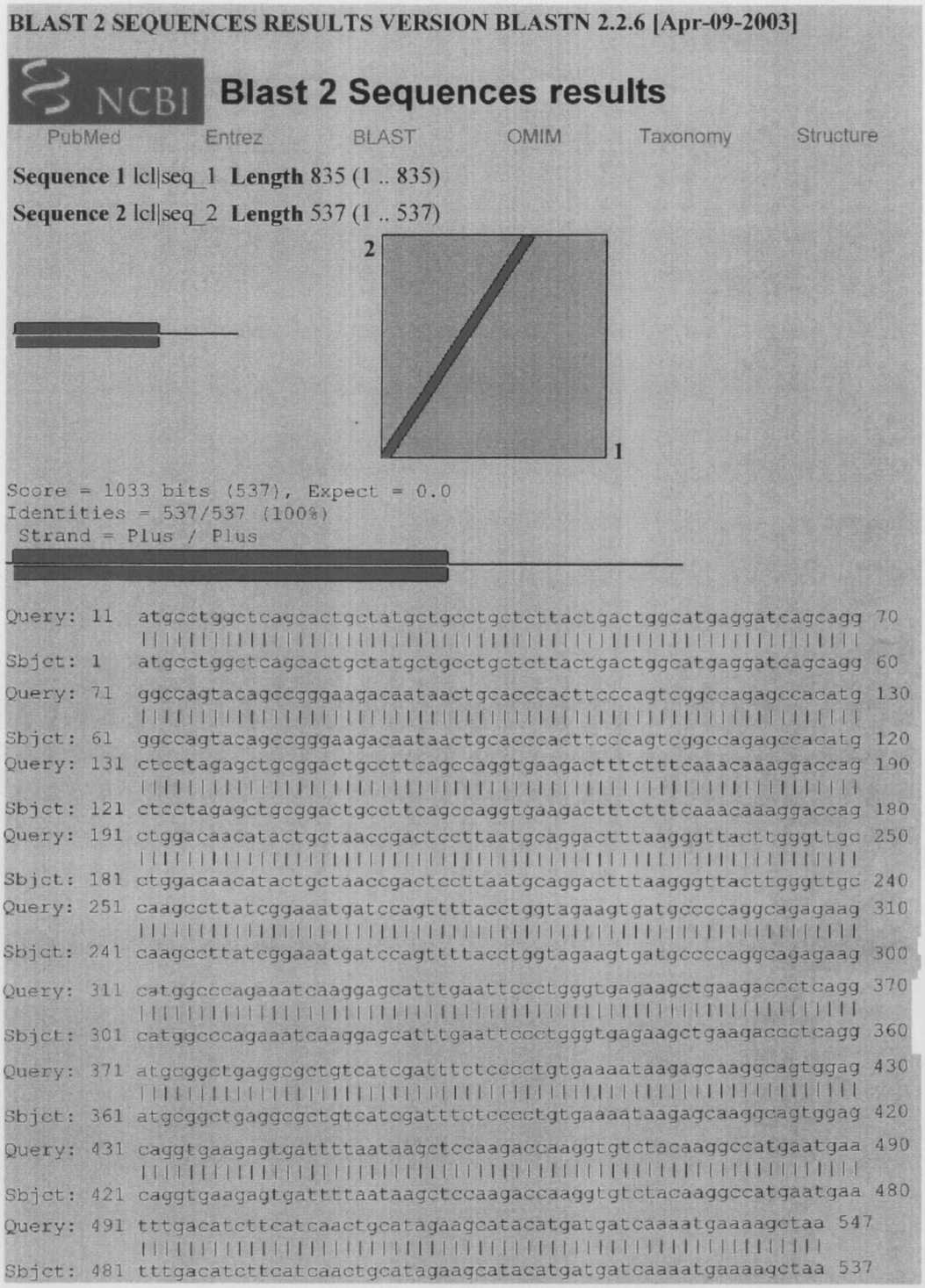

Figure 3.16 IL-10 sequence analyses

Sequence obtained from the cloned IL-10 gene from pSFV1-IL10 (using insert primers) was blasted against the original mouse IL-10 sequence from the GenBank database. A homology of 100% was obtained with an expected value of 0.0, indicating a perfect match. Results also confirmed sequence was in correct orientation, as indicated in the figure.

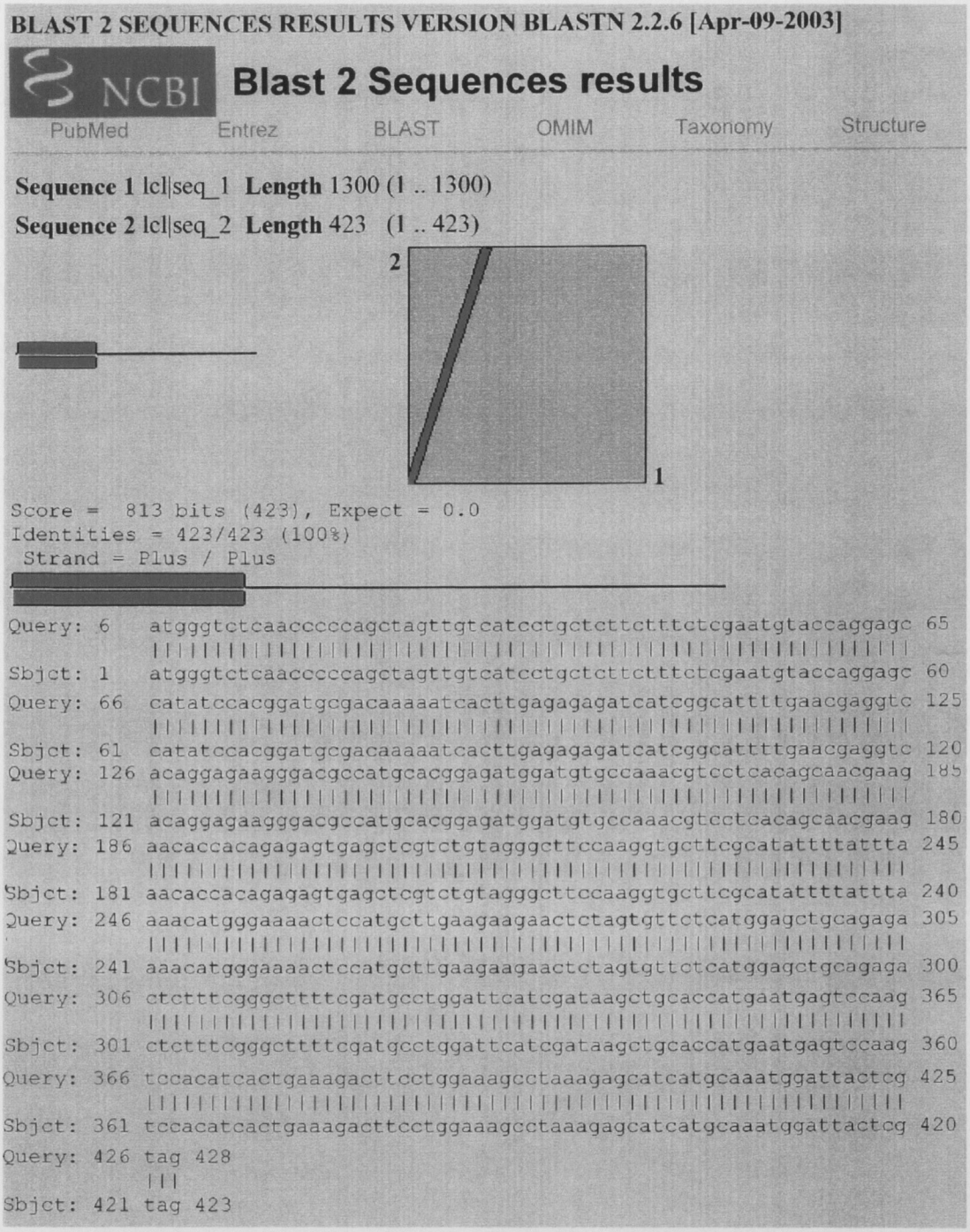

Figure 3.17 IL-4 sequence analyses

Sequence obtained from the cloned IL-4 gene from pSFV1-IL4 (using insert primers) was blasted against the original mouse IL-4 sequence from the GenBank database. A homology of 100% was obtained with an expected value of 0.0, indicating a perfect match. Results also confirmed sequence was in correct orientation, as indicated in the figure.

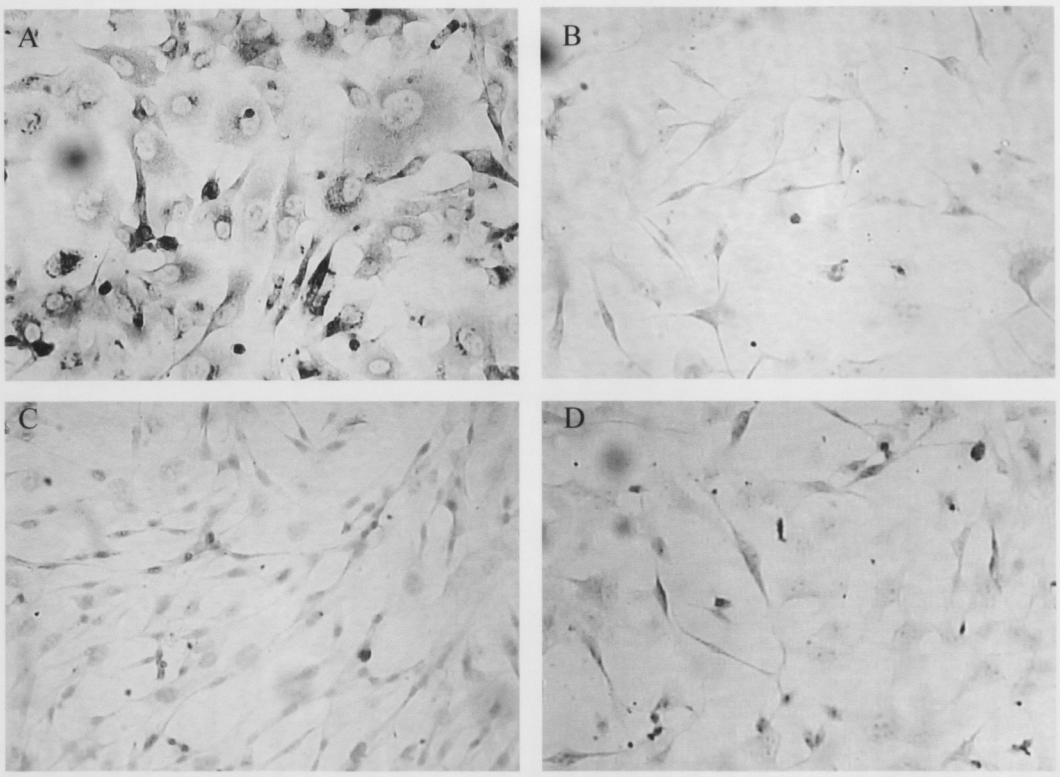

Figure 3.18 Expression of IL-10 in BHK-21 cells

RNA transcribed from pSFV1-IL10 was electroporated into BHK-21 cells, and expression visualized 18-20 h later by immunocytochemistry using mouse IL-10 monoclonal antibody as described in section 3.2.2.3. As negative controls, cells were transfected with pSFV1-IL4 RNA, pSFV-EGFP RNA, and PBS buffer alone. All cells counterstained in 2% (wt/vol) methyl green. **(A)** Cells transfected with rSFV-IL10 RNA, showing high levels of IL-10, as indicated by substrate (brown staining). **(B)** Cells transfected with rSFV-IL4 RNA. **(C)** Cells transfected with rSFV-EGFP RNA. **(D)** Cells transfected with PBS alone. None of the controls showed any expression of IL-10.

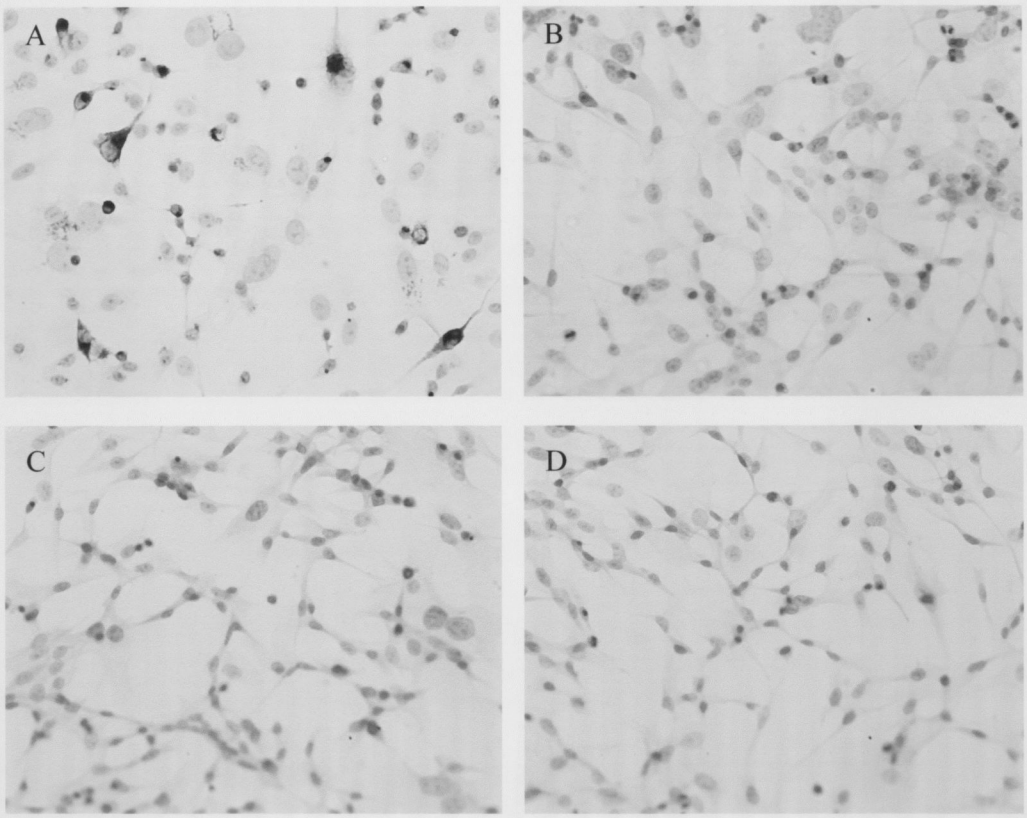

Figure 3.19 Expression of IL-4 in BHK-21 cells

RNA transcribed from pSFV1-IL4 was electroporated into BHK-21 cells, and expression visualized 18-20 h later by immunocytochemistry using mouse IL-4 monoclonal antibody as described in section 3.2.2.3. As negative controls, cells were transfected with pSFV1-IL10 RNA, pSFV-EGFP RNA, and PBS buffer alone. All cells were counterstained with Haematoxylin Harris. **(A)** Cells transfected with rSFV-IL4 RNA, showing high levels of IL-4, as indicated by substrate (brown staining). **(B)** Cells transfected with rSFV-IL10 RNA. **(C)** Cells transfected with rSFV-EGFP RNA. **(D)** Cells transfected with PBS alone. None of the controls showed any expression of IL-4.

2.3.4 *In vitro* cytokine secreted levels

High levels of secreted cytokines were detected by ELISA in cell supernatants following infection with rSFV-IL10 (figure 3.20) or rSFV-IL4 (figure 3.21) particles. This was compared to levels produced when cells were infected with SFV particles expressing other cytokines, reporter gene, empty vector, or PBS only. Levels were measured for BHK cells, Cos-7 cells, and two mouse cell lines, Balb/3T3 and L929. No detectable levels of TGF-β were detected in any cell line following infection with rSFV-TGFb by either ELISA or western blot analyses.

3.4 DISCUSSION

Both IL-10 and IL-4 gene were successfully cloned into the SFV vector system. The newly formed vector was capable of secreting the cytokines at extremely high levels in culture, following infection of different cell lines. It is known from the EGFP expression experiment that the vector is capable of expressing proteins from cloned genes in cells of the olfactory bulb. Cytokines as opposed to the EGFP are soluble proteins, which are secreted and therefore would have the ability to reach other areas of the CNS when delivered by an i.n. route. When a cytokine is released into a specific environment, it evokes a biological response once it binds to receptors on responsive target cells. Two distinct classes of cells, T_H1 or T_H2, secrete cytokines depending on biological function. More commonly a T_H1 response is directed against viral infections and intracellular pathogens because it secrets IL-2 and IFN-γ, leading to activation of T_C cells and macrophages. Allergic reactions evoke a T_H2 response, by secretion of cytokines such as IL-4 and IL-5 known to induce IgE and eosinophil activation.

Cloned IL-10 has been used as a therapeutic gene in EAE (Burkhart *et al,* 1999, Croxford *et al,* 2001, Cua *et al,* 1999, Massey *et al,* 2002). By inhibiting the activation of monocytes, dendritic cells, and macrophages IL-10 directly reduces production of pro-inflammatory mediators leading to a diminish T-cell stimulation (Beebe *et al,* 2002). IL-4 has also been extensively used in EAE (Falcone *et al,* 1998, Furlan *et al,* 1998, Furlan *et al,* 2001, Liblau *et al,* 1997, Pal *et al,* 1999, Poliani *et al,* 2001). TGF-β, an

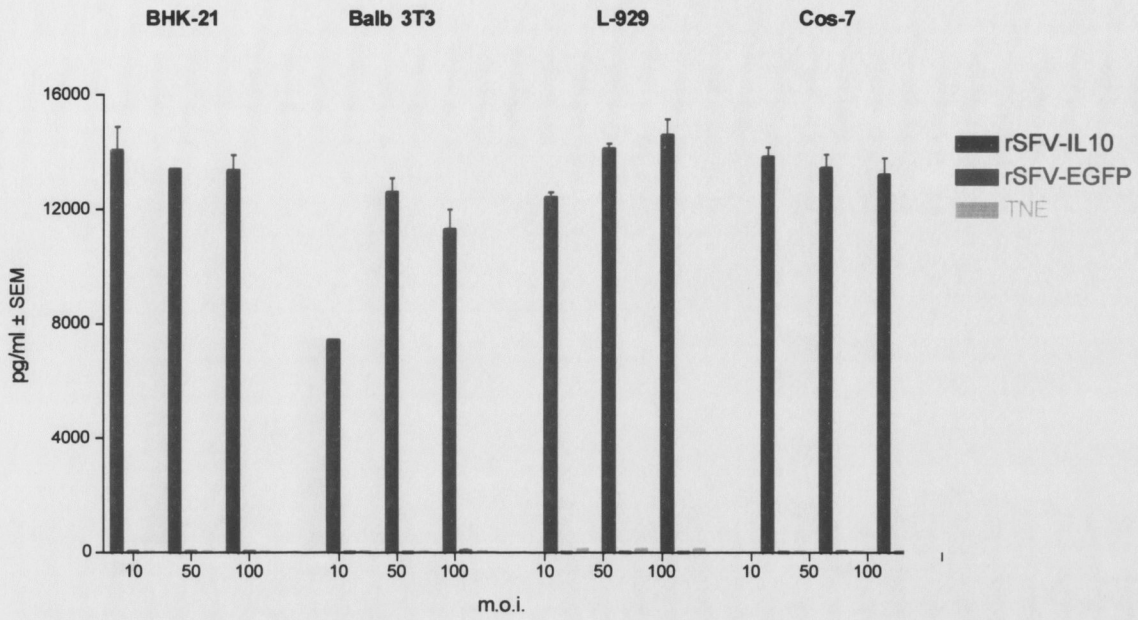

Figure 3.20 Secreted levels of IL-10 in different cell lines

The cell lines BHK-21, Balb3T3, L929, and Cos-7 were infected with rSFV-IL10, rSFV-EGFP (vector control), and TNE buffer only (uninfected control), at a multiplicity of infection (m.o.i.) of 10, 50, 100 as described in section 3.2.2.4.3. Supernatant samples were tested for the presence of IL-10 by use of a capture ELISA as described in section 3.2.2.4.3.1. Significantly higher levels of IL-10 were detected in supernatant of cells infected with rSFV-IL10 compared to controls.

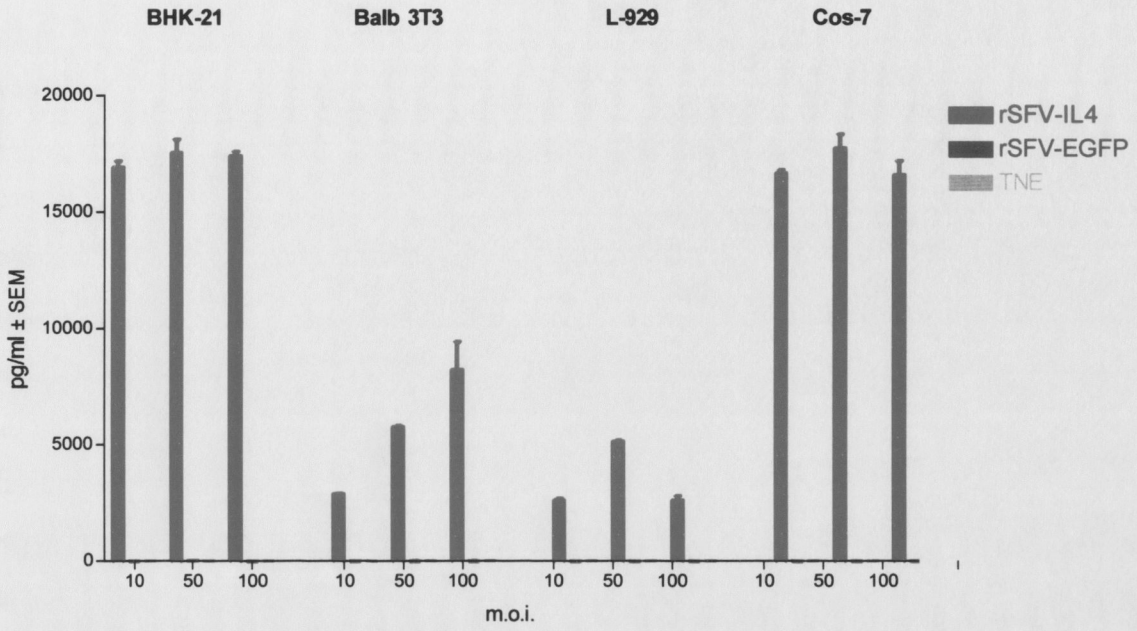

Figure 3.21 Secreted levels of IL-4 in different cell lines

The cell lines BHK-21, Balb3T3, L929, and Cos-7 were infected with rSFV-IL4, rSFV-EGFP (vector control), and TNE buffer only (uninfected control), at a multiplicity of infection (m.o.i.) of 10, 50, 100 as described in section 3.2.2.4.3. Supernatant samples were tested for the presence of IL-4 by use of a capture ELISA as described in section 3.2.2.4.3.1. Significantly higher levels of IL-4 were detected in supernatant of cells infected with rSFV-IL4 compared to controls.

immunoregulatory cytokine, has also been widely used in the treatment of EAE (Croxford *et al,* 1998, Piccirillo and Prud'homme 1999, Young *et al,* 2000). TGF-β has been implicated in suppression of primary autoimmune disease and in mediating the effects of tolerance (D'Orazio and Niederkorn 1998, Letterio and Roberts 1998). Previously, TGF-β1 was cloned into pSFV-1, and showed expression in BHK-21 cells by M.M. Morris-Downes. It was necessary however to verify that the cytokine was also being secreted by infected cells. Neither ELISA nor western blot analyses detected secreted levels in four different cell lines. This led to further investigation into the reason why TGF-β was not being secreted from infected cells. TGF-β is a complex protein, in that it is expressed in cells as the biologically inactive 390 a.a. precursor polypeptide, necessary for secretion of the active form. The N-terminus of the precursor molecule, called latency-associated peptide LAP, binds to the mature peptide (112 a.a.) creating a latent complex, which facilitates secretion of active TGF-β. Figure 3.22 demonstrated this principle. Only the gene coding for the 112 a.a. mature peptide was cloned into pSFV-1, which explains why TGF-β is being detected within cells by immunocytochemistry, but not in cell supernatant as secreted proteins.

From both the expression and secretion experiments, it was concluded that neither the vector alone, nor vector encoding IL-4 or TGF-β were leading to expression of IL-10 by infected cells. The same holds true for IL-4 expression in cells infected with empty, IL-10 or TGF-β vector. How this vector behaves *in vivo*, in an immunologically active animal, is the subject of chapter four.

A.

.....agcacc**atg**gccctggataccaactattgcttcagctccacagag
aagaactgctgtgtgcggcagctgtacattgactttaggaaggacctgggttggaagtggatccacgagcccaag
ggctaccatgccaacttctgtctgggaccctgcccctatatttggagcctggacacacagtacagcaaggtccttgc
cctctacaaccaacacaacccgggcgcttcggcgtcaccgtgctgcgtgccgcaggctttggagccactgcccat
cgtctactacgtgggtcgcaagcccaaggtggagcagttgtccaacatgattgtgcgctcctgcaagtgcagctga
.....

B.

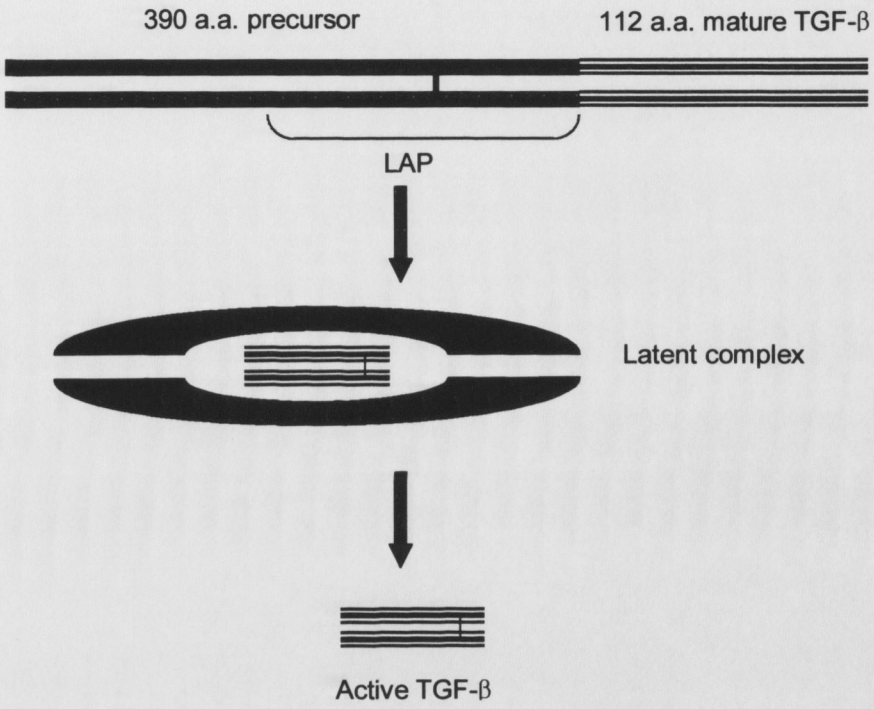

Figure 3.22 TGF-β latent complex and sequence

Both the mature and precursor peptides are needed for TGF-β secretion. Sequencing of pSFV1-TGFb confirmed that only the mature form was cloned into the plasmid. **(A)** Sequence segment taken from sequencing of pSFV1-TGFb with RBS site underlined, start codon in bold, followed by sequence of mature form. Nucleotides on both ends not shown in above sequence belong to pSFV-1. **(B)** Formation of the latent complex, and release of active TGF-β by the precursor and mature peptides.

Chapter 4

In-vivo expression and analyses of SFV particles expressing different cytokines

4.1 INTRODUCTION

With cytokines cloned into the SFV vector system, it was necessary to determine what effects they would have when delivered to the CNS of healthy animals. It is important to realise that cytokines are secreted proteins that can act as humoral regulators at nano- to picomolar concentrations; therefore the site of their expression does not necessarily predict the site at which they exert their biological function. This is observed in EAE, where peripheral cytokine delivery results in amelioration of disease (Braciak *et al,* 2003, Johns *et al,* 1991, Piccirillo and Prud'homme 1999, Santambrogio *et al,* 1993). Within the immune system there is a delicate balance of cytokine levels. Since a cytokine is capable of interacting with a variety of cell types as well as other cytokines, a process known as a cytokine cascade occurs when they are introduced into an environment. This is where one cytokine initially triggers the expression of one or more other cytokines that, in turn, trigger the expression of further factors and create complicated feedback regulatory circuits. This cascade leads to production of various regulatory effects, both local and systemic. Of key importance for the current work was to determine if the cytokine delivered (IL-4 or IL-10) by the rSFV vector system was up-regulating the production of other T_H2 cytokines, or even down regulating T_H1 produced cytokines. Of equal importance was to determine what response is induced by vector administration alone, since it is known that the wild-type virus induces a T_H1 response. It is known from previous experiments that proteins cloned into the SFV vector system delivered i.n. reach the olfactory bulb area of the CNS. Cytokines being soluble secreted proteins should have the ability to reach other areas of the CNS, and possibly change the cytokine balance in the animal. Since viruses induce a T_H1 response in infected animals, it was also expected that the SFV vector system would behave similarly. It will be interesting to determine if the cytokine cloned into the vector system is able to overcome this response.

In the present study, healthy mice were inoculated with rSFV-IL10, rSFV-IL4, rSFV-EGFP, and buffer alone. The nasal passage, olfactory bulb, cerebrum and cerebellum were removed and homogenised for cytokine analyses by means of ELISA. The rSFV-EGFP vector was used as a control vector, since EGFP is non-imunogenic and is not secreted by the vector. The main limitation of the current study is that there will be no distinction between produced cytokines and cytokines released by the vector. By

measuring cytokine levels in non-inoculated control animals, this problem can be circumvented.

4.2 EXPERIMENTAL PROCEDURES

4.2.1 NEW MATERIALS

4.2.1.1 Expression Vectors

The SFV expression vector, pSFV1-IL10, and pSFV1-IL4, in addition to pSFV-EGFP, and helper vectors, pSFV-Helper S2 and pSFV-Helper CS219A were used.

4.2.1.2 Particle production

Ultracentrifuge tubes and the SW28 rotor and swing buckets from Beckman-Coulter Instruments Inc. were used as opposed to the SW40Ti.

4.2.1.3 Mice

Female C57BL/6 mice aged 40-60 days were obtained from Harlan (UK). Mice were maintained in accordance with the principles outlined in S1 17/94 European Communities regulations 1994, for care and use of laboratory animals.

4.2.1.4 Enzyme Linked Immunoabsorbancy Assay

The OptEIA mouse IFN-γ set from BD PharMingen was used in addition to mouse IL-10 and mouse IL-4. All buffers for IFN-γ set are similar to those of IL-4 set.

4.2.1.5 Miscellaneous

0.25M Tris-HCl buffer was prepared by dissolving 6.06 g of Tris in 200 ml of sterile distilled water, pH lowered to 8.0 with HCl, and final solution filter sterilized. Bradford protein assay was from Sigma. Homogenizer type RZR 1 was from Heidolph (Germany).

4.2.2 METHODS

4.2.2.1 SFV Particle production

The SFV particles rSFV-EGFP, rSFV-IL10, and rSFV-IL4 were prepared in a manner similar to previously described in section 2.2.2.5.3, with the following modifications. Six flasks of confluent sBHK cells and 6 sets of recombinant and helper RNAs were used. Cells suspended in PBS were centrifuged as before, and resuspended in a total of 4.4 ml of PBS. 800 µl of PBS was mixed with 150 µl aliquot of the 3 RNAs, and electroporated as before. Four sets of electroporated cells were mixed with 20 ml of fresh BHK medium, and 2 sets with 10 ml. Cells were pooled and transferred into two 150-cm^2 tissue culture flasks each containing 50 ml of cells. They were incubated as before for 36 h at 33°C in a humidified atmosphere of 5% CO_2. The process was repeated so that a total of 4 flasks were incubated.

Cells were harvested as before, with the following modifications. Following initial centrifugation to remove cell debris, a total of 200 ml were pooled into a glass conical flask kept on ice. 30 ml aliquots of particle supernatant were placed in 6 Beckman SW28 ultracentrifuge tubes. A sucrose cushion was added as before, and tubes balanced with remaining supernatant. The tubes were placed into 6 SW29 swing buckets, balanced and centrifuged (28,000g, 2.0 h, 4°C). Following ultracentrifugation, the supernatant was removed, and tubes dried as before. Each tube was resuspended in 400 µl of TNE buffer overnight, followed by a wash with a further 265 µl in a same manner as before. A final volume of 4 ml, was aliquoted into 50-200 µl volumes, on ice, and rapidly frozen using dry-ice-cooled ethanol or liquid nitrogen, before storage at -70°C. Titration of particles was carried out as before.

4.2.2.2 Mice infection with particles

A total of 48 C57BL/6 mice were infected i.n. with 10^7 IU of either rSFV-IL10, rSFV-IL4, rSFV-EGFP, or mock infected with TNE. A further 6 mice were used as uninfected controls. Three mice infected with each particle or TNE were sampled at days 1, 7, 14, and 21.

4.2.2.3 Tissue homogenates

At designated time points the nasal passage, olfactory bulbs, cerebrum, and cerebellum were removed. Tissue was then homogenated in 2.0 ml of 0.25M Tris-HCl buffer. Homogenized solution was transferred to a fresh 15 ml tube, and centrifuged (1,000g, 10 min, 4°C). Clear supernatant was transferred to a clean tube and stored at -70°C. Blood taken from animals was kept at 4°C overnight, centrifuged (13,000g, 5 min, 4°C), and serum stored at -70°C.

4.2.2.4 Protein assays

The Bradford reagent was used to determine protein concentration of homogenized sample. The assay consists of mixing 1 part of protein sample with 30 parts of the Bradford reagent. A serial dilution of a protein standard (BSA) solution was used to generate a standard curve. To each well of a 96 well plate, 5 µl of each protein and standard were added in duplicate. 250 µl of Bradford reagent was then added to each well containing protein. Samples were mixed for 30 sec, incubated at RT for 5 to 45 min, and absorbance read at 595 nm in a spectrophotometer. Concentrations were recorded as mg/ml of total protein.

4.2.2.5 ELISA

Homogenized tissue and serum samples were tested for the presence of cytokines by use of a capture ELISA specific for IL-4, IL-10 or IFN-γ, as described in section 3.2.2.4.3.1. Dilutions for IFN-γ set were as follows: capture antibody 1:200, detection antibody 1:250, and avidin-HRP reagent 1:250 in same buffers as previously described. Values obtained from protein assay and ELISA were normalized using a spreadsheet (Microsoft Excel) to a final concentration of 1 mg of total protein.

Measured cytokine levels were compared using the one-way analyses of variance (ANOVA) statistical test. When a statistically significance difference between groups was calculated, the Bonferroni's multiple comparison test was used to compare between individual pairs of groups. All statistical tests were calculated using Prism 4.0 (GraphPad software Inc.).

4.3 RESULTS

4.3.1 SFV Particle production

A few modifications were made to the particle production system in order to achieve slightly higher particle titers. The use of 6 flasks of cells as opposed to 5, and the use of sBHK cells consistently yielded titers of at least 4.0×10^9 IU/ml, and as high as 4×10^{10} IU/ml. With the use of a SW28 rotor, larger volumes of particle were produced in half the time required for the original protocol.

4.3.2 Cytokine levels in tissue following infection

No significant data was obtained from ELISAs performed on serum samples. Data obtained from tissue homogenates was interpreted using statistical analyses. IL-4 levels are demonstrated in figures 4.1 and 4.2. In the nasal passage, at day 1 post inoculation, there was a very clear difference in levels between rSFV-IL4 group compared to all other groups ($P < 0.001$). Though not as high a difference, by day 7 there still was a significant

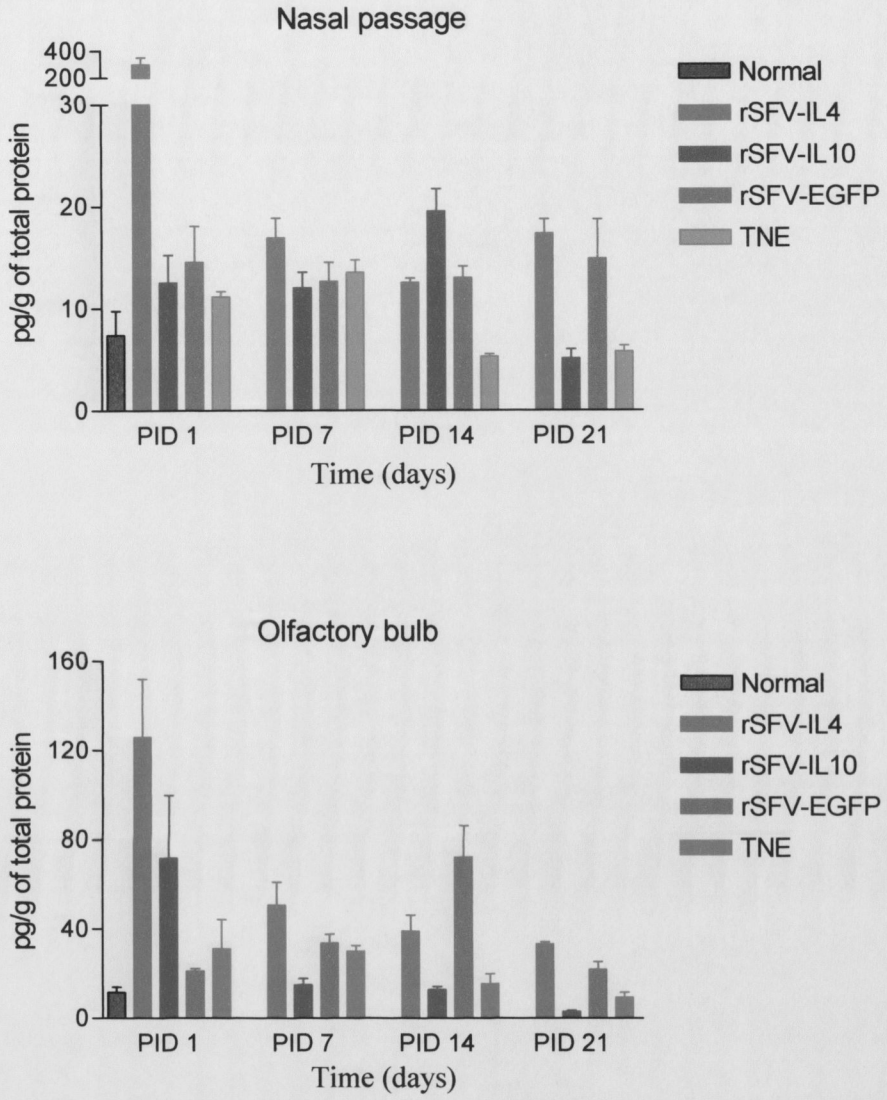

Figure 4.1 IL-4 levels in mice following particle administration

C57BL/6 mice were infected i.n. with rSFV-IL10, rSFV-IL4, rSFV-EGFP, or mock infected with TNE. Uninfected mice were used for normal controls. Nasal passage and olfactory bulb tissue were removed at designated time points and homogenized as described in section 4.2.2.3. Homogenized tissue samples were tested for the presence of IL-4 by capture ELISA as described in section 3.2.2.4.3.1.

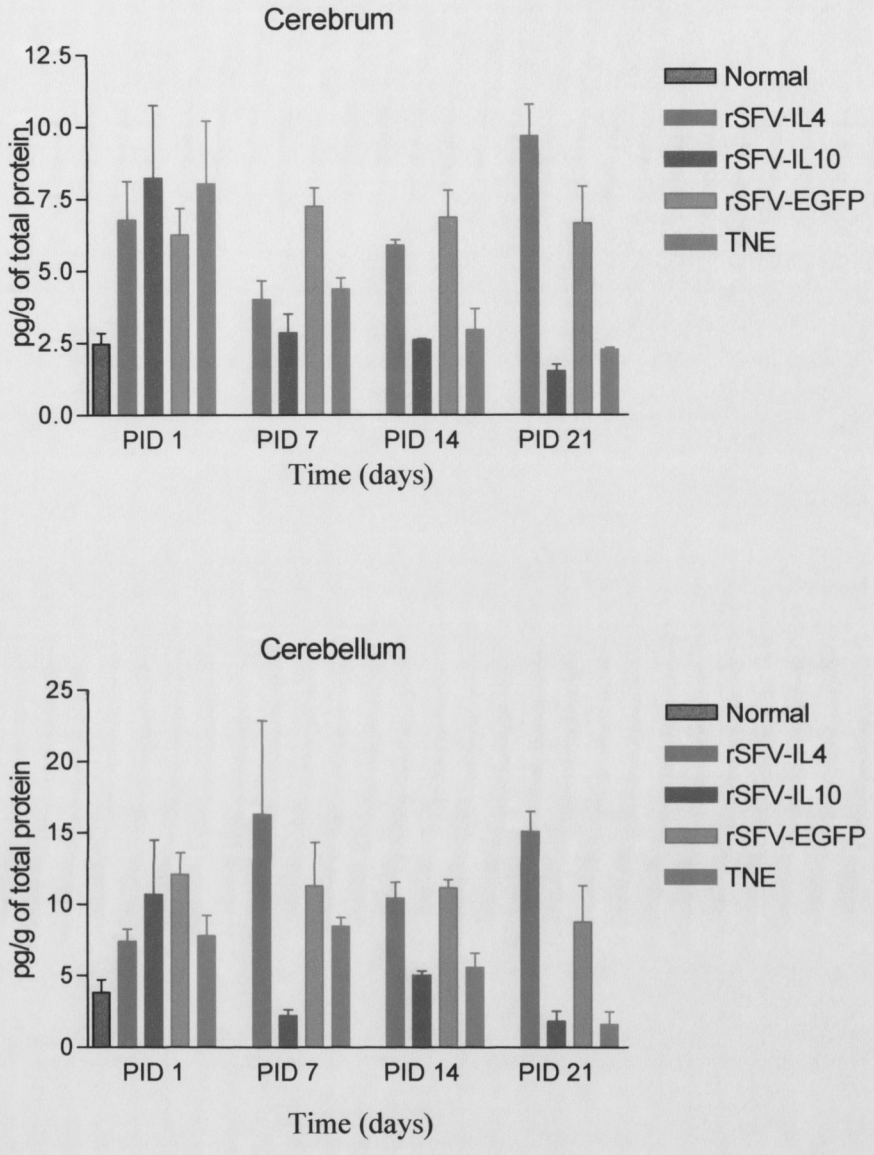

Figure 4.2 IL-4 levels in mice following particle administration

C57BL/6 mice were infected i.n. with rSFV-IL10, rSFV-IL4, rSFV-EGFP, or mock infected with TNE. Uninfected mice were used for normal controls. Cerebrum and cerebellum tissue were removed at designated time points and homogenized as described in section 4.2.2.3. Homogenized tissue samples were tested for the presence of IL-4 by capture ELISA as described in section 3.2.2.4.3.1.

difference between all groups ($P = 0.0488$). Comparing individual groups, only the normal group had IL-4 levels significantly lower then the rSFV-IL4 group. By day 14, mice given TNE had returned to normal levels. The rSFV-IL10 group had slightly higher levels of IL-4 compared to other groups, though values were significantly higher then TNE and normal groups only. At day 21, IL-4 levels as a result of rSFV-IL10 were back to normal (figure 4.1). A similar result was found on the olfactory bulbs of infected mice. A statistical difference ($P = 0.0203$) was found between all groups, with levels higher for the rSFV-IL4 group at day 1. Comparison between each group was only statistically different when normal levels were compared to rSFV-IL4 group. At day 7, a statistical difference ($P = 0.0028$) between rSFV-IL4 and normal groups was still detected. The rSFV-IL10 group had lower levels, similar to normal group, and was also statistically different to rSFV-IL4 group. By day 14, IL-4 levels as a result of rSFV-IL4 were lowered. Levels as a result of control vector (EGFP) were statistically higher ($P < 0.05$) then other groups with the exception of the rSFV-IL4 group. By day 21, IL-4 levels as a result of the control vector were again lowered; similarly, the rSFV-IL10 group had very low levels of IL-4. Measured levels as a result of rSFV-IL4 were again statistically higher ($P < 0.05$) then normal and TNE groups (figure 4.1). No significant differences between groups were found in cerebrum IL-4 levels at 1 day post infection. At day 7, levels as a result of control vector were significantly higher ($P = 0.0010$) then other groups. Finally at day 14, IL-4 levels as a result of rSFV-IL4 were significantly higher ($P < 0.05$) then normal. By day 21, IL-4 levels following rSFV-IL4 were higher then levels from control vector, and statistically higher ($P < 0.05$) then other groups (figure 4.2). No significant differences were calculated between IL-4 levels in the cerebellum in all groups at days 1 and 7. By day 14, both rSFV-IL4 and control vector had levels significantly higher then other groups. At day 21, the only statistically significant difference ($P < 0.05$) was calculated between the rSFV-IL4 group to normal and TNE groups (figure 4.2). Statistical differences obtained from one-way analyses of variance are described in table 4.1.

IL-10 levels obtained following infection are demonstrated in figures 4.3 and 4.4. As with IL-4 levels in the nasal passage following treatment, measured levels were significantly higher in the rSFV-IL10 treated group then all other groups at day 1. At day 7, no significant difference was calculated between groups. By day 14, there was again a difference between rSFV-IL10 and other groups. IL-10 levels in the rSFV-IL-10 group were lowered back to normal levels by day 21, though no significant difference was

Table 4.1 Statistical analyses of IL-4 levels in tissue homogenates

Homogenized tissue samples were tested for the presence of IL-4 by use of a capture ELISA as described in section 3.2.2.4.3.1. Measured cytokine levels were compared using the one-way analyses of variance (ANOVA) statistical test using Prism 4.0 (GraphPad software Inc.).

Location	d.p.i.	P value	P value summary *
Nasal passage	1	< 0.0001	Extremely significant
	7	0.0488	Significant
	14	0.0006	Extremely significant
	21	0.0073	Very significant
Olfactory bulb	1	0.0203	Significant
	7	0.0028	Very significant
	14	0.0014	Very significant
	21	< 0.0001	Extremely significant
Cerebrum	1	> 0.05	Not significant
	7	0.0010	Very significant
	14	0.0014	Very significant
	21	< 0.0001	Extremely significant
Cerebellum	1	> 0.05	Not significant
	7	> 0.05	Not significant
	14	0.0002	Extremely significant
	21	0.0089	Very significant

* P value significance obtained using Prism 4.0 (GraphPad software Inc.), where:

P value:	> 0.05	not significant
P value	0.01 to 0.05	significant
P value	0.001 to 0.01	very significant
P value	< 0.001	extremely significant

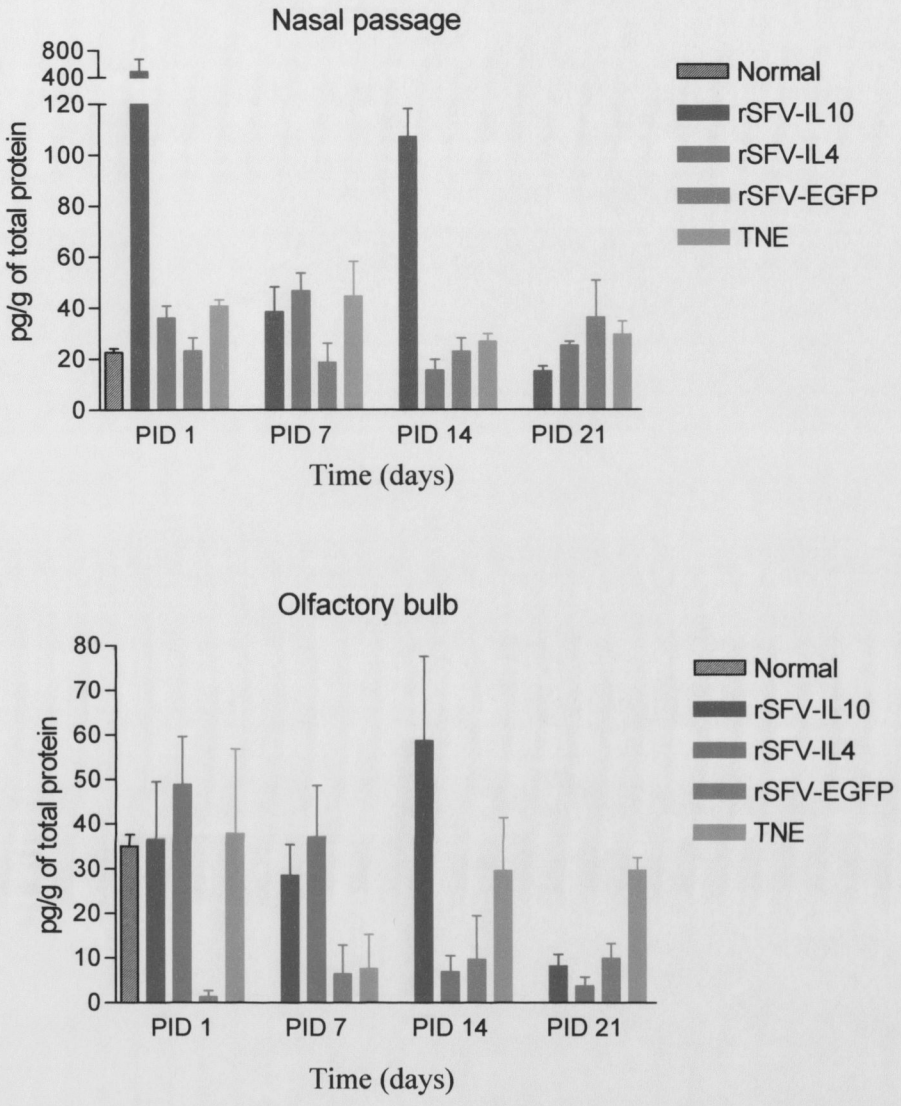

Figure 4.3 IL-10 levels in mice following particle administration

C57BL/6 mice were infected i.n. with rSFV-IL10, rSFV-IL4, rSFV-EGFP, or mock infected with TNE. Uninfected mice were used for normal controls. Nasal passage and olfactory bulb tissue were removed at designated time points and homogenized as described in section 4.2.2.3. Homogenized tissue samples were tested for the presence of IL-10 by capture ELISA as described in section 3.2.2.4.3.1.

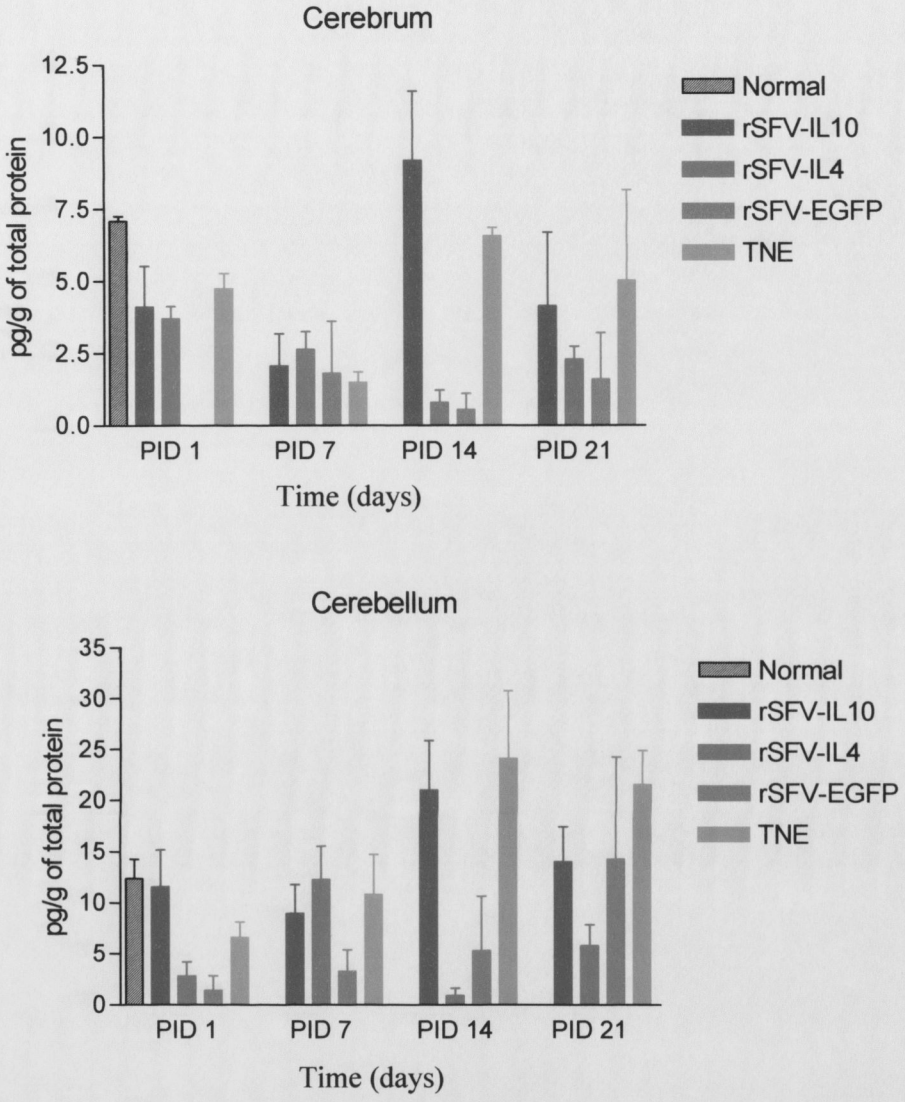

Figure 4.4 IL-10 levels in mice following particle administration

C57BL/6 mice were infected i.n. with rSFV-IL10, rSFV-IL4, rSFV-EGFP, or mock infected with TNE. Uninfected mice were used for normal controls. Cerebrum and cerebellum tissue were removed at designated time points and homogenized as described in section 4.2.2.3. Homogenized tissue samples were tested for the presence of IL-10 by capture ELISA as described in section 3.2.2.4.3.1.

calculated between groups (figure 4.3). No significant difference was calculated between groups at day 1 following treatment in the olfactory bulb, however extremely low levels of IL-10 were measured in the control vector group. At day 7 only the rSFV-IL10 and rSFV-IL4 groups had levels comparable to the normal group, with control vector and TNE group levels significantly lower. TNE group had levels return to normal by day 14, with levels from rSFV-IL10 higher then all others. Control and rSFV-IL4 vectors had statistically ($P < 0.05$) lower levels then other groups. By day 21, all vector treated groups (rSFV-IL10, rSFV-IL4, rSFV-EGFP) had levels significantly ($P < 0.05$) lower then the normal and TNE control groups (figure 4.3). As in the olfactory bulb, cerebrum levels following control vector administration were very low, and at day 1 they were significantly lower then all other groups. A small statistical difference ($P < 0.0375$) was calculated between groups at day 7, with all treated groups having lower levels of IL-10 then normal untreated group. Levels return to normal in the TNE group by day 14, while rSFV-IL10 levels were higher. Control and rSFV-IL4 vector treated groups had significantly lower ($P < 0.05$) levels of IL-10. The same was observed for day 21, though there was no statistical significant difference calculated between groups (figure 4.4). IL-10 levels in the cerebellum at day 1 were no different from cerebrum levels, in that the rSFV-IL10 group had normal levels of IL-10, and other vector treated groups had significantly ($P < 0.05$) lower levels. No significant differences were found for day 7, though the control vector had lower levels of IL-10 then all other groups. At day 14, the only group to have lower levels then normal was the rSFV-IL4 treated group. By day 21, all groups had levels return to normal with the exception of rSFV-IL4 (figure 4.4). Statistical differences between groups obtained from one-way analyses of variance are described in table 4.2.

IFN-γ levels in the nasal passage had different profiles to IL-4 and IL-10 following treatment. A statistically significant difference was found for all time points. Following rSFV-IL10 administration, levels were higher at days 1 and 7, returning to normal at days 14 and 21. Similarly, rSFV-IL4 had higher levels at days 1 and 7, normal levels at day 14, and again higher levels at day 21. TNE group only had levels of IFN-γ higher then normal at day 1 post infection. The control vector group behaved in opposite manner to rSFV-IL10, and had normal levels at days 1 and 7, and elevated levels of the cytokine at days 14 and 21 (figure 4.5). The only statistical significant difference found for groups in the olfactory bulb was for the rSFV-IL4 treated group at days 1 and 7, which had higher levels ($P < 0.05$) then others. All remaining groups had levels similar to normal untreated group

Table 4.2 Statistical analyses of IL-10 levels in tissue homogenates

Homogenized tissue samples were tested for the presence of IL-10 by use of a capture ELISA as described in section 3.2.2.4.3.1. Measured cytokine levels were compared using the one-way analyses of variance (ANOVA) statistical test using Prism 4.0 (GraphPad software Inc.).

Location	d.p.i.	P value	P value summary *
Nasal passage	1	0.0096	Very significant
	7	> 0.05	Not significant
	14	0.0052	Very significant
	21	> 0.05	Not significant
Olfactory bulb	1	> 0.05	Not significant
	7	0.0375	Significant
	14	0.0358	Significant
	21	< 0.0001	Extremely significant
Cerebrum	1	0.0005	Extremely significant
	7	0.0155	Very significant
	14	0.0007	Extremely significant
	21	> 0.05	Not significant
Cerebellum	1	0.0149	Significant
	7	> 0.05	Not significant
	14	0.0114	Significant
	21	> 0.05	Not significant

* P value significance obtained using Prism 4.0 (GraphPad software Inc.), where:

P value:	> 0.05	not significant
P value	0.01 to 0.05	significant
P value	0.001 to 0.01	very significant
P value	< 0.001	extremely significant

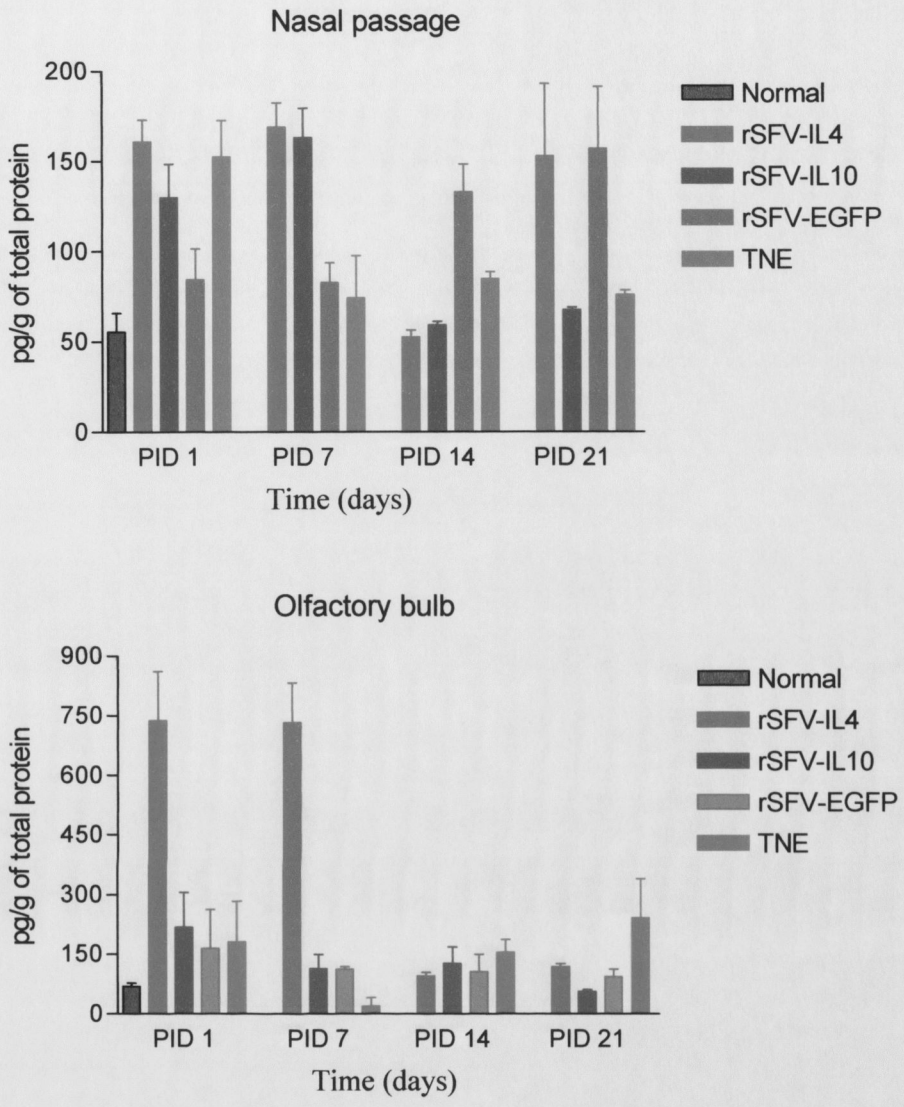

Figure 4.5 IFN-γ levels in mice following particle administration

C57BL/6 mice were infected i.n. with rSFV-IL10, rSFV-IL4, rSFV-EGFP, or mock infected with TNE. Uninfected mice were used for normal controls. Nasal passage and olfactory bulb tissue were removed at designated time points and homogenized as described in section 4.2.2.3. Homogenized tissue samples were tested for the presence of IFN-γ by capture ELISA as described in section 3.2.2.4.3.1.

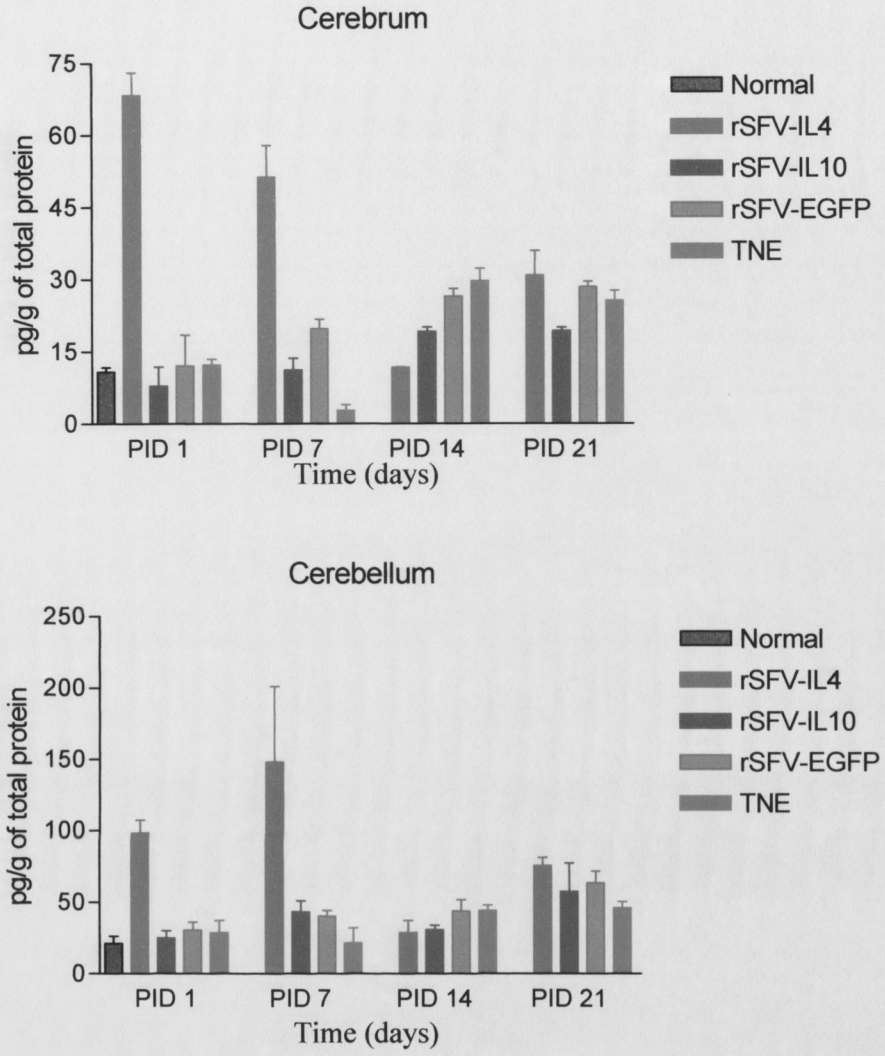

Figure 4.6 IFN-γ levels in mice following particle administration

C57BL/6 mice were infected i.n. with rSFV-IL10, rSFV-IL4, rSFV-EGFP, or mock infected with TNE. Uninfected mice were used for normal controls. Cerebrum and cerebellum tissue were removed at designated time points and homogenized as described in section 4.2.2.3. Homogenized tissue samples were tested for the presence of IFN-γ by capture ELISA as described in section 3.2.2.4.3.1.

(figure 4.5). Much like the olfactory bulb, the rSFV-IL4 group had significantly higher ($P < 0.05$) levels of IFN-γ in the cerebrum at days 1 and 7. By day 14, all groups except rSFV-IL4 had significantly higher levels then normal. By day 21 however, all groups except rSFV-IL10 had higher levels then the normal group (figure 4.6). Levels in the cerebellum were similar to those of the cerebrum. At days 1 and 7, rSFV-IL4 treated group had higher levels then others, which were similar to normal levels. All groups had similar levels of IFN-γ at day 14, with no statistical difference between them. Again at day 21, only the rSFV-IL4 group had higher levels then the normal untreated group (figure 4.6). Statistical differences obtained from one-way analyses of variance are described in table 4.3.

4.4 DISCUSSION

Cytokines behave *in vivo* very differently then *in vitro*. They have the ability to initiate cascade events that will further enhance an immune response. As a result of their ability to act at nano- to picomolar concentrations, the site of their expression does not necessarily predict the site at which they exert their biological function.

It was previously demonstrated that extremely high levels of secreted cytokines were present in cell supernatants following infection with rSFV vectors containing both IL-4 and IL-10. It was also demonstrated in previous experiments that proteins cloned into the rSFV vector system delivered i.n. could reach both the olfactory mucosa, and the olfactory bulb area of the brain. The current study goes further in showing that there is a definite change in the cytokine profile within the CNS of animals infected with the same vector.

The main problem in using a viral vector to treat inflammatory autoimmune diseases of the CNS is that the vector will induce a T_H1 response, which could enhance disease severity. The current study involves infecting mice with rSFV-IL10, rSFV-IL4, rSFV-EGFP, and buffer alone to detect changes in cytokine profiles of infected mice. Levels of the T_H2 cytokines IL-10 and IL-4, and the T_H1 cytokine IFN-γ were measured in the nasal passage, and in different areas of the brain. Since a great deal of raw data was obtained from this experiment, the one-way analyses of variance statistical test was used to interpret results. Taking into account the behavior of individual vectors the following

Table 4.3 Statistical analyses of IFN-γ levels in tissue homogenates

Homogenized tissue samples were tested for the presence of IFN-γ by use of a capture ELISA as described in section 3.2.2.4.3.1. Measured cytokine levels were compared using the one-way analyses of variance (ANOVA) statistical test using Prism 4.0 (GraphPad software Inc.).

Location	d.p.i.	P value	P value summary *
Nasal passage	1	0.0038	Very significant
	7	0.0006	Significant
	14	0.0003	Extremely significant
	21	0.0313	Significant
Olfactory bulb	1	0.0035	Very significant
	7	< 0.0001	Extremely significant
	14	> 0.05	Not significant
	21	> 0.05	Not significant
Cerebrum	1	< 0.0001	Extremely significant
	7	< 0.0001	Extremely significant
	14	< 0.0001	Extremely significant
	21	0.0017	Very significant
Cerebellum	1	< 0.0001	Extremely significant
	7	0.0065	Very significant
	14	> 0.05	Not significant
	21	0.0352	Significant

* P value significance obtained using Prism 4.0 (GraphPad software Inc.), where:

P value:	> 0.05	not significant
P value	0.01 to 0.05	significant
P value	0.001 to 0.01	very significant
P value	< 0.001	extremely significant

conclusions can be reached. IL-10 levels produced as a result of the rSFV-IL10 vector are significantly higher in the nasal passage for up to 14 days following vector administration. By day 14, higher levels of IL-10 could be detected in areas of the brain, also as a result of rSFV-IL10 administration. Higher IL-4 levels as a result of this vector could also be detected in areas of the brain immediately after vector administration. IFN-γ levels were only higher as a result of this vector in the early days following infection, and only in the nasal passage. Similarly, rSFV-IL4 resulted in increased levels of IL-4 in the nasal passage and different areas of the brain. This vector however was not effective in raising levels of IL-10 in either the brain or nasal passage. IFN-γ levels on the other hand, were considerably higher as a result of rSFV-IL4 administration, for up to 21 days in the nasal passage, and 7 days in areas of the brain. A possible explanation for the raised levels of the inflammatory cytokine IFN-γ following i.n. administration of rSFV-IL4 could be due to raised levels of IL-4 in the lungs, airways and bronchial epithelial cells. It has been demonstrated that IL-4 plays a key role in the inflammatory response of hypersensitive reactions. This cytokine promotes the production of IgG1 and IgE. IgE plays a role in mediating immediate hypersensitive reactions responsible for such conditions as fever, asthma, and hives. Studies on allergen-induced airway eosinophilic inflammation and bronchial hyperresponsiveness have demonstrated raised IL-4 levels associated with inflammation (Hodge *et al,* 2001, Tanaka *et al,* 2000). Since IL-4 is being delivered i.n. by a rSFV vector, it would be likely that IL-4 would accumulate in the airways, lungs, and bronchial epithelial cells. This would in turn lead to an inflammatory response; therefore raising IFN-γ levels. The control vector (rSFV-EGFP) worked as expected. It caused IL-10 levels in the areas of the brain to decrease, and IFN-γ levels to increase. IL-4 levels as a result of the control vector were higher in some areas of the brain, but not on the nasal passage.

The main limitation of this study was that no distinction was made between the cloned cytokine, and cytokines produced as a result of vector administration. To distinguish between cloned and cytokines normally present in the body, uninfected controls were used. In order to differentiate between cloned cytokines and cytokines produced by the body as a result of the vector, cloned cytokines would need to be tagged, which involves construction of a new vector including a HA-tagged IL-10. This would in theory allow for exact localization, by immunohistochemistry, of the expressed cytokine in the CNS. This method of identification however is not quantitative; therefore no indication of

cytokine levels delivered would be detected. In the context of the current research, it was more important to determine levels of cytokine produced in areas of the CNS following vector administration than to know where the cloned cytokine was localized. Furthermore, most pathology lesions in EAE occur in the spinal cord, and the likelihood of proteins being delivered there by this non-replicative vector is highly unlikely. A second alternative to cloning a tagged form of the protein would be to use cytokine knockout mice. This however, would lead to a similar problem, in that no cytokines would be produced as a result of the vector. Furthermore the extreme high cost of these animals would severely limit the number available for use. All these reasons combined led to the use of C57BL/6 mice, the same strain used for the EAE experiment. These mice are healthy and capable of normally producing cytokines.

Chapter 5

Treatment of experimental autoimmune encephalomyelitis with the rSFV expression vector

5.1 INTRODUCTION

EAE is the most widely used animal model for the human disease MS. This model was first described in 1933 by Rivers et al, where it was demonstrated that immunization of experimental animals with myelinated tissue led to what is now considered EAE (Rivers *et al,* 1933). The method was perfected over many years, especially with the discovery that Freund's adjuvant results in a rapid development of the disease at a much higher incidence (Kabat *et al,* 1947, Morgan 1947). For the next 70 years EAE has been considered an essential model for study of demyelinating diseases, with special emphasis given to MS. EAE is an acute or chronic relapsing experimental autoimmune disease of the CNS characterized by focal areas of inflammation and demyelination. It is easily induced in susceptible animal strains by immunization with myelin components in appropriate adjuvant. It is well established that EAE is mediated by MHC class II-restricted CD4+ T-cells specific for the portion of the peptide used which is encephalitogenic to a particular animal strain (Fritz *et al,* 1985, Zamvil and Steinman 1990). EAE pathology varies considerably between species. In mice, it is characterized by perivascular lymphocytic and monocytic infiltrates, demyelination, and some limited remyelination (Raine 1983, Raine 1984). Similar to MS, not every animal is susceptible to EAE. In mice, different strains are susceptible to different autoantigens. Two commonly used strains that are susceptible to EAE are SJL and C57BL/6 mice. One method of inducing the disease in SJL mice is with spinal cord homogenate (SCH), and in C57BL/6 with the peptide MOG 35-55 (Amor *et al,* 1994, Okuda *et al,* 2002).

The use of cytokines to treat EAE has been extensively exploited. T_H2 producing cytokines are commonly in use, due to their anti-inflammatory characteristics. One such cytokine is IL-10, which has been widely studied in EAE (Bettelli *et al,* 1998, Croxford *et al,* 2001, Cua *et al,* 2001, D'Orazio and Niederkorn 1998, Samoilova *et al,* 1998, Xiao *et al,* 1998). It has been further demonstrated that elevated levels of T_H2 cells producing IL-10 are associated with the spontaneous recovery from EAE (Kennedy *et al,* 1992), and that chronic relapsing EAE is associated with low IL-10 production (Issazadeh *et al,* 1996). Much like IL-10, IL-4 has been commonly studied in EAE. Also produced by T_H2 cells, it plays an important role in EAE, as demonstrated by IL-4 knockout mice, which develop a more severe form of the disease (Falcone *et al,* 1998). TGF-β has also been successfully demonstrated as an important cytokine in EAE, where it was shown to prevent the

incidence of relapses in EAE mice (Kuruvilla *et al,* 1991). It was further demonstrated that administration of anti-TGF-β increased severity of EAE (Johns and Sriram 1993, Racke *et al,* 1992, Santambrogio *et al,* 1993). TGF-β has also been shown to inhibit the adoptive transfer of EAE in vitro by preventing activation and proliferation of encephalitogenic precursors (Racke *et al,* 1991).

A number of different viral vectors and delivery routes have been used in the treatment of EAE. Viral vectors delivered by the i.c. route have successfully demonstrated cytokine expression in the CNS, and an effect on the outcome of EAE. That was the case of herpes virus, and adeno-associated viral vectors (Cua *et al,* 2001, Furlan *et al,* 2001, Martino *et al,* 1998, Martino *et al,* 2000a). It has also been shown that i.m. injection of plasmid-based DNA vectors expressing IL-4 or TGF-β inhibit the development of EAE (Piccirillo and Prud'homme 1999). The i.n. mode of inoculation has only been used to deliver the cytokine protein directly, that is with no vector. It has been demonstrated that i.n. delivery of IL-10 given as protein to rats was effective in inhibiting EAE when given in large amounts (Xiao *et al,* 1998). The present study investigated the effects of treating mice sensitized for EAE with rSFV vectors expressing different cytokines. The main problem with the use of this vector to treat EAE is that it has been shown that the wild-type avirulent virus given peripherally can potentiate or exacerbate EAE (Eralinna *et al,* 1996, Mokhtarian and Swoveland 1987). It is possible therefore, that administration of the SFV vector by peripheral inoculations could have the same effect.

Higher levels of cytokine were observed in previous experiments following i.n. delivery by the rSFV vector system. It is possible therefore, that a desired biological response will be obtained with an inhibition of the disease. The use of the i.n. inoculation of rSFV in the treatment of EAE has recently been demonstrated. We demonstrated that the i.n. treatment of EAE with rSFV expressing IL-10 inhibited the disease (Jerusalmi *et al,* 2003 data included in this thesis). Treatment with rSFV expressing other cytokines generated numerous results.

5.2 EXPERIMENTAL PROCEDURES

5.2.1 NEW MATERIALS

5.2.1.1 Mice

Female SJL and C57BL/6 mice aged 40-60 days were obtained from Harlan (UK). Mice were maintained in accordance with the principles outlined in S1 17/94 European Communities regulations 1994, for care and use of laboratory animals. Syringes (20 ml, 10 ml, and 1.0 ml) and needles, (21G), were from Terumo (Leuven, Belgium)

5.2.1.2 EAE induction

MOG peptide 35-55 (MEVGWYRSPFSRVVHLYRNGK) was from Genemed Synthesis, Inc (CA, USA). Spinal cord homogenate (SCH) was obtained by homogenizing spinal cord of either SJL or BALB/c mice, freezing it overnight at -20°C, then freeze drying it overnight. Incomplete Freund's adjuvant (IFA), *Mycobacterium tuberculosis*, and *Mycobacterium butyricium* were from DIFCO (Detroit, USA). Pertussis toxin (PT) was from CAMR (UK). A Clifton ultrasonic bath model DU-4 was obtained from Laboratory Instruments & Supplies Ltd. (Meath, Ireland).

5.2.1.3 Particle production

An empty vector was constructed from the plasmid pSFV-1. An antibody specific for the nsP4 region of SFV was obtained from Dr. Marina Fleeton, and used for the titration of the viral like particle. The vector was produced and titrated as described for rSFV-IL10 in sections 3.2.2.4.1 and 3.2.2.4.2, with the following modification: cells were blocked in goat serum, primary antibody dilution was 1:2000, and a goat anti-rabbit secondary antibody was used.

5.2.2 METHODS

5.2.2.1 Particle production

rSFV vectors expressing EGFP, IL-10, IL-4, TGF-β, and an empty vector were prepared as described in sections 4.2.2.1. All viral like particles contained a titer ranging from 5×10^9 to 3×10^{10} IU/ml.

5.2.2.2 Setting up the EAE model for C57BL/6 mice

A working stock was of adjuvant and bacteria was prepared by dissolving 16.0 mg of *Mycobacterium tuberculosis* and 2.0 mg of *Mycobacterium butyricium* in 4.0 ml of incomplete Freud's adjuvant (IFA). This stock was kept for 7 days at 4°C and used for a booster immunization. An enriched adjuvant was prepared by mixing 1.0 ml of freshly prepared working stock with 11.5 ml of IFA. Two different concentrations of MOG peptide were prepared for immunization. The first involved immunizing each mouse with 100 μg of the peptide emulsified in enriched adjuvant, while a second group contained 200 μg of peptide per mouse in enriched adjuvant.

A total of 24 mice were used. Four groups each containing 6 mice were immunized with the following: 100 μg per mouse with and without PT, and 200 μg per mouse with and without PT. To prepare the 100 μg group, 2.0 mg of peptide was dissolved in 3.0 ml of PBS, and mixed with 3.0 ml of enriched adjuvant in a 10 ml plugged syringe. Solution was sonicated for 10 min at RT in an ultrasonic bath, and mixed with a 1 ml syringe until an emulsion was complete. The 200 μg group was prepared by mixing 4.0 mg of peptide in 3.0 ml of PBS and 3.0 ml of enriched adjuvant in same manner. A CSF needle was used to fill 1 ml syringes with freshly prepared emulsion. Needles were super-glued to 1 ml syringe prior to use. Each mouse was immunized s.c. with 0.15 ml of emulsion into both femoral region. Mice were also injected i.p. with 200 ηg of pertussis toxin derived from *Bordetella pertussis*, dissolved in 0.1 ml water, 1 h following immunization, and 24 h later. A booster with same emulsion as well as PT was given 7 days later.

Animals were monitored daily and disease severity graded on a scale of 0 to 6 with 0.5 points for intermediate clinical findings. Score design was as follows: 0, no clinical

sign; 1, limp tail and feet; 2, impaired righting reflex; 3, partial hind limb paralysis; 4, total hind limb paralysis; 5, moribund; 6, death. The Mann Whitney test was used for statistical analyses (GraphPad Prism 4.0) on EAE progression after the onset of disease.

5.2.2.3 Effect of 3 inoculations of rSFV on EAE

EAE was induced in 40 female C57BL/6 mice with 100 μg of MOG 35-55 enriched in adjuvant with PT as described in section 5.2.2.2. Four groups of 10 mice each were then treated i.n. with 10^7 IU of the following: rSFV-IL4, rSFV-IL10, rSFV-TGFb, and TNE buffer at days 8, 10, and 12 following EAE induction. Animals were monitored as described in section 5.2.2.2 for a period of 27 days. At day 27, all mice were perfused with NBF as described in section 2.2.2.6.2, kept in fixative overnight, and whole brains and spinal cords removed for pathological analyses. Paraffin embedding and sectioning was performed by Ms. Alex Whelan (Veterinary Pathology Laboratory, UCD), as described in section 2.2.2.9.2. Professor Brian J. Sheahan (Veterinary Pathology Laboratory, UCD) analyzed all samples for pathology. A tentative grading system was devised assigning each section a grade of 1 to 3, based on severity of pathology lesions. The Mann Whitney test was used for statistical analyses (GraphPad Prism 4.0) on EAE scores based on EAE progression after the onset of disease.

5.2.2.4 Effect of 4 inoculations of rSFV on EAE

EAE was induced in 54 female C57BL/6 mice with 100 μg of MOG 35-55 enriched in adjuvant with PT as described in section 5.2.2.2. Mice were grouped in 9 groups of 6 mice. Groups were treated either i.n. with 10^7 IU or i.m. with 10^6 IU with each of the following: rSFV-IL4, rSFV-IL10, rSFV-EGFP, and TNE buffer at days 6, 9, 12, and 15 following EAE induction. Final group was left untreated. Animals were monitored as described in section 5.2.2.2 for up to 42 days.

At varying time points ranging from days 23 to 42 post EAE induction, animals were taken for cytokine analyses. Mice from each group were taken during the acute phase of disease, disease remission, or no disease when possible. Brain and spinal cord were

homogenized as described in section 4.2.2.3, and protein assays performed as described in section 4.2.2.4. IL-10, IL-4, and IFN-γ levels were measured by ELISA on tissue homogenates and serum from each mice as outlined in section 4.2.2.5. The Mann Whitney test was used for statistical analyses (GraphPad Prism 4.0) on EAE progression after the onset of disease.

5.2.2.5 Effect of 5 inoculations of rSFV on EAE

EAE was induced in 60 female C57BL/6 mice with 100 μg of MOG 35-55 enriched in adjuvant with PT as described in section 5.2.2.2. Mice were grouped in 6 groups of 10 mice. Groups were treated i.n. with 10^7 IU of rSFV-IL10, rSFV-EGFP, rSFV-IL4 or mock-treated with TNE buffer; remaining groups were treated i.p. with 10^6 IU of rSFV-IL10 or rSFV-EGFP. Treatment days were 5, 8, 11, 14, and 17 following EAE induction. Animals were monitored as described in section 5.2.2.2 for 31 days following treatment. The Mann Whitney test was used for statistical analyses (GraphPad Prism 4.0) of EAE scores based on EAE progression after the onset of disease. Six mice randomly selected from each group were processed for pathological examination as outlined in section 5.2.2.3. Both olfactory bulbs were sectioned sagittally, and coronal sections were taken of the forebrain, midbrain, hindbrain and cerebellum. Longitudinal and transverse sections were examined from the cervical, thoracic, and lumbar spinal cord. A semi-quantitative histological grading system was adopted based on a scale of one plus for lesions which were isolated and mild to five plus for lesions which were diffuse and severe. A final composite score for each individual mouse was obtained by adding the scores allocated to lesions in the olfactory bulbs, brain, and spinal cord. Cumulative scores for the 6 mice in each group were added to obtain a final group score. All sections were coded to ensure they would be graded without knowledge of the origin or treatment.

5.2.2.6 Effect of 5 early inoculations of rSFV on EAE

EAE was induced in 42 female C57BL/6 mice with 100 μg of MOG 35-55 enriched in adjuvant with PT as described in section 5.2.2.2. Mice were grouped in 6

groups of 7 mice. Groups were treated i.n. with 10^7 IU with each of the following: rSFV-IL4, rSFV-IL10, rSFV-TGFb, rSFV-EGFP, and TNE buffer at days –1, 2, 5, 8, and 11 following EAE induction. The final group remained untreated. Animals were monitored as described in section 5.2.2.2 for 38 days. The Mann Whitney test was used for statistical analyses (GraphPad Prism 4.0) on EAE progression after the onset of disease.

5.2.2.7 Effect of rSFV on EAE induced on SJL mice

A working stock of bacteria, adjuvant, and enriched adjuvant were prepared as described in section 5.2.2.2. Each mouse was immunized with 1 mg of SCH emulsified in enriched adjuvant. A total of 42 SJL mice were used. Emulsion was prepared by dissolving 60 mg of SCH in 9.0 ml of PBS and mixing it with 9.0 ml of enriched adjuvant. Solution was sonicated for 10 min and a CSF needle used to fill 1 ml syringes as before. Mice were immunized as before with 0.15 ml of the emulsion s.c. in each femoral region. 200 ng of PT was also given at day of injection and 24 hrs later as before. A booster with the same emulsion and PT was given 7 days later. Animals were monitored as described in section 5.2.2.2. The Mann Whitney test was used for statistical analyses (GraphPad Prism 4.0) on EAE progression after the onset of disease.

Five groups of 7 mice were treated i.n. with 10^7 IU of one of the following: rSFV-IL10, rSFV-TGFb, rSFV or TNE at days 5, 8, 11, 14, and 17 following EAE induction. The final group remained untreated. Mice were monitored for a total of 42 days following disease induction.

5.2.2.8 Effect of rSFV on EAE induced on SJL mice - 2

EAE was induced in 30 female SJL mice with SCH enriched in adjuvant with PT as described in section 5.2.2.7. Five groups of 6 mice were treated i.n. with 10^7 IU with each of the following: rSFV-IL10, rSFV-TGFb, rSFV-EGFP, and TNE buffer at days –1, 2, 5, 8, and 11 following EAE induction. The final group remained untreated. Animals were monitored as described in section 5.2.2.2 for 38 days. The Mann Whitney test was used for statistical analyses (GraphPad Prism 4.0) on EAE progression after the onset of disease.

Four mice from each group were sent for pathology as outlined in section 5.2.2.3. A similar pathology grading system and analyses as used in section 5.2.2.5 was utilized.

5.3 RESULTS

5.3.1 Setting up EAE model on C57BL/6 mice

A working model of the disease was induced on C57BL/6 mice. Only animals that were given PT showed clinical signs of EAE, therefore, it was concluded that PT was needed to achieve disease. Both groups (100 μg and 200 μg) showed signs of EAE in all mice. Even though no significant statistical difference was measured between groups, a slightly higher acute disease profile was observed with group sensitized with 100 μg of MOG peptide compared to the 200 μg group, as observed by clinical score and weight loss graphs (figure 5.1). A mean EAE score of 3.1 ± 0.5 and a mean day of onset of 11.8 ± 0.6 was obtained for 100 μg group compared to 2.7 ± 0.4 and 10.2 ± 0.2 in 200 μg group. The mean EAE score for each group was obtained by averaging maximum EAE score of each mouse within group, expressed with standard error. Since a better acute disease model was established with the 100 μg per mouse group, this was used for further experiments.

5.3.2 Effect of 3 inoculations of rSFV on EAE

To detect an effect of rSFV vector administration on the course of EAE, mice sensitized for EAE were inoculated with rSFV-IL10, rSFV-IL4, rSFV-TGFb, or TNE buffer by the i.n. route at 3 time intervals (8, 10, and 12 days post disease induction). There was no significant difference between the mean maximum EAE scores of groups. When progression of disease after onset was analyzed, treatment with rSFV-IL10 significantly exacerbated disease compared to buffer control, rSFV-IL4 and rSFV-TGFb ($P < 0.05$). No significant difference was observed between any of the other treatment groups (figures 5.2 and 5.3). A pathology scale varying from 0 to 3 was devised dependent on severity of lesions observed in both brain and spinal cord. Main pathology observed in mice were perivascular lymphocytic cuffing, gliosis, and demyelination, which are

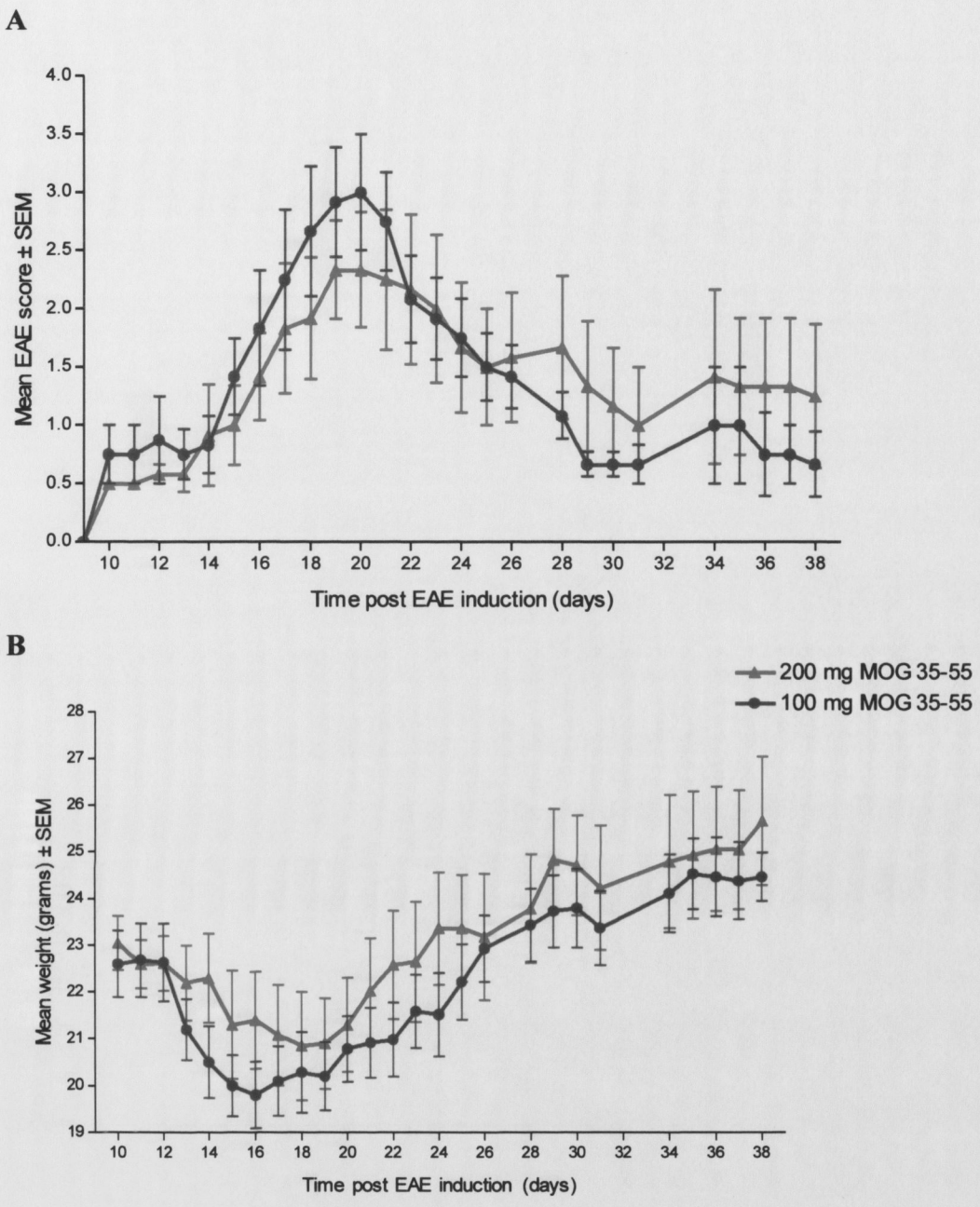

Figure 5.1 EAE model disease

EAE was induced in C57BL/6 mice using the encephalogenic peptide MOG 35-55. Animals were injected subcutaneously with either 100 μg or 200 μg peptide emulsified in IFA supplemented with *Mycobacterium* on days 0 and 7. In addition mice received 200 ng of PT 1 h and 24 h after peptide immunization. Animals were monitored daily, weighed and graded based on a neurological scale as outlined in section 5.2.2.2. **(A)** Progression of disease expressed as EAE score after the induction of disease. **(B)** Weight gain in grams after disease induction.

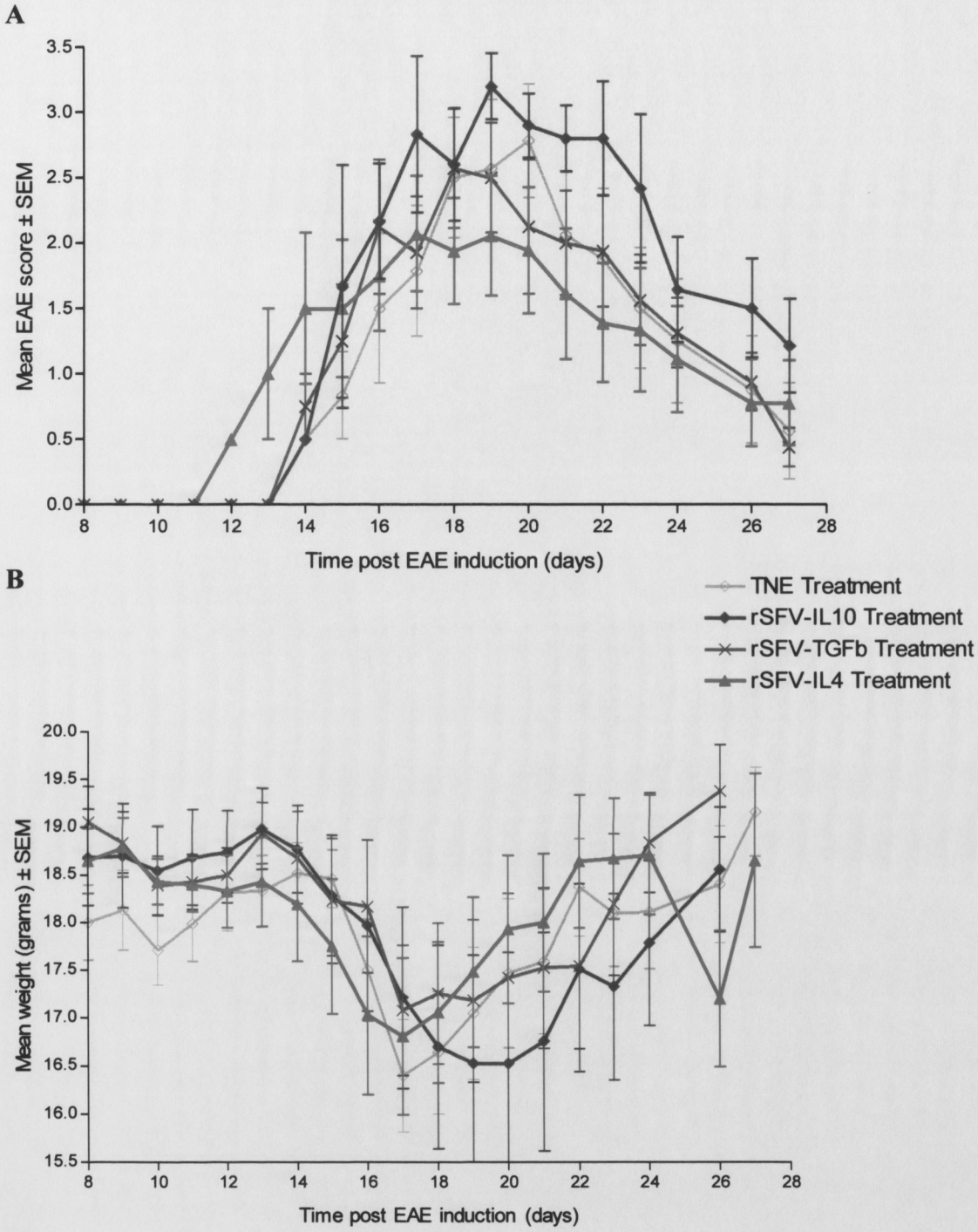

Figure 5.2 Effect of 3 inoculations of rSFV on EAE

Four groups of 10 EAE induced mice were treated i.n. with rSFV-IL10, rSFV-IL4, rSFV-TGFb, and TNE at days 8, 10 and 12 post disease induction. Animals were monitored daily, weighed and graded based on a neurological scale as outlined in section 5.2.2.2. **(A)** Progression of disease expressed as EAE score after the induction of disease. **(B)** Weight gain in grams after disease induction.

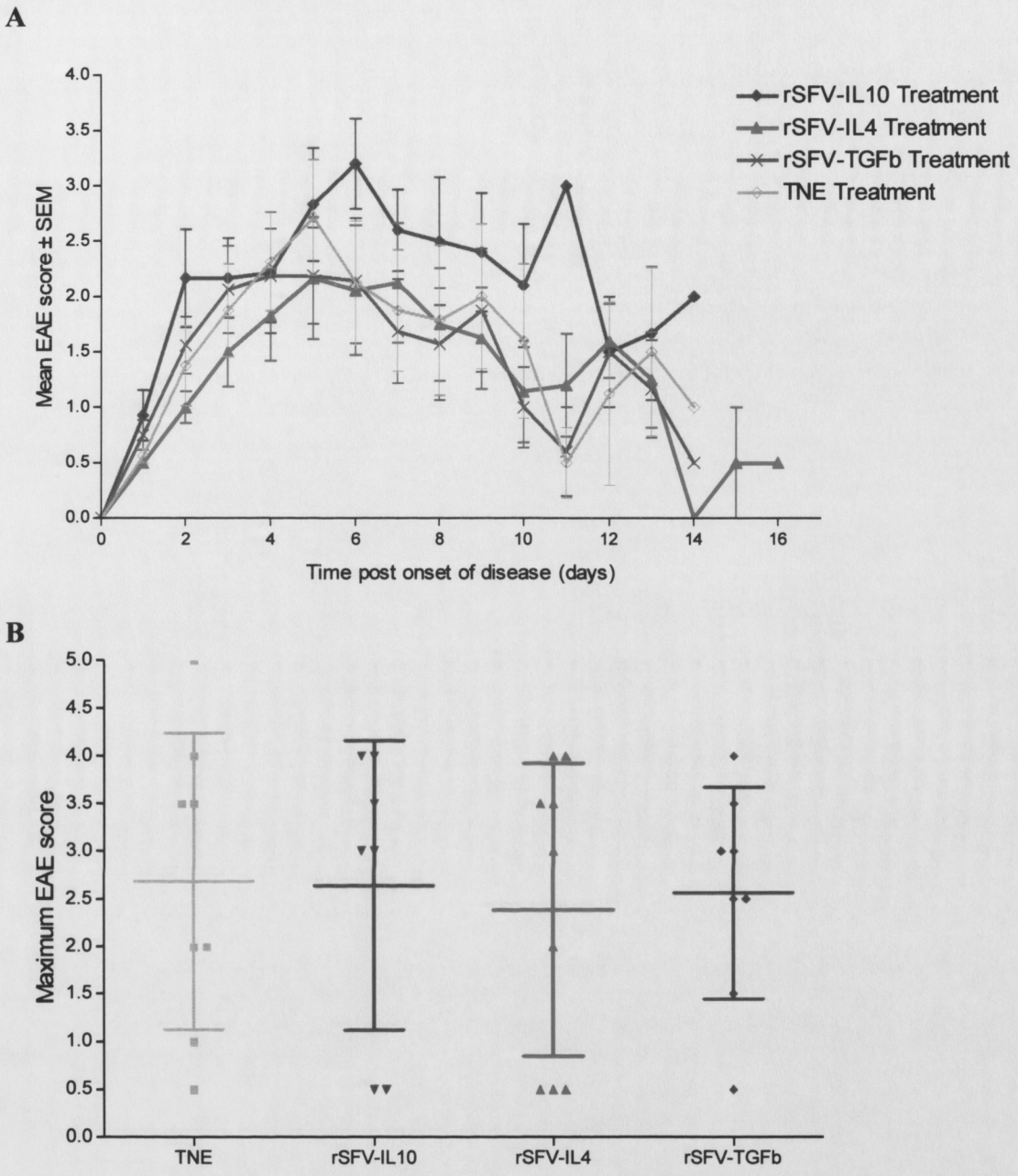

Figure 5.3 Effect of 3 inoculations of rSFV on EAE

Four groups of 10 EAE induced mice were treated i.n. with rSFV-IL10, rSFV-IL4, rSFV-TGFb, and TNE at days 8, 10 and 12 post disease induction. Animals were monitored daily, weighed and graded based on a neurological scale as outlined in section 5.2.2.2. **(A)** Progression of disease expressed as EAE score after disease onset. **(B)** Scatter plot graph of maximum EAE score of individual mice in each group with mean group score ± SD.

routinely observed in EAE lesions of the spinal cord. Milder lesions were noted in brains compared to spinal cord. No clear correlation was noted between pathology lesions and treatment groups, in that degree of pathology of each individual mouse correlated with clinical disease, rather then treatment agent. Table 5.1 summarizes findings with mean EAE scores, mean day of onset, disease incidence, and mean pathology grade for each group.

5.3.3 Effect of 4 inoculations of rSFV on EAE

Mice sensitized for EAE were treated with 4 doses of rSFV vectors expressing IL-10, IL-4, EGFP, or mock treated with TNE buffer. Mice were treated either i.n. or i.m. at 6, 9, 12 and 15 days post disease induction. Treatment by the i.m. method significantly exacerbated the disease compared to buffer treated group, independent of vector used (figures 5.4 and 5.5). In addition, no statistical difference was observed between cytokine treated groups to control vector (rSFV-EGFP) group (table 5.2). Treatment by the i.n. route exacerbated EAE only when the control vector was used, while both rSFV-IL10 and rSFV-IL4 had no statistical effect on disease outcome (figures 5.6 and 5.7). Furthermore, a statistical difference ($P < 0.05$) between i.n and i.m. treatments was only observed for cytokine treated groups (figure 5.8). No statistical difference was noted between control groups treated (both i.n. and i.m.) to untreated group, therefore only one control group was plotted in each graph, and used for statistical analyses.

Protein analyses by ELISA revealed no conclusive data. It did however suggest that animals recovering from the disease had higher levels of IL-10, while animals with EAE had higher levels of the T_H1 cytokine IFN-γ. No apparent difference was noted between groups treated with particles by the i.n. or i.m. methods, including all control groups.

5.3.4 Effect of 5 inoculations of rSFV on EAE

EAE mice were treated i.n. with 5 doses of rSFV vectors expressing IL-10, IL-4, EGFP, or mock treated with TNE buffer. Two further groups were treated i.p with rSFV-

Table 5.1 Analysis of EAE mice treated with rSFV particles

Four groups of 10 mice sensitized for EAE were treated i.n. with rSFV-IL10, rSFV-IL4, rSFV-TGFb, and TNE at days 8, 10 and 12 post disease induction. Animals were monitored daily, weighed and graded based on a neurological scale as outlined in section 5.2.2.2. Table demonstrates key findings for each group.

Group	Maximum EAE score (mean ± SEM)	Day of onset (mean ± SEM)	EAE mice (sick / total)	Pathology (mean ± SD)
rSFV-IL10	2.6 ± 0.6	18.1 ± 1.5	7 / 10	2.3 ± 0.9
rSFV-IL4	2.4 ± 0.5	15.6 ± 0.8	9 / 10	2.7 ± 0.5
rSFV-TGFb	2.6 ± 0.4	16.1 ± 0.7	8 / 10	2.3 ± 0.9
TNE	2.7 ± 0.6	16.4 ± 0.8	8 / 10	2.3 ± 0.7

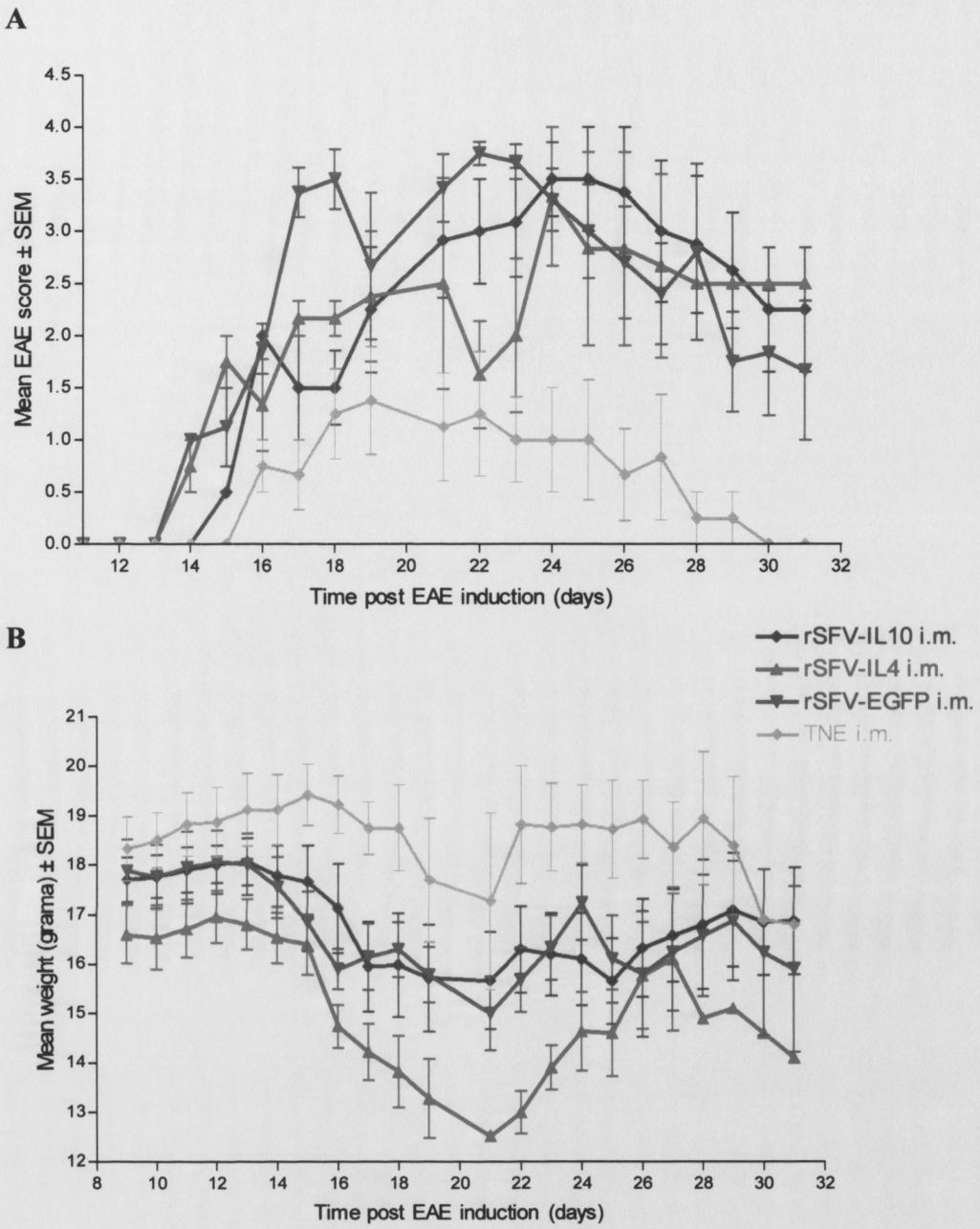

Figure 5.4 Effect of 4 i.m. inoculations of rSFV on EAE

Four groups of 6 EAE induced mice were treated i.m. with rSFV-IL10, rSFV-IL4, rSFV-EGFP, and TNE at days 6, 9, 12 and 15 post disease induction. Animals were monitored daily, weighed and graded based on a neurological scale as outlined in section 5.2.2.2. **(A)** Progression of disease expressed as EAE score after the induction of disease. **(B)** Weight gain in grams after disease induction.

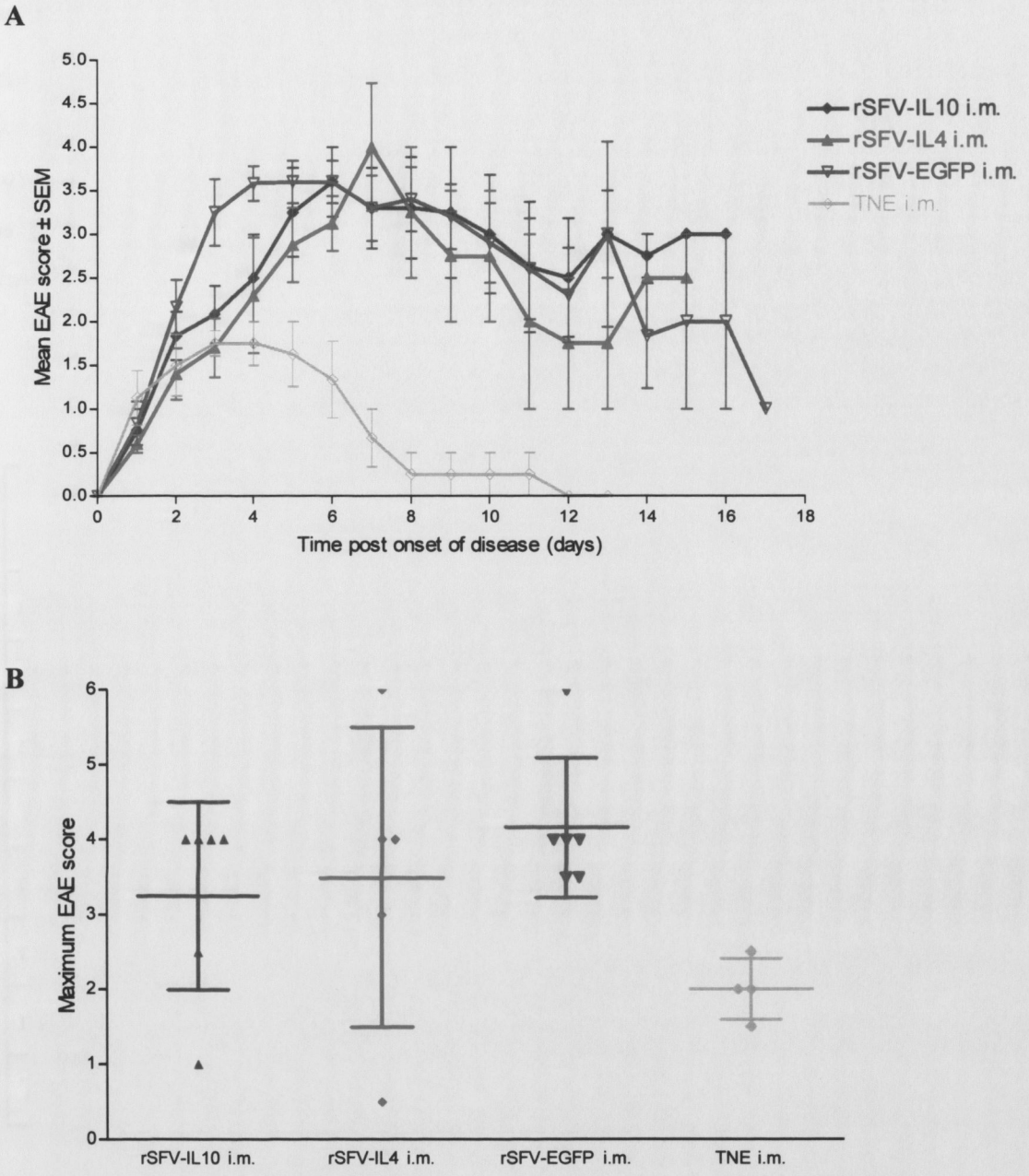

Figure 5.5 Effect of 4 i.m. inoculations of rSFV on EAE

Four groups of 6 EAE induced mice were treated i.m. with rSFV-IL10, rSFV-IL4, rSFV-EGFP, and TNE at days 6, 9, 12 and 15 post disease induction. Animals were monitored daily, weighed and graded based on a neurological scale as outlined in section 5.2.2.2. **(A)** Progression of disease expressed as EAE score after disease onset. **(B)** Scatter plot graph of maximum EAE score of individual mice in each group with mean group score ± SD. Statistical analyses performed by the Mann Whitney non-parametric ranking test showed that rSFV treatment exacerbated disease compared to controls ($P<0.005$).

Table 5.2 Analysis of EAE mice treated with rSFV particles

Mice sensitized for EAE were treated at days 6, 9, 12 and 15 post disease induction. Table demonstrates key findings for each group. All i.n. treated groups were compared to i.n. controls and i.m. treated groups to i.m. controls. Statistical significance was calculated using the Mann-Whitney nonparametric ranking test (GraphPad Prism 4.0) using data for the onset of clinical scores of mice showing EAE.

Group	Inoc. route	Maximum EAE score (mean ± SEM)	Day of onset (mean ± SEM)	EAE mice	P value vs TNE control	P value vs EGFP control
rSFV-IL4	i.n.	2.7 ± 0.8	16.8 ± 0.8	6/6	n.s.	0.0016**
rSFV-IL10	i.n.	2.1 ± 0.5	17.2 ± 1.3	5/6	n.s.	<0.0001**
rSFV-EGFP	i.n.	3.2 ± 0.5	17.2 ± 1.0	5/6	0.0005*	n.a.
TNE	i.n.	2.6 ± 0.2	14.2 ± 0.6	5/6	n.a	n.a.
rSFV-IL4	i.m.	3.5 ± 0.9	16.8 ± 1.4	5/6	0.0005*	n.s.
rSFV-IL10	i.m.	3.3 ± 0.5	17.2 ± 0.7	6/6	<0.0001*	n.s.
rSFV-EGFP	i.m.	4.2 ± 0.4	16.2 ± 0.9	6/6	0.0001*	n.a.
TNE	i.m.	2.0 ± 0.2	18.3 ± 1.7	4/6	n.a.	n.a.

* EAE score significantly higher than control ($p<0.005$)

** EAE score significantly lower than control ($p<0.005$)

n.s., not significant

n.a., not applicable

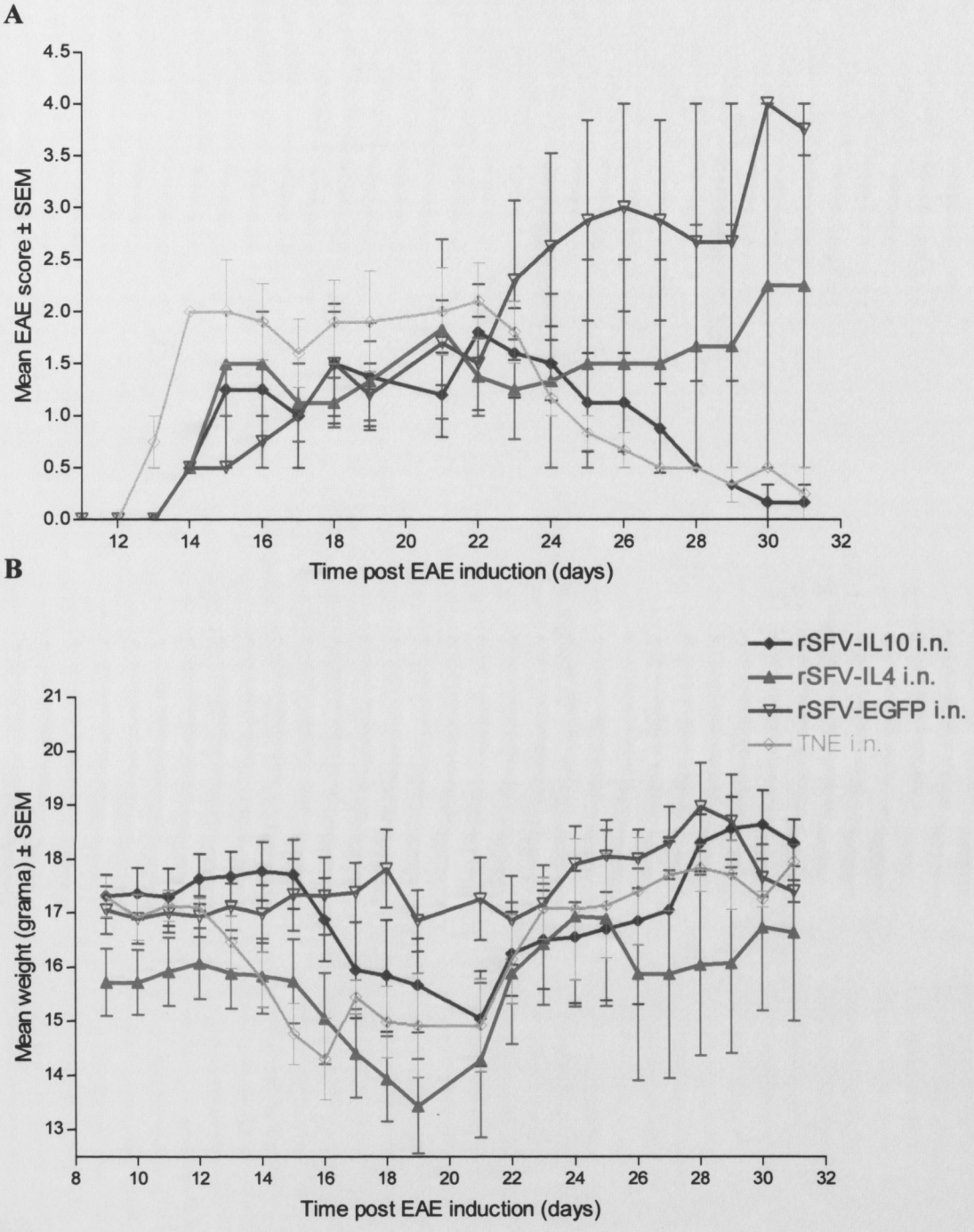

Figure 5.6 Effect of 4 i.n. inoculations of rSFV on EAE

Four groups of 6 EAE induced mice were treated i.n. with rSFV-IL10, rSFV-IL4, rSFV-EGFP, and TNE at days 6, 9, 12 and 15 post disease induction. Animals were monitored daily, weighed and graded based on a neurological scale as outlined in section 5.2.2.2. **(A)** Progression of disease expressed as EAE score after the induction of disease. **(B)** Weight gain in grams after disease induction.

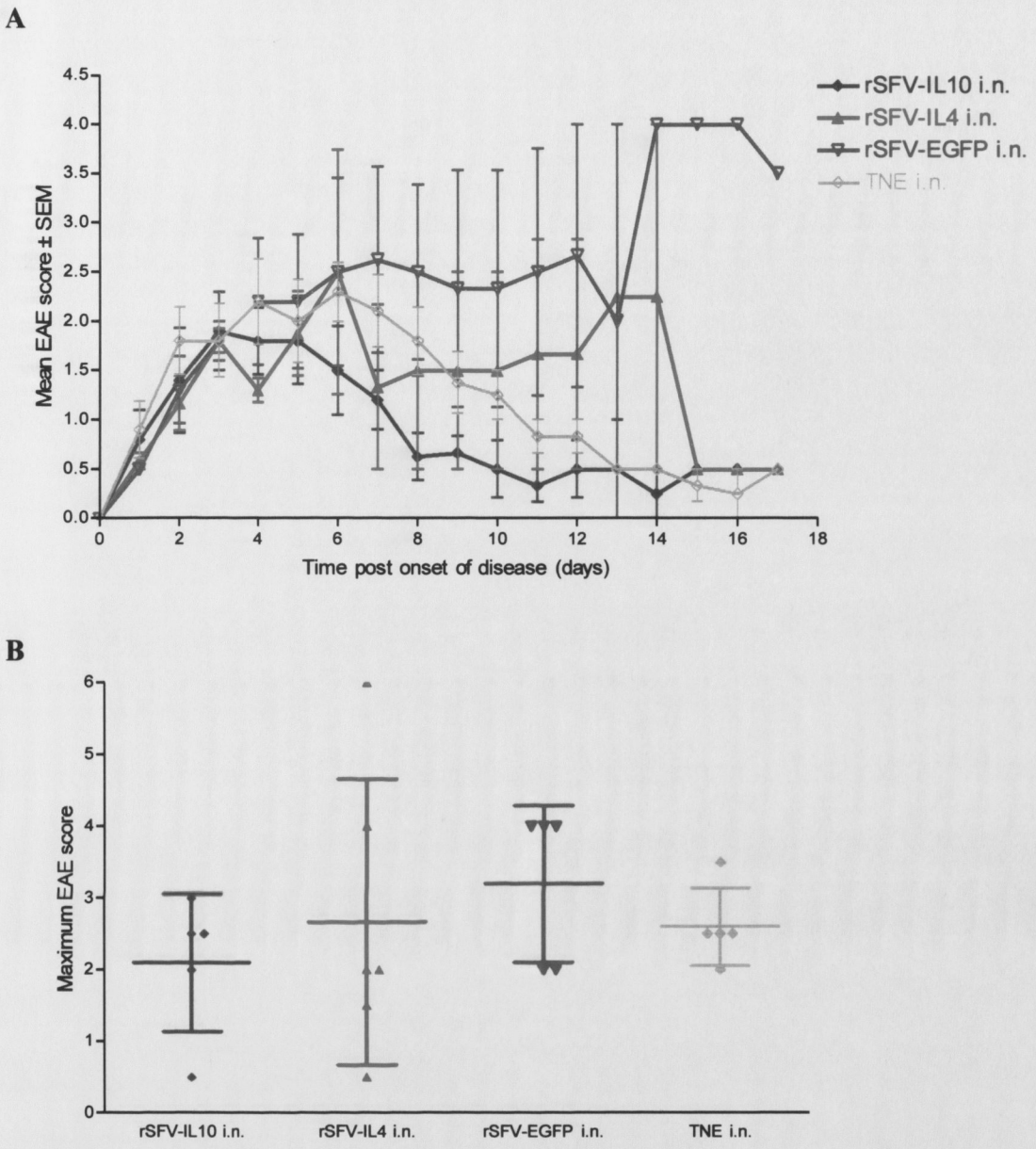

Figure 5.7 Effect of 4 i.n. inoculations of rSFV on EAE

Four groups of 6 EAE induced mice were treated i.n. with rSFV-IL10, rSFV-IL4, rSFV-EGFP, and TNE at days 6, 9, 12 and 15 post disease induction. Animals were monitored daily, weighed and graded based on a neurological scale as outlined in section 5.2.2.2. **(A)** Progression of disease expressed as EAE score after disease onset. **(B)** Scatter plot graph of maximum EAE score of individual mice in each group with mean group score ± SD. Statistical analyses was carried out by the Mann Whitney non-parametric ranking test on progression of disease showed that rSFV-EGFP treatment exacerbated disease compared to control and cytokine treated groups ($P<0.005$).

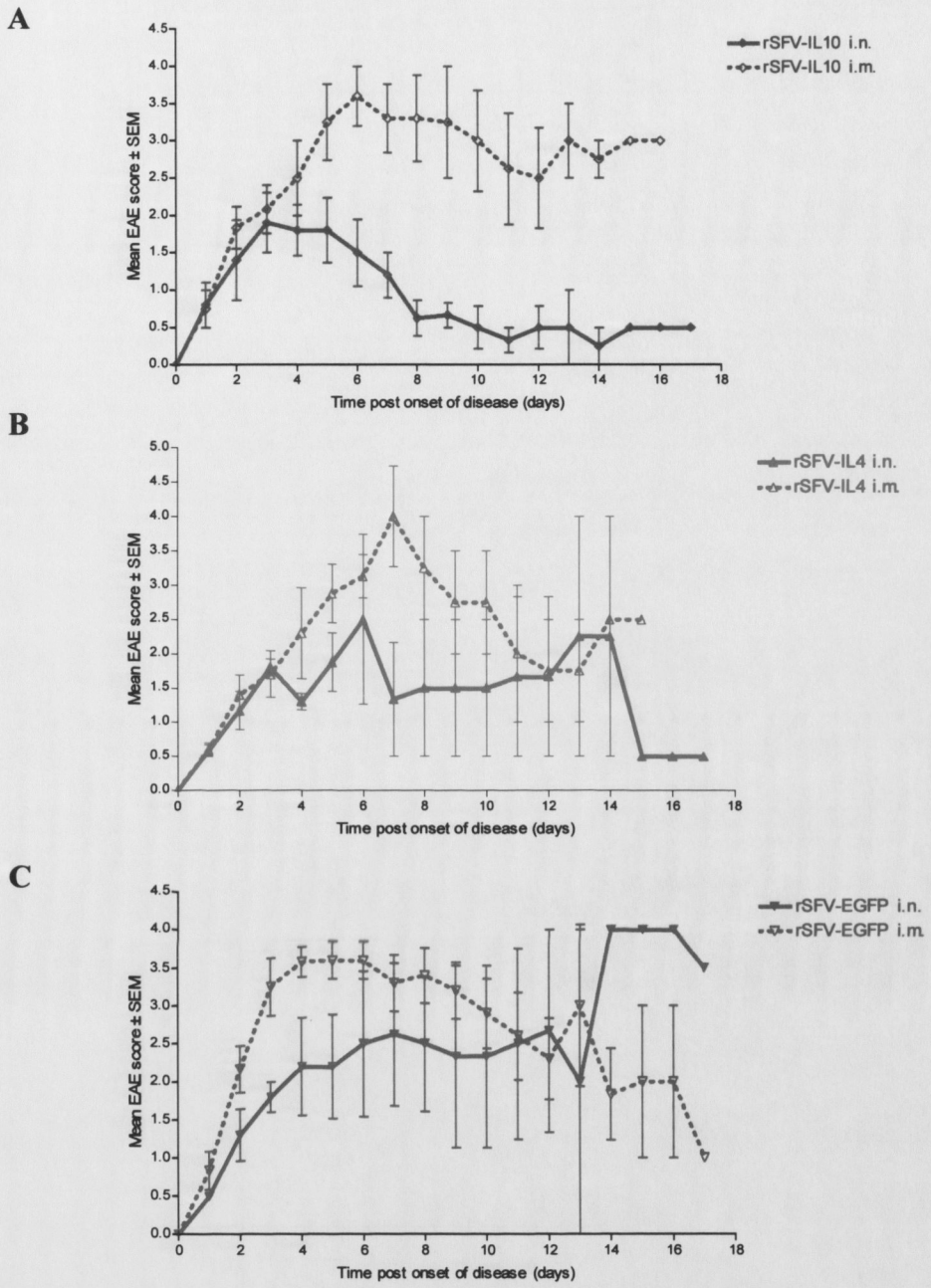

Figure 5.8 Comparison of i.n and i.m. treatment of rSFV on EAE

Three groups of 6 EAE induced mice were treated either i.n. or i.m. with rSFV-IL10, rSFV-IL4, and rSFV-EGFP at days 6, 9, 12 and 15 post disease induction. Animals were monitored daily, weighed and graded based on a neurological scale as outlined in section 5.2.2.2. Treatment routes for each vector is demonstrated as progression of disease expressed as EAE score after disease onset. **(A)** Comparison of rSFV-IL-10 treated groups showing significant difference between groups ($P<0.0001$). **(B)** Comparison of rSFV-IL-4 treated groups showing significant difference between groups ($P<0.005$). **(C)** Comparison of rSFV-EGFP treated groups showing no significant difference between groups. Statistical analyses was carried out by the Mann Whitney non-parametric ranking test.

IL10 and rSFV-EGFP. All mice were treated at 5, 8, 11, 14 and 17 days post disease induction. Treatment by the i.p. route delayed the onset of the disease, however it significantly exacerbated EAE compared to the buffer treated group (figures 5.9 and 5.10). Control vector treatment as on previous occasions significantly exacerbated EAE. IL-4 treatment delayed the onset of the disease, and also significantly exacerbated EAE compared to controls, as observed by clinical scores and pathological analyses. In contrast, IL-10 treatment not only considerably delayed the onset of the disease, but also significantly inhibited EAE (figures 5.11 and 5.12). The maximum recorded clinical EAE score was 2.0 for one mouse, compared to control mice treated with TNE, which had clinical scores as high as 3.5 for two mice. Furthermore, duration of disease was much shorter then all other groups (figure 5.13). As in previous experiment, severity of pathology lesions correlated with clinical disease score. Mostly lesions were concentrated in the white matter of the spinal cord, and less frequently in the cerebellum and hind brain. Typical lesions were characterized by gliosis, perivascular cuffing (mostly lymphocytes, with occasional macrophages), axonal swellings, and myelin vacuolation. Table 5.3 reflects a summarized finding of the pathology results and clinical scores. Table 5.4 describes pathology findings for individual mice. Figures 5.14 and 5.15 illustrated the semi-quantitative histological grading system utilized for pathology assessments.

5.3.5 Effect of 5 early inoculations of rSFV on EAE

When the timing of the treatment was modified to start prior to EAE induction, different results were obtained. Similarly, IL-4 treatment had no significant difference on the outcome of EAE when compared to IL-10 treated or buffer treated groups; but it once gain had a statistical significant difference ($P < 0.03$) when compared to empty vector (rSFV-EGFP and rSFV-TGFb). Treatment with IL-10 again inhibited the disease, however only slightly. There was a statistical difference between this and the buffer treated group ($P = 0.0308$) as well as a significant difference to control treated groups ($P < 0.002$). Once again, treatments with empty vector (rSFV-EGFP and rSFV-TGFb) significantly exacerbated the disease ($P < 0.02$). A graphical representation of the findings can be seen in figure 5.16.

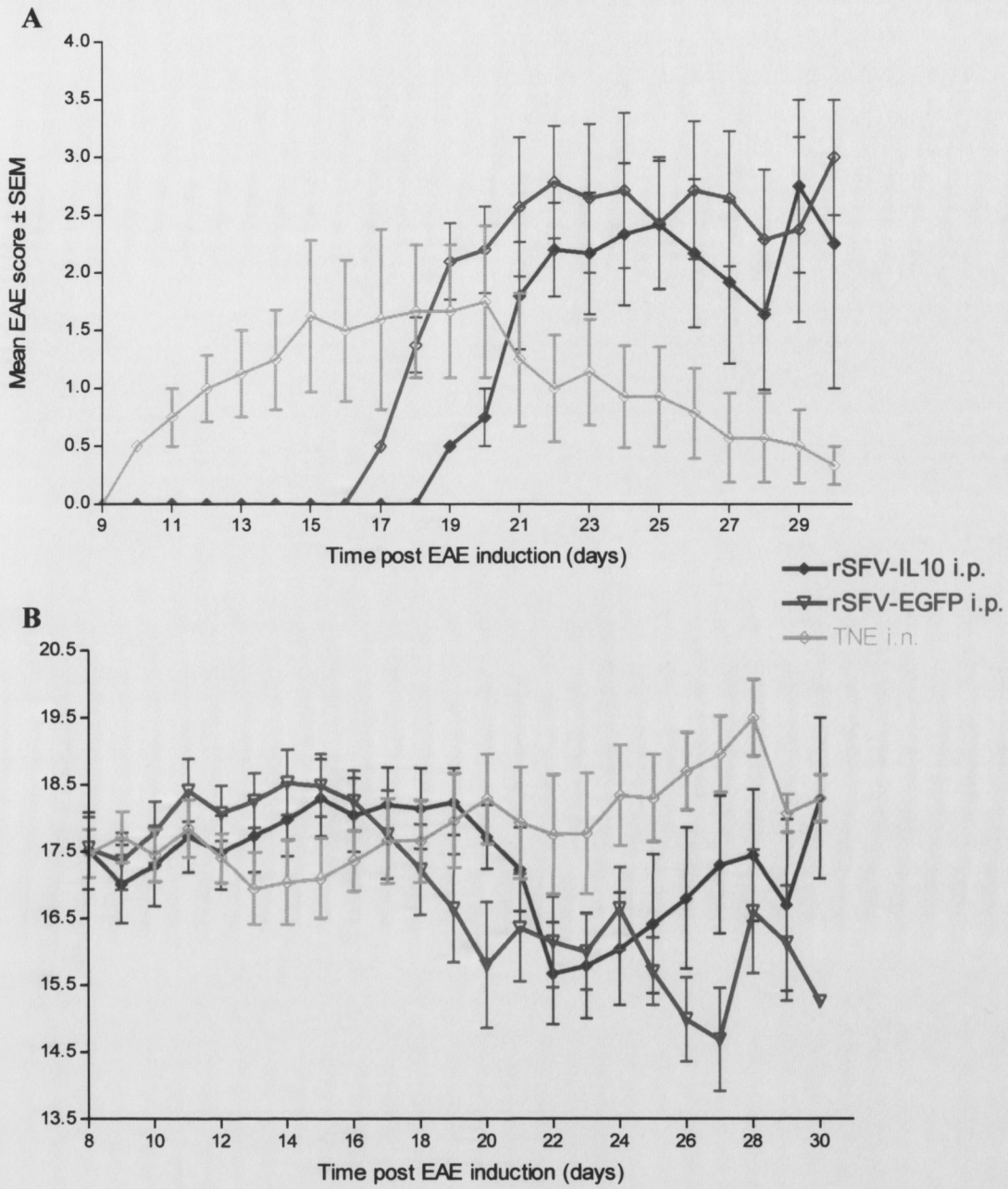

Figure 5.9 Effect of 5 i.p. inoculations of rSFV on EAE

Two groups of 10 EAE induced mice were treated i.p. with rSFV-IL10 and rSFV-EGFP at days 5, 8, 11, 14 and 17 post disease induction. Animals were monitored daily, weighed and graded based on a neurological scale as outlined in section 5.2.2.2. **(A)** Progression of disease expressed as EAE score after the induction of disease. **(B)** Weight gain in grams after disease induction.

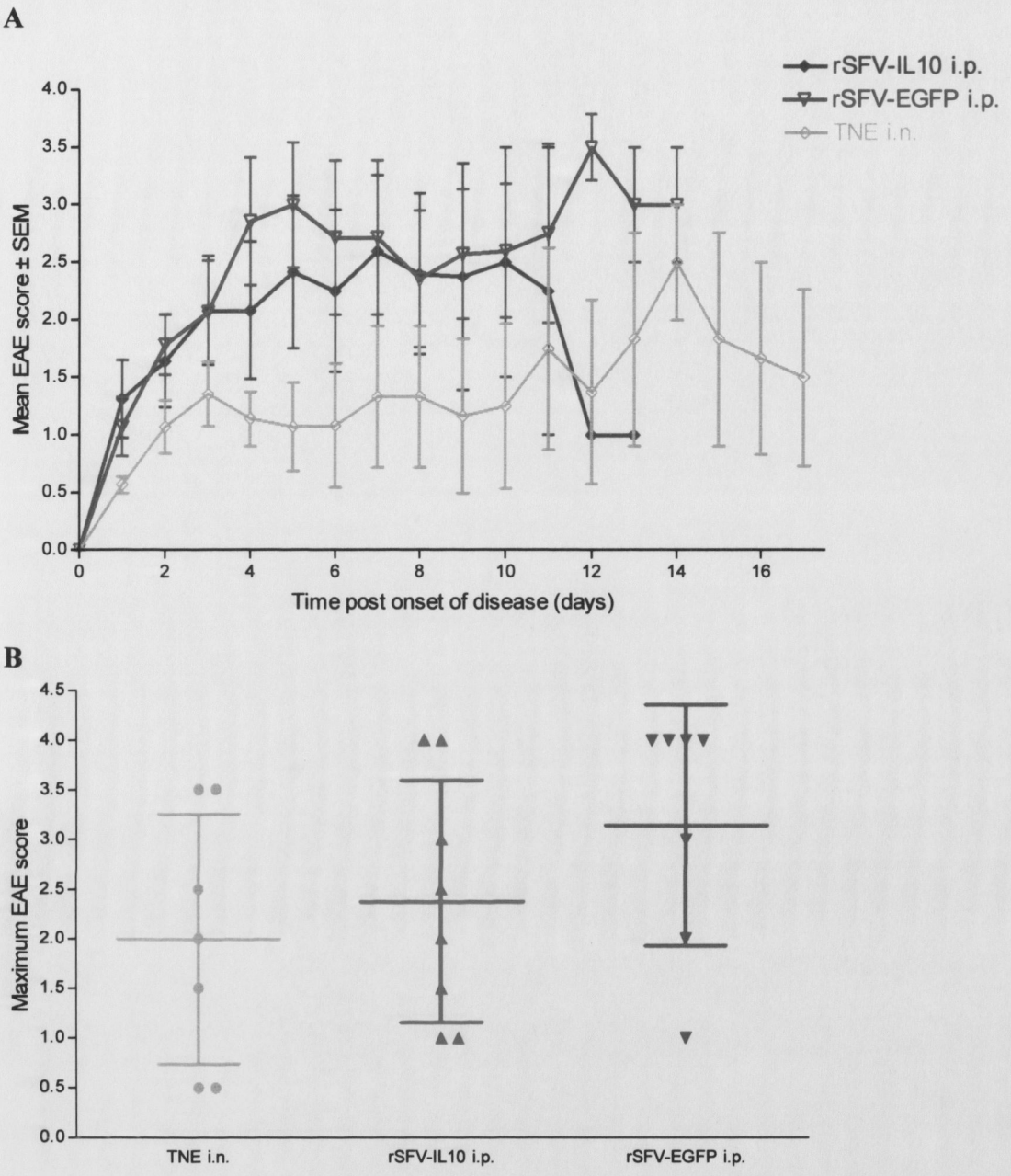

Figure 5.10 Effect of 5 i.p. inoculations of rSFV on EAE

Two groups of 10 EAE induced mice were treated i.p. with rSFV-IL10 and rSFV-EGFP at days 5, 8, 11, 14 and 17 post disease induction. Animals were monitored daily, weighed and graded based on a neurological scale as outlined in section 5.2.2.2. **(A)** Progression of disease expressed as EAE score after disease onset. **(B)**. Scatter plot graph of maximum EAE score of individual mice in each group with mean group score ± SD. Statistical analyses was carried out by the Mann Whitney non-parametric ranking test showed that rSFV treatment exacerbated disease compared to control treated groups ($P<0.005$).

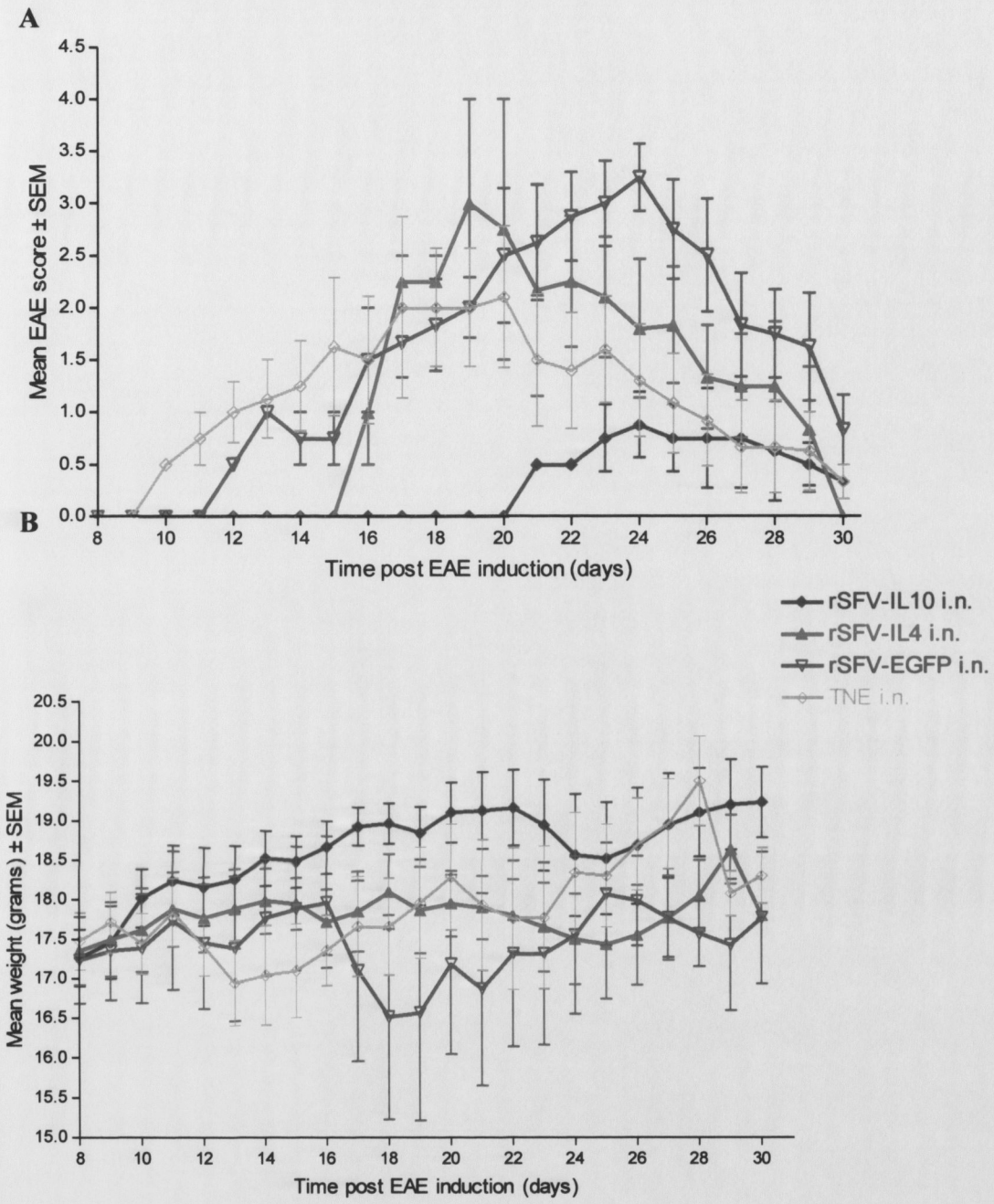

Figure 5.11 Effect of 5 i.n. inoculations of rSFV on EAE

Four groups of 10 EAE induced mice were treated i.n. with rSFV-IL10, rSFV-IL4, rSFV-EGFP and TNE buffer at days 5, 8, 11, 14 and 17 post disease induction. Animals were monitored daily, weighed and graded based on a neurological scale as outlined in section 5.2.2.2. **(A)** Progression of disease expressed as EAE score after the induction of disease. **(B)** Weight gain in grams after disease induction.

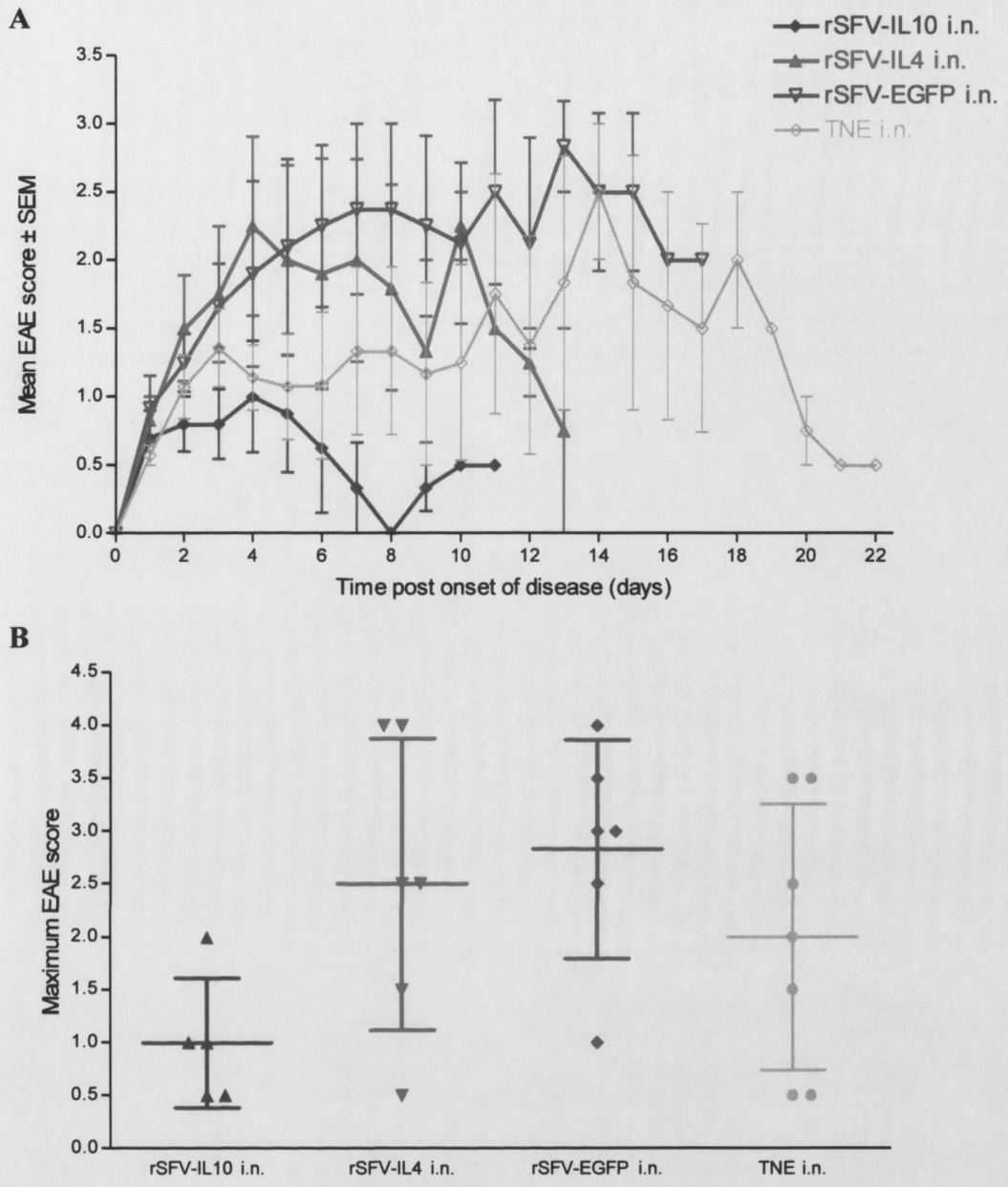

Figure 5.12 Effect of 5 i.n. inoculations of rSFV on EAE

Four groups of 10 EAE induced mice were treated i.n. with rSFV-IL10, rSFV-IL4, rSFV-EGFP and TNE buffer at days 5, 8, 11, 14 and 17 post disease induction. Animals were monitored daily, weighed and graded based on a neurological scale as outlined in section 5.2.2.2. **(A)** Progression of disease expressed as EAE score after disease onset. **(B)** Scatter plot graph of maximum EAE score of individual mice in each group with mean group score ± SD. Statistical analysis was carried out by the Mann Whitney non-parametric ranking test showed that rSFV-IL10 treatment inhibited disease compared to control treated groups ($P<0.005$).

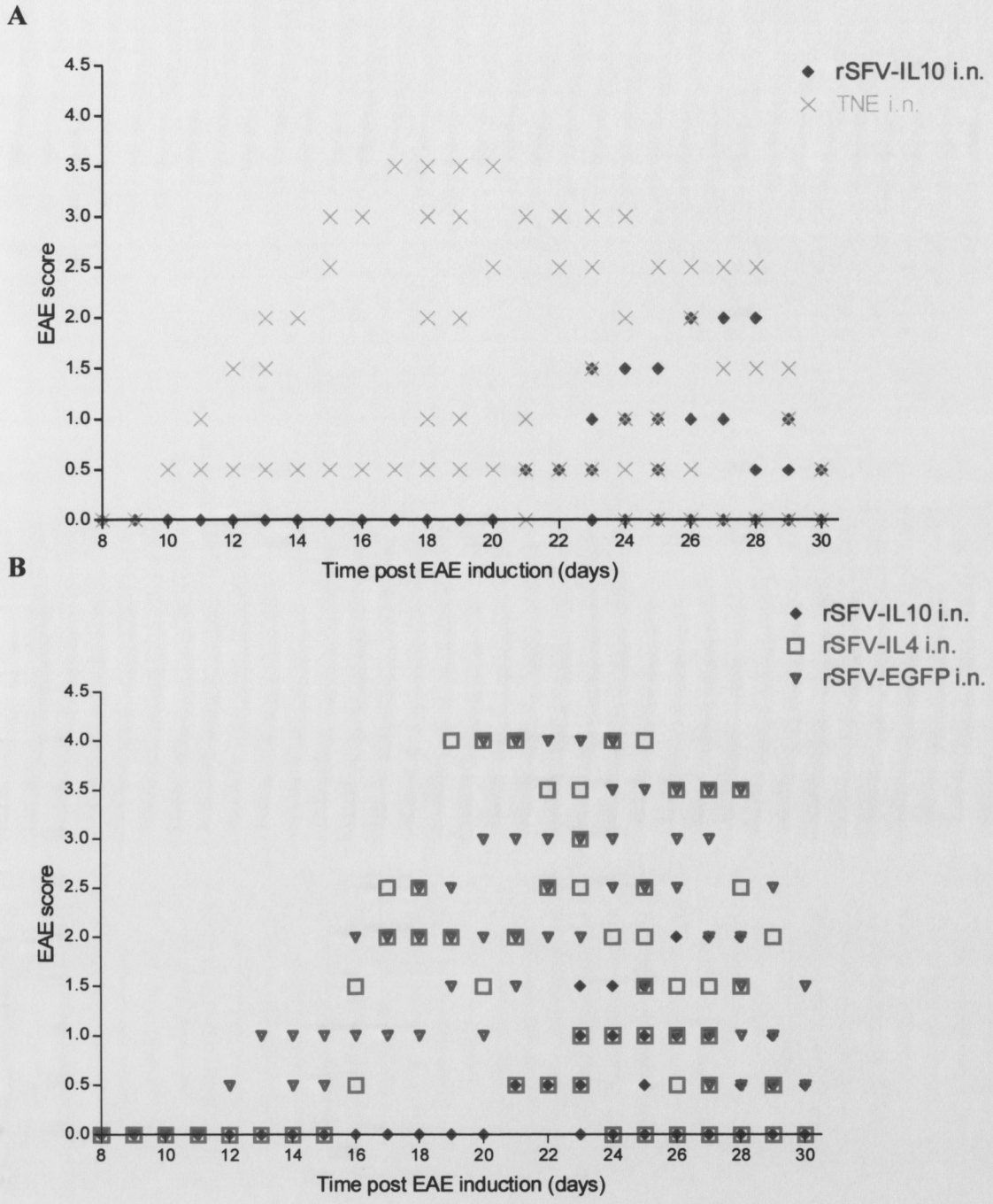

Figure 5.13 Analyses of 5 rSFV treatments on EAE

Four groups of 10 EAE induced mice were treated i.n. with rSFV-IL10, rSFV-IL4, rSFV-EGFP and TNE buffer at days 5, 8, 11, 14 and 17 post disease induction. Animals were monitored daily and graded based on a neurological scale as outlined in section 5.2.2.2. Graph represents daily EAE scores of each mouse **(A)** rSFV-IL10 and buffer treated group. **(B)** rSFV-IL10, rSFV-IL4 and rSFV-EGFP.

Table 5.3 Analysis of EAE mice treated with rSFV particles

Mice sensitized for EAE were treated at days 5, 8, 11, 14 and 17 post disease induction as indicated in section 5.2.2.5. Table demonstrates key findings for each group. Statistical significance was calculated using the Mann-Whitney nonparametric ranking test (GraphPad Prism 4.0) using data for the onset of clinical scores of mice showing EAE. Pathology grade demonstrates composite scores of olfactory bulb, brain, and spinal cord of all mice in group.

Group	Inoc. route	Max EAE score (mean ± SEM)	Day of onset (mean ± SEM)	EAE mice	P value vs TNE control	P value vs EGFP control[a]	Pathology grade
rSFV-IL4	i.n.	2.5 ± 0.6	20.5 ± 1.5	6/10	0.0040*	n.s.	25
rSFV-IL10	i.n.	1.0 ± 0.3	23.4 ± 1.5	5/10	0.0005**	<0.0001**	7
rSFV-EGFP	i.n.	2.8 ± 0.4	19.5 ± 2.6	6/10	<0.0001*	n.a.	22
TNE	i.n.	2.0 ± 0.5	14.1 ± 1.7	7/10	n.a	n.a.	12
rSFV-IL10	i.p.	2.4 ± 0.4	23.0 ± 1.5	8/10	0.0013*	n.s.	27
rSFV-EGFP	i.p.	3.1 ± 0.5	18.9 ± 0.6	7/10	<0.0001*	n.a.	22

[a] i.n. treated were compared to i.n. control, and i.p. treated to i.p. control.

* EAE score significantly higher than control ($p<0.005$)

** EAE score significantly lower than control ($p<0.005$)

n.s., not significant

n.a., not applicable

Table 5.4 Pathology analysis of EAE mice treated with rSFV particles

Mice sensitized for EAE were treated at days 5, 8, 11, 14 and 17 post disease induction as indicated in section 5.2.2.5. Table demonstrates findings for individual mice in each group. Pathology grade for each group represents the cumulative score for the bulbs, brain, and spinal cord of all mice.

Group	#	Olf. Bulb	Brain	Spinal Cord	Total	Pathology grade
rSFV-IL4 i.n.	1	NAD	+++	++	5	25
	2	NAD	++	+++++	7	
	3	NAD	+	+++	4	
	4	NAD	NAD	++	2	
	5	++	++	+++	7	
	6	NAD	NAD	NAD	0	
rSFV-IL10 i.n.	1	NAD	NAD	+	1	7
	2	NAD	NAD	NAD	0	
	3	NAD	NAD	++++	4	
	4	NAD	NAD	NAD	0	
	5	NAD	NAD	++	2	
	6	NAD	NAD	NAD	0	
rSFV-EGFP i.n.	1	NAD	NAD	++	2	22
	2	++	++	+	6	
	3	NAD	+	+++++	6	
	4	NAD	NAD	NAD	0	
	5	NAD	NAD	+	1	
	6	NAD	+++	++++	7	
TNE	1	NAD	+	++	3	12
	2	NAD	+	+	2	
	3	NAD	+	++	3	
	4	NAD	NAD	NAD	0	
	5	NAD	+	+	2	
	6	NAD	+	+	2	
rSFV-IL10 i.p.	1	NAD	+	++++	5	27
	2	NAD	NAD	++	2	
	3	NAD	+	++	3	
	4	NAD	NAD	+++	3	
	5	NAD	++	+++++	7	
	6	+	++	++++	7	
rSFV-EGFP i.p.	1	NAD	+	+++	4	22
	2	NAD	+	+++	4	
	3	NAD	NAD	++	2	
	4	NAD	+	+	2	
	5	NAD	NAD	++	2	
	6	+	++	+++++	8	

NAD no abnormality detected

Figure 5.14 Pathology analysis of EAE mice

H&E stained spinal cord sagittal sections of EAE mice taken from day 31. Mice were treated at days 5, 8, 11, 14 and 17 post disease induction and graded on severity of lesions as described in section 5.2.2.5. Figure illustrates the semi-quantitative histological grading system utilized for pathology assessments. **(A)** One plus (1+) lesion. Localized area of gliosis (G) and occasional myelin vacuoles and axonal swellings (arrowheads) in the superficial white matter. The central gray matter (bottom) appears normal. **(B)** Three plus (3+) lesion. Localized lesion in the superficial white matter showing myelin vacuolation, gliosis and axonal swellings (arrowheads). A small aggregate of lymphocytes is present in the leptomeninges (arrow). **(C)** Five plus (5+) lesion. Diffuse lesion showing severe gliosis, myelin vacuolation, axonal swellings and perivascular cuffing with lymphocytes and histiocytes (P). The spinal nerve root (top) appears normal.

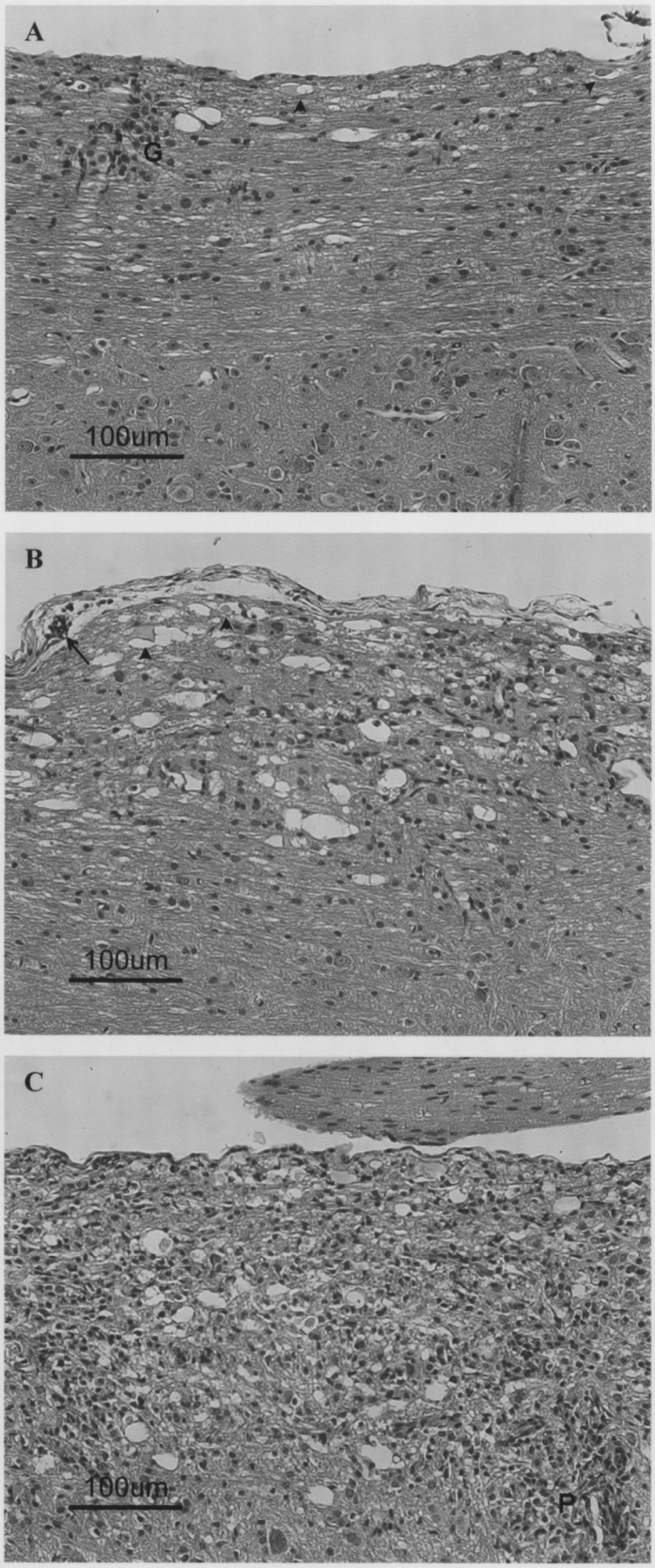
A
G
100um
B
100um
C
100um
P

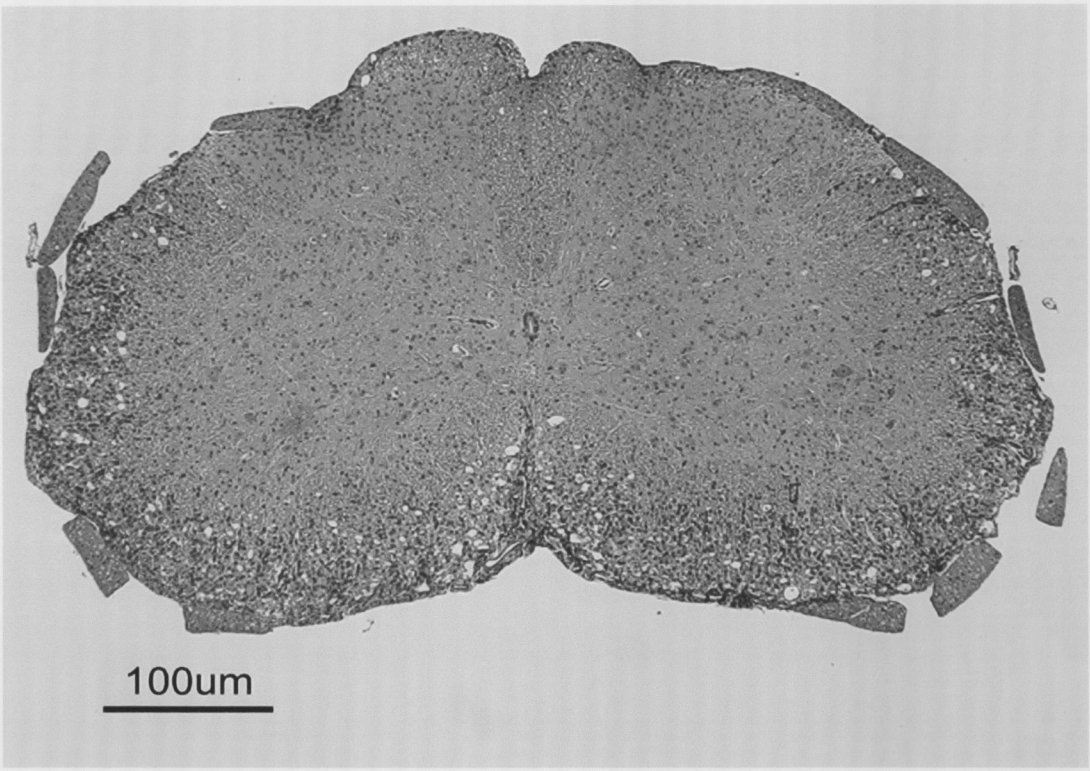

Figure 5.15 Pathology analysis of EAE mice

H&E stained spinal cord coronal section of EAE mice taken from day 31. Mice were treated at days 5, 8, 11, 14 and 17 post disease induction and graded on severity of pathology lesions as described in section 5.2.2.5. Figure illustrates the semi-quantitative histological grading system utilized for pathology assessments. Five plus (5+) lesion. Severe lesions diffusely distributed in the white matter. The central gray matter and spinal nerve roots appear normal.

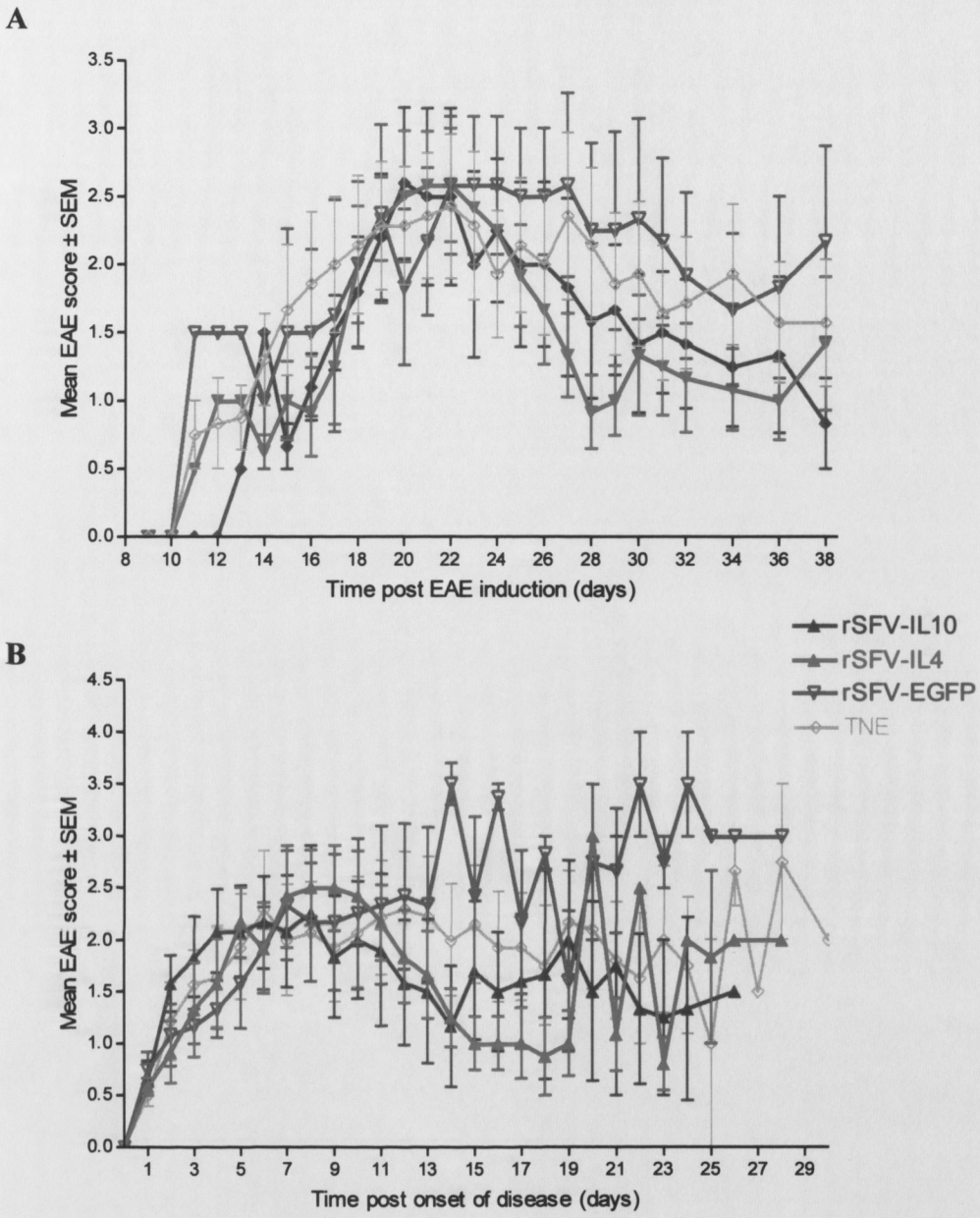

Figure 5.16 Effect of 5 early i.n. inoculations of rSFV on EAE

Six groups of 7 EAE induced mice were treated i.n. with rSFV-IL10, rSFV-IL4, rSFV-EGFP, rSFV-TGFb and TNE buffer at days 5, 8, 11, 14 and 17 post disease induction plus an untreated group. Animals were monitored daily, weighed and graded based on a neurological scale as outlined in section 5.2.2.2. Since no statistical difference was noted between the control groups (rSFV-EGFP and rSFV-TGFb as well as TNE and untreated) only one of each is represented. **(A)** Progression of disease expressed as EAE score after the induction of disease. **(B)** Progression of disease expressed as EAE score after disease onset.

5.3.6 Effect of rSFV on EAE induced on SJL mice

A working model of EAE in SJL mice using spinal cord homogenate had previously been established in our laboratory. Clinically and pathologically, disease is more severe in this model then one observed in C57BL/6 mice model. This increase in severity is observed by both clinical scores and pathology lesions on brain and spinal cord. Mice were treated i.n. with 5 doses of either an empty rSFV vector, a second control vector (rSFV-TGFb), an IL-10 containing vector, and mock treated with TNE buffer. A final group remained untreated. All mice were treated at 5, 8, 11, 14 and 17 days post disease induction, and monitored for 42 days. Since 5 out of the 7 untreated mice succumbed to the disease, this group was not included in statistical analyses. No significant differences were found between groups treated with empty vectors and group mock treated with TNE; however treatment with IL-10 slightly exacerbated disease severity compared to TNE group ($P = 0.0384$), and to groups treated with empty vector ($P < 0.009$). This severity was mostly detected in the later stages of the disease, where animals treated with IL-10 did not fully recover from EAE (figure 5.17). An empty vector was used in this treatment to further confirm that there is no difference in using this vector to other control vectors used previously (rSFV-EGFP and rSFV-TGFb). Since only a small amount of the antibody used for the titration of this particle was obtained, this vector was not used again.

5.3.7 Effect of rSFV on EAE induced on SJL mice - 2

The timing of the above treatment was again modified to start prior to EAE induction, to determine if a different outcome would be obtained. No significant difference was measured between any of the groups. Graphical interpretation of the data however yielded interesting results. Animals treated with IL-10 expressing particles did not get as sick as all other groups. In contrast, animals treated with empty particles (rSFV-EGFP and rSFV-TGFb) seemed to recover slightly faster then other groups, including rSFV-IL10 treated group (figure 5.18). If only the first 10 days of disease onset are taken into consideration, a statistically significant difference is measured between group treated with IL-10 and untreated group ($P = 0.0452$). Samples taken for pathology at day 30

A

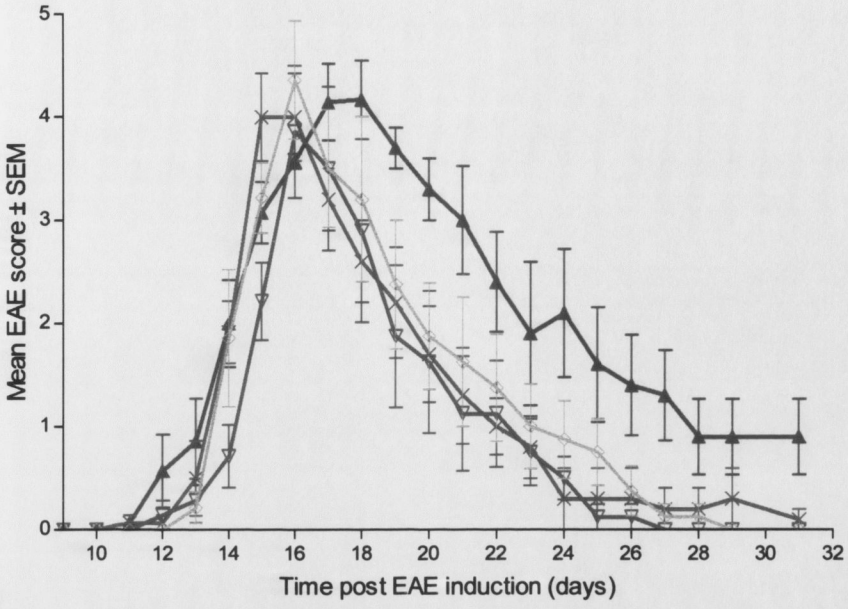

B

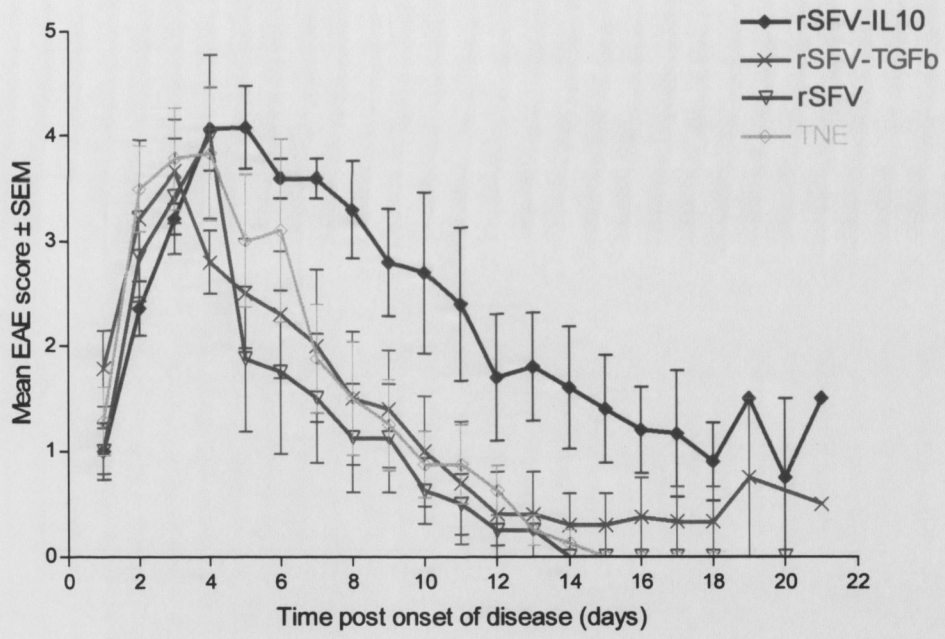

Figure 5.17 Effect of rSFV on EAE induced on SJL mice

Four groups of 7 EAE induced mice were treated i.n. with rSFV-IL10, rSFV-TGFb, rSFV, and TNE buffer at days 5, 8, 11, 14 and 17 post disease induction. Animals were monitored daily, weighed and graded based on a neurological scale as outlined in section 5.2.2.2. **(A)** Progression of disease expressed as EAE score after the induction of disease. **(B)** Progression of disease expressed as EAE score after disease onset.

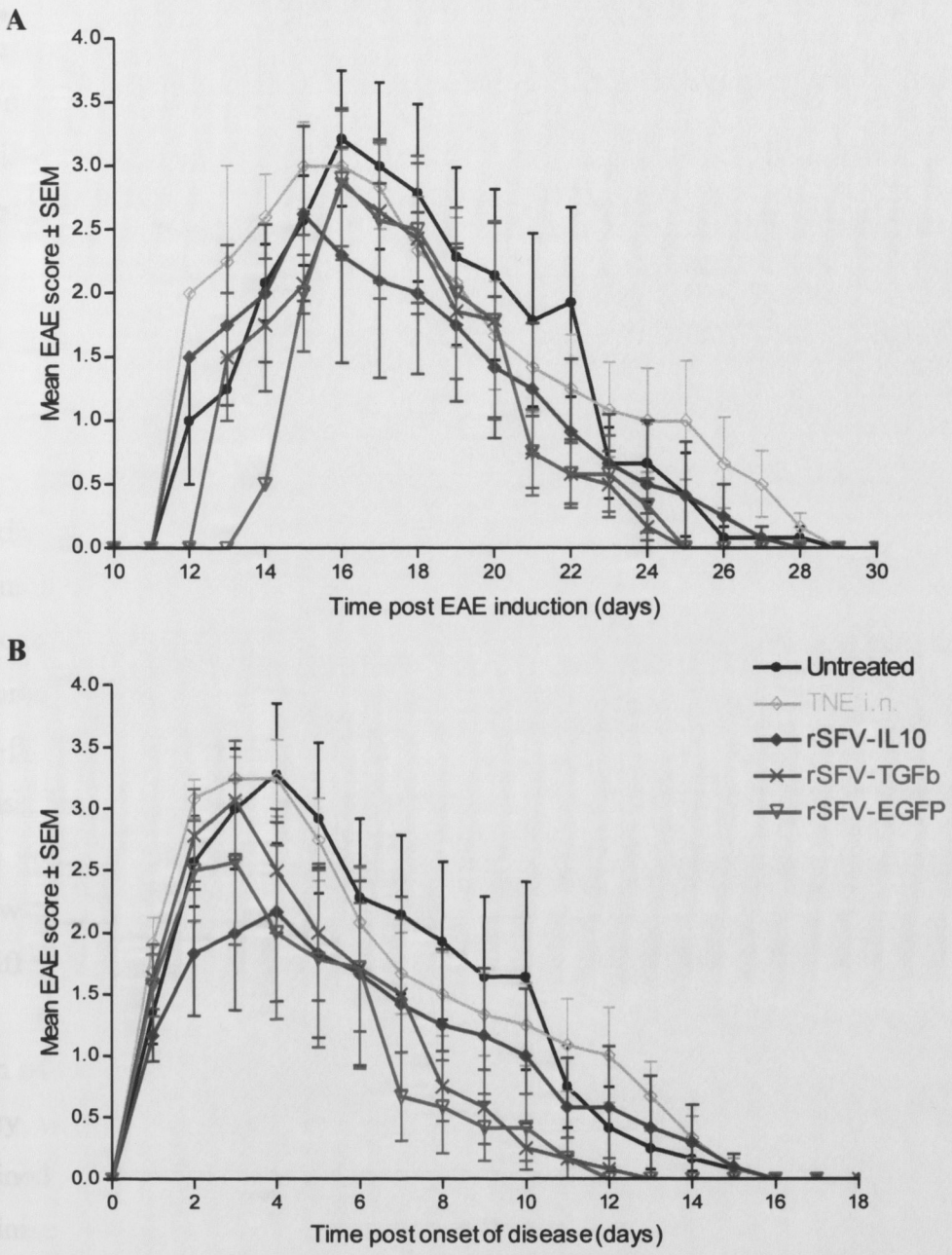

Figure 5.18 Effect of rSFV on EAE induced on SJL mice - 2

Four groups of 7 EAE induced mice were treated i.n. with rSFV-IL10, rSFV-TGFb, rSFV-EGFP, and TNE buffer at days –1, 2, 5, 8, and 11 post disease induction. Animals were monitored daily, weighed and graded based on a neurological scale as outlined in section 5.2.2.2. **(A)** Progression of disease expressed as EAE score after the induction of disease. **(B)** Progression of disease expressed as EAE score after disease onset.

indicated again that pathology severity correlated with clinical scores. Table 5.5 demonstrated key findings obtained in study. Table 5.6 describes pathology findings for individual mice in groups. Furthermore, no clear difference was obtained between each treated group based on pathology findings.

5.4 DISCUSSION

There is a delicate cytokine balance within an immune system. When new cytokines are introduced into this system, a number of outcomes could occur, depending on amount delivered and location. Previous research has demonstrated that different methods of IL-10 delivery into mice sensitized for EAE have differing results on disease outcome (Croxford *et al,* 2001). The same is true for other cytokines, such as IL-4 or TGF-β. Furthermore, the timing of delivery also profoundly affects the outcome of the disease, as was reviewed by Martino et al, where delivery of IL-4 by a herpes simplex virus vector had slightly differing outcomes on EAE when delivered at different times following disease induction. (Martino *et al,* 2000a). Results from the current work, were no different.

An important result obtained was that the vector, much like the wild-type avirulent strain of SFV, exacerbated EAE when delivered peripherally. This was the case for both empty vectors, and vectors encoding IL-4 or IL-10. Different results however were obtained when treatment was performed by the more direct i.n. route. Vector administration with no therapeutic protein (rSFV-EGFP and rSFV-TGFb) consistently exacerbated clinical disease, regardless of treatment regime. The reason for this exacerbation is likely a direct effect of the inflammatory response caused by the vector. EAE is a T_H1 mediated disease, viral infections also lead to a T_H1 response by the immune system; therefore, it is expected one will up-regulate the other leading to an exacerbation of the disease. This was indeed the case, where it was observed that both vectors not secreting any cytokine augmented the effects of EAE. When rSFV vectors expressing either IL-10 or IL-4 were used, different results were obtained. Treatment with IL-4 at lower doses (either 3 or 4 treatments) had no significant effect on disease outcome. It did however, successfully counter the inflammatory effects of the vector, preventing exacerbation of the disease. When the amount given was increased to 5 doses, there was a

Table 5.5 Analysis of EAE mice treated with rSFV particles

Mice sensitized for EAE were treated at days –1, 2, 5, 8, and 11 post disease induction as indicated in section 5.2.2.8. Table demonstrates key findings for each group. Statistical significance was calculated using the Mann-Whitney nonparametric ranking test (GraphPad Prism 4.0) using data for the onset of clinical scores of mice showing EAE. Pathology grade demonstrates composite scores of olfactory bulbs, brain, and spinal cord mice in each group.

Group	Max EAE score (mean ± SEM)	Day of onset (mean ± SEM)	Mortality	Pathology grade
rSFV-IL10	2.8 ± 0.6	14.7 ± 0.9	0/6	24
rSFV-EGFP	2.9 ± 0.6	15.6 ± 0.4	1/7	22
rSFV-TGFb	3.4 ± 0.6	14.1 ± 0.3	1/7	20
TNE	3.5 ± 0.2	13.6 ± 0.4	0/6	27
Untreated	3.7 ± 0.6	13.3 ± 0.4	1/7	26

Table 5.6 Pathology analysis of EAE mice treated with rSFV particles

Mice sensitized for EAE were treated at days –1, 2, 5, 8, and 11 post disease induction as indicated in section 5.2.2.8. Table demonstrates findings for individual mice in each group. Pathology grade for each group represents the cumulative score for the bulbs, brain, and spinal cord of all mice.

Group	#	Olf. Bulb	Brain	Spinal Cord	Total	Pathology grade
rSFV-IL10.	1	++	+++	++	7	24
	2	+	+++	++	6	
	3	+	+++	++	6	
	4	+	++	++	5	
rSFV-EGFP	1	NAD	+	++	3	22
	2	++	+	++	5	
	3	++	+++	+++	8	
	4	+	+++	++	6	
rSFV-TGFb	1	NAD	++	++	4	20
	2	++	+++	+++	8	
	3	NAD	++	+	3	
	4	+	++	++	5	
TNE	1	++	+++	++	7	27
	2	++	+++	+++	8	
	3	++	+++	+++	8	
	4	NAD	++	++	4	
Untreated	1	+	+++	+++	7	26
	2	+	+++	+++	7	
	3	NAD	+++	++	5	
	4	++	+++	++	7	

NAD no abnormality detected

delay of disease onset, however clinical disease was slightly higher then the control. This was measured both clinically and as seen by the severity of pathology lesions. The delayed onset of EAE observed correlated with previous finding where IL-4 administered by the intracisternal route with a recombinant HSV-1 vector also delayed the onset of EAE, though it also slightly inhibited disease (Furlan *et al,* 1998). These results are in direct contradiction with other researchers who demonstrated successful treatment of EAE with IL-4 using a HSV-1 vector by the i.c. route (Martino *et al,* 1998, Martino *et al,* 2000b). A number of reasons could be associated with these differences. The different vectors used in each treatment could account for the different outcomes, since differing amounts of protein were delivered during treatment. The route of inoculation, could also account for the difference in outcomes. The elevated levels of IFN-γ measured following administration of rSFV-IL4 by the i.n. route could explain why disease inhibition was not obtained with this vector. It has been previously discussed that higher levels of IL-4 in the airways and bronchial epithelial cells contribute to inflammation, which would have negative effects on the outcome of EAE. This is not the case when IL-4 was delivered by the i.c. method, where cytokine delivery is concentrated to the CNS only.

Treatment with IL-10 expressing vectors yielded the most promising results. When an EAE model set on C57BL/6 mice was used, treatment was dependent on amount of cytokine delivered (figure 5.19). Lower administrations of the vector had an adverse effect on the clinical outcome of the disease, exacerbating it compared to untreated control. Treatment with 4 doses neither exacerbated nor inhibited disease. It did however counter the inflammatory effects of the vector, much like treatment with IL-4. When the treatment was increased to 5 doses, the result was either a strong inhibition of disease, or very mild disease amelioration depending on time of treatment. Animals in which treatment started very early, before induction of EAE only showed slight disease inhibition compared to control groups. When the treatment was started shortly after the induction of EAE (at day 5), a very strong inhibition of the disease was measured. Clinically animals showed very mild symptoms, with only 2 mice reaching scores of 1.5 (controls consistently reach scores of above 3). Furthermore, the onset of EAE was delayed considerably by up to 12 days in some animals. The duration of disease was much shorter than any other treated or control animals. Pathological analyses of these mice indicated a direct correlation with clinical scores. Milder and less frequent lesions were observed in all mice, with the exception of 1, which had more infiltrating lymphocytes in the white matter despite only achieving a

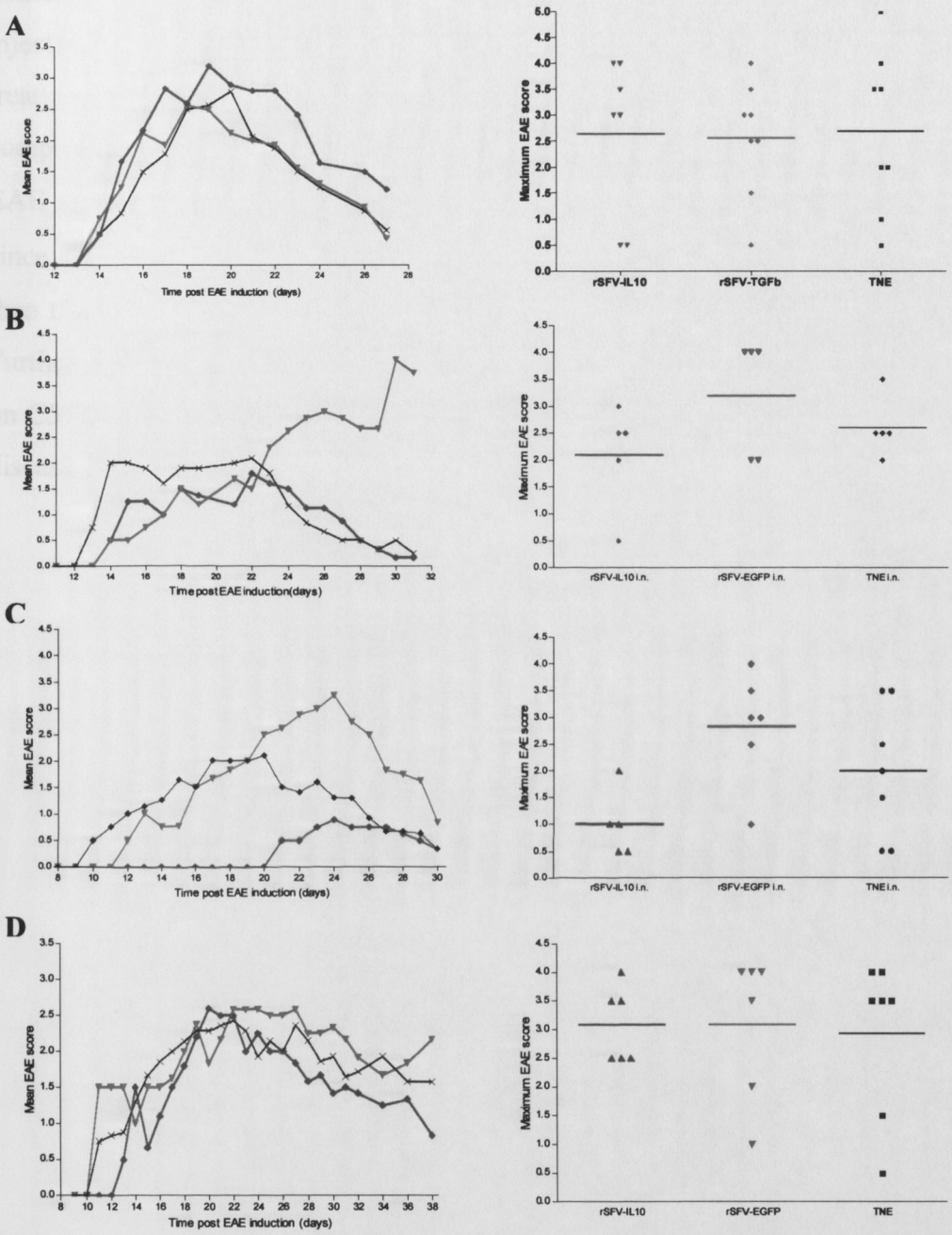

Figure 5.19 Comparison of all rSFV treatments on C57BL/6 mice

Mice sensitized for EAE were treated with rSFV-IL10 (blue), control vector (green), or mock treated with buffer (black). A comparison of all 4-treatment routines is represented. **(A)** Mice treated at days 8, 10, and 12 following EAE induction. **(B)** Mice treated at days 6, 9, 12, and 15 following EAE induction. **(C)** Mice treated at days 5, 8, 11, 14, and 17 following EAE induction. **(D)** Mice treated at days –1, 2, 5, 8, and 11 following EAE induction.

clinical score of 1.5. SJL mice treated with the IL-10 by same treatment routines (5 injections at 2 different time points) did not have the desired results. With an earlier treatment routine, the group treated with rSFV-IL10 had a slightly milder disease compared to other groups, though not enough for a statistically significant difference. EAE models set up on SJL mice are generally used when a TGF-β treatment is desired, since these mice have a small deficiency in their TGF-β production. It is not surprising then that since only IL-10 was given to these mice, no significant results were obtained. Furthermore, clinical and pathological signs of this model are much more severe then that on C57BL/6 mice. It is possible that more administrations of the cytokine are needed for disease inhibition to occur.

Chapter 6

Treatment of experimental autoimmune encephalomyelitis with Linoleic acid compounds

6.1 INTRODUCTION

Polyunsaturated fatty acids have been the subject of recent research in the treatment of MS. It has been suggested that the intake of compounds rich in such fatty acids could alter the course of the disease, as they are one of the components that make up myelin in the nervous system. A dietary supplement of polyunsaturated fatty acids is linoleic acid, a major component of evening primrose oil, sunflower oils, and sunflower seeds. Linoleic acid is an omega-6 fatty acid, considered an essential fatty acid. Essential fatty acids are essential to human health but cannot be made in the human body; therefore must be obtained from food. Two types of essential fatty acids play a crucial role in brain function and normal growth and development: the omega-6 and omega-3 fatty acids. In the body, linoleic acid is converted to gamma-linoleic acid and then further broken down to arachidonic acid. Both of these can be consumed directly from food, arachidonic acid from meat and gamma-linoleic acid from several plant-based oils. In excess, linoleic acid and arachidonic acid are unhealthy, as they promote inflammation. Gamma-linoleic acid on the other hand may reduce inflammation. When gamma-linoleic acid is taken as a supplement, it does not get converted to arachidonic acid, rather to a substance called dihomogamma-linoleic acid. This acid competes with arachidonic acid and prevents the negative inflammatory effects that would otherwise be caused in the body. In addition, DGLA becomes part of a series of substances called prostaglandins (PGE_1 and PGE_2), hormone-like molecules that have shown to have physiological immunoregulatory functions (Goetzl *et al,* 1995, Harbige *et al,* 1995, Phipps *et al,* 1991).

Studies on omega-6 have shown an increased TGF-β1 production in peripheral blood mononuclear cells of volunteers taking oral supplements (Fisher and Harbige 1997). Prostaglandins can be potent anti-inflammatory mediators and inhibit the production of IFN-γ and IL-4 production in human T-cell clones stimulated by antigens and mitogens (Harbige *et al,* 1997, Watanabe *et al,* 1994). Both LA and GLA have been previously used in the treatment of EAE. LA was found to partially inhibit clinical signs of EAE in the Lewis rat model (Mertin and Stackpoole 1978, Mertin and Stackpoole 1979), while GLA was able to completely protect animals depending on dose (Harbige *et al,* 1995). GLA has more recently been shown to protect SJL mice from developing EAE following oral administration (Harbige *et al,* 2000).

The current study, involves treatment of mice sensitized for EAE with a number of synthetic made compounds, which are pure polyunsaturated fatty acids of a homologous series related metabolically.

6.2 EXPERIMENTAL PROCEDURES

6.2.1 NEW MATERIALS

6.2.1.1 Mice

Female SJL mice aged 40-60 days were obtained from the Harlan (UK). Mice were maintained in accordance with the principles outlined in S1 17/94 European Communities regulations 1994, for care and use of laboratory animals. Syringes (20 ml, 10 ml, and 1.0 ml) and needles, (21G), were from Terumo (Leuven, Belgium).

6.2.1.2 Compounds

The following polyunsaturated fatty acids synthetic compounds were obtained from Dr. Laurence S. Harbige (School of Chemical and Life Sciences, University of Greenwich, London, UK): compounds A, B, C, and D. Due to confidentiality reasons the chemical structure and names of the compounds may not be published. Compounds are pure polyunsaturated fatty acids of a homologous series related metabolically; and were produced by Dr. Harbige and his collaborators.

6.2.2 METHODS

6.2.2.1 Study 1

EAE was induced in 60 female SJL mice with SCH enriched in adjuvant with PT as described in section 5.2.2.7. Six groups of 10 mice were treated with different concentrations of each compound. Compound B was given to groups 1, 2, and 3 at a

volume of 350 µl, 150 µl, and 50 µl respectively. Compound C was given to groups 4 and 5 at a volume of 350 µl and 50 µl respectively. The inert compound A was given to group 6 (350 µl) to be used as a control. Compounds were administered daily to mice by gavage from day 8 to day 21 post EAE induction, and animals were monitored as described in section 5.2.2.2 for a total of 25 days. The Mann Whitney test was used for statistical analyses (GraphPad Prism 4.0) on maximum EAE scores. Mice that died immediately following treatment or were found dead within 24h and had not previously displayed weight loss >1.5g or clinical signs of EAE were assigned 'DFT' – died following treatment and were not included in analysis. Mice that were found dead after 24h and had weight loss >1.5g and/or clinical EAE were scored '6' and included in data analysis.

6.2.2.2 Study 2

EAE was induced in 135 female SJL mice with SCH enriched in adjuvant with PT as described in section 5.2.2.7. Fourteen groups of mice were treated with different concentrations of each compound. Compound A was given to groups 1, 2, and 3 at a volume of 50 µl, 150 µl, and 350 µl respectively. Compound B was given to groups 4, 5, 6 and 7 at a volume of 25 µl, 50 µl, 150 µl, and 350 µl respectively. Compound C was given to groups 8, 9, and 10 at a volume of 50 µl, 150 µl, and 350 µl respectively. Finally, compound D was given to groups 11, 12, 13, and 14 at a volume of 25 µl, 50 µl, 150 µl, and 350 µl respectively. Compounds were administered daily to mice by gavage from day 7 to day 21 post EAE induction, and animals were monitored as described in section 5.2.2.2 for a total of 25 days. The Mann Whitney test was used for statistical analyses (GraphPad Prism 4.0) on maximum EAE scores. Mice that died immediately following treatment or were found dead within 24h and had not previously displayed weight loss >1.5g or clinical signs of EAE were assigned 'DFT' – died following treatment and were not included in statistical analysis. Mice that were found dead after 24h and had weight loss >1.5g and/or clinical EAE were scored '6' and included in data analysis.

6.3 RESULTS

6.3.1 Study 1

To detect an effect of the lipid compounds on the outcome of EAE, mice sensitized for EAE were treated with different concentrations of synthetic pure polyunsaturated fatty acid homologues. Mice were fed the compound daily from day 8 to 21 following EAE induction. Table 6.1 demonstrates key results obtained. A graphical representation of the results is demonstrated in figures 6.1 and 6.2. Administration of a high dose of compound C significantly ($P < 0.05$) inhibited the mean maximum EAE score compared to control group. Furthermore, a statistical difference ($P < 0.05$) was also observed between the high and low dose of this same compound. All other treated groups showed no significant difference compared to control group. There was no difference in the day of onset of disease between any treated groups.

A notable difference in the mortality rate was observed between treated groups. Compound B given at high doses (350 μl and 150 μl) and the low dose treatment of compound C (50 μl) resulted in a high mortality rate, similar to control group A. Group treated with a low dose of compound B had fewer deaths then other groups, while treatment with a high dose of compound C resulted in no deaths from the disease.

6.3.2 Study 2

Study 1 was repeated to include extra concentrations of compounds, as well as a new compound (D). Table 6.2 demonstrates key findings of experiment. Each treatment was plotted against control groups. As in previous experiment compound B was not effective in inhibiting the severity of EAE (figure 6.3); furthermore, 9 out of 37 mice died as a result of treatment alone. A similar result was obtained with compound B. Again, no mice died as a result of treatment alone, prior to developing EAE. A notable difference between both treatments was that the newly incorporated 150 μl group was the one effective in inhibiting EAE, as opposed to the 350 μl group (figure 6.4). Compound D, was not effective in inhibiting EAE (figure 6.5), and resulted in 8 deaths from treatment alone. There were also a high number of animals that died as a result of the disease. As in

Table 6.l Analysis of EAE mice study 1 treated with fatty acid compounds

Six groups of 10 SJL mice sensitized for EAE were treated orally with different amounts of synthetic omega-6 fatty acids. Animals were monitored daily, weighed and graded based on a neurological scale as outlined in section 5.2.2.2. Table demonstrates key findings for each group.

GROUP	TREATMENT	Mean Group EAE Score Mean ± SEM	Mean Day of Onset Mean ± SEM	EAE Mice	EAE Mortality
1	B 350 µl	5.06 ± 0.6	14.78 ± 0.3	9/10	7/9
2	B 150 µl	4.33 ± 0.8	15.00 ± 0.8	9/9	6/9
3	B 50 µl	3.90 ± 0.6	13.20 ± 0.4	10/10	3/10
4	C 350 µl	2.39 ± 0.5 *	13.63 ± 0.6	8/10	0/8
5	C 50 µl	5.33 ± 0.5	13.67 ± 0.4	9/10	7/9
6	A 350 µl	4.61 ± 0.8	13.88 ± 0.3	9/10	6/9

* A statistical difference was measured between this group and control group A, where $P < 0.05$ using the Mann Whitney t-Test

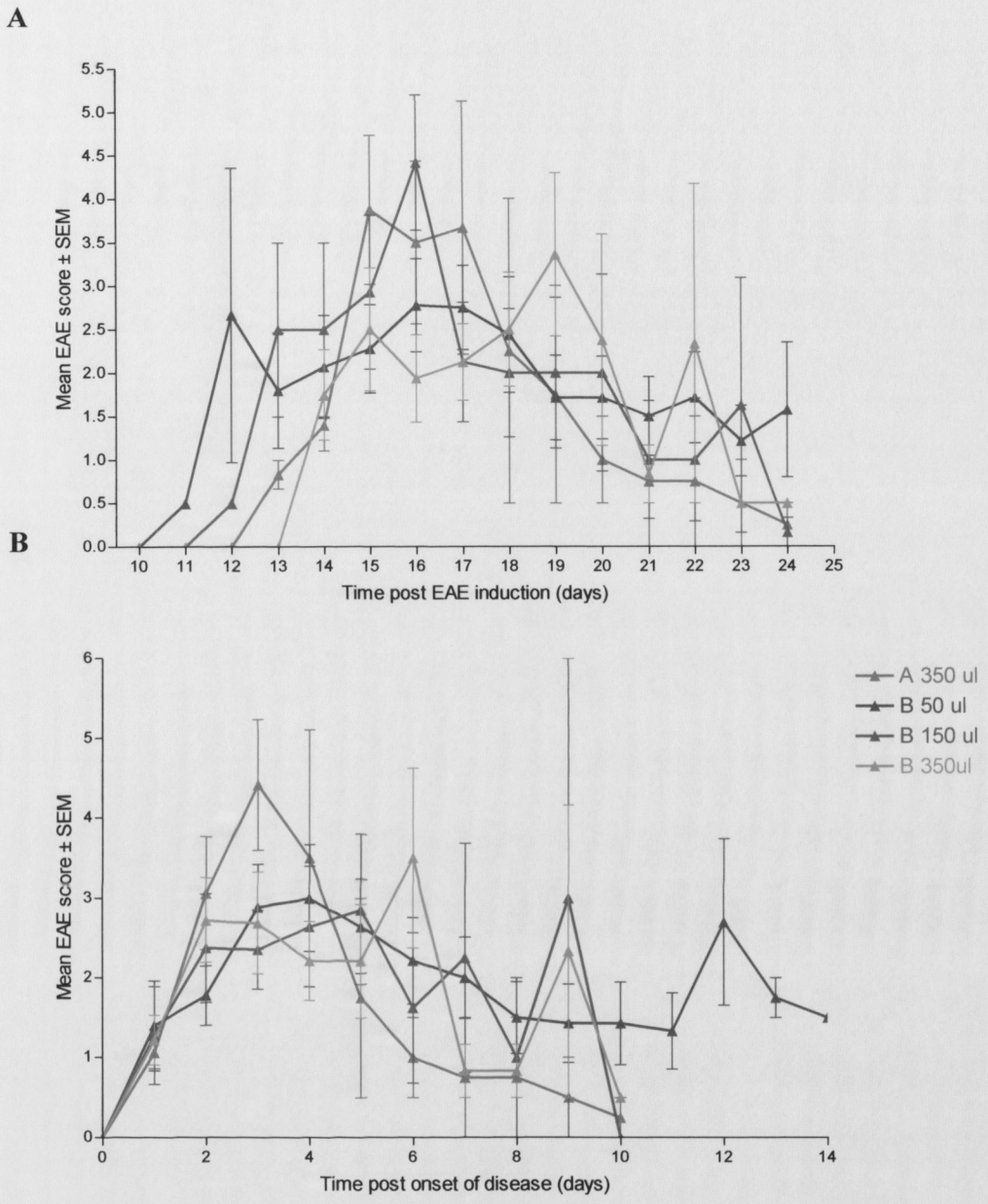

Figure 6.1 Effect of omega-6 fatty acid study 1 on EAE

Four groups of 10 EAE induced mice were treated orally with lipid compounds A and B daily from 7 to 21 days post disease induction. Animals were monitored daily, weighed and graded based on a neurological scale as outlined in section 5.2.2.2. **(A)** Progression of disease expressed as EAE score after the induction of disease **(B)** Progression of disease expressed as EAE score after disease onset.

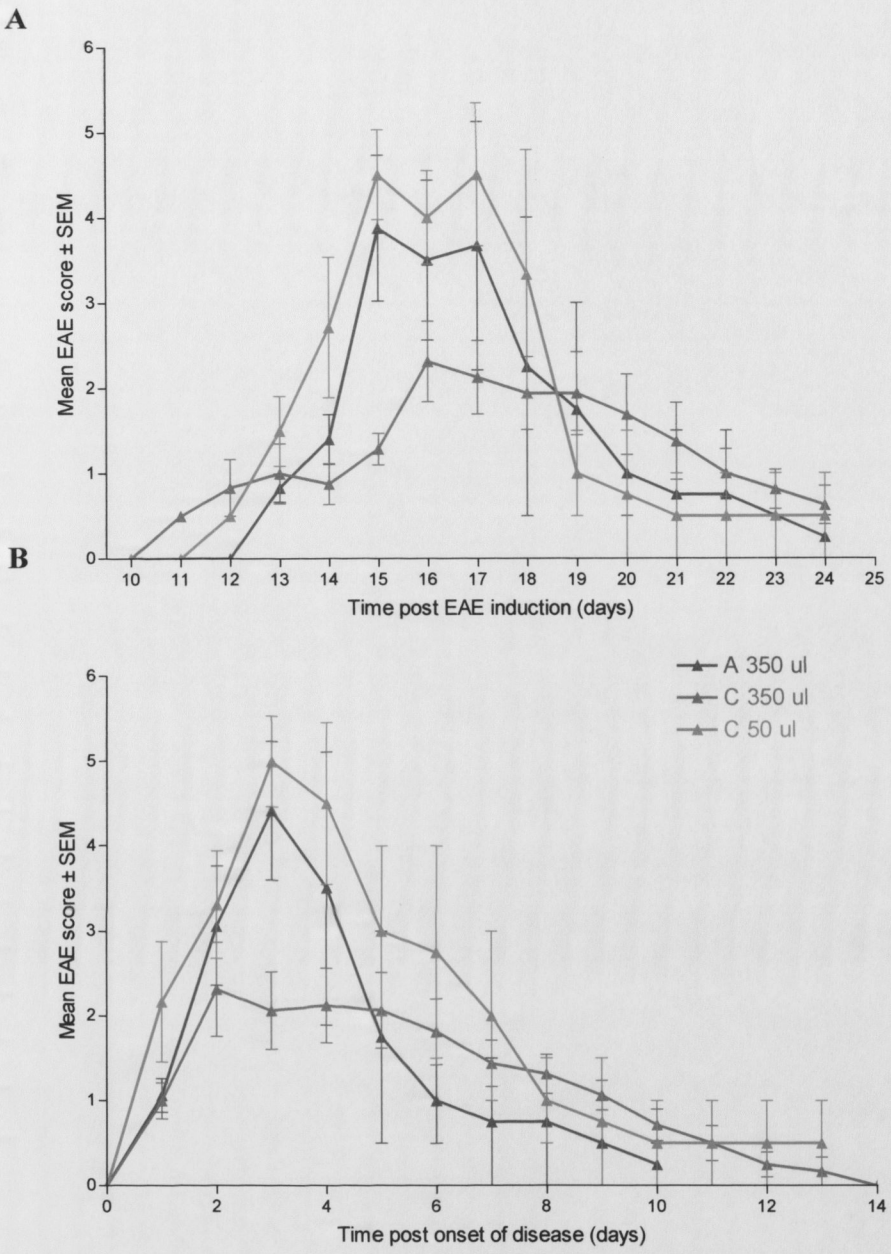

Figure 6.2 Effect of omega-6 fatty acid study 1 on EAE

Three groups of 10 EAE induced mice were fed orally with lipid compounds alpha and gamma daily from 7 to 21 days post disease induction. Animals were monitored daily, weighed and graded based on a neurological scale as outlined in section 5.2.2.2. **(A)** Progression of disease expressed as EAE score after the induction of disease **(B)** Progression of disease expressed as EAE score after disease onset.

Table 6.2 Analysis of EAE mice study 2 treated with fatty acid compounds

Fourteen groups of SJL mice sensitized for EAE were treated orally with different amounts of synthetic omega-6 fatty acids. Animals were monitored daily, weighed and graded based on a neurological scale as outlined in section 5.2.2.2. Table demonstrates key findings for each group.

GROUP	TREATMENT	Mean Group EAE Score Mean ± SEM	Mean Day of Onset Mean ± SEM	EAE mice	EAE Mortality
1	A 50 µl	6.0 ± 0.0	12.7 ± 0.4	9/9	9/9
2	A 150 µl	4.6 ± 0.7	12.2 ± 0.4	8/10	5/8
3	A 350 µl	5.4 ± 0.6	13.1 ± 0.6	8/9	7/8
4	B 25 µl	4.9 ± 0.7	13.0 ± 0.5	7/10	5/7
5	B 50 µl	4.1 ± 0.5	13.8 ± 0.5	9/9	3/9
6	B 150 µl	4.2 ± 0.7	13.1 ± 0.5	7/9	3/7
7	B 350 µl	4.7 ± 0.7	12.5 ± 0.4	6/9	3/6
8	C 50 µl	5.6 ± 0.4	12.6 ± 0.3	10/10	9/10
9	C 150 µl	3.4 ± 0.7	13.4 ± 0.6	9/10	3/9
10	C 350 µl	5.2 ± 0.5	13.5 ± 0.7	10/10	8/10
11	D 25 µl	4.9 ± 0.6	12.8 ± 0.5	9/10	6/9
12	D 50 µl	5.4 ± 0.6	12.3 ± 0.2	6/10	5/6
13	D 150 µl	4.7 ± 0.6	13.5 ± 0.4	10/10	7/10
14	D 350 µl	4.4 ± 0.8	12.7 ± 0.3	7/10	4/7

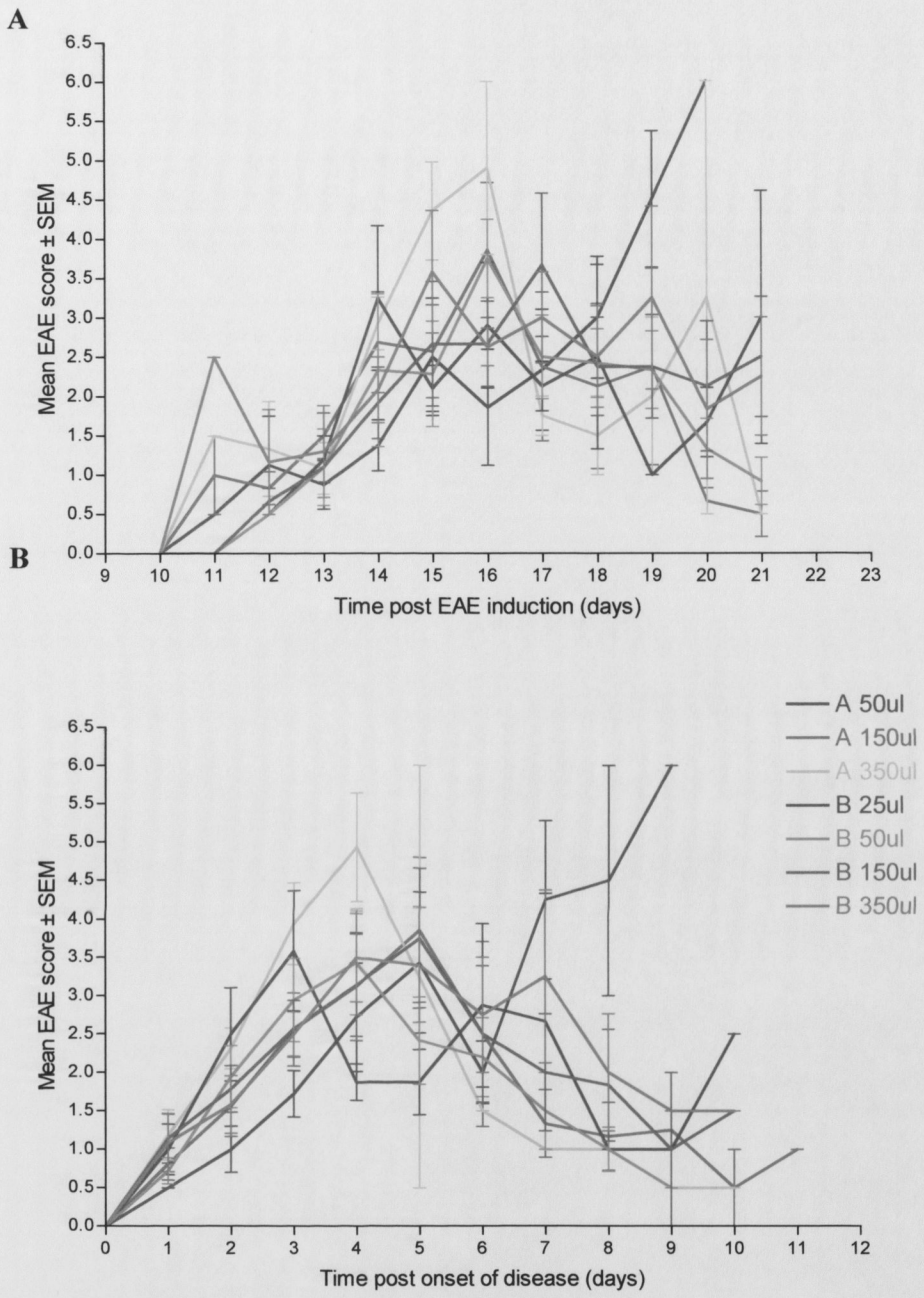

Figure 6.3 Effect of omega-6 fatty acid study 2 on EAE

Seven groups of EAE induced mice were treated orally with lipid compounds alpha and beta daily from 7 to 21 days post disease induction. Animals were monitored daily, weighed and graded based on a neurological scale as outlined in section 5.2.2.2. **(A)** Progression of disease expressed as EAE score after the induction of disease **(B)** Progression of disease expressed as EAE score after disease onset.

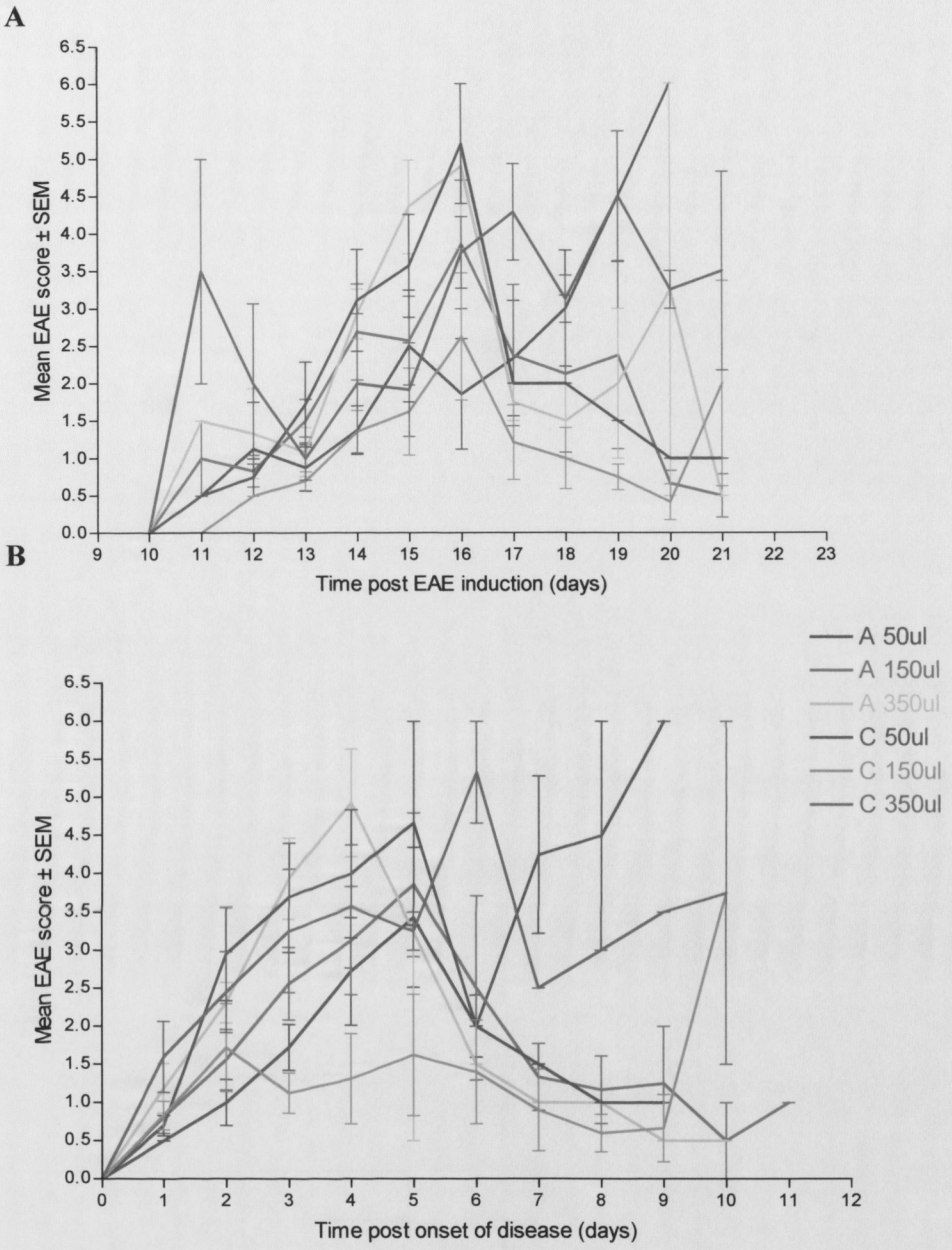

Figure 6.4 Effect of omega-6 fatty acid study 2 on EAE

Six groups of EAE induced mice were treated orally with lipid compounds alpha and gamma daily from 7 to 21 days post disease induction. Animals were monitored daily, weighed and graded based on a neurological scale as outlined in section 5.2.2.2. **(A)** Progression of disease expressed as EAE score after the induction of disease **(B)** Progression of disease expressed as EAE score after disease onset.

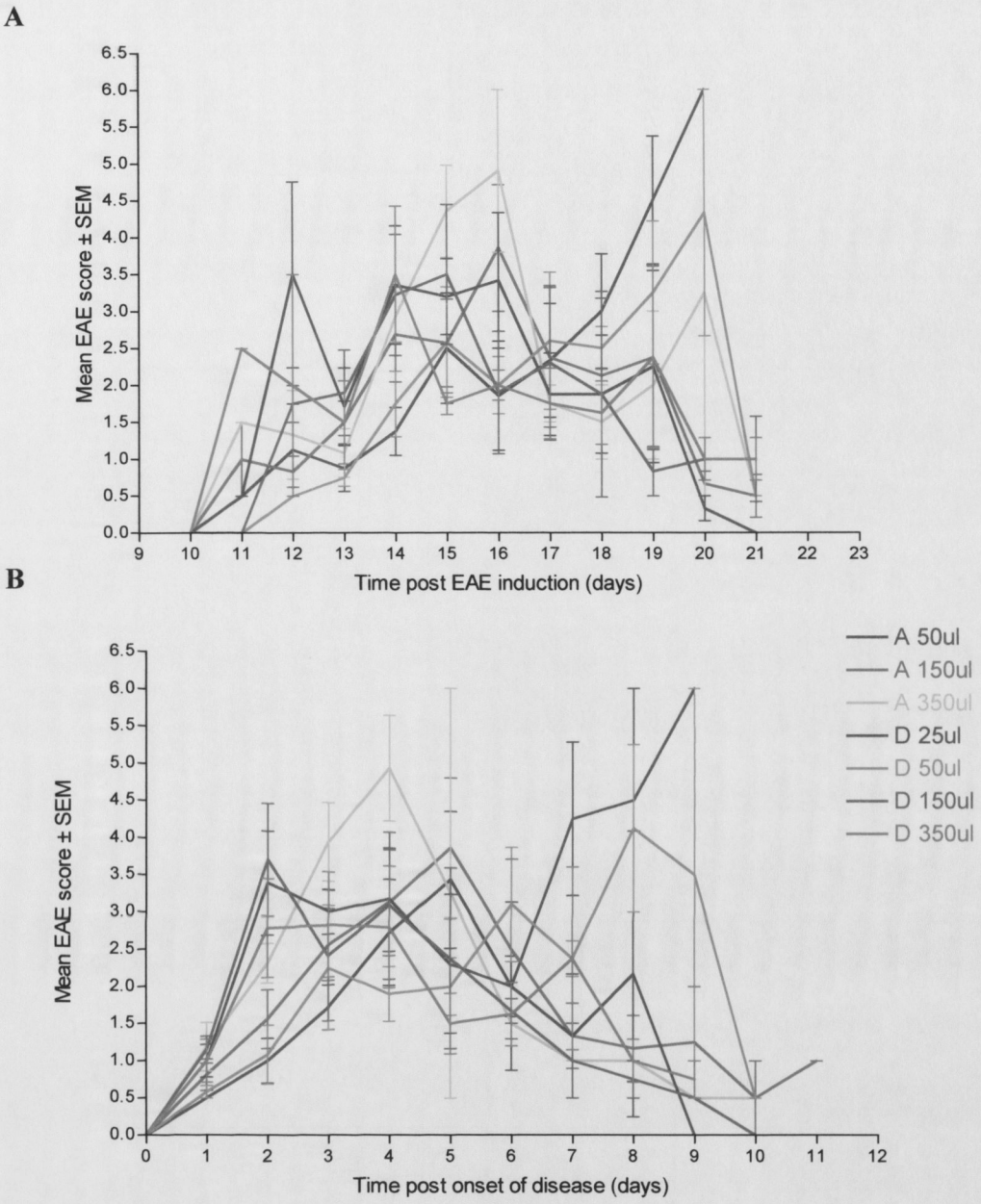

Figure 6.5 Effect of omega-6 fatty acid study 2 on EAE

Seven groups of EAE induced mice were treated orally with lipid compounds alpha and delta daily from 7 to 21 days post disease induction. Animals were monitored daily, weighed and graded based on a neurological scale as outlined in section 5.2.2.2. **(A)** Progression of disease expressed as EAE score after the induction of disease **(B)** Progression of disease expressed as EAE score after disease onset.

previous experiment, no difference in the day of disease onset was observed between groups.

6.4 DISCUSSION

Epidemiological studies indicate MS as a disease more prevalent in higher latitudes, away from the equator. It is speculated environmental factors could play a role in this geographical distribution observed. Another possible explanation could be dietary factors. This is suggested based on MS incidence in Japan and costal regions of Norway, where diets consist of a high consumption of fish combined with lower consumption of meats and dairy products. Both are located in higher latitudes; however do not have a high incidence of MS. Native Japanese who migrate to Hawaii and change their diets (more western) observe a higher incidence of MS. The same is observed for inland inhabitants of Norway, who have higher MS incidence then coastal residents (Hutter and Laing 1996, Lauer 1997). Another example can be found in the Faroe islands, where MS incidence was extremely low until their diet was changed as a result of western influence (Kurtzke *et al,* 1993). It can be concluded that dietary factors do play a role in the etiology of MS.

It is known from previous studies that GLA is effective in the treatment of EAE (Harbige *et al,* 1995, Harbige *et al,* 2000, Mertin and Stackpoole 1978, Mertin and Stackpoole 1979). Attempts to use synthetic made polyunsaturated fatty acids for the treatment of EAE introduce a series of difficulties. It is hard to mimic exact chemical, physical, and biological properties of the compound, in order to achieve similar results. This study utilized different pure polyunsaturated fatty acid homologues related metabolically in an attempt to treat EAE.

Out of the three homologues used only one (C) appears to have a desired effect on the outcome of EAE. Though the mean EAE score of treated groups varied in studies, this was the only compound not to cause death to any mice used (from treatment alone, prior to EAE signs). Furthermore, this compound had the lowest mean group EAE scores in both treatments. The first study indicated that higher doses of the compound were needed to partially inhibit EAE. When the experiment was repeated, the same dose of 350 µl, which on the first study was effective, was no longer effective; however, a new dose of 150 µl was. The different days in which treatment was started in each study (8 for the first and 7

for the second) could have accounted for the difference observed. It is possible that the compound takes a few days to start working following administration, therefore by changing the date treatment starts would most certainly slightly change results obtained. There was also a notable difference in disease severity observed between the first and second EAE studies, as measured by controls. The second study had a more severe form of the disease, which could also account for the compound working on a different dose than previously.

All data obtained from study is preliminary. Further research is required in the mechanism of action of the compounds tested. Cytokine profile studies need to be conducted to determine if higher levels of TGB-β and IL-10 are found in mice following treatment. A comprehensive histo-pathological analysis also needs to be conducted. It would be interesting to conduct the studies in various EAE models, not only with different mice strains, but also in different animals.

Chapter 7

General Discussion

7.1 DISCUSSION

The main objective of this work has been to establish the rSFV vector system as a means of gene delivery to the CNS. Extensive work on the use of SFV as a vector system has been conducted to date. A number of characteristics make the SFV an effective virus for vector development. The genome is of positive polarity; viral replication is very efficient and takes place in the cytoplasm of infected cells. SFV has a very broad host range, and most people outside of Africa have no pre-existing immunity against the virus. In addition, extremely high titers of viral particles can be easily generated. The vector system was developed in the Karolinska Institute in Sweden by Professor Peter Liljestrom. It consists of three self-replicating RNA molecules, one containing the non-structural genes where a foreign gene replaces the structural gene, and the structural protein genes are supplied *in trans* by helper RNAs (Liljestrom and Garoff 1991a, Smerdou and Liljestrom 1999). Since the cloned gene is only expressed transiently during a single round of viral multiplication, this system is also known as a suicide vector.

To date, the two main uses of this vector system have been for vaccine construction and for tumor therapy. It has been previously demonstrated that high levels of immune responses to a particular antigen could be achieved following peripheral inoculation of the vector. This was verified by vaccination of sheep with a vector containing the prME and NS1 proteins of the Louping Ill virus, where animals survived challenge with the wild type virus (Morris-Downes *et al,* 2001b). Work performed by M. Murphy showed the apoptotic nature of the vector system and its use as an anti-tumor agent. Direct infection of murine tumor with rSFV particles was effective in inhibiting tumor growth and inducing regression in the *p53*-deleted human non-small cell lung carcinoma cell line H358a (Murphy *et al,* 2000). A vector encoding the *Bax* gene was used to augment the p53-independent apoptosis characteristic of the SFV vector, resulting in an enhanced cytopathic and anti-tumour potential of the vector (Murphy *et al,* 2001). Later work by James Smyth demonstrated that vectors encoding the p62-6K gene of SFV were much more effective in enhancing inhibition of tumor growth by inducing an immune response directed towards the tumor (Smyth, *unpublished work*). Both anti-tumour studies performed with the SFV vector show that there is a considerable potential for this system to be used for genotoxic cancer therapy.

The theory behind using the rSFV vector for the CNS comes from extensive data obtained from work on i.n. infection of mice with wild-type SFV. The virus is neurotrophic for mice, and is capable of infecting a number of cells in the CNS, including neurons and oligodendrocytes (Atkins *et al,* 1990, Balluz *et al,* 1993, Ehrengruber *et al,* 1999, Glasgow *et al,* 1997). It was demonstrated that virulent strains of SFV (SFV4) induce lethal encephalitis in mice when given i.n. (Atkins et al, 1990, Fazakerley 2002). In contrast, avirulent strains infect neurons at a slower pace allowing for the animals to clear the virus; they do however lead to immune mediated demyelination of the CNS in some mice (Balluz et al, 1993, Sheahan *et al,* 1981, Sheahan *et al,* 1996). The virus reaches the CNS by binding to receptors in the nasal epithelium, and traveling through the axons of neurons in the nasal cavity to reach the olfactory bulb area of the brain. Once there, it infects neurons and oligodendrocytes and proceeds to further infect other areas of the brain (Sheahan et al, 1996, Smyth *et al,* 1990). Previous studies have also demonstrated reporter gene expression in hippocampal brain slices in culture or in other *in vitro* systems following gene transfer using alphavirus vectors (Ehrengruber *et al,* 1999).

Based on the pathway taken by the virus upon i.n. infection and the vector's ability to infect neuronal cells, it was postulated the vector system would be capable of expressing its cloned genes in the CNS. This was indeed verified by data obtained when the vector system expressing the reporter gene *EGFP* was administered i.n. to mice (Jerusalmi *et al,* 2003). The reporter gene EGFP was selected for a number of reasons. The protein is easily visualized under a fluorescence microscope, with no need for complicated staining or labeling procedures. EGFP is known to be immunologically inactive, which leads to no ill effect as a result of protein administration in infected animals. Furthermore, EGFP is not secreted from infected cells, allowing for a simple identification of cells infected with the vector. Finally, titration of these particles is extremely easy and takes little time.

It was demonstrated that the vector is capable of penetrating the CNS via the olfactory bulb area of the brain, by a non-invasive method, causing no damage to recipient cells. High levels of expression were detected in incoming axons from the receptor cells in the olfactory epithelium that terminate in the glomeruli area of the olfactory bulbs. Expression levels of the protein on the CNS were high, especially during the first 48 hours following inoculation. Intense expression was observed in the olfactory bulbs of the majority of mice up to 5 d.p.i., and was observed in occasional animals up to 14 d.p.i. The location of protein expression was consistent throughout the time course of the experiment.

It was further demonstrated that no vector RNA was present in any areas of the CNS. This observation, together with the finding that the RNA of the vector could be detected only in the nasal passage of infected animals, suggests that duration of expression in the CNS is dependent on the half-life of the protein, and that the viral vector does not enter the CNS. These findings also suggest that transcription and/or replication of the vector RNA was taking place in the cells of the olfactory mucosa, which have the capability to regenerate, as is the case with most upper respiratory infections. Viral RNA persisted for 7 days at the site of inoculation only, which was consistent with previous findings (Morris-Downes *et al,* 2001a), as opposed to dispersing in the host and persisting for many weeks, which is the case for DNA vectors (Donnelly *et al,* 1997a). Though the mechanism is not fully understood, protein was transported to the CNS by axonal transport from the nasal epithelium to the olfactory bulb. Within the bulb expression terminated in the glomeruli area, which is where synaptic contacts are formed between incoming axons and the dendrites from mitral and tufted cells found in the olfactory bulb. Axons from these cells extend to the anterior olfactory nucleus of the brain. Histological analyses of brain tissue of mice infected with rSFV-EGFP showed no pathology associated with particle administration. Infected tissue remained healthy for the entire duration of the experiment. This study indicated the possibility of cloning therapeutic genes into the rSFV vector system, and utilizing them as agents for the treatment of CNS disorders.

Previous studies have utilized several different viral vectors for protein expression in the CNS, with mixed results. Usually the intracerebral route of administration is employed. A modified herpes simplex virus vector was able to infect neurons within the cortex, thalamus, and striatum of rats following stereotactic injection. Protein expression was reported for up to 5 weeks, and though the vector alone caused no damage, tissue damage was seen as a result of the method of administration (Sandler *et al,* 2002). Other studies utilizing herpes vectors delivered to the CNS by stereotactic inoculation have detected long lasting expression, but with some damage to recipient cells (Fukuda *et al,* 2003, Lilley *et al,* 2001). Adeno-associated virus vectors have also been used for protein expression in the CNS by stereotactic inoculation, and long-term but relatively low level expression obtained (Klein *et al,* 1998, Klein *et al,* 1999, Peel *et al,* 1997, Peel and Klein 2000). For lentivirus vectors, transgene expression has been detected for over 3 months following injection into the striatum and hippocampus (Lai and Brady 2002). Though most studies were able to show transgene expression in the CNS, tissue damage was

usually noted, not caused by the vector, but as a result of mechanical damage from the stereotactic injection process. Compared to other vector systems, it is clear that the currently used SFV recombinant particle system is a transient expression system, and not suitable for the long-term expression of transgenes in the CNS (Atkins *et al,* 1999, Lundstrom 2003). Direct injection of the vector, for example by stereotactic inoculation, may also induce neuronal damage or inflammation. However, as shown in this study, intranasal administration does not induce CNS damage, and transient high-level expression may in some circumstances be an advantage. This would be the case, for example, in the treatment of disease episodes such as occur in EAE or human multiple sclerosis, or to treat transient infections of the CNS.

The rSFV has a few other advantages over other vectors. High titers can easily be produced with the vector, which is not the case with retroviral, adeno-associated, and HSV-1 vectors. Furthermore, the genome of the vector is very easily manipulated allowing for easier insertion of foreign genes. That is not the case with all vectors. HSV-1 vectors for example are more difficult to manipulate due to its large size, and the fact that many genes are duplicated. Few people with the exception of Africans have any immunity against the SFV. The use of HSV-1 may not be possible if patients are seropositive for anti-herpes virus antibodies, or are being treated with anti-herpes drugs.

Measured levels of both IL-4 and IL-10 cytokines in the CNS were higher when either IL-4 or IL-10 expressing vector were given i.n. to mice, compared to vectors containing only a reporter gene. It was previously determined that following i.n. infection of mice with the rSFV particle system, the vector did not infect cells of the CNS, and that only the cloned gene was detected in the olfactory bulb. It can be concluded therefore that the cloned cytokine is successfully being secreted into the CNS, since it was found in higher levels in areas of the brain. Furthermore, since the vector RNA does not persist for longer then 7 days in infected tissue, it is possible that the effect of the cytokine expressing vector is due to induction of a cytokine cascade effect, rather than just the local action of IL-10 or IL-4 expressed by the vector. It is also possible that the cytokine is released from the site of expression and spreads systemically.

This can be concluded from the fact that cytokines are short-lived molecules that would not be detected for longer than 7 or 8 days. It was clear that the delivery of IL-10 led to the production of more of the same cytokine; with similar taking place with IL-4. A notable difference was that higher levels of IFN-γ were detected following rSFV-IL4

administration. This could be due to inflammation of the airways and bronchial epithelial cells due to raised levels of IL-4 (Hodge *et al,* 2001, Tanaka *et al,* 2000). It is not clear if all the cytokine detected in the CNS is that which was cloned and delivered by the vector system, or if it was produced as a result of the vector. The length of expression as previously mentioned indicated that most of the cytokine detected is a direct result of a change in cytokine balance caused by the vector's addition of other cytokines in the system. To differentiate between endogenous and delivered cytokines either knockout mice or a tagged form of the cytokine cloned in the vector system would need to be used. The limitation in using knockout mice is that the animal would not be able to produce cytokines as a result of new cytokines being introduced to the immune system, which is of key importance in the current research. The use of a tagged form of the cytokine would allow for easy localization of the protein within the CNS of animals. This measure however would not be quantitative, which is the type of result needed to determine whether this system would be useful in the treatment of CNS diseases. As the main objective of the study was to determine if the immune system would produce more cytokines as a result of infection, there was no reason to conduct the mentioned studies. The costs involved, the time required, and the extra use of animals would not be justified.

The nasal route of administration has previously been used to deliver cytokines to down-regulate EAE (Xiao *et al,* 1998). The therapeutic uses of IL-4 and IL-10 in EAE have also been widely researched, with conflicting results. Studies conducted on knockout mice clearly indicated that each play an important role in the treatment or severity of EAE (Bettelli *et al,* 1998, Cua *et al,* 1999, Samoilova *et al,* 1998). How important a role still remains to be seen. Work with transgenic mice showed that only the IL-10 transgene did not develop EAE, opposed to the IL-4 transgene, which had no effect on disease outcome (Bettelli et al, 1998, Cua et al, 1999). It has previously been reported that avirulent SFV infection potentiates or exacerbates EAE (Eralinna *et al,* 1996, Mokhtarian and Swoveland 1987). Also, intramuscular administration of plasmids encoding DNA vaccines can potentiate EAE, if such plasmids are administered within 10 weeks of EAE induction. This effect is associated with induction of a Th1 cytokine response (Selmaj *et al,* 2000, Tsunoda *et al,* 1999). In this study, it was showed that i.n. administration of recombinant SFV particles, expressing reporter gene only or a non-secreting form of a cytokine, exacerbated EAE. This was also observed for peripheral administration (intramuscular or intraperitoneal) of recombinant SFV particles encoding either cytokines or a reporter gene.

The exacerbation of EAE is likely therefore to be a direct effect of the vector rather than the encoded gene. However, i.n. administration of recombinant SFV particles encoding IL-10 abrogated this effect and indeed inhibited EAE. This is consistent with previous studies in which vectors encoding IL-10, or i.n. administration of IL-10 protein down-regulated EAE (Cua *et al,* 2001, Rott *et al,* 1994, Xiao et al, 1998). Many studies have described the use of various combinations of vectors and cytokines to treat autoimmune animal disease models. Different vectors and different routes of administration often lead to conflicting results (Croxford *et al,* 2001). In this study, we showed that i.n. administration of recombinant SFV particles encoding IL-10 inhibited EAE, whereas this is not the case for a defective herpes virus vector encoding IL-10 (Broberg *et al,* 2001). In contrast, the use of recombinant SFV particles encoding IL-4 did not inhibit EAE, whereas IL-4 delivered by a HSV-1 vector inhibited the disease (Furlan *et al,* 1998, Martino *et al,* 1998, Martino *et al,* 2000b). The reason for this apparent anomaly is not clear at present.

There are a number of directions the current study could go in the future. Since IFN-β is the most widely used cytokine currently in use to treat MS, it would be interesting to clone the gene for this protein into the vector system, and test its therapeutic efficacy on EAE. A second cytokine which has been the subject of much research for its role in EAE is TGF-β. Once this cytokine is properly cloned into the vector system, it could also be used in the treatment of EAE. A number of other models of demyelinating disease are currently in use. The vector has proven successful in the inhibition of EAE; however, how it would act on other demyelinating diseases of the CNS remains to be seen. One such model that was attempted in the current project was on the treatment of SFV induced demyelination. Since infected mice present mild clinical signs, the model relies solely on pathology assessment to determine effectiveness. The main problem encountered was that the demyelination observed in control animals is very variable, making it difficult to compare treated versus untreated groups. A better model to work on would be Theilers virus, which also induces demyelination. Furthermore, by using this virus rather then SFV, there is no problem of animals developing an immune reaction to the vector prior to treatment.

The use of polyunsaturated fatty acids in the treatment of EAE is an alternative to gene therapy with viral vectors. Since lipids are fed to animals, it is also a non-invasive method of treatment. There has been some research suggesting that linoleic acid plays a role as an anti-inflammatory agent. There has also been some association with raised

levels of TGF-β following treatment with this compound (Harbige *et al,* 1995, Harbige *et al,* 2000). This research is still in a very early stage; however results obtained have been promising. A more comprehensive analysis is needed to determine the mode of action of the different compounds, a comprehensive pathological analysis, as well as determining any possible side effects. During treatment there were some animals that died as a result of treatment, prior to developing EAE. Some of these animals could have accidentally received the compound in their lungs, which is a complication of orally feeding the compounds.

Comparing the two forms of treatment, there are advantages as well as disadvantages to each. Both are non-invasive, and cause no damage to treated animals. The cost of producing synthetic compounds could be high, and the treatment does involve injection of large volumes in order to achieve disease inhibition. The use of the rSFV vector has the stigma of being a viral vector, which many people who do not understand the nature of the vector might be afraid to use such treatment in fears of being infected with a virus. In terms of tolerance, the vector has the advantage over lipid compounds, since there are people who might not tolerate the oil well, and have allergic reactions to it; this would not the case with a viral vector delivered intranasally.

MS is a central nervous system disease that affects a large part of young adults worldwide. The need for a more comprehensive treatment is urgently needed. The biggest challenge to finding a cure has been to achieve expression of the therapy within the CNS. A number of drugs are currently in use for the treatment of MS relapses. The most common treatment is interferon-beta delivered either intravenously or intramuscularly. The main challenge facing researchers has been to find a method of getting treatment agents to successfully cross the blood-brain barrier. The blood-brain barrier is a capillary barrier that results from a continuous layer of endothelial cells bound together with tight junctions, allowing very little transcellular or pericellular transport of blood-borne molecules. Molecules are excluded from the brain based on electric charge, lipid solubility, and molecular weight (Neuwelt 1989, Rapoport and Robinson 1986). To be able to circumvent the blood-brain barrier and gain access of therapeutic agents in the brain is an area where more research is needed. Gene therapy using viral vectors delivered to the CNS of animals by the intracisternal and intracranial route have managed to circumvent this barrier, though these methods are somewhat traumatic to animals. The rSFV vector

system delivered i.n. has also proven an effective method of bypassing this barrier and reaching the CNS, with no trauma or physical injury to tested animals.

In conclusion, it has been demonstrated that SFV recombinant particles, when administered by the i.n. route, represent a novel non-invasive vector system for protein delivery to the CNS. There is a need to develop safe, non-invasive vectors to treat neurological conditions. Previous studies have demonstrated the safety and efficacy of rSFV vectors (Morris-Downes et al, 2001a), while the ability to produce stable high titer particles combined with the findings of this study indicate that they are potential candidates to be developed as therapeutic agents for the CNS.

Chapter 8

References

Aliperti G, Schlesinger MJ. 1978. Evidence for an autoprotease activity of sindbis virus capsid protein. *Virology*. **90**(2): 366-369.

Allen I, Brankin B. 1993. Pathogenesis of multiple sclerosis--the immune diathesis and the role of viruses. *J Neuropathol Exp Neurol*. **52**(2): 95-105.

Amor S, Groome N, Linington C, Morris MM, Dornmair K, Gardinier MV, et al. 1994. Identification of epitopes of myelin oligodendrocyte glycoprotein for the induction of experimental allergic encephalomyelitis in SJL and Biozzi AB/H mice. *J Immunol*. **153**(10): 4349-4356.

Atkins GJ, Sheahan BJ. 1982. Semliki forest virus neurovirulence mutants have altered cytopathogenicity for central nervous system cells. *Infect Immun*. **36**(1): 333-341.

Atkins GJ, Sheahan BJ, Dimmock NJ. 1985. Semliki Forest virus infection of mice: a model for genetic and molecular analysis of viral pathogenicity. *Journal of General Virology*. **66**: 395-408.

Atkins GJ, Sheahan BJ, Mooney DA. 1990. Pathogenicity of Semliki Forest virus for the rat central nervous system and primary rat neural cell cultures: possible implications for the pathogenesis of multiple sclerosis. *Neuropathol Appl Neurobiol*. **16**(1): 57-68.

Atkins GJ, Sheahan BJ, Liljestrom P. 1996. Manipulation of the Semliki Forest virus genome and its potential for vaccine construction. *Molecular biotechnology*. **5**: 33-38.

Atkins GJ, Sheahan BJ, Liljestrom P. 1999. The molecular pathogenesis of Semliki Forest virus: a model virus made useful? *Journal of General Virology*. **80**: 2287-2297.

Atkins GJ, McQuaid S, Morris-Downes MM, Galbraith SE, Amor S, Cosby SL, et al. 2000. Transient virus infection and multiple sclerosis. *Rev Med Virol*. **10**(5): 291-303.

Baig S, Olsson T, Yu-Ping J, Hojeberg B, Cruz M, Link H. 1991. Multiple sclerosis: cells secreting antibodies agains myelin-associated glycoprotein are present in cerebrospinal fluid. *Scand J Immunol*. **33**: 73-79.

Balluz IM, Glasgow GM, Killen HM, Mabruk MJ, Sheahan BJ, Atkins GJ. 1993. Virulent and avirulent strains of Semliki Forest virus show similar cell tropism for the murine central nervous system but differ in the severity and rate of induction of cytolytic damage. *Neuropathology and Applied Neurobiology*. **19**: 233-239.

Baranzini SE, Oksenberg JR, Hauser SL. 2002. New insights into the genetics of multiple sclerosis. *J Rehabil Res Dev*. **39**(2): 201-209.

Barbarese E, Carson JH, Braun PE. 1978. Accumulation of the four myelin basic proteins in mouse brain during development. *J Neurochem*. **31**: 779-782.

Barna BP, Estes ML, Jacobs BS, Hudson S, Ransohoff RM. 1990. Human astrocytes proliferate in response to tumor necrosis factor alpha. *J Neuroimmunol.* **30**: 239-243.

Barth BU, Suomalainen M, Liljestrom P, Garoff H. 1992. Alphavirus assembly and entry: role of the cytoplasmic tail of the E1 spike subunit. *J Virol.* **66**(12): 7560-7564.

Barth BU, Wahlberg JM, Garoff H. 1995. The oligomerization reaction of the Semliki Forest virus membrane protein subunits. *J Cell Biol.* **128**(3): 283-291.

Baum HM, Rothschild BB. 1981. The incidence and the prevalence of reported multiple sclerosis. *Ann Neurol.* **10**: 420-428.

Beck J, Rondot P, Catinot L, Falcoff E, Kirchner H, Wietzerbin J. 1988. Increased production of interferon gamma and tumor necrosis factor precedes clinical manifestations in multiple sclerosis: do cytokines trigger exarcerbations? *Acta Neurol Scand.* **78**: 318-323.

Beebe AM, Cua DJ, de Waal Malefyt R. 2002. The role of interleukin-10 in autoimmune disease: systemic lupus erythematosus (SLE) and multiple sclerosis (MS). *Cytokine Growth Factor Rev.* **13**(4-5): 403-412.

Berg DJ, Kuhn R, Rajewsky K, Muller W, Menon S, Davidson N, et al. 1995a. Interleukin-10 is a central regulator of the response to LPS in murine models of endotoxic shock and the Shwartzman reaction but not endotoxin tolerance. *J Clin Invest.* **96**: 2339-2347.

Berg DJ, Leach MW, Kuhn R, Rajewsky K, Muller W, Davidson NJ, et al. 1995b. Interleukin 10 but not interleukin 4 is a natural suppressant of cutaneous inflammatory responses. *J Exp Med.* **182**: 99-108.

Berglund, P., Tubulekas, I., Liljestrom, P. 1996. Alphaviruses as vectors for gene delivery. *TIBTECH.* **14**:130-134.

Berglund P, Quesada-Rolander M, Putkonen P, Biberfeld G, Thorstensson R, Liljestrom P. 1997. Outcome of immunization of cynomolgus monkeys with recombinant Semliki Forest virus encoding human immunodeficiency virus type 1 envelope protein and challenge with a high dose of SHIV-4 virus. *AIDS research and human retroviruses.* **13**: 1487-1495.

Berglund P, Fleeton MN, Smerdou C, Liljestrom P. 1999. Immunization with recombinant Semliki Forest virus induces protection against influenza challenge in mice. *Vaccine.* **17**: 497-507.

Besnard F, Parraud F, Sensenbrenner M, Labourdette G. 1987. Platelet-derived growth factor is a mitogen for glial but not for neuronal rat brain cells in vitro. *Neurosci Lett.* **73**: 287-292.

Bettelli E, Das MP, Howard ED, Weiner HL, Sobel RA, Kuchroo VK. 1998. IL-10 is critical in the regulation of autoimmune encephalomyelitis as demonstrated by studies of IL-10- and IL-4-deficient and transgenic mice. *J Immunol.* **161**(7): 3299-306.

Blomer U, Naldini L, Kafri T, Trono D, Verma IM, Gage FH. 1997. Highly efficient and sustained gene transfer in adult neurons with a lentivirus vector. *J Virol.* **71**(9): 6641-6649.

Bonatti S, Migliaccio G, Blobel G, Walter P. 1984. Role of the signal recognition particle in the membrane assembly of Sindbis viral glycoprotein. *Eur J Biochem.* **140**: 499-502.

Braciak TA, Pedersen B, Chin J, Hsiao C, Ward ES, Maricic I, et al. 2003. Protection against experimental autoimmune encephalomyelitis generated by a recombinant adenovirus vector expressing the V beta 8.2 TCR is disrupted by coadministration with vectors expressing either IL-4 or -10. *J Immunol.* **170**(2): 765-774.

Bradish CJ, Allner K, Maber HB. 1971. The virulence of original and derived strains of Semliki forest virus for mice, guinea-pigs and rabbits. *J Gen Virol.* **12**(2): 141-160.

Brand D, Lemiale F, Turbica I, Buzelay L, Brunet S, Barin F. 1998. Comparative analysis of humoral immune responses to HIV type 1 envelope glycoproteins in mice immunized with a DNA vaccine, recombinant Semliki Forest virus RNA, or recombinant Semliki Forest virus particles. *AIDS Res Hum Retroviruses.* **14**(15): 1369-1377.

Bridoux F, Badou A, Saoudi A, Bernard I, Druet E, Pasquier R, et al. 1997. Transforming growth factor beta (TGF-beta)-dependent inhibition of T helper cell 2 (Th2)-induced autoimmunity by self-major histocompatibility complex (MHC) class II-specific, regulatory CD4(+) T cell lines. *J Exp Med.* **185**(10): 1769-1775.

Broberg E, Setala N, Roytta M, Salmi A, Eralinna JP, He B, et al. 2001. Expression of interleukin-4 but not of interleukin-10 from a replicative herpes simplex virus type 1 viral vector precludes experimental allergic encephalomyelitis. *Gene Ther.* **8**(10): 769-777.

Bron R, Wahlberg JM, Garoff H, Wilschut J. 1993. Membrane fusion of Semliki Forest virus in a model system: correlation between fusion kinetics and structural changes in the envelope glycoprotein. *Embo J.* **12**(2): 693-701.

Brown DT, Condreay LD. Replication of alphaviruses in mosquito cells. In: Schlesinger S, Schlesinger MJ, editors. 1986. The Togaviridae and Flaviviridae. New York: Plenum Press. p. 171-207.

Brunner C, Lassmann H, Waehneldt TV, Matthieu JM, Linington C. 1989. Differential ultrastructural localization of myelin basic protein, myelin/oligodendroglial glycoprotein, and 2',3'-cyclic nucleotide 3'-phosphodiesterase in the CNS of adult rats. *J Neurochem.* **52**: 296-304.

Burkhart C, Liu GY, Anderton SM, Metzler B, Wraith DC. 1999. Peptide-induced T cell regulation of experimental autoimmune encephalomyelitis: a role for IL-10. *Int Immunol.* **11**(10): 1625-1634.

Burns CP, Haugstad BN, Mossman CJ, North JA, Ingraham LM. 1988. Membrane lipid alteration: effect on cellular uptake of mitoxantrone. *Lipids.* **23**(5): 393-397.

Callard R, Gearing A. 1994. The Cytokine Facts Book: Harcourt Brace & Company.

Cammer W, Tansey FA, Brosnan CF. 1990. Reactive gliosis in the brains of Lewis rats with experimental allergic encephalomyelitis. *J Neuroimmunol.* **27**: 111-120.

Cannella B, Gao YL, Brosnan C, Raine CS. 1996. IL-10 fails to abrogate experimental autoimmune encephalomyelitis. *J Neurosci Res.* **45**(6): 735-746.

Cantorna MT, Hayes CE, DeLuca HF. 1996. 1,25-Dihydroxyvitamin D3 reversibly blocks the progression of relapsing encephalomyelitis, a model of multiple sclerosis. *Proc Natl Acad Sci U S A.* **93**(15): 7861-7864.

Cassetta I, Granieri E. 2000. Clinical infections and multiple sclerosis: contribution from analytical epidemiology. *J Neurovirol.* **6**: S147-S151.

Cautain B, Damoiseaux J, Bernard I, van Straaten H, van Breda Vriesman P, Boneu B, et al. 2001. Essential role of TGF-beta in the natural resistance to experimental allergic encephalomyelitis in rats. *Eur J Immunol.* **31**(4): 1132-1140.

Cerwenka A, Bevec D, Majdic O, Knapp W, Holter W. 1994. TGF-*b* 1 is a potent inducer of human effector T cells. *J Immunol.* **153**: 4367-4377.

Chen Y, Kuchroo VK, Inobe J, Hafler DA, Weiner HL. 1994. Regulatory T cell clones induced by oral tolerance: suppression of autoimmune encephalomyelitis. *Science.* **265**(5176): 1237-1240.

Choi HK, Tong L, Minor W, Dumas P, Boege U, Rossmann MG, et al. 1991. Structure of Sindbis virus core protein reveals a chymotrypsin-like serine proteinase and the organization of the virion. *Nature.* **354**(6348): 37-43.

Christensen T, Dissing Sorensen P, Riemann H, Hansen HJ, Moller-Larsen A. 1998. Expression of sequence variants of endogenous retrovirus RGH in particle form in multiple sclerosis. *Lancet.* **352**: 1033.

Clark HF, Cohen MM, Lunger PD. 1973. Comparative characterization of a C-type virus-producing cell line (VSW) and a virus-free cell line (VH2) from *Vipera russelli. J Natl Cancer Inst.* **51**: 645-657.

Compston A. 2000. The genetics of multiple sclerosis. *Clin Chem Lab Med.* **38**(2): 133-135.

Cornell-Bell AH, Finkbeiner SM, Cooper MS, Smith SJ. 1990. Glutamate induces calcium waves in cultured astrocytes: long range glial signaling. *Science.* **247**: 470-473.

Croxford JL, Triantaphyllopoulos K, Podhajcer OL, Feldmann M, Baker D, Chernajovsky Y. 1998. Cytokine gene therapy in experimental allergic encephalomyelitis by injection of plasmid DNA-cationic liposome complex into the central nervous system. *J Immunol.* **160**(10): 5181-5187.

Croxford JL, Feldmann M, Chernajovsky Y, Baker D. 2001. Different therapeutic outcomes in experimental allergic encephalomyelitis dependent upon the mode of delivery of IL-10: a comparison of the effects of protein, adenoviral or retroviral IL-10 delivery into the central nervous system. *J Immunol.* **166**(6): 4124-4130.

Cua DJ, Groux H, Hinton DR, Stohlman SA, Coffman RL. 1999. Transgenic interleukin 10 prevents induction of experimental autoimmune encephalomyelitis. *J Exp Med.* **189**(6): 1005-1010.

Cua DJ, Hutchins B, LaFace DM, Stohlman SA, Coffman RL. 2001. Central nervous system expression of IL-10 inhibits autoimmune encephalomyelitis. *J Immunol.* **166**(1): 602-608.

Dani JW, Chernjavsky A, Smith SJ. 1992. Neuronal activity triggers calcium waves in hippocampal astrocyte networks. *Neuron.* **8**: 429-440.

Dau PC. 1991. Plasmapheresis in acute multiple sclerosis: rationale and results. *J Clin Apheresis.* **6**(4): 200-204.

de Curtis I, Simons K. 1988. Dissection of Semliki Forest virus glycoprotein delivery from the trans-Golgi network to the cell surface in permeabilized BHK cells. *Proc Natl Acad Sci U S A.* **85**(21): 8052-8056.

De Keyser J, Zwanikken CM, Zorgdrager A, Oenema D, Boon M. 1999. Treatment of acute relapses in multiple sclerosis at home with oral dexamethasone: a pilot study. *J Clin Neurosci.* **6**(5): 382-384.

de Waal Malefyt R, Haanen J, Spits H, Roncarolo M-G, te Velde A, Figdor C, et al. 1991. IL-10 and viral IL-10 strongly reduce antigen-specific human T cell proliferation by diminishing the antigen-presenting capacity of monocytes via downregulation of class II MHC expression. *J Exp Med.* **174**: 915–924.

Dermietzel R, Hertzberg EL, Kessler JA, Spray DC. 1991. Gap junctions between cultured astrocytes: immunocytochemical, molecular, and electrophysiological analyses. *J Neurosci.* **11**: 1421-1432.

Despres P, Griffin JW, Griffin DE. 1995. Effects of anti-E2 monoclonal antibody on sindbis virus replication in AT3 cells expressing *bcl-2*. *J Virol.* **69**(11): 7006-7014.

DeTulleo L, Kirchhausen T. 1998. The clathrin endocytic pathway in viral infection. *Embo J.* **1998**(17): 4585-4593.

Ding L, Shevach EM. 1992. IL-10 inhibits mitogen-induced T-cell proliferation by selectively inhibiting macrophage co-stimulatory function. *J Immunol.* **148**: 3133–3139.

Ding MX, Schlesinger MJ. 1989. Evidence that Sindbis virus NSP2 is an autoprotease which processes the virus nonstructural polyprotein. *Virology.* **171**(1): 280-284.

Donnelly JJ, Ulmer JB, Shiver JW, Liu MA. 1997a. DNA vaccines. *Annual review of Immunology.* **15**: 617-648.

Donnelly SM, Sheahan BJ, Atkins GJ. 1997b. Long-term effects of Semliki Forest virus infection in the mouse central nervous system. *Neuropathol Appl Neurobiol.* **23**(3): 235-241.

D'Orazio TJ, Niederkorn JY. 1998. A novel role for TGF-beta and IL-10 in the induction of immune privilege. *J Immunol.* **160**(5): 2089-2098.

Dryga SA, Dryga OA, Schlesinger S. 1997. Identification of mutations in a Sindbis virus variant able to establish persistent infection in BHK cells: the importance of a mutation in the nsP2 gene. *Virology.* **228**(1): 74-83.

Dubuisson J, Rice CM. 1993. Sindbis virus attachment: isolation and characterization of mutants with impaired binding to vertebrate cells. *J Virol*. **67**(6): 3363-3374.

Duchen LW. General pathology of neurons and neuroglia. In: Adams JH, Corsellis JAN, Duchen LW, editors. 1984. Greenfield's Neuropathology. 4th ed. Arnold, London. p. 1-52.

Dworkin RH, Bates D, Millar JH, Paty DW. 1984. Linoleic acid and multiple sclerosis: a reanalysis of three double-blind trials. *Neurology*. **34**(11): 1441-1445.

Ebers GC, Sadovnick AD, Risch NJ. 1995. A genetic basis for familial aggregation in multiple sclerosis. Canadian colaborative sudy group. *Nature*. **377**: 150-151.

Ehrengruber MU, Lundstrom K, Schweitzer C, Heuss C, Schlesinger S, Gahwiler BH. 1999. Recombinant Semliki Forest virus and Sindbis virus efficiently infect neurons in hippocampal slice cultures. *Proc Natl Acad Sci U S A*. **96**(12): 7041-7046.

Embry AF, Snowdon LR, Vieth R. 2000. Vitamin D and seasonal fluctuations of gadolinium-enhancing magnetic resonance imaging lesions in multiple sclerosis. *Ann Neurol*. **48**: 271-272.

Eng LF, D'Amelio FE, Smith ME. 1989. Dissociation of GFAP intermediate filaments in EAE: observations in the lumbar spinal cord. *Glia*. **2**: 308-317.

Eralinna JP, Soilu-Hanninen M, Roytta M, Hukkanen V, Salmi AA, Salonen R. 1996. Blood-brain barrier breakdown and increased intercellular adhesion molecule (ICAM-1/CD54) expression after Semliki Forest (A7) virus infection facilitates the development of experimental allergic encephalomyelitis. *J Neuroimmunol*. **66**(1-2): 103-114.

Falcone M, Rajan AJ, Bloom BR, Brosnan CF. 1998. A critical role for IL-4 in regulating disease severity in experimental allergic encephalomyelitis as demonstrated in IL-4-deficient C57BL/6 mice and BALB/c mice. *J Immunol*. **160**(10): 4822-4830.

Fan YY, Chapkin RS, Ramos KS. 1995. A macrophage-smooth muscle cell co-culture model: applications in the study of atherogenesis. *In Vitro Cell Dev Biol Anim*. **31**(7): 492-493.

Favre D, Studer E, Michel MR. 1996. Semliki Forest virus capsid protein inhibits the initiation of translation by upregulating the double-stranded RNA-activated protein kinase (PKR). *Biosci Rep*. **16**(6): 485-511.

Fazakerley JK, Webb HE. 1987. Semliki Forest virus-induced, immune-mediated demyelination: adoptive transfer studies and viral persistence in nude mice. *J Gen Virol.* **68 (Pt 2)**: 377-385.

Fazakerley JK, Pathak S, Scallan M, Amor S, Dyson H. 1993. Replication of the A7(74) strain of Semliki Forest virus is restricted in neurons. *Virology.* **195**(2): 627-637.

Fazakerley JK. 2002. Pathogenesis of Semliki Forest virus encephalitis. *J Neurovirol.* **8 Suppl 2**: 66-74.

Fidler JM, DeJoy SQ, Gibbons JJ, Jr. 1986a. Selective immunomodulation by the antineoplastic agent mitoxantrone. I. Suppression of B lymphocyte function. *J Immunol.* **137**(2): 727-732.

Fidler JM, DeJoy SQ, Smith FR, 3rd, Gibbons JJ, Jr. 1986b. Selective immunomodulation by the antineoplastic agent mitoxantrone. II. Nonspecific adherent suppressor cells derived from mitoxantrone-treated mice. *J Immunol.* **136**(8): 2747-2754.

Fiorentino DF, Zlotnik A, Vieira P, Mosmann TR, Howard M, Moore KW, et al. 1991. IL-10 acts on the antigen-presenting cell to inhibit cytokine production by Th1 cells. *J Immunol.* **146**: 3444-3451.

Fisher BA, Harbige LS. 1997. Effect of omega-6 lipid-rich borage oil feeding on immune function in healthy volunteers. *Biochem Soc Trans.* **25**(2): 343S.

Fischer G, Kettenmann H. 1985. Cultured astrocytes from a syncytium after maturation. *Exp Cell Res.* **159**: 273-279.

Fleeton MN, Sheahan BJ, Gould EA, Atkins GJ, Liljestrom P. 1999. Recombinant Semliki Forest virus particles encoding the prME or NS1 proteins of louping ill virus protect mice from lethal challenge. *Journal of General Virology.* **80**: 1189-1198.

Fleeton MN, Liljestrom P, Sheahan BJ, Atkins GJ. 2000. Recombinant Semliki Forest virus particles expressing louping ill virus antigens induce a better protective response than plasmid-based DNA vaccines or an inactivated whole particle vaccine. *J Gen Virol.* **81**(Pt 3): 749-758.

Fleeton MN, Chen M, Berglund P, Rhodes G, Parker SE, Murphy M, et al. 2001. Self-replicative RNA vaccines elicit protection against influenza A virus, respiratory syncytial virus, and a tickborne encephalitis virus. *J Infect Dis.* **183**(9): 1395-1398.

Fritz RB, Skeen MJ, Chou CH, Garcia M, Egorov IK. 1985. Major histocompatibility complex-linked control of the murine immune response to myelin basic protein. *J Immunol.* **134**(4): 2328-2332.

Frolov I, Schlesinger S. 1994. Comparison of the effects of Sindbis virus and Sindbis virus replicons on host cell protein synthesis and cytopathogenicity in BHK cells. *J Virol.* **68**(3): 1721-1727.

Frolov I, Agapov E, Hoffman TAJ. 1999. Selection of RNA replicons capable of persistent noncytopathic replication in mammalian cells. *J Virol.* **73**: 3854-3865.

Froshauer S, Kartenbeck J, Helenius A. 1988. Alphavirus RNA replicase is located on the cytoplasmic surface of endosomes and lysosomes. *J Cell Biol.* **107**(6 Pt 1): 2075-2086.

Fukuda Y, Yamamura J, Uwano T, Nishijo H, Kurokawa M, Fukuda M, et al. 2003. Regulated transgene delivery by ganciclovir in the brain without physiological alterations by a live attenuated herpes simplex virus vector. *Neurosci Res.* **45**(2): 233-241.

Furlan R, Poliani PL, Galbiati F, Bergami A, Grimaldi LM, Comi G, et al. 1998. Central nervous system delivery of interleukin 4 by a nonreplicative herpes simplex type 1 viral vector ameliorates autoimmune demyelination. *Hum Gene Ther.* **9**(17): 2605-2617.

Furlan R, Poliani PL, Marconi PC, Bergami A, Ruffini F, Adorini L, et al. 2001. Central nervous system gene therapy with interleukin-4 inhibits progression of ongoing relapsing-remitting autoimmune encephalomyelitis in Biozzi AB/H mice. *Gene Ther.* **8**(1): 13-19.

Garoff H, Simons K. 1974. Location of the spike glycoproteins in the Semliki Forest virus membrane. *Proc Natl Acad Sci U S A.* **71**(10): 3988-3992.

Garoff H, Simons K, Renkonen O. 1974. Isolation and characterization of the membrane proteins of Semliki Forest virus. *Virology.* **61**(2): 493-504.

Garoff H, Simons K, Dobberstein B. 1978. Assembly of the Semliki Forest virus membrane glycoproteins in the membrane of the endoplasmic reticulum in vitro. *J Mol Biol.* **124**(4): 587-600.

Garoff H, Frischauf AM, Simons K, Lehrach H, Delius H. 1980. Nucleotide sequence of cDNA coding for Semliki Forest virus membrane glycoproteins. *Nature.* **288**(5788): 236-241.

Garoff H, Kondor-Koch C, Riedel H. 1982. Structure and assembly of alphaviruses. *Curr Top Microbiol Immunol.* **99**: 1-50.

Garoff H, Huylebroeck D, Robinson A, Tillman U, Liljestrom P. 1990. The signal sequence of the p62 protein of Semliki Forest virus is involved in initiation but not in completing chain translocation. *J Cell Biol.* **111**(3): 867-876.

Gascan H, Gauchat JF, Roncarolo MG, Yssel H, Spits H, de Vries JE. 1991. Human B cell clones can be induced to proliferate and to switch to IgE and IgG4 synthesis by interleukin 4 and a signal provided by activated CD4 C T cell clones. *J Exp Med.* **173**: 747-750.

Gates MC, Sheahan BJ, O'Sullivan MA, Atkins GJ. 1985. The pathogenicity of the A7, M9 and L10 strains of Semliki Forest virus for weanling mice and primary mouse brain cell cultures. *J Gen Virol.* **66 (Pt 11)**: 2365-2373.

Genain CP, Roberts T, Davis RL, Nguyen MH, Uccelli A, Faulds D, et al. 1995. Prevention of autoimmune demyelination by a cAMP-specific phosphodiesterase inhibitor. *Proc Natl Acad Sci U S A.* **92**: 3601-3605.

Giulian D, Lachman LB. 1985. Interleukin-1 stimulation of astroglial proliferation after brain injury. *Science.* **228**: 497-499.

Glanville N, Ranki M, Morser J, Kaariainen L, Smith AE. 1976. Initiation of translation directed by 42S and 26S RNAs from Semliki Forest virus in vitro. *Proc Natl Acad Sci U S A.* **73**(9): 3059-3063.

Glasgow GM, Sheahan BJ, Atkins GJ, Wahlberg JM, Salminen A, Liljestrom P. 1991. Two mutations in the envelope glycoprotein E2 of Semliki Forest virus affecting the maturation and entry patterns of the virus alter pathogenicity for mice. *Virology.* **185**(2): 741-748.

Glasgow GM, McGee MM, Sheahan BJ, Atkins GJ. 1997. Death mechanisms in cultured cells infected by Semliki Forest virus. *J Gen Virol.* **78 (Pt 7)**: 1559-1563.

Glasgow GM, McGee MM, Tarbatt CJ, Mooney DA, Sheahan BJ, Atkins GJ. 1998. The Semliki Forest virus vector induces p53-independent apoptosis. *Journal of General Virology.* **79**: 2405-2410.

Goetzl EJ, An S, Smith WL. 1995. Specificity of expression and effects of eicosanoid mediators in normal physiology and human diseases. *Faseb J.* **9**(11): 1051-1058.

Gold R, Hartung HP, Toyka KV. 2000. Animal models for autoimmune demyelinating disorders of the nervous system. *Med Mol Today.* **6**: 88.

Goldmuntz EA, Brosnan CF, Chiu F-C, Norton WT. 1986. Astrocytic reactivity and intermediate filament metabolism in experimental autoimmune encephalomyelitis: the effect of suppression with prazosin. *Brain Res.* **397**: 16-26.

Graca DL, Bondan EF, Pereira LA, Fernandes CG, Maiorka PC. 2001. Behaviour of oligodendrocytes and Schwann cells in an experimental model of toxic demyelination of the central nervous system. *Arq Neuropsiquiatr.* **59**(2-B): 358-361.

Grakoui A, Levis R, Raju R, Huang HV, Rice CM. 1989. A cis-acting mutation in the Sindbis virus junction region which affects subgenomic RNA synthesis. *J Virol.* **63**(12): 5216-5227.

Grandgirard GM, Studer E, Monney L, Belser T, Fellay I, Borner C, et al. 1998. Alphaviruses induce apoptosis in *Bcl-2* expressing cells: evidence for a caspase-mediated, proteolytic inactivation of *Bcl-2*. *EMBO J.* **17**: 1268-1278.

Griffin DE. Alphavirus pathogenesis and immunity. In: Schlesinger SS, Schlesinger MJ, editors. 1986. The togaviridae and Flaviridae. New York: Plenum Press. p. 209-250.

Gruber MF, Williams CC, Gerrard TL. 1994. Macrophage-colony-stimulating factor expression by anti-CD45 stimulated human monocytes is transcriptionally up-regulated by IL-1 beta and inhibited by IL-4 and IL-10. *j immunol.* **152**: 1354–1361.

Haahr S, Sommerlund M, Christensen T, Jensen AW, Hansen HJ, Moller-Larsen A. 1994. A putative new retrovirus associated with multiple sclerosis and the possible involvement of Epstein-Barr virus in this disease. *Ann N Y Acad Sci.* **724**: 148-156.

Haberly LB, Price JL. 1977. The axonal projection patterns of the mitral and tufted cells of the olfactory bulb in the rat. *Brain Res.* **129**: 152-157.

Hahn CS, Strauss JH. 1990. Site-directed mutagenesis of the proposed catalytic amino acids of the Sindbis virus capsid protein autoprotease. *J Virol.* **64**(6): 3069-3073.

Hahn YS, Grakoui A, Rice CM, Strauss EG, Strauss JH. 1989. Mapping of RNA-temperature-sensitive mutants of Sindbis virus: complementation group F mutants have lesions in nsP4. *J Virol.* **63**(3): 1194-1202.

Harber M, Sundstedt A, Wraith D. 2000. The role of cytokines in immunological tolerance: potential for therapy. *Exp. Rev. Mol. Med.* **27**(November): 1-20.

Harbige LS, Yeatman N, Amor S, Crawford MA. 1995. Prevention of experimental autoimmune encephalomyelitis in Lewis rats by a novel fungal source of gamma-linolenic acid. *Br J Nutr.* **74**(5): 701-715.

Harbige LS, Layward L, Morris MM, Amor S. 1997. Cytokine secretion by human T cell clones is differentially regulated by eicosanoids. *Biochem Soc Trans.* **25**(2): 347S.

Harbige LS, Layward L, Morris-Downes MM, Dumonde DC, Amor S. 2000. The protective effects of omega-6 fatty acids in experimental autoimmune encephalomyelitis (EAE) in relation to transforming growth factor-beta 1 (TGF-beta1) up-regulation and increased prostaglandin E2 (PGE2) production. *Clin Exp Immunol.* **122**(3): 445-452.

Hardy WR, Strauss JH. 1989. Processing the nonstructural polyproteins of sindbis virus: nonstructural proteinase is in the C-terminal half of nsP2 and functions both in *cis* and in trans. *J Virol.* **63**(11): 4653-4664.

Hauser SL, Doolittle TH, Lincoln R, Brown RH, Dinarello CA. 1990. Cytokine accumulations in CSF of multiple sclerosis patients: frequent detection of interleukin-1 and tumor necrosis factor but not interleukin-6. *Neurology.* **40**: 1735-1739.

Heber-Katz E. 1995. The relationship between human multiple sclerosis and rodent experimental allergic encephalomyelitis. *Ann N Y Acad Sci.* **756**: 283-293.

Helenius A, Morein B, Fries E, Simons K, Robinson P, Schirrmacher V, et al. 1978. Human (HLA-A and HLA-B) and murine (H-2K and H-2D) histocompatibility antigens are cell surface receptors for Semliki Forest virus. *Proc Natl Acad Sci U S A.* **75**(8): 3846-3850.

Hodge S, Hodge G, Holmes M, Flower R, Scicchitano R. 2001. Interleukin-4 and tumour necrosis factor-α inhibit transforming growth factor-β production in a human bronchial epithelial cell line: Possible relevance to inflammatory mechanisms in chronic obstructive pulmonary disease. *Respirology.* **6**: 205-211.

Hofman RM, Hinton DR, Johnson K, Merrill JE. 1989. Tumor necrosis factor identified in multiple sclerosis brain. *J Exp Med.* **170**: 607-612.

Hohlfeld R. 1997. Biotechnological agents for the immunotherapy of multiple sclerosis. Principles, problems and perspectives. *Brain.* **120 (Pt 5)**: 865-916.

Holder MJ, Knox K, Gordon JK. 1992. Factors modifying survival pathways of germinal center B cells. Glucocorticoids and transforming growth factor-beta, but not cyclosporin A or anti-CD19, block surface immunoglobulin-mediated rescue from apoptosis. *Eur J Immunol.* **22**: 2725-2728.

Honegger P, Metthieu JM, Lassmann H. 1989. Demyelination in brain cell aggregate cultures, induced by a monoclonal antibody against the myelin/oligodendrocyte glycoprotein (MOG). *Schweiz Arch Neurol Psychiatr.* **140**: 10-13.

Huber G, Matus A. 1984. Differences in the cellular distributions of two microtubule-associated proteins, MAP1 and MAP2, in rat brain. *The Journal of neuroscience.* **4**: 151-160.

Hughes D, Keith AB, Mertin J, Caspary EA. 1980. Linoleic acid therapy in severe experimental allergic encephalomyelitis in the guinea-pig: suppression by continuous treatment. *Clin Exp Immunol.* **40**(3): 523-31.

Hurst EW. 1932. The effects of the injection of normal brain emulsion into rabbits, with special reference to the aetiology of the paralytic accidents of antirabic treatment. *J Hygiene.* **32**: 3-44.

Hutter CD, Laing P. 1996. Multiple sclerosis: sunlight, diet, immunology and aetiology. *Med Hypotheses.* **46**(2): 67-74.

Inobe J, Slavin AJ, Komagata Y, Chen Y, Liu L, Weiner HL. 1998. IL-4 is a differentiation factor for transforming growth factor-beta secreting Th3 cells and oral administration of IL-4 enhances oral tolerance in experimental allergic encephalomyelitis. *Eur J Immunol.* **28**(9): 2780-2790.

Inobe JI, Chen Y, Weiner HL. 1996. In vivo administration of IL-4 induces TGF-beta-producing cells and protects animals from experimental autoimmune encephalomyelitis. *Ann N Y Acad Sci.* **778**: 390-392.

Issa LL, Leong GM, Eisman JA. 1998. Molecular mechanism of vitamin D receptor action. *Inflamm Res.* **47**: 451-475.

Issazadeh S, Mustafa M, Ljungdahl A, Hojeberg B, Dagerlind A, Elde R, et al. 1995. Interferon gamma, interleukin 4 and transforming growth factor beta in experimental autoimmune encephalomyelitis in Lewis rats: dynamics of cellular mRNA expression in the central nervous system and lymphoid cells. *J Neurosci Res.* **40**(5): 579-590.

Issazadeh S, Lorentzen JC, Mustafa MI, Hojeberg B, Mussener A, Olsson T. 1996. Cytokines in relapsing experimental autoimmune encephalomyelitis in DA rats: persistent mRNA expression of proinflammatory cytokines and absent expression of interleukin-10 and transforming growth factor-beta. *J Neuroimmunol.* **69**(1-2): 103-115.

Itoyama Y, Sternberg NH, Webster HF, Quarles RH, Cohen SR, Richardson EP. 1980. Immunocytochemical observations on the distribution of myelin-associated glycoprotein and myelin basic protein in multiple sclerosis lesions. *Ann Neurol.* **7:**167-177.

Jerusalmi A, Morris-Downes MM, Sheahan BJ, Atkins GJ. 2003. Effect of intranasal administration of semliki forest virus recombinant particles expressing reporter and cytokine genes on the progression of experimental autoimmune encephalomyelitis. *Molecular Therapy.* **8**(6): 886-894.

Jingwu ZR, Madaer R, Hashim GA, Chin Y, Van der Berg-Loonen E, Raus JCM. 1992. Myelin basic protein-specific T lymphocytes in multiple sclerosis and controls. Precursor frequency, fine specificity and cytotoxicity. *Ann Neurol.* **32**: 330-338.

Johns LD, Flanders KC, Ranges GE, Sriram S. 1991. Successful treatment of experimental allergic encephalomyelitis with transforming growth factor-beta 1. *J Immunol.* **147**(6): 1792-1796.

Johns LD, Sriram S. 1993. Experimental allergic encephalomyelitis: neutralizing antibody to TGF beta 1 enhances the clinical severity of the disease. *J Neuroimmunol.* **47**(1): 1-7.

Joshi N, Usuku K, Hauser SL. 1993. The T-cell response to myelin basic protein in familial multiple sclerosis: diversity of fine specificity, restricting elements, and T-cell receptor usage. *Ann Neurol.* **34**: 385-393.

Kabat EA, Wolf A, Bezer AE. 1947. The rapid production of acute disseminated encephalomyelitis in rhesus monkeys by injection of heterologous and homologous brain tissue with adjuvants. *J Exp Med.* **85**: 117-130.

Kamholz J, Toffenetti J, Lazzarini RA. 1988. Organization and expression of the human myelin basic protein gene. *J Neurosci.* **21**: 62-70.

Karpf AR, Brown DT. 1998. Comparison of Sindbis virus-induced pathology in mosquito and vertebrate cell cultures. *Virology.* **240**(2): 193-201.

Kennedy MK, Torrance DS, Picha KS, Mohler KM. 1992. Analysis of cytokine mRNA expression in the central nervous system of mice with experimental autoimmune encephalomyelitis reveals that IL-10 mRNA expression correlates with recovery. *J Immunol.* **149**(7): 2496-505.

Keranen S, Kaariainen L. 1975. Proteins synthesized by Semliki Forest virus and its 16 temperature-sensitive mutants. *J Virol.* **16**(2): 388-396.

Khoury SJ, Hancock WW, Weiner HL. 1992. Oral tolerance to myelin basic protein and natural recovery from experimental autoimmune encephalomyelitis are associated with downregulation of inflammatory cytokines and differential upregulation of transforming growth factor beta, interleukin 4, and prostaglandin E expression in the brain. *J Exp Med.* **176**(5): 1355-1364.

Kies MW, Roboz E, Alvord ECJ. 1956. Experimental encephalitogenic activity in glycoprotein fraction of bovine spinal cord. *Federation Proc.* **15**: 288.

Kimelberg HK, Goderie SK, Higman S, Pang S, Waniewski RA. 1990. Swelling-induced release of glutamate, aspartate, and taurine from astrocyte cultures. *J Neurosci.* **10**: 1583-1591.

Kimelberg HKe. 1988. Glial Cell Receptors. New York: Raven Press.

Kishi K, Mori K, Ojima H. 1984. Distribution of local axon collaterals of mitral, displaced mitral, and tufted cells in the rabbit olfactory bulb. *J Comp Neurol.* **225**: 511-526.

Klein RL, Meyer EM, Peel AL, Zolotukhin S, Meyers C, Muzyczka N, et al. 1998. Neuron-specific transduction in the rat septohippocampal or nigrostriatal pathway by recombinant adeno-associated virus vectors. *Exp Neurol.* **150**(2): 183-94.

Klein RL, Muir D, King MA, Peel AL, Zolotukhin S, Moller JC, et al. 1999. Long-term actions of vector-derived nerve growth factor or brain-derived neurotrophic factor on choline acetyltransferase and Trk receptor levels in the adult rat basal forebrain. *Neuroscience.* **90**(3): 815-821.

Kronquist KE, Crandall BF, Macklin WB, Campagnoni AT. 1987. Expression of myelin proteins in the developing human spinal cord: cloning and sequencing of human proteolipid protein cDNA. *J Neurosci Res.* **18**: 395-401.

Kruse F, Mailhammer R, Werneckle H, Faissner A, Sommer I, Goridis C, et al. 1984. Neural cell adhesion molecules and myelin-associated glycoproteins share a common carbohydrate moiety recognized by monoclonal antibodies L2 and HNK-1. *Nature.* **311**: 153-155.

Kuhn R, Lohler J, Rennick D, Rajewsky K, Muller W. 1993. Interleukin-10 deficient mice develop chronic enterocolitis. *Cell.* **75**: 263-274.

Kurtzke JF, Hyllested K. 1975. Multiple sclerosis. An epidemic disease in the Faeroes. *Trans Am Neurol Assoc.* **100**: 213-315.

Kurtzke JF. 1993. Epidemiologic evidence for multiple sclerosis as an infection. *Clin Microbiol Rev.* **6**: 382-427.

Kurtzke JF, Hyllested K, Heltberg A, Olsen A. 1993. Multiple sclerosis in the Faroe Islands. 5. The occurrence of the fourth epidemic as validation of transmission. *Acta Neurol Scand.* **88**: 161-173.

Kurtzke JF, Delasnerie-Laupretre N, Wallin T. 1998. Multiple sclerosis in North African migrants to France. *Acta Neurol Scand.* **98**: 302-309.

Kurtzke JF. 2000. Multiple sclerosis in time and space-geographic clues to cause. *J Neurovirol.* **6 Suppl 2**: S134-40.

Kuruvilla AP, Shah R, Hochwald GM, Liggitt HD, Palladino MA, Thorbecke GJ. 1991. Protective effect of transforming growth factor beta 1 on experimental autoimmune diseases in mice. *Proc Natl Acad Sci U S A.* **88**(7): 2918-21.

La Mantia L, Eoli M, Milanese C, Salmaggi A, Dufour A, Torri V. 1994. Double-blind trial of dexamethasone versus methylprednisolone in multiple sclerosis acute relapses. *Eur Neurol.* **34**(4): 199-203.

Lachmi BE, Kaariainen L. 1976. Sequential translation of nonstructural proteins in cells infected with a Semliki Forest virus mutant. *Proc Natl Acad Sci U S A.* **73**(6): 1936-1940.

Lai Z, Brady RO. 2002. Gene transfer into the central nervous system *in vivo* using a recombinant lentivirus vector. *J Neurosci Res.* **67**(3): 363-71.

LaStarza MW, Lemm JA, Rice CM. 1994. Genetic analysis of the nsP3 region of Sindbis virus: evidence for roles in minus-strand and subgenomic RNA synthesis. *J Virol.* **68**(9): 5781-5791.

Lauer K. 1997. Diet and multiple sclerosis. *Neurology.* **49**: S55-S61.

Leake CJ, Varma MG, Pudney M. 1977. Cytopathic effect and plaque formation by Arboviruses in a continuous cell line (XTC-2) from the toad Xenopuslaevis. *J Gen Virol.* **35**: 335-339.

Lebar R, Lubetzki C, Vincent C, Lombrail P, Boutry JM. 1986. The M2 autoantigen of central nervous system myelin, a glycoprotein present in oligodendrocyte membrane. *Clin Exp Immunol.* **66**: 423-434.

Lees MB, Brostoff SW. Proteins of myelin. In: Morell P, editor. 1984. Myelin. New York: Plenum Press. p. 197-224.

Letterio JJ, Roberts AB. 1998. Regulation of immune responses by TGF-b. *Annu Rev Immunol*. **16**: 137-161.

Leutz A, Schachner M. 1981. Epidermal growth factor stimulates DNA-synthesis of astrocytes in primary cerebellar cultures. *Cell Tissue Res*. **220**: 393-404.

Levine B, Huang Q, Isaacs JT, Reed JC, Griffin DE, Hardwick JM. 1993. Conversion of lytic to persistent alphavirus infection by the *bcl-2* cellular oncogene. *Nature*. **361**(6414): 739-742.

Levis R, Schlesinger S, Huang HV. 1990. Promoter for Sindbis virus RNA-dependent subgenomic RNA transcription. *J Virol*. **64**(4): 1726-1733.

L'Heritier P. Drosophila viruses and their role as evolutionary factors. 1970. In: Evolutionary Biology. p. 185-209.

Li GP, La Starza MW, Hardy WR, Strauss JH, Rice CM. 1990. Phosphorylation of Sindbis virus nsP3 in vivo and in vitro. *Virology*. **179**(1): 416-427.

Liblau R, Steinman L, Brocke S. 1997. Experimental autoimmune encephalomyelitis in IL-4-deficient mice. *Int Immunol*. **9**(5): 799-803.

Liljestrom P, Garoff H. 1991a. A new generation of animal cell expression vectors based on the Semliki Forest virus replicon. *Biotechnology (N Y)*. **9**(12): 1356-1361.

Liljestrom P, Garoff H. 1991b. Internally located cleavable signal sequences direct the formation of Semliki Forest virus membrane proteins from a polyprotein precursor. *J Virol*. **65**(1): 147-154.

Liljestrom P, Lusa S, Huylebroeck D, Garoff H. 1991. In vitro mutagenesis of a full-length cDNA clone of Semliki Forest virus: the small 6,000-molecular-weight membrane protein modulates virus release. *J Virol*. **65**(8): 4107-4113.

Lilley CE, Groutsi F, Han Z, Palmer JA, Anderson PN, Latchman DS, et al. 2001. Multiple immediate-early gene-deficient herpes simplex virus vectors allowing efficient gene delivery to neurons in culture and widespread gene delivery to the central nervous system in vivo. *J Virol*. **75**(9): 4343-4356.

Linington C, Webb M, Woodhams PL. 1984. A novel myelin-associated glycoprotein defined by a mouse monoclonal antibody. *J Neuroimmunol*. **6**: 387-396.

Linington C, Bradl M, Lassmann H, Brunner C, Vass K. 1988. Augmentation of demyelination in rat acute allergic encephalomyelities by circulating mouse monoclonal antibodies directed against a myelin/oligodendrocyte glycoprotein. *Ann J Pathol*. **130**: 443-454.

Link H, Sun JB, Wang Z, Xu Z, Love A. 1992. Virus-reactive and autoreactive T cells are accumulated in cerebrospinal fluid in multiple sclerosis. *J Neuroimmunol.* **38**: 63-73.

Lobigs M, Garoff H. 1990. Fusion function of the Semliki Forest virus spike is activated by proteolytic cleavage of the envelope glycoprotein precursor p62. *J Virol.* **64**(3): 1233-1240.

Lobigs M, Zhao HX, Garoff H. 1990. Function of Semliki Forest virus E3 peptide in virus assembly: replacement of E3 with an artificial signal peptide abolishes spike heterodimerization and surface expression of E1. *J Virol.* **64**(9): 4346-4355.

Lomo J, Blomhoff HK, Beiske K, Stokke T, Smeland EB. 1995. TGF-*b*1 and cyclic AMP promote apoptosis in resting human B lymphocytes. *J Immunol.* **154**: 1634-1643.

Losy J, Michalowska-Wender G, Wender M. 1994. The effect of large-dose prednisone therapy on IgG subclasses in multiple sclerosis. *Acta Neurol Scand.* **89**(1): 69-71.

Lucchinetti C, Bruck W, Parisi JE, Scheithauer B, Rodrigues M, Lassmann H. 2000. Heterogeneity of multiple sclerosis lesions: implications for the pathogenesis of demyelination. *Ann Neurol.* **47**: 707-717.

Lundstrom K. 2003. Semliki Forest virus vectors for gene therapy. *Expert Opin Biol Ther.* **3**(5): 771-777.

Lusa S, Garoff H, Liljestrom P. 1991. Fate of the 6K membrane protein of Semliki Forest virus during virus assembly. *Virology.* **185**(2): 843-846.

Macklin WB, Campagnoni DW, Deininger PL, Gardinier MV. 1987. Structure and expression of the mouse myelin proteolipid protein gene. *J Neurosci Res.* **18**: 383-394.

Macrides F, Schneider SP. 1982. Laminar organization of mitral and tufted cells in the main olfactory bulb of the adult hamster. *J Comp Neurol.* **208**: 419-430.

Marquardt MT, Phalen T, Kielian M. 1993. Cholesterol is required in the exit pathway of Semliki Forest virus. *J Cell Biol.* **123**(1): 57-65.

Marth T, Strober W, Seder RA, Kelsall BL. 1997. Regulation of transforming growth factor-beta production by interleukin-12. *Eur J Immunol.* **27**: 1213-1220.

Martin R, McFarland HF, McFarlin DE. 1992. Immunological aspects of demyelinating diseases. *Ann Rev Immunol.* **10**: 153.

Martinez-Caceres EM, Barrau MA, Brieva L, Espejo C, Barbera N, Montalban X. 2002. Treatment with methylprednisolone in relapses of multiple sclerosis patients:

immunological evidence of immediate and short-term but not long-lasting effects. *Clin Exp Immunol.* **127**(1): 165-171.

Martino G, Furlan R, Galbiati F, Poliani PL, Bergami A, Grimaldi LM, et al. 1998. A gene therapy approach to treat demyelinating diseases using non-replicative herpetic vectors engineered to produce cytokines. *Mult Scler.* **4**(3): 222-227.

Martino G, Poliani PL, Furlan R, Marconi P, Glorioso JC, Adorini L, et al. 2000a. Cytokine therapy in immune-mediated demyelinating diseases of the central nervous system: a novel gene therapy approach. *J Neuroimmunol.* **107**(2): 184-190.

Martino G, Poliani PL, Marconi PC, Comi G, Furlan R. 2000b. Cytokine gene therapy of autoimmune demyelination revisited using herpes simplex virus type-1-derived vectors. *Gene Therapy.* **7**(13): 1087-1093.

Massa PT, Mugnaini E. 1982. Cell functions and intramembrane particles of astrocytes and oligodendrocytes: a freeze fracture study. *Neuroscience.* **7**: 523-538.

Massey EJ, Sundstedt A, Day MJ, Corfield G, Anderton S, Wraith DC. 2002. Intranasal peptide-induced peripheral tolerance: the role of IL-10 in regulatory T cell function within the context of experimental autoimmune encephalomyelitis. *Vet Immunol Immunopathol.* **87**(3-4): 357-372.

Mathiot CC, Grimaud G, Garry P, Bouquety JC, Mada A, Daguisy AM, et al. 1990. An outbreak of human Semliki Forest virus infections in Central African Republic. *Am J Trop Med Hyg.* **42**(4): 386-393.

Matthieu JM, Amiguet P. 1990. Myelin/oligodendrocyte glycoprotein expression during development in normal and myelin-deficient mice. *Dev Neurosci.* **12**: 293-302.

McIntosh BM, Brookworth C, Kokernot RH. 1961. Isolation of Semliki Forest virus from *Aedes (Aedimorphus) argenteopunctatus* (Theobald) collected in Portuguese East Africa. *Translations of the Royal Society of Tropical Medicine and Hygiene.* **55**: 192-198.

McKenzie A, Culpepper J, de Waal Malefyt R, Briere F, Punnonen J, Aversa G, et al. 1993. Interleukin-13, a T-cell-derived cytokine that regulates human monocyte and B-cell function. *Proc Natl Acad Sci U S A.* **90**: 3735-3739.

McKenzie AN. 2000. Regulation of T helper type 2 cell immunity by interleukin-4 and interleukin-13. *Pharmacol Ther.* **88**(2): 143-151.

McLeod BC. 2003. Plasmapheresis in multiple sclerosis. *J Clin Apheresis.* **18**(2): 72-74.

McQuillen MP. 1991. Plasmapheresis in chronic progressive multiple sclerosis: pro. *J Clin Apheresis*. **6**(4): 207-210.

Meade CJ, Mertin J, Sheena J, Hunt R. 1978. Reduction by linoleic acid of the severity of experimental allergic encephalomyelitis in the guinea pig. *J Neurol Sci*. **35**(2-3): 291-308.

Melancon P, Garoff H. 1986. Reinitiation of translocation in the Semliki Forest virus structural polyprotein: identification of the signal for the E1 glycoprotein. *Embo J*. **5**(7): 1551-1560.

Melancon P, Garoff H. 1987. Processing of the Semliki Forest virus structural polyprotein: role of the capsid protease. *J Virol*. **61**(5): 1301-1309.

Mertin J, Stackpoole A. 1978. Suppression by essential fatty acids of experimental allergic encephalomyelitis is abolished by indomethacin. *Prostaglandins Med*. **1**(4): 283-291.

Mertin J, Stackpoole A. 1979. The spleen is required for the suppression of experimental allergic encephalomyelitis by prostaglandin precursors. *Clin Exp Immunol*. **36**(3): 449-455.

Metsikko K, Garoff H. 1990. Oligomers of the cytoplasmic domain of the p62/E2 membrane protein of Semliki Forest virus bind to the nucleocapsid in vitro. *J Virol*. **64**(10): 4678-4683.

Mi S, Durbin R, Huang HV, Rice CM, Stollar V. 1989. Association of the Sindbis virus RNA methyltransferase activity with the nonstructural protein nsP1. *Virology*. **170**(2): 385-391.

Mi S, Stollar V. 1991. Expression of Sindbis virus nsP1 and methyltransferase activity in *Escherichia coli*. *Virology*. **184**(1): 423-427.

Milanov I, Topalov N, Kmetski T. 1999. Prevalence of multiple sclerosis in Gypsies and Bulgarians. *Epidemiol*. **18**: 218-222.

Mokhtarian F, Swoveland P. 1987. Predisposition to EAE induction in resistant mice by prior infection with Semliki Forest virus. *J Immunol*. **138**(10): 3264-3268.

Moller JR, Johnson D, Brady RO, Tourtellotte WW, Quarles RH. 1989. Antibodies to myeliN-associated glyco-protein (MAG) in the cerebrospinal fluid of multiple sclerosis patients. *J Neuroimmunol*. **22**: 55-61.

Monastra G, Cross AH, Bruni A, Raine CS. 1993. Phosphatidylserine, a putative inhibitor of tumor necrosis factor, prevents autoimmune demyelination. *Neurology.* **43**: 153-163.

Moore KW, de Waal Malefyt R, Coffman RL, O'Garra A. 2001. Interleukin-10 and the interleukin-10 receptor. *Annu Rev Immunol.* **19**: 683-765.

Moore PM. 1997. Herpesvirus 6 might trigger multiple sclerosis. *Lancet.* **350**: 1685-1687.

Morgan IM. 1947. Allergic encephalomyelitis in monkeys in response to injection of normal monkey nervous tissue. *J Exp Med.* **85**: 131-140.

Morris-Downes MM, Phenix KV, Smyth J, Sheahan BJ, Lileqvist S, Mooney DA, et al. 2001a. Semliki Forest virus-based vaccines: persistence, distribution and pathological analysis in two animal systems. *Vaccine.* **19**: 1978-1988.

Morris-Downes MM, Sheahan BJ, Fleeton MN, Liljestrom P, Reid HW, Atkins GJ. 2001b. A recombinant Semliki Forest virus particle vaccine encoding the prME and NS1 proteins of louping ill virus is effective in a sheep challenge model. *Vaccine.* **19**(28-29): 3877-3884.

Mossman T, Coffman R. 1989. TH1 and TH2 cells: different patterns of lymphokine secretion lead to different functional properties. *Annu Rev Immunol.* **5**: 429-459.

Mumford CJ, Wood NW, Kellar Wood HF, Thorpe J, Miller D, Compston DAS. 1994. The British Isles survey of multiple sclerosis in twins. *Neurology.* **44**: 11-15.

Murphy AM, Morris-Downes MM, Sheahan BJ, Atkins GJ. 2000. Inhibition of human lung carcinoma cell growth by apoptosis induction using Semliki Forest virus recombinant particles. *Gene Therapy.* **7**: 1477-1482.

Murphy AM, Sheahan BJ, Atkins GJ. 2001. Induction of apoptosis in Bcl-2-expressing rat prostate cancer cells using the Semliki Forest virus vector. *International Journal of Cancer.* **94**: 572-578.

Murphy S, Pearce B. 1987. Functional receptors for neurotransmitters on astroglial cells. *Neuroscience.* **22**: 381-394.

Nagelkerken L, Blauw B, Tielemans M. 1997. IL-4 abrogates the inhibitory effect of IL-10 on the development of experimental allergic encephalomyelitis in SJL mice. *Int Immunol.* **9**(9): 1243-1251.

Nave KA, Lai C, Bloom FE, Milner RJ. 1987. Splice site selection in the proteolipid protein (PLP) gene transcript and primary structure of the DM-20 protein of central nervous system myelin. *Proc Natl Acad Sci U S A.* **84**: 5665-5669.

Nedergaard M, Cooper AJL, Goldman SA. 1995. Gap junctions are required for the propagation spreading depression. *J Neurobiol.* **28**: 433-444.

Neuwelt EA. 1989. Implications of the blood-brain barrier and its manipulation. New York: Plenum Publishing Co.

Newman PK, Saunders M, Tilley PJ. 1982. Methylprednisolone therapy in multiple sclerosis. *J Neurol Neurosurg Psychiatry.* **45**(10): 941-942.

Nieva JL, Bron R, Corver J, Wilschut J. 1994. Membrane fusion of Semliki Forest virus requires sphingolipids in the target membrane. *Embo J.* **13**(12): 2797-2804.

Nieves J, Cosman F, Herbert J, Shen V, Lindsay R. 1994. High prevalence of vitamin D deficiency and reduced bone mass in multiple sclerosis. *Neurol.* **44**: 1687-1692.

Oksenberg JR, Barcellos LF. 2000. The complex genetic aetiology of multiple sclerosis. *J Neurovirol.* **6 Suppl 2**: S10-14.

Okuda Y, Okuda M, Bernard CC. 2002. Gender does not influence the susceptibility of C57BL/6 mice to develop chronic experimental autoimmune encephalomyelitis induced by myelin oligodendrocyte glycoprotein. *Immunol Lett.* **81**(1): 25-29.

Oldstone MB, Tishon A, Dutko FJ, Kennedy SI, Holland JJ, Lampert PW. 1980. Does the major histocompatibility complex serve as a specific receptor for Semliki Forest virus? *J Virol.* **34**(1): 256-265.

Omlin FX, Webster HD, Palkovits CG, Cohen SR. 1982. Immunocytochemical localization of basic protein in major dense line regions of central and peripheral myelin. *J Cell Biol.* **95**: 242-248.

Orona E, Rainer EC, Scott JW. 1984. Dendritic and axonal organization of mitral and tufted cells in the rat olfactory bulb. *J Comp Neurol.* **226**: 346-356.

Pal E, Yamamura T, Tabira T. 1999. Autonomic regulation of experimental autoimmune encephalomyelitis in IL-4 knockout mice. *J Neuroimmunol.* **100**(1-2): 149-155.

Panitch HS, Hooper CJ, Johnson KP. 1980. CSF antibody to myelin basic protein. Measurement in patients with multiple sclerosis and subacute sclerosing panencephalitis. *Arch Neurol.* **37**: 206-209.

Peel AL, Zolotukhin S, Schrimsher GW, Muzyczka N, Reier PJ. 1997. Efficient transduction of green fluorescent protein in spinal cord neurons using adeno-associated virus vectors containing cell type-specific promoters. *Gene Ther.* **4**(1): 16-24.

Peel AL, Klein RL. 2000. Adeno-associated virus vectors: activity and applications in the CNS. *J Neurosci Methods.* **98**(2): 95-104.

Peranen J, Kaariainen L. 1991. Biogenesis of type I cytopathic vacuoles in Semliki Forest virus-infected BHK cells. *J Virol.* **65**(3): 1623-1627.

Perraud F, Besnard F, Pettmann B, Sensenbrenner M, Labourdette G. 1988. Effects of acidic and basic fabroblastic growth factors (aFGF and bFGF) on the proliferation and the glutamine synthetase expression of rat astroblasts in culture. *Glia.* **1**: 124-131.

Pette M, Fujita K, Wilkinson D, Altman DM, Trowsdale J, Giegerich G, et al. 1990. Myelin autoreactivity in multiple sclerosis: recognition of myelin basic protein in the context of HLA-DR2 products by T lymphocytes of multiple sclerosis patients and healthy donors. *Proc Natl Acad Sci U S A.* **87**: 7968-7972.

Phalen T, Kielian M. 1991. Cholesterol is required for infection by Semliki Forest virus. *J Cell Biol.* **112**(4): 615-623.

Phipps RP, Stein SH, Roper RL. 1991. A new view of prostaglandin E regulation of the immune response. *Immunol Today.* **12**(10): 349-352.

Phylactos AC, Harbige LS, Crawford MA. 1994. Essential fatty acids alter the activity of manganese-superoxide dismutase in rat heart. *Lipids.* **29**(2): 111-115.

Piccirillo CA, Prud'homme GJ. 1999. Prevention of experimental allergic encephalomyelitis by intramuscular gene transfer with cytokine-encoding plasmid vectors. *Hum Gene Ther.* **10**(12): 1915-1922.

Poliani PL, Brok H, Furlan R, Ruffini F, Bergami A, Desina G, et al. 2001. Delivery to the central nervous system of a nonreplicative herpes simplex type 1 vector engineered with the interleukin 4 gene protects rhesus monkeys from hyperacute autoimmune encephalomyelitis. *Hum Gene Ther.* **12**(8): 905-920.

Price JL, Powell TBS. 1970a. An electron microscopic study of the termination of the afferent fibers to the olfactory bulb from the cerebral hemisphere. *J Cell Sci.* **7**: 157-187.

Price JL, Powell TBS. 1970b. The synaptology of the granule cells of the olfactory bulb. *J Cell Sci.* **7**:125-155.

Quarles RH. 1989. Myelin-associated glycoprotein in demyelinating disorders. *Crit Rev Neurobiol.* **51**: 1-28.

Racke MK, Dhib-Jalbut S, Cannella B, Albert PS, Raine CS, McFarlin DE. 1991. Prevention and treatment of chronic relapsing experimental allergic encephalomyelitis by transforming growth factor-beta 1. *J Immunol.* **146**(9): 3012-3017.

Racke MK, Cannella B, Albert P, Sporn M, Raine CS, McFarlin DE. 1992. Evidence of endogenous regulatory function of transforming growth factor-beta 1 in experimental allergic encephalomyelitis. *Int Immunol.* **4**(5): 615-20.

Raine CS. Multiple sclerosis and chronic relapsing EAE: comparative ultrastructural neuropathology. In: Hallpike JF, Adams CW, Tourtellotte WW, editors. 1983. Multiple sclerosis. Baltimore: Williams & Wilkins. p. 413-478.

Raine CS. 1984. Biology of disease. Analysis of autoimmune demyelination: its impact upon multiple sclerosis. *Lab Invest.* **50**(6): 608-35.

Rao K, Lund RD. 1989. Degeneration of optic axons induces the expression of major histocompatibility antigens. *Brain.* **488**: 332-335.

Rapoport SI, Robinson PJ. 1986. Tight-junctional modification as the basis of osmotic opening of the blood-brain barrier. *Ann N Y Acad Sci.* **481**: 250-267.

Riedl E, Strobl H, Majdic O, Knapp W. 1997. TGF-*beta* 1 promotes in vitro generation of dendritic cells by protecting progenitor cells from apoptosis. *J Immunol.* **158**: 1591-1597.

Rikkonen M. 1996. Functional significance of the nuclear-targeting and NTP-binding motifs of Semliki Forest virus nonstructural protein nsP2. *Virology.* **218**(2): 352-361.

Rivers TM, Sprunt DH, Berry GP. 1933. Observations on attempts to produce acute disseminated encephalomyelitis in monkeys. *J Exp Med.* **58**: 39-53.

Ross RH, Romrell LJ. 1989. Histology: A text and atlas. 2nd edition ed. Baltimore, MD, USA.

Rott O, Fleischer B, Cash E. 1994. Interleukin-10 prevents experimental allergic encephalomyelitis in rats. *Eur J Immunol.* **24**: 1434-1440.

Ruddle NH, Bergman CM, McGrath KM, Lingenheld EG, Grunnet ML, Padula SJ, et al. 1990. An antibody to lymphotoxin and tumor necrosis factor prevents transfer of experimental allergic encephalomyelitis. *J Exp Med.* **172**: 1193-1200.

Rumbsy MG. 1978. Organisation and structure in central nerve myelin. *Biochem Soc Trans.*

Salminen A, Wahlberg JM, Lobigs M, Liljestrom P, Garoff H. 1992. Membrane fusion process of Semliki Forest virus. II: Cleavage-dependent reorganization of the spike protein complex controls virus entry. *J Cell Biol.* **116**(2): 349-357.

Salzer JI, Holmes WP, Colman DR. 1987. The amino acid sequences of the myelin-associated glycoproteins: homology to the immunoglobulin gene superfamily. *J Cell Biol.* **104**: 957-965.

Sammin DJ, Butler D, Atkins GJ, Sheahan BJ. 1999. Cell death mechanisms in the olfactory bulb of rats infected intranasally with Semliki Forest virus. *Neuropathology and Applied Neurobiology.* **25**: 236-243.

Samoilova EB, Horton JL, Chen Y. 1998. Acceleration of experimental autoimmune encephalomyelitis in interleukin-10-deficient mice: roles of interleukin-10 in disease progression and recovery. *Cell Immunol.* **188**(2): 118-124.

Sandler VM, Wang S, Angelo K, Lo HG, Breakefield XO, Clapham DE. 2002. Modified herpes simplex virus delivery of enhanced GFP into the central nervous system. *J Neurosci Methods.* **121**(2): 211-219.

Santambrogio L, Hochwald GM, Saxena B, Leu CH, Martz JE, Carlino JA, et al. 1993. Studies on the mechanisms by which transforming growth factor-beta (TGF-beta) protects against allergic encephalomyelitis. Antagonism between TGF-beta and tumor necrosis factor. *J Immunol.* **151**(2): 1116-1127.

Sariola M, Saraste J, Kuismanen E. 1995. Communication of post-Golgi elements with early endocytic pathway: regulation of endoproteolytic cleavage of Semliki Forest virus p62 precursor. *J Cell Sci.* **108 (Pt 6)**: 2465-2475.

Sawcer S, Goodfellow PN. 1998. Inheritance of susceptibility to multiple sclerosis. *Curr Opin Immunol.* **10**(6): 697-703.

Sawicki D, Barkhimer DB, Sawicki SG, Rice CM, Schlesinger S. 1990. Temperature sensitive shut-off of alphavirus minus strand RNA synthesis maps to a nonstructural protein, nsP4. *Virology.* **174**(1): 43-52.

Sawicki DL, Gomatos PJ. 1976. Replication of Semliki forest virus: polyadenylate in plus-strand RNA and polyuridylate in minus-strand RNA. *J Virol.* **20**(2): 446-64.

Scallan MF, Allsopp TE, Fazakerley JK. 1997. *bcl-2* acts early to restrict Semliki Forest virus replication and delays virus-induced programmed cell death. *J Virol.* **71**(2): 1583-1590.

Schlesinger, S. and Schlesinger, M. J. 1996. Togaviridae: the viruses and their replication. p825-868. In, *Fields virology 3rd edition.* B. N. Fields, D. M. Knipe, P. M. Howley *et al* (*eds*). Lippincott-Raven publishers, Philadelphia.

Schluesener HJ, Sobel RA, Linington C, Weiner HL. 1987. A monoclonal antibody against a myelin oligodendrocyte glycoprotein induces relapses and demyelination in the central nervous system autoimmune disease. *J immunol.* **139**: 4016-4021.

Scolding NJ, Frith S, Linington C, Morgan BP, Campbell AK, Compston DA. 1989. Myelin-oligodendrocyte glycoprotein (MOG) is a surface marker for oligodendrocyte maturation. *J Neuroimmunol.* **22**: 169-176.

Scolding NJ, Compston DA. 1991. Oligodendrocyte-macrophage interactions in vitro triggered by specific antibodies. *Immunology.* **72**: 127-132.

Scott JW. 1981. Electrophysiological identification of mitral and tufted cells and distributions of their axons in olfactory system of the rat. *J Neurophysiol.* **46**: 918-931.

Selmaj K, Raine CS, Cannella B, Brosnan CF. 1991. Identification of lymphotoxin and tumor necrosis factor in multiple sclerosis lesions. *J Clin Invest.* **87**(3): 949-54.

Selmaj K, Kowal C, Walczak A, Nowicka J, Raine CS. 2000. Naked DNA vaccination differentially modulates autoimmune responses in experimental autoimmune encephalomyelitis. *J Neuroimmunol.* **111**(1-2): 34-44.

Sheahan BJ, Barrett PN, Atkins GJ. 1981. Demyelination in mice resulting from infection with a mutant of Semliki Forest virus. *Acta Neuropathol (Berl).* **53**(2): 129-136.

Sheahan BJ, Ibrahim MA, Atkins GJ. 1996. Demyelination of olfactory pathways in mice following intranasal infection with the avirulent A7 strain of Semliki Forest virus. *European Journal of Veterinary Pathology.* **2**: 117-125.

Shepherd GM. 1972. Synaptic organization of the mammalian olfactory bulb. *Physiol Rev.* **52**: 864-917.

Simmons K, Garoff H. 1980. The budding mechanisms of enveloped animal viruses. *J Gen Virol.* **50**: 1-21.

Singh I, Helenius A. 1992. Role of ribosomes in Semliki Forest virus nucleocapsid uncoating. *J Virol.* **66**(12): 7049-7058.

Skoging U, Vihinen M, Nilsson L, Liljestrom P. 1996. Aromatic interactions define the binding of the alphavirus spike to its nucleocapsid. *Structure.* **4**(5): 519-529.

Slavin AJ, Maron R, Weiner HL. 2001. Mucosal administration of IL-10 enhances oral tolerance in autoimmune encephalomyelitis and diabetes. *International Immunology.* **13**(6): 825-833.

Smerdou C, Liljestrom P. 1999. Two-helper RNA system for production of recombinant Semliki forest virus particles. *J Virol.* **73**(2): 1092-1098.

Smit JM, Bittman R, Wilschut J. 1999. Low-pH-dependent fusion of Sindbis virus with receptor-free cholesterol- and sphingolipid-containing liposomes. *J Virol.* **73**(10): 8476-8484.

Smith ME, Gibbs MA, Forno LS, Eng LF. 1987. [3H]Thymidine labeling of astrocytes in experimental autoimmune encephalomyelitis. *J Neuroimmunol.* **15**: 309.

Smithburn KC, Haddow AJ. 1944. Semliki Forest virus. Isolation and pathogenic properties. *J Iimmunol.* **49**: 141-173.

Smyth JM, Sheahan BJ, Atkins GJ. 1990. Multiplication of virulent and demyelinating Semliki Forest virus in the mouse central nervous system: consequences in BALB/c and SJL mice. *J Gen Virol.* **71 (Pt 11)**: 2575-2583.

Snell R.S. Clinical Neuroanatomy 3rd edition 2001. Lippincott Williams & Wilkins

Soderlund H. 1973. Kinetics of formation of the Semliki Forest virus nucleocapsid. *Intervirology.* **1**(5-6): 354-361.

Sprinkle TJ. 1989. 2',3'-cyclic nucleotide 3'-phosphodiesterase, an oligodendrocyte-Schwann cell and myelin-associated enzyme of the nervous system. *Critical reviews in Neurobiology.* **43**: 235-301.

Stollar V. Defective interfering alphaviruses. In: Schlesinger RW, editor. 1980. The Togaviruses. New York: Academic Press. p. 427-457.

Strauss JH, Wang KS, Schmaljohn AL, Kuhn RJ, Strauss EG. 1994. Host-cell receptors for Sindbis virus. *Arch Virol Suppl.* **9**: 473-484.

Streit WJ, Graeber MB, Kreutzberg GW. 1988. Functional plasticity of microglia: a review. *Glia.* **1**: 301-307.

Strober W, Kelsall B, Fuss I, Marth T, Ludviksson B, Ehrhardt R, et al. 1997. Reciprocal IFN-gamma and TGF-*beta* responses regulate the occurrence of mucosal inflammation. *Immunol Today.* **18**: 61-64.

Strobl H, Riedl E, Scheinecker C, Bello-Fernandez C, Pickl WF, Rappersberger K, et al. 1996. TGF-*beta* 1 promotes in vitro development of dendritic cells from $CD34^+$ hemopoietic progenitors. *J immunol.* **157**: 1499-1507.

Subak-Sharpe I, Dyson H, Fazakerley J. 1993. In vivo depletion of CD8+ T cells prevents lesions of demyelination in Semliki Forest virus infection. *J Virol.* **67**(12): 7629-7633.

Sun J, Link H, Olsson T, Xiao BG, Andersson G, Ekre HP, et al. 1991a. T and B cell response to myelin-oligodendrocyte glycoprotein in multiple sclerosis. *J immunol.* **146**: 1490-1495.

Sun JB, Olsson T, Wang WZ, Xiao BG, Kostulas V, Fredrikson S, et al. 1991b. Autoreactive T and B cells responding to myelin proteolipid protein in multiple sclerosis and controls. *Eur J Immunol.* **21**: 1461-1468.

Suomalainen M, Liljestrom P, Garoff H. 1992. Spike protein-nucleocapsid interactions drive the budding of alphaviruses. *J Virol.* **66**(8): 4737-4747.

Takkinen K. 1986. Complete nucleotide sequence of the nonstructural protein genes of Semliki Forest virus. *Nucleic Acids Res.* **14**(14): 5667-5682.

Tanaka H, Kawada N, Yamada T, Kawada K, Nagai H. 2000. Interleukin-4 is involved in allergen-induced airway eosinophilic inflammation and bronchial hyperresponsiveness independent of genetic background. *Allergology International.* **49**: 253-261.

Tourtellotte WW, Potvin AR, Fleming JO, Murthy KN, Levy J, Syndulco K, et al. 1980. Multiple sclerosis: measurament and validation of central nervous system IgG synthesis rate. *Neurology.* **30**: 240-244.

Trotter JL, Hickey WF, van der Veen RC, Sulze L. 1991. Peripheral blood mononuclear cells from multiple sclerosis patients recognize myelin proteolipid protein and selected peptides. *J Neuroimmunol.* **33**: 55-62.

Tsunoda I, Tolley ND, Theil DJ, Whitton JL, Kobayashi H, Fujinami RS. 1999. Exacerbation of viral and autoimmune animal models for multiple sclerosis by bacterial DNA. *Brain Pathol.* **9**(3): 481-493.

Tubulekas I, Berglund P, Fleeton M, Liljestrom P. 1997. Alphavirus expression vectors and their use as recombinant vaccines: a minireview. *Gene.* **190**(1): 191-195.

Ubol S, Tucker PC, Griffin DE, Hardwick JM. 1994. Neurovirulent strains of Alphavirus induce apoptosis in bcl-2-expressing cells: role of a single amino acid change in the E2 glycoprotein. *Proc Natl Acad Sci U S A.* **91**(11): 5202-5206.

van de Wyngaert FA, Beguin C, D'Hooghe MB, Dooms G, Lissoir F, Carton H, et al. 2001. A double-blind clinical trial of mitoxantrone versus methylprednisolone in relapsing, secondary progressive multiple sclerosis. *Acta Neurol Belg.* **101**(4): 210-216.

von Bonsdorff CH, Harrison SC. 1975. Sindbis virus glycoproteins form a regular icosahedral surface lattice. *J Virol.* **16**(1): 141-145.

Wahlberg JM, Boere WA, Garoff H. 1989. The heterodimeric association between the membrane proteins of Semliki Forest virus changes its sensitivity to low pH during virus maturation. *J Virol.* **63**(12): 4991-4997.

Wahlberg JM, Bron R, Wilschut J, Garoff H. 1992. Membrane fusion of Semliki Forest virus involves homotrimers of the fusion protein. *J Virol.* **66**(12): 7309-7318.

Wahlberg JM, Garoff H. 1992. Membrane fusion process of Semliki Forest virus. I: Low pH-induced rearrangement in spike protein quaternary structure precedes virus penetration into cells. *J Cell Biol.* **116**(2): 339-348.

Waksman BH, Porter H, Lees MD, Adams RD, Folch J. 1954. A study of the chemical nature of components of bovine white matter effective in producing allergic encephalomyelitis in the rabbit. *J Exp Med.* **100**: 451-471.

Waksman BH, Reingold SC. 1986. Viral etiology of multiple sclerosis: Where does the truth lie? *TINS.* **9**: 388-391.

Wang BS, Lumanglas AL, Silva J, Ruszala-Mallon VM, Durr FE. 1986. Inhibition of the induction of alloreactivity with mitoxantrone. *Int J Immunopharmacol.* **8**(8): 967-973.

Warren KG, Catz I, Johnson E, Mielke B. 1994. Antimyelin basic protein specific forms of multiple sclerosis. *Ann Neurol.* **35**: 280-289.

Watanabe S, Yssel H, Harada Y, Arai K. 1994. Effects of prostaglandin E2 on Th0-type human T cell clones: modulation of functions of nuclear proteins involved in cytokine production. *Int Immunol.* **6**(4): 523-32.

Weiss B, Rosenthal R, Schlesinger S. 1980. Establishment and maintenance of persistent infection by Sindbis virus in BHK cells. *J Virol.* **33**(1): 463-474.

Weiss B, Nitschko H, Ghattas I, Wright R, Schlesinger S. 1989. Evidence for specificity in the encapsidation of Sindbis virus RNAs. *J Virol.* **63**(12): 5310-5318.

Wekerle H, Linington C, Lassmann H, Meyermann R. 1986. Cellular immune reactivity within the CNS. *Trends Neurosci.* **9**: 271-277.

Wender M, Zwyrzykowska-Kierys E. 1984. Multiple sclerosis and the history of infectious diseases in childhood. *Neurol Neurochir Pol.* **18**: 429-434.

Wender M, Losy J, Michalowska-Wender G, Kozubski W, Sosnowski P. 1999. The effect of large dose prednisone therapy on immunological markers in multiple sclerosis]. *Neurol Neurochir Pol.* **33**(4): 771-779.

Wengler G, Wengler G. 1976. Localisation of the 26S RNA sequence on the viral genome type 42S RNA isolated from SFV-infected cells. *Virology*. **73**: 190-199.

Willems WR, Kaluza G, Boschek CB, Bauer H, Hager H, Schutz HJ, et al. 1979. Semliki forest virus: cause of a fatal case of human encephalitis. *Science*. **203**(4385): 1127-1129.

Williams KA, Deber CM. 1993. The structure and function of central nervous system myelin. *Crit Rev Clin Lab Sci*. **30**: 29-64.

Wolff JA, Ludtke JJ, Acsadi G, Williams P, Jani A. 1992. A long-term persistence of plasmid DNA and foreign gene expression in mouse muscle. *Hum Mol Genet*. **1**: 363-369.

Xiao BG, Linington C, Link H. 1991. Antibodies to myelin-oligodendrocyte glycoprotein in cerebrospinal fluid from patients with multiple sclerosis and controls. *J Neuroimmunol*. **31**: 91-96.

Xiao BG, Bai XF, Zhang GX, Link H. 1998. Suppression of acute and protracted-relapsing experimental allergic encephalomyelitis by nasal administration of low-dose IL-10 in rats. *J Neuroimmunol*. **84**(2): 230-237.

Xu LY, Huang YM, Yang JS, Van Der Meide PH, Link H, Xiao BG. 2000a. Suppression of ongoing experimental allergic encephalomyelitis (EAE) in Lewis rats: synergistic effects of myelin basic protein (MBP) peptide 68-86 and IL-4. *Clin Exp Immunol*. **120**(3): 526-531.

Xu LY, Yang JS, Huang YM, Levi M, Link H, Xiao BG. 2000b. Combined nasal administration of encephalitogenic myelin basic protein peptide 68-86 and IL-10 suppressed incipient experimental allergic encephalomyelitis in Lewis rats. *Clin Immunol*. **96**(3): 205-211.

Yong VW, Moumdjian R, Yong FP, Ruijs TCG, Freedman MS, Cashman N, et al. 1991. γ-interferon promotes proliferation of adult human astrocytes in vitro and reactive gliosis in the adult mouse brain in vivo. *Proc Natl Acad Sci U S A*. **88**: 7016-7020.

Yoshimoto T, Paul WE. 1994. CD4pos, NK1.1pos T-cells promptly produce Interleukin-4 in response to in-vivo challenge with anti-CD3. *J Exp Med*. **179**: 1285–1295.

Young DA, Lowe LD, Booth SS, Whitters MJ, Nicholson L, Kuchroo VK, et al. 2000. IL-4, IL-10, IL-13, and TGF-beta from an altered peptide ligand-specific Th2 cell

clone down-regulate adoptive transfer of experimental autoimmune encephalomyelitis. *J Immunol.* **164**(7): 3563-3572.

Zamvil SS, Steinman L. 1990. The T lymphocyte in experimental allergic encephalomyelitis. *Annu Rev Immunol.* **8**: 579.

Zhao H, Garoff H. 1992. Role of cell surface spikes in alphavirus budding. *J Virol.* **66**(12): 7089-7095.

Zhou X, Berglund P, Rhodes G, Parker SE, Jondal M, Liljestrom P. 1994. Self-replicating Semliki Forest virus RNA as recombinant vaccine. *Vaccine.* **12**: 1510-1514.

Zhou X, Berglund P, Zhao H, Liljestrom P, Jondal M. 1995. Generation of cytotoxic and humoral immune responses by nonreplicative recombinant Semliki Forest virus. *Proc Natl Acad Sci U S A.* **92**(7): 3009-3013.